TIMON VANDAMME

Pancreatic Neuroendocrine Neoplasms

From Genetics to Everolimus Resistance

Pancreatic Neuroendocrine Neoplasms: from Genetics to Everolimus Resistance

TIMON VANDAMME

The studies described in this thesis were conducted at the Center for Oncological Research (CORE) / Center fo Medical Genetics, University of Antwerp, Belgium and the Section of Endocrinology, Department of Internal Medicine, Erasmus Medical Center Rotterdam, the Netherlands

Layout: Esther Vandamme

Printing: Optima Grafische Communicatie, Rotterdam

ISBN 978-94-6361-526-6

PANCREATIC NEUROENDOCRINE NEOPLASMS: FROM GENETICS TO EVEROLIMUS RESISTANCE

Pancreatische neuroendocriene neoplasieën: van genetica tot everolimusresistentie

Proefschrift
ter verkrijging van de graad van
doctor aan de Erasmus Universiteit Rotterdam
en
doctor in de Medische Wetenschappen aan de Universiteit Antwerpen

op gezag van
de rector magnificus
Prof. dr. F.A. van der Duyn Schouten (EUR)
en
de rector
Prof. dr. H. Van Goethem (UAntwerpen)

en volgens besluit van het College voor Promoties van de Erasmus Universiteit.

De openbare verdediging zal plaatsvinden op
20 april 2021 om 13 uur

door
Timon Arnold Lieve Vandamme
geboren te Antwerpen, België

Erasmus University Rotterdam

University of Antwerp

PROMOTIECOMMISSIE

PROMOTOREN:

Prof. dr. L.J. Hofland

Prof. dr. P. Pauwels

Prof. dr. M. Peeters

Dr. K. Op de Beeck

OVERIGE LEDEN:

Prof. dr. W.N.M. Dinjens

Prof.dr. J.W.M. Martens

Prof. dr. G.D. Valk

Table of contents

General introduction

Partially based upon

Resistance to targeted treatment of gastroenteropancreatic neuroendocrine tumors

Matthias Beyens[1,2], Timon Vandamme[1,2,3], Marc Peeters[2], Guy Van Camp[2], Ken Op de Beeck[1,2]. Endocrine-related Cancer, 2019; 25 (3): R109–R130. doi: 10.1530/ERC-18-0420.

Clinical applications of (epi) genetics in gastroenteropancreatic neuroendocrine neoplasms: moving towards liquid biopsies

Boons Gitta[1,2], Vandamme Timon[1,2,3], Peeters Marc[2], Van Camp Guy[1,2], Op de Beeck Ken[1,2]. Reviews in Endocrine and Metabolic Disorders, 2019; 20 (3), 333-351. doi: 10.1007/s11154-019-09508-w.

[1]Center of Medical Genetics Antwerp, University of Antwerp, Universiteitsplein 1, 2610 Antwerp, Belgium
[2]Center for Oncological Research, University of Antwerp, Universiteitsplein 1, 2610 Antwerp, Belgium
[3]Section of Endocrinology, Department of Internal Medicine, Erasmus Medical Center. Dr Molenwaterplein 40, 3015GD Rotterdam, the Netherlands

I. INTRODUCTION

Neuroendocrine neoplasms (NENs) are rare malignancies that arise from neuroendocrine cells present in many organs, including lung, pancreas, small intestine, thyroid and adrenal glands (Figure 1). The origin of the cells from which NENs arise is not well understood. For instance, in the gastrointestinal tract at least 17 different neuroendocrine cell types are found. The term “neuroendocrine” is used for cell types that exhibit mixed morphological and physiological attributes of both the neural and endocrine regulatory systems. Phenotypically, these NENs express certain proteins, such as synaptophysin, neuron-specific enolase, and chromogranin A (CgA) akin to neural cells while also exhibiting secretory granules typically seen in endocrine cells[1]. Despite these common features, NENs are very heterogeneous in biological behavior[2]. In the pancreas, the α-, β-, δ-, PP- and VIP-cells in the islets can give rise to pancreatic neuroendocrine neoplasms (pNENs)[1]. Functional pNENs, which are symptomatic due to massive secretion of cell-type specific hormones, are called respectively glucagonoma, insulinoma, somatostatinoma, PPoma, and VIPoma[1]. However, only 25% of pNENs are functional and the majority present without hormonal symptoms[3]. pNENs comprise only 1-2% of all pancreatic neoplasms, with an incidence of about 0.48 per 100,000 person years, according to the Surveillance, Epidemiology, and End Results (SEER) program[4,5]. The median overall survival (mOS) for patients with pNEN is 3.6 years[2]. pNENs are graded according to the World Health Organization

(WHO) classification system, which is based on proliferation markers Ki-67 and mitotic count. In 2017 the WHO revised the classification system and introduced “neuroendocrine neoplasm” as the common denominator across all tumor grades, effectively replacing “neuroendocrine tumor” as the preferred terminology for low and intermediate grade neoplasms. In this thesis, neuroendocrine neoplasm is preferably used. However, as some chapters were published before the change in nomenclature, “neuroendocrine tumor” is used instead of “neuroendocrine neoplasm” in those chapters in line with the previous WHO 2010 nomenclature. In addition to the changed terminology, WHO 2017 added differentiation grade as an additional parameter for pNEN classification. Well-differentiated pNENs can be Grade G1, G2 or G3 based on their proliferation rate, while neuroendocrine carcinomas (NECs) are poorly differentiated neoplasms with a high proliferation rate (G3). G3 neoplasms have a poor prognosis [2]. Surgical resection is the primary treatment in locoregional pNENs, and the only curative treatment option. However, more than 50% of patients present with unresectable disease at time of diagnosis [6,7]. For these advanced cases, different therapeutic strategies are available, which are mostly a combination of ablative surgery, peptide receptor radionuclide therapy (PRRT), and medical treatment. Medical treatment can be divided in chemotherapy, biological treatment with somatostatin analogs (SSAs), and targeted therapies[8]. SSAs are molecules that resemble somatostatin, a peptide hormone whose receptors are commonly found at high density on the surface of pNEN tumor cells. Binding of SSAs to these receptors inhibits both hormone secretion and

tumor growth[9]. PRRT is also based on the interaction between a somatostatin receptor (SSTR) and an SSA. However, in PRRT a radionuclide is attached to the SSA, which will kill tumor cells upon internalization.

In pNEN, the focus for targeted therapy has been angiogenesis, through the pan-tyrosine kinase inhibitor sunitinib, and the mammalian target of rapamycin (mTOR). In the late 1970s, the cellular mTOR protein complex was discovered along with its natural inhibitor rapamycin. Rapamycin is isolated from *Streptomyces hygroscopicus* and named after the ancient residents of its discovery place (Easter Island, Rapa Nui)[10–13]. In mammals, rapamycin has strong anti-fungal, immune-suppressive and anticancer properties via the inhibition of mTOR complex 1 and 2 (mTORC1 and mTORC2), two protein complexes part of the phosphoinositide-3-kinase/Akt/mammalian target of rapamycin (PI3K/Akt/mTOR) pathway[14]. The PI3K/Akt/mTOR pathway plays a pivotal role in gastroenteropancreatic neuroendocrine tumors (GEP-NENs) by regulating cell growth, proliferation, survival and protein synthesis[15–17]. The contributing role of the PI3K/Akt/mTOR signaling in NEN carcinogenesis has led to the introduction of the mTOR inhibitor everolimus, a so-called rapalog, in the clinic.

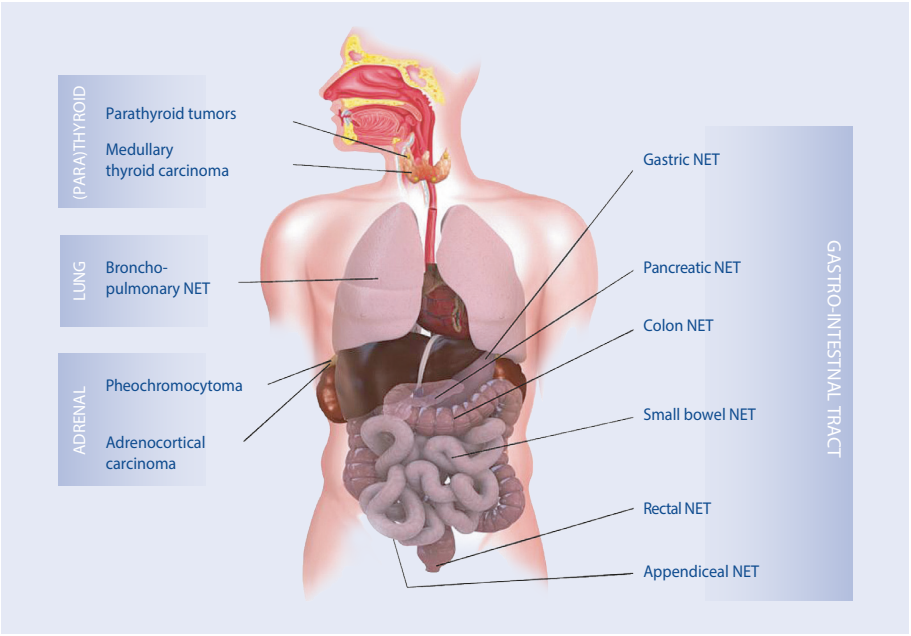

Figure 1 | Neuroendocrine tumors locations and types

II. MUTATIONS AND COPY NUMBER VARIATIONS

Most GEP-NENs are sporadic, but they can also develop as part of genetic syndromes. Approximately 10% of the GEP-NENs, mainly pNENs, arise in the context of a genetic syndrome[18].

1. GENETIC SYNDROMES AND FAMILIAL PNEN CASES

Multiple familial syndromes exist in which pNENs can develop. The syndrome with the highest risk for pNENs (60%) is multiple endocrine neoplasia 1 (MEN1), which is caused by inactivating mutations in the *MEN1* gene[19]. *MEN1* encodes for the protein Menin, which is mainly localized in the nucleus, has many interaction partners and plays a role in multiple pathways, including PI3K/Akt/mTOR, chromatine remodeling, DNA repair and cell cycle control[20]. The von Hippel Lindau (VHL) syndrome is caused by germline mutations in the *VHL* gene. VHL functions within a complex that regulates activity of hypoxia inducible factors (HIFs) which can stimulate angiogenesis[21]. Other syndromes include MEN4, Neurofibromatosis Type 1 (NF1) and Tuberous Sclerosis (TS), caused by mutations in *CDKN1B*, *NF1* and *TSC1* or *TSC2*, respectively[22–24]. Gene products of *NF1*, *TSC1* and *TSC2* all play a role in the PI3K/Akt/mTOR pathway. Remarkably, sequencing of sporadic pNEN cases led to the identification of likely pathogenic germline mutations in cancer susceptibility genes in 10-16% of patients, including *MEN1*, *VHL*, *CDKN1B*, *APC*, *TSC2*, *MUTYH*, *CHEK2* and *BRCA1*. This suggests that a higher than previously anticipated proportion of patients may have inheritable disease[25,26] (Table 1).

2. SPORADIC PNENS

Our understanding of the genetic constitution of sporadic (non-familial) pNENs is supported by a growing body of evidence, mainly based upon next-generation sequencing (NGS) data. With

the introduction of NGS, it became possible to sequence multiple genes simultaneously and even perform unbiased whole-exome sequencing (WES) and whole-genome sequencing (WGS). Most NGS studies have focused on G1 and G2 pNENs. CNV analysis of pNENs, at first via DNA arrays and later via NGS, showed frequent alterations, including whole or partial loss of chromosomes 1, 2, 3, 6, 8, 10, 11, 15,16, 21 and 22, gain of chromosomes 5, 7, 12, 14 and 17, as well as loss of heterozygosity[25–27]. Initial sequencing analysis of sporadic pNEN cases has identified somatic mutations in the *MEN1* gene, previously identified in familial pNENs[28]. Thereafter, two landmark studies have strongly advanced the understanding of genetics of sporadic pNENs, being the WES study of Jiao et al. in 2011 and the WGS study of Scarpa et al. in 2017[17,25]. Jiao et al. performed WES on 10 patients, followed by Sanger sequencing of a selection of genes in 58 additional cases. They detected mutations in *MEN1* (44%) and in PI3K/Akt/mTOR pathway genes (15%), in line with previous studies in pNENs, and identified *DAXX* (25%) and *ATRX* (18%) as new frequently mutated genes[17,28,29]. Scarpa et al. performed WGS on 102 sporadic cases, which were mainly early stage. In 2018, Raj et al. performed targeted sequencing of 80 metastatic pNENs and showed that the mutational burden in these metastasized tumors was 2.95 mutations/megabase, which is higher than the 0.82 mutations/megabase identified by Scarpa[25,26]. Molecular alterations in pNENs were associated with four main pathways, being (1) chromatin remodeling including *MEN1, SETD2*, (2) DNA damage repair including *MUTYH, CHEK2*, (3) activation of mTOR signaling including *TSC2, PTEN* and (4) telomere maintenance including *DAXX, ATRX*. However,

also genes implicated in cell cycle regulation were affected, including *TP53, CDKN2A* and *CDKN1B*[25,26] (Table 1). Five mutation signatures could be distinguished in pNENs, being APOBEC, age, BRCA, "signature 5" and a novel signature associated with loss of MUTYH[25]. In addition, based on an integrative analysis of 57 pNEN cases using shallow WGS, WES, RNA sequencing and DNA methylation analysis, Lawrence et al. conclude that aneuploidy, i.e. abnormal chromosome numbers, is more important than single mutations in tumor development[30]. Sequencing of insulinomas, a type of functional pNENs, has led to the discovery of a hotspot mutation in transcription factor *YY1* present in 30% of a Chinese, 0% of an Indian and 8%-33% of Western/Caucasian insulinoma populations[31–36]. This suggests that functional and non-functional neoplasms may also differ genetically. In different tumor types, the existence of genetic heterogeneity has been demonstrated[37,38]. Various studies have shown that the genetic make-up of primary tumors evolves dynamically in time[37,38]. This time-dependent change of the genetic alterations present in a tumor reflects the appearance and disappearance of subsets of tumor cells within one tumor[37,38]. The existence of genetic intratumor heterogeneity could possibly impact tumor proliferation and therapy resistance. Despite its possible clinical significance, no data was available on the existence of mutations heterogeneity in pNEN until recently.

Table 1 | Genes mutated in familial and sporadic pNENs

Familial pNENs		Sporadic pNENs		
Gene	**Syndrome**	**Gene**		
*MEN1**+	Multiple endocrine neoplasia 1	*MEN1**+	*DAXX*	*MUTYH*
*VHL**+	von Hippel Lindau	*VHL**+	*ATRX*	*BRCA1*
*CDKN1B**	Multiple endocrine neoplasia 4 (MEN4)	*CDKN1B**	*SETD2*	*YY1*
NF1+	Neurofibromatosis Type 1	*TSC2**+	*PTEN* +	
TSC1 +	Tuberous Sclerosis	*CHEK2*	*TP53*	
*TSC2**+	Tuberous Sclerosis	*APC*	*CDKN2A*	

* Genes involved in familial syndromes that are also altered in sporadic neoplasms; +Genes involved in PI3K/Akt/mTOR pathway

3. COPY NUMBER VARIATIONS AND MUTATIONS AS BIOMARKERS

3.1. COPY NUMBER VARIATIONS AS PROGNOSTIC BIOMARKER

CNVs are frequently observed in GEP-NENs and some alterations have been associated with prognosis. Genome-wide loss of heterozygosity was found to be associated with inferior survival in pNENs[26]. CNV profiles also allow subgrouping of pNENs in groups characterized by different mutational profiles and clinical features, including different metastatic potential[25,39]. pNEN patients with a higher level of chromosomal instability show a trend towards longer survival in the RADIANT trials[40].

3.2. MUTATIONS IN DAXX/ATRX AS PROGNOSTIC BIOMARKER

A large fraction of pNENs has mutations in *DAXX* and *ATRX* which correlates with loss of DAXX and ATRX protein expression[17,41,42]. pNENs usually have mutations in either *DAXX* or *ATRX*, which can be readily understood as their encoded proteins function in the same pathway, where they form a complex. The DAXX/ATRX complex has an important role in maintaining telomeric chromatin by deposition of the Histone H3.3 variant at the telomeres[43]. Absence of DAXX/ATRX results in homologous recombination at the telomeres leading to an alternative lengthening of telomeres (ALT), as opposed to the more common activation of telomerase in cancer cells to maintain telomere length[44]. The ALT phenotype can be evaluated using fluorescence in situ hybridization (FISH) with telomere-specific probes. Heaphy et al. even found a 100% correlation between loss of ATRX or DAXX and the ALT phenotype in pNENs[45]. Additional studies reported loss of DAXX/ATRX or ALT activation in 20%-79% of pNEN cases. These diverse prevalences could be explained by a different ethnic background of the patients or by differences in the composition of the study population regarding, for example, tumor stage. ALT positivity and DAXX/ATRX loss associated with higher grade, higher Ki-67 index, larger size and tumor stage[46,47]. Furthermore, it has been shown that loss of DAXX/ATRX was a late event in MEN1-associated pNEN development as 47 small adenomas (<0.5cm) showed no ATRX/DAXX loss or ALT positivity[48]. Singhi et al. showed that DAXX/ATRX status is concordant between primary and metastatic tissue of 52 sporadic pNEN cases[47]. This suggests that, although

loss of DAXX/ATRX expression is a late event, it still occurs prior to development of metastatic disease and it might therefore also play a role in driving tumor metastasis. Interestingly, Jiao et al. described a significant association between *DAXX/ATRX* mutations and an improved survival in metastatic cases[17]. Following these observations, many additional studies have investigated DAXX/ATRX mutation and expression status and ALT status in relation to prognosis. However, controversy is still present. In several studies including between 16 and 321 pNEN patients, DAXX/ATRX mutations and/or loss were significantly associated with worse survival, including disease-free (DFS), relapse-free (RFS), disease-specific (DSS) and overall (OS) survival[41,46,47,49–53]. The worse prognosis in ATRX/DAXX-negative patients might seem contradictory to the findings of Jiao et al.[17]. However, all these studies mainly included early stage patients. In a subset analysis on metastatic patients or in studies including only metastatic patients, DAXX/ATRX-negative tumors showed a trend towards or association with longer survival[41,46,53,54]. Furthermore, ALT positivity has been found to be an independent risk factor for liver metastases[39]. In some studies, DAXX/ATRX status is significantly associated with DFS, but not with OS or DSS in multivariate analysis. This is possibly due to a strong correlation with other prognostic factors, a too short follow-up time or the presence of confounding factors[41,46,47]. In a large pNEN cohort (N=269), ALT activation or loss of ATRX/DAXX was only an independent poor prognostic factor for OS when the cohort was limited to patients with synchronous or metachronous metastatic pNENs, with ALT-positive patients having a significantly better OS[46]. In a study on

105 unselected pNENs, loss of ATRX or DAXX was associated with poor OS in univariate analysis, but not in multivariate analysis. However, in a separate analysis of DAXX and ATRX, only ATRX loss was significantly associated with a worse OS in both univariate and multivariate analysis[53]. A 4-marker panel, including DAXX/ATRX expression analysis, was tested on 347 mainly early-stage pNENs and showed that loss of DAXX/ATRX was associated with a shorter DFS and DSS. These findings are in line with previous studies reporting that loss of DAXX/ATRX is a marker for poor prognosis in metastasis-free patients[55]. Targeted sequencing of 80 metastatic pNEN patients showed an improved survival in *DAXX/ATRX*-mutated tumors compared to wild-type tumors, further adding to the evidence that loss associates with better prognosis in metastatic patients[26]. As an overall conclusion, we can state that the prognostic value of DAXX/ATRX loss depends on disease status, with loss in non-metastatic patients associated with worse survival and loss in metastatic patients associated with better survival. Therefore, when studying DAXX/ATRX loss, a very precise definition of the targeted study population is crucial. In addition, a large meta-analysis that includes all cases and makes relevant stratifications, e.g. metastatic versus non-metastatic, could lead to better insights. A possible explanation for this phenomenon could be that ALT positive tumors more easily progress and metastasize, but because of the intact telomeres, they have less chromosomal instability and might therefore have more difficulties adapting to the new microenvironment, resulting in a slower growth[46,56]. In addition, DAXX/ATRX loss might also indicate that micro metastasis has already occurred

in some cases without clinical apparent metastasis. In metastatic cases, loss of DAXX/ATRX might indicate a subtype of NENs that is associated with a better prognosis.

III. PI3K/AKT/MTOR SIGNALING

1. PI3K/AKT/MTOR SIGNALING IN THE NORMAL CELL

The PI3K/Akt/mTOR signaling cascade plays a pivotal role in cell growth, proliferation, survival and protein synthesis. The physiological intracellular signaling cascade is triggered through binding of growth factors to their respective receptors, either receptor tyrosine kinases (RTKs) or G-protein coupled receptors (GPCRs) at the cell membrane (Figure 2). One such signal transduction involves the activation of phosphoinositide 3-kinase (PI3K) lipid kinase[57]. PI3K phosphorylates the membrane bound phosphatidylinositol-4-5-biphosphate (PIP_2), to generate phosphatidylinositol-3,4,5-triphosphate (PIP_3)[58]. PI3K activity is regulated by phosphatase and tensin homologue (PTEN), which converts PIP_3 back to PIP_2[59]. PIP_3 effectors are proteins with pleckstrin homology (PH) domains. One such effector is the serine/threonine kinase Akt, also known as protein kinase B (PKB)[59]. Upon PIP_3 PH-domain binding, Akt localizes to the membrane and gets activated by phosphoinositide-dependent kinase 1 (PDK1) phosphorylation at Thr308[60]. Akt has a myriad of downstream substrates: glycogen synthase kinase 3 (GSK3, insulin signaling),

B-cell lymphoma 2 (Bcl-2) antagonist of cell death (BAD, pro-apoptotic signaling), p21 and p27 (cell cycle regulation), Forkhead box O (FOXO transcription factor) and mTOR[14,61–65].

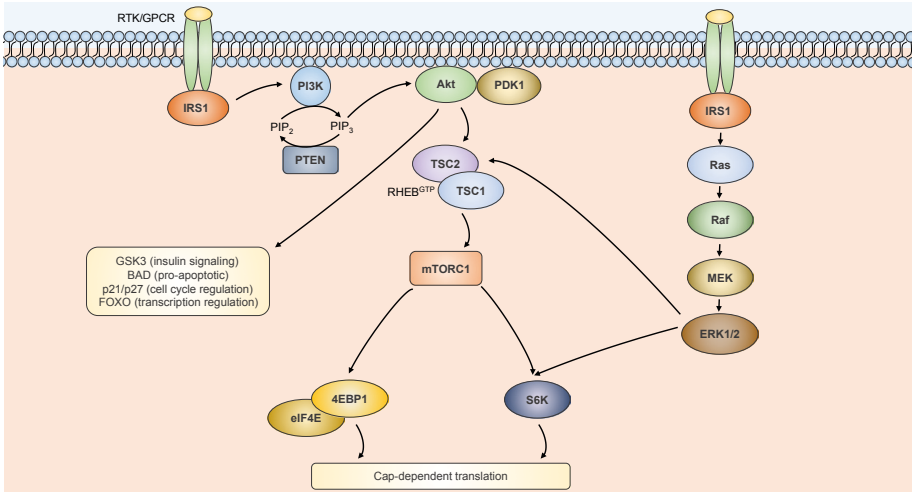

Figure 2 | Schematic representation of the PI3K/Akt/mTORC1 pathway.

Important components involved in the PI3K/Akt/mTOR pathway and their interactions in a cellular context are depicted. The components upstream of mTOR regulate insulin signaling, pro-apoptotic signals, cell cycle regulation and transcription factors. Downstream of mTOR are the effectors that stimulate the cap-dependent translation of proteins.

2. TWO MTOR PROTEIN COMPLEXES

mTOR exerts its kinase activity within two distinct multiprotein complexes designated mTORC1 and mTORC2 with both a combination of unique and common components (Figure 4). mTORC1 is built around its main protein mTOR and different subunits, regulatory-associated protein of mTOR (Raptor), and mammalian lethal with SEC13 protein 8 (mLST8), plus two inhibitors 40kDa proline-rich Akt substrate (PRAS40) and DEP domain-containing mTOR-interacting protein (DEPTOR)[14]. Once mTORC1 is activated, it can regulate the activity of eukaryotic translation initiation factor 4E (eIF4E)-binding proteins (4E-BPs) and ribosomal S6 kinase 1 and 2 (S6K1/2) (Figure 3A). Under basal conditions, 4E-BP1 remains bound to eIF4E in its hypo-phosphorylated form. Upon activation 4E-BP1 is phosphorylated at Thr37, Thr46, Thr70 and Ser65 by mTOR, and induces dissociation of the 4E-BP-eIF4E complex. eIF4E is not inhibited anymore and stimulates the initiation of cap-dependent mRNA translation[66]. Further, S6K1 is phosphorylated at Thr389 by mTORC1 and at Thr229 by PDK1[67]. Activation of S6K1/2 promotes the cells' translational machinery and interacts with transcription factors to promote transcription of cell cycle regulation genes. On the other hand, mTORC2 is assembled with its main protein mTOR and rapamycin-insensitive subunit (Rictor), and mLST8, plus one inhibitor DEPTOR[14] (Figure 4). mTORC2 is a distinct complex from mTORC1 and it regulates the activity of Akt via a feedback circuit[68] (Figure 3**A**). Maximal allosteric kinase activation of Akt is accomplished by mTORC2-dependent Ser473 phosphorylation[69].

Another regulatory function of mTORC2 is the phosphorylation of serum and glucocorticoid-activated kinase 1 (SGK1), thereby regulating cell proliferation and apoptosis via FOXO transcription factors[70]. Furthermore, the Rictor component of the complex causes insensitivity to rapalogs[71], although prolonged treatment can inhibit mTORC2 in some cell types. mTORC2 is mainly involved in cell proliferation, survival and migration via cytoskeletal remodeling[72]. In addition, mTORC2 promotes tumorigenesis via stimulation of the lipid synthesis[73].

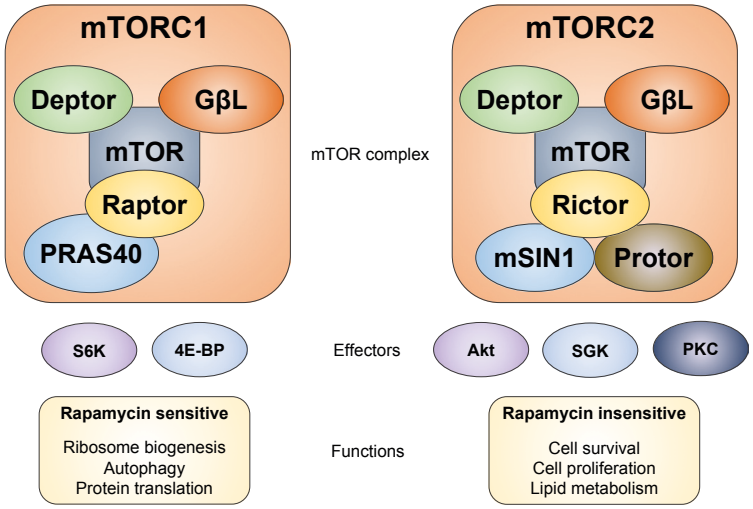

Figure 4 | Two distinct mTOR complexes.

mTOR is the common protein in two different complexes, mTORC1 and mTORC2. The first mTOR complex, mTORC1, contains Deptor, GβL, PRAS40 and Raptor. The second complex, mTORC2, contains Deptor, GβL, mSIN1, Protor and Rictor. Every complex has its own downstream effectors and hence specific functions.

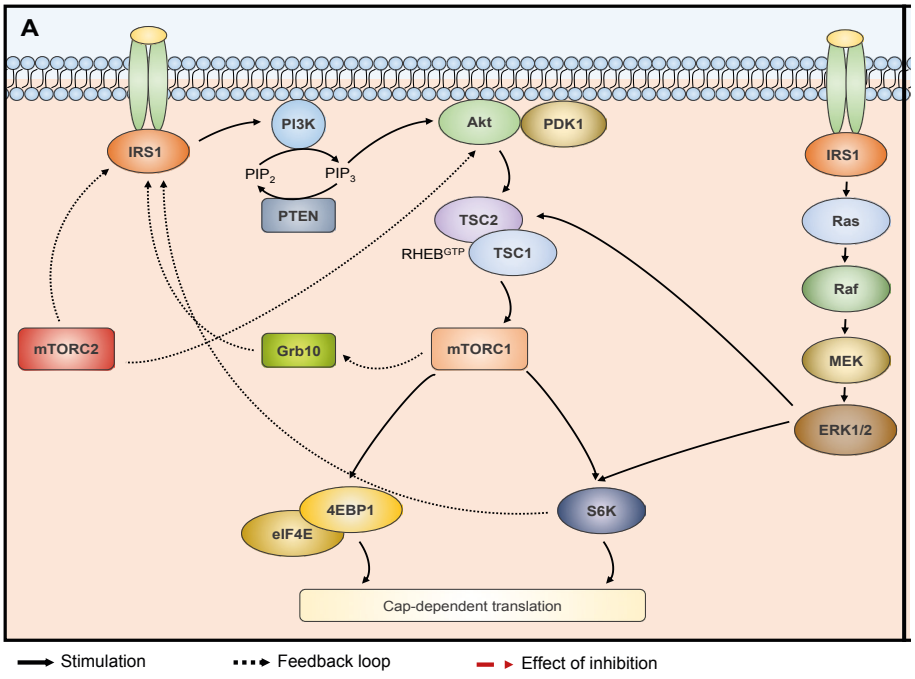

Figure 3 | PI3K/Akt/mTOR feedback circuits and mechanism of action of pharmacological compounds.

Negative feedback is depicted through black, dashed arrows. Effect of inhibitors is shown through red, dashed arrows. Panel A. The physiological feedback circuit of the PI3K/Akt/mTOR signaling. mTORC1 activity is modulated by Akt through tuberous sclerosis complex (TSC). TSC includes three proteins: Hamartin (TSC1), Tuberin (TSC2) and TBC1D792,93. TSC has a small GTPase-activating protein (GAP) activity and inhibits Ras homologue enriched in brain (RHEB) kinase. Phosphorylation of TSC2 by Akt, weakens its interaction with TSC1 and destabilizes TSC2. The phosphorylation relieves the TSC2 inhibition of RHEB and allows it to activate mTORC1 kinase activity. Simultaneously, Akt phosphorylates PRAS40 at Thr246, and mTORC1 phosphorylates

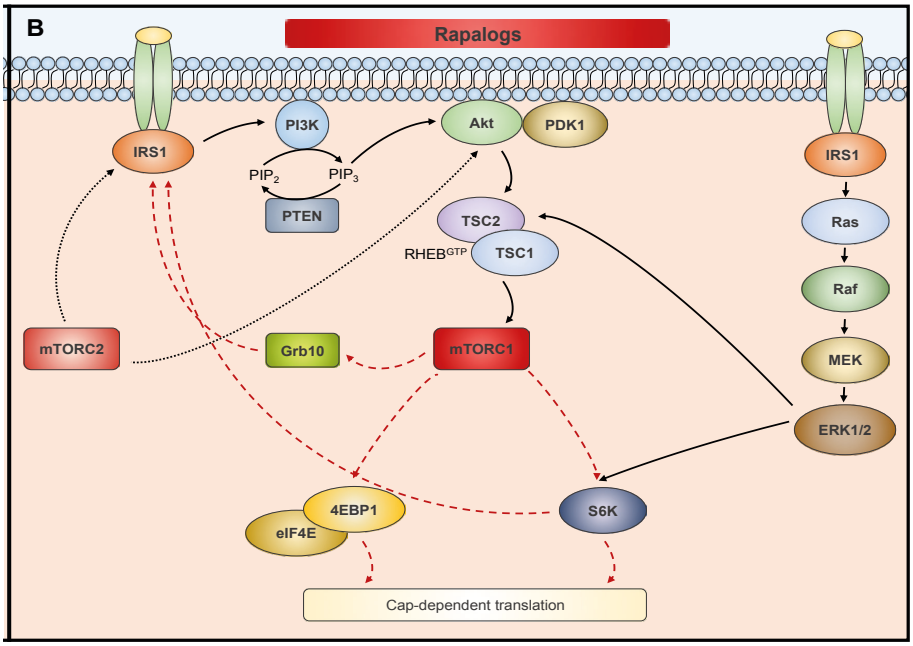

PRAS40 at Ser183 and Ser221, which induces its dissociation and loss of inhibition of mTORC194. The Ras-ERK-MAPK signaling pathway can activate mTORC1 by ERK-directed phosphorylation of TSC2 at Ser66495, or phosphorylation of S6 kinase 1 (S6K1), which in turn phosphorylates TSC2 at Ser179896. In addition, mTORC2 requires an intact TSC1/2 complex for activation by growth factors, as TSC1/2 associates with Rictor and activates mTORC2 independently of the GAP activity of TSC2 towards RHEB. A negative feedback on mTORC1 occurs through proteasomal degradation of insulin receptor substrate 1 and 2 (IRS1 and IRS2), through S6K1-dependent phosphorylation and through phosphorylation of growth factor receptor-bound protein 10 (Grb10)97–100. Panel B. Inhibition of mTORC1 by rapalogs.

Table 2 | Median progression free survival (mPFS) and overall survival (mOS) in RADIANT clinical trials evaluating everolimus in neuroendocrine neoplasms

Study	Phase	Year	Cohort	Treatment	mPFS (months)	mOS (months)
RADIANT-1	II	2010	160 progressive, chemo-resistant pNENs	Everolimus	9.7	24.9
				Everolimus + Octreotide LAR	16.7	NR
RADIANT-2	III	2011	429 advanced carcinoid tumors	Everolimus + Octreotide LAR	16.4	29.2
				Placebo + Octreotide LAR	11.3	35.2
RADIANT-3	III	2011	410 advanced pNENs	Everolimus	11	44
				Placebo	4.6	37.7
RADIANT-4	III	2016	302 advanced, well differentiated NENs	Everolimus vs placebo	11	NR
					3.9	NR

NR: not reported.

3. PI3K/AKT/MTOR SIGNALING IN NEUROENDOCRINE NEOPLASMS

In recent studies, alterations in genes and encoded products involved in the PI3K/Akt/mTOR signaling were linked in both familial and sporadic NEN cases. Familial NENs are more rare than sporadic ones and often have incomplete penetrance. These familial syndromes are caused by germline mutations in genes such as Neurofibromatosis (*NF1*), Von Hippel-Lindau (*VHL*), Multiple Endocrine Neoplasia-1 (*MEN1*), and Tuberous sclerosis (*TSC1/2*), which are involved in the PI3K/Akt/mTOR pathway[24] (Table 1). Sporadic NENs are more frequent and the tumors frequently harbor somatic mutations in genes associated to the PI3K/Akt/mTOR signaling. Next-generation sequencing (NGS) experiments revealed alterations in 14-29% of the pNEN patients having mutations in the mTOR pathway genes and 21-44% somatic inactivating mutations in *MEN1*[17,74] (Table 1). *PHLDA3*, a potent inhibitor of Akt activation, is inactivated by loss-of-heterozygosity in 72% of pNENs[75,76]. In addition, Scarpa and colleagues identified a gain-of-function gene fusion that indirectly activates mTORs kinase activity. In 3% of the examined pNENs, somatic Ewing Sarcoma Breakpoint Region 1 (*EWSR1*) fusion events with *BEND2* or *FLI-1* were detected[25]. Another structural variation includes the amplification of Persephin (*PSPN*) in 13% of the investigated samples[25]. PSPN binds the rearranged during transfection (RET) receptor and activates PI3K catalytic subunit alfa (PI3KCA)[77]. Abnormal activation of the mTOR signaling in pNEN is also driven by dysfunctional tyrosine

kinase receptors, such as EGFR, VEGFR, PDGFR, FGFR3 and IGF-1R, all activating the mTOR axis[78]. Most of the alterations have been associated with known oncogenes and tumor suppressors upstream of mTOR, eventually leading to an increase in mTOR activity. Nevertheless, there is evidence to suggest that mTOR's downstream effectors 4E-BPs and S6Ks are also altered in NENs. Gene expression profiling and immunohistochemistry (IHC) staining studies in pNENs have shown overexpression of mTOR in 67% and aberrant activation of Akt in 61%. In addition a positive correlation of mTOR downstream targets protein levels and phosphorylation status with clinicopathological variables and patient prognosis was found[16,79,80]. Loss or severe reduction of expression of negative regulatory components of mTOR signaling, such as TSC2 and PTEN, was observed in multiple independent pNEN studies[15,25,81]. TSC2 expression is lowered or absent in 35% of pNENs, in comparison to normal pancreatic islet cells. Similarly, PTEN expression is lost in 7-29% of pNENs. In another study involving 72 pNENs, PTEN expression levels were lowered or absent in 60% of the samples. TSC2 or PTEN levels in pNENs are of clinical relevance as both gene products correlate to a less favorable disease-free, progression-free and overall survival outcome[15]. More recently, the role of phosphorylated (p-)mTOR, the expression of somatostatin receptor 2A (SSTR2A) and insulin growth factor receptor 1 (IGF-1R) was evaluated via IHC staining as a prognostic marker in 64 GEP-NENs[82]. Low SSTR2A expression and higher p-mTOR levels were associated with advanced disease.

IV. RAPALOG THERAPY IN NEUROENDOCRINE NEOPLASMS

1. MECHANISM OF ACTION OF RAPALOGS

Rapalogs inhibit the mTORC1-dependent activation of S6K1/2 and 4E-BP1. These effectors regulate cap-dependent protein translation of key proteins involved in cell cycle progression, including cyclin D1, c-MYC and HIF-1α (Figure 1 and 2)[83]. Consequently, mTORC1-inhibitors suppress protein translation and growth of cells, limit cell progression through cell cycle G1-S phase inhibition, induce autophagy, modulate apoptotic processes and disrupt angiogenesis[14]. To inhibit mTORC1 activity, rapalogs bind to the intracellular FK506 binding protein 12 kDa (FKBP12). The FKBP12-rapalog complex binds to mTOR at the FRB domain[84,85]. Subsequently, this complex binding induces conformational changes and allosteric inhibition of mTOR, resulting in dissociation of raptor from mTOR in mTORC1[86]. The altered mTORC1 structure drastically reduces the accessibility of the catalytic cleft and reduces its kinase activity on downstream components including S6K1/2 and 4E-BP1 (Figure 4B). However, cell-type-specific treatment effects on phosphorylation status exist[87]. In addition, auto-phosphorylation of the Ser2481 mTOR residue is significantly reduced and further decreases the kinase activity[88]. In 2006, it has been shown that short-term rapalog therapy inhibits mTORC1, while mTORC2, assembled with rapalog-insensitive component Rictor, was not inhibited by short-

term treatment[89]. However, recent studies show that long-term rapamycin treatment inhibits both mTORC1 and mTORC2 as the FKBP12-rapalog complex directly binds mTOR under long-term treatment and prevents its assembly to the multi-protein mTOR complex[90,91].

2. CLINICAL TRIALS EVALUATING RAPALOG SAFETY AND EFFICACY IN NEUROENDOCRINE NEOPLASMS

In 2008, O'Donnell and colleagues have published the first phase I study evaluating the pharmacokinetic and pharmacodynamics of everolimus in patients with advanced solid tumors[101]. In the same year, Yao and colleagues have reported the first phase II study evaluating everolimus in NENs[102]. This study included 30 patients with carcinoids and 30 patients with pNENs, who were given a combination of octreotide-LAR and everolimus. Radiological response rates (RRs) were 17% and 27% with a progression free survival rate (PFS) of 63 and 50 weeks respectively. Patients treated with everolimus obtained a higher RR (30% versus 13%) and prolonged PFS (72 versus 50 weeks). In both groups, mOS was not reached by the end of the study.

Evidence for anti-proliferative activity of everolimus in advanced, non-functional NENs of the lung, pancreas and gastrointestinal tract has been obtained in four clinical trials, named the 'RAD001 In Advanced Neuroendocrine Tumors' (RADIANT) (Table 2). The first confirmatory phase-II study (RADIANT-1), evaluated everolimus alone or in combination with long-acting octreotide

in progressive chemo-resistant pNENs[103]. The first cohort (115 patients) received everolimus and the second cohort (45 patients) received long-acting octreotide and everolimus. The overall RR plus stabilization was higher with the combination (84% versus 77%) as was mPFS (16.7 versus 9.7 months). Two other phase-III trials with everolimus have been completed: RADIANT-2 studying the effect of everolimus and octreotide in advanced carcinoid tumors and the prospective RADIANT-3 in advanced pNENs[104]. The latter study compared best supportive care plus everolimus placebo in 410 patients. Two-hundred and seven patients were included in the everolimus stratum and 203 in the placebo stratum. Everolimus prolonged mPFS from 4.6 to 11 months and demonstrated a 65% risk reduction for progression compared with placebo. The rather limited mPFS of about 11 months could be explained by acquired resistance to everolimus in the subset of patients with pNENs.

The most recent study is the RADIANT-4 trial[105]. This randomized, double-blinded phase-III trial included 302 patients with advanced, well-differentiated NENs. In this study, patients received the best supportive care plus everolimus or placebo. Two-hundred and five patients were included in the everolimus stratum and 97 patients in the placebo stratum. The mPFS was 11 months in the everolimus treated group and 3.9 months in the placebo group. Everolimus was associated with a 52% RR for progression compared with placebo. Based upon these studies, everolimus has been approved in the treatment of advanced lung, pancreatic and gastro-intestinal NEN. However, primary and

acquired resistance to everolimus may limit their efficacy as single treatment modality[106,107]. Acquired resistance is the mechanism where patients that initially respond to everolimus and other rapalogs, later relapse and develop resistance, whereas primary resistance, e.g. patients that do not respond at all, can occur as well. Studies demonstrated a role for serum chromogranin A (CgA) and serum neuron-specific enolase (NSE) as a prognostic factor for progression-free and overall survival, but predictive biomarkers for everolimus in pNEN have yet to be identified[108,109]. By identifying these biomarkers, those patients benefiting most from everolimus treatment could be selected, maximizing treatment efficacy while minimizing treatment burden to the patient and treatment-associated costs to society. Next to predictive biomarkers, a better understanding of resistance mechanisms could facilitate the development of novel drugs and treatment strategies to overcome everolimus resistance

V. PRECLINICAL GEP-NEN MODELS

Preclinical GEP-NEN models have been used to elucidate novel drugs. Several rapalogs were first evaluated in two-dimensional (2D) cell culture models, such as BON-1 and QGP-1[112–115]. The BON-1 cell line was established in 1986 from a peripancreatic lymph node metastasis of a 28-year-old male with a pNEN[115]. In 1980, the QGP-1 cell line was developed from pancreatic NEN tumor tissue obtained from a 61-year-old male[116]. Both cell lines retain expression of typical neuroendocrine neoplasm markers, such as

synaptophysin and neuron-specific enolase[117]. Additionally, both cell lines secrete hormones, a pathognomonic characteristic of NENs. The BON-1 cell line secretes neurotensin, pancreastatin, chromogranin A, serotonin (5-HT), 5-hydroxytryptophan (5-HTP) and 5-hydroxyindoleactic acid (5-HIAA)[118]. The QGP-1 cell line is a 5HT-, somatostatin- and carcinoembryonic antigen (CEA)-secreting cell line[119,120]. To study GEP-NENs *in vivo*, different animal models have been developed. The most used rodent GEP-NEN model relies on the promotor of rat insulin gene2 (RIP), which drives the transgenic expression of simian virus 40 (SV40) large T antigen (Tag). In this RIP-Tag GEP-NEN model, β cell-specific, and exceptionally pancreatic polypeptide cell-specific, transgenic oncogene expression after activation of the insulin promotor drives tumorigenesis[121,122]. The most frequently used lineages are RIP-Tag2 and RIP-Tag5[121,123,124]. Patient-derived xenograft models (PDXs) have emerged as a preclinical tool, as these implanted human biopsy samples maintain the cellular and genetic context of the primary tumor[125–127]. Since zebrafish (*Danio rerio*) embryos have highly conserved angiogenesis signaling compared to mammals, they often function as acceptor organism in the PDX approach[128–131]. Vitale and colleagues established a novel angiogenesis NEN assay by xenotransplantation of human TT (medullary thyroid cancer) and DMS79 (small-cell lung carcinoma secreting ACTH) cells into zebrafish embryos[132]. Gaudenzi and colleagues also successfully developed GEP-NEN xenotransplantation models using cell lines from primary human tumor samples[133]. These experiments show that zebrafish can be a useful, high-throughput tool for screening novel compounds

for GEP-NEN treatment. Many insights in the pathophysiology of these GEP-NENs originate from research on pre-clinical models of these rare tumors. Despite its usefulness to evaluate novel therapies, results obtained in models cannot always be translated to the clinic. Hence, understanding of cell line and animal models is needed for preclinical research into treatment resistance. The advent of large-scale genomics techniques has made it possible to better understand the genetic make-up of clinical tumor samples and the corresponding pre-clinical cell line models for many cancer types[134,135]. However, until recently only limited data was available on the genetic constitution of BON-1 and QGP-1[136]. In addition, only limited data is available on the RNA expression profile in both cell lines. A whole transcriptome analysis may elucidate the role of BON-1 and QGP-1 as pNEN disease models.

VI. AIMS OF THIS THESIS

The aims of the studies in this thesis are:

1. To unravel the genetic constitution of pNEN cell lines
2. To provide further insight in the genetic heterogeneity in pNEN patient samples and to make a comparison with pNEN cell line models
3. To establish a pNEN cell model for long-term acquired everolimus resistance
4. To understand genetic and genomic changes in long-term acquired everolimus resistance
5. To overcome long-term acquired everolimus resistance using novel drugs

VI. OUTLINE OF THIS THESIS

Chapter 1 gives an overview of the current understanding of pNEN genetics and its prognostic implications, the role of the PI3K-Akt-mTOR pathway in pNEN, the establishment of everolimus as pNEN treatment and the importance of pNEN models in its development. In **chapter 2**, whole-exome sequencing provides insight in the genetics of the most-used pNEN cell lines, BON-1 and QGP-1. Ultra-deep sequencing of pNEN patient samples in **chapter 3** leads to the identification of low-frequency mutations in pNEN, which indicates genetic tumor heterogeneity and could have clinical implications. **Chapter 4** describes the establishment of the first long-term acquired everolimus resistance model in pNEN and demonstrates that this resistance can be overcome by novel PI3K-Akt-mTOR inhibitors. In **chapter 5** whole-genome sequencing of everolimus-resistant and everolimus-sensitive pNEN cel lines implicates cell cycle components in everolimus resistance. The first full transcriptomic profile of BON-1 and QGP-1 is presented in **chapter 6**. Additionally, in this chapter, mRNA expression changes after short-term everolimus exposure and in long-term everolimus resistance are described. Finally, **chapter** 7 and **chapter 8** provide a general discussion and summary of the presented data.

VII. REFERENCES

1. Schimmack, S., Svejda, B., Lawrence, B., Kidd, M. & Modlin, I. M. The diversity and commonalities of gastroenteropancreatic neuroendocrine tumors. *Langenbecks Arch Surg* **396**, 273–298 (2011).
2. Dasari, A. *et al.* Trends in the Incidence, Prevalence, and Survival Outcomes in Patients With Neuroendocrine Tumors in the United States. *JAMA Oncol.* **3**, 1335–1342 (2017).
3. Zerbi, A. *et al.* Surgical treatment of pancreatic endocrine tumours in Italy: results of a prospective multicentre study of 262 cases. *Langenbecks Arch Surg* **396**, 313–321 (2011).
4. Verbeke, C. S. Endocrine tumours of the pancreas. *Histopathology* **56**, 669–682 (2010).
5. Eriksson, B. & Öberg, K. Neuroendocrine tumours of the pancreas. *British Journal of Surgery* **87**, 129–131 (2000).
6. Yao, J. C. *et al.* One hundred years after 'carcinoid': epidemiology of and prognostic factors for neuroendocrine tumors in 35,825 cases in the United States. *J Clin Oncol* **26**, 3063–3072 (2008).
7. Kulke, M. H. *et al.* Neuroendocrine tumors, version 1.2015. *JNCCN J. Natl. Compr. Cancer Netw.* (2015). doi:10.6004/jnccn.2015.0011
8. Herrera-Martínez, A. D. *et al.* Targeted Systemic Treatment of Neuroendocrine Tumors: Current Options and Future Perspectives. *Drugs* (2019). doi:10.1007/s40265-018-1033-0
9. Hofland, L. J., Vandamme, T., Albertelli, M. & Ferone, D. Hormone and Receptor Candidates for Target and Biotherapy of Neuroendocrine Tumors. *Front. Horm. Res.* **44**, (2015).
10. VÉZINA, C., KUDELSKI, A. & SEHGAL, S. N. Rapamycin (AY-22,989), a new antifungal antibiotic. I. Taxonomy of the producing streptomycete and isolation of the active principle. *J. Antibiot. (Tokyo).* **28**, 721–726 (1975).
11. Sehgal, S. N., Baker, H. & Vézina, C. Rapamycin (AY-22,989), a new antifungal antibiotic. II. Fermentation, isolation and characterization. *J. Antibiot. (Tokyo).* **28**, 727–732 (1975).
12. BAKER, H., SIDOROWICZ, A., SEHGAL, S. N. & VÉZINA, C. Rapamycin (AY-

22,989), a new antifungal antibiotic. III. In vitro and in vivo evaluation. *J. Antibiot. (Tokyo).* **31**, 539–545 (1978).
13. Singh, K., Sun, S. & Vezina, C. Rapamycin (AY-22,989), a new antifungal antibiotic. IV. Mechanism of action. *J Antibiot* **32**, 630–645 (1979).
14. Saxton, R. A. & Sabatini, D. M. mTOR Signaling in Growth, Metabolism, and Disease. *Cell* **168**, 960–976 (2017).
15. Missiaglia, E. *et al.* Pancreatic endocrine tumors: Expression profiling evidences a role for AKT-mTOR pathway. *J. Clin. Oncol.* **28**, 245–255 (2010).
16. Kasajima, A. *et al.* mTOR expression and activity patterns in gastroenteropancreatic neuroendocrine tumours. *Endocr. Relat. Cancer* **18**, 181–192 (2011).
17. Jiao, Y. *et al.* DAXX/ATRX, MEN1, and mTOR pathway genes are frequently altered in pancreatic neuroendocrine tumors. *Science (80-.).* **331**, 1199–1203 (2011).
18. O'Shea, T. & Druce, M. When should genetic testing be performed in patients with neuroendocrine tumours? *Reviews in Endocrine and Metabolic Disorders* (2017). doi:10.1007/s11154-017-9430-3
19. Lemos, M. C. & Thakker, R. V. Multiple endocrine neoplasia type 1 (MEN1): Analysis of 1336 mutations reported in the first decade following identification of the gene. *Hum. Mutat.* (2008). doi:10.1002/humu.20605
20. Matkar, S., Thiel, A. & Hua, X. Menin: A scaffold protein that controls gene expression and cell signaling. *Trends in Biochemical Sciences* (2013). doi:10.1016/j.tibs.2013.05.005
21. Tsang, S. H. & Sharma, T. Von Hippel-Lindau disease. *Adv. Exp. Med. Biol.* **1085**, 201–203 (2018).
22. Pellegata, N. S. *et al.* Germ-line mutations in p27Kip1 cause a multiple endocrine neoplasia syndrome in rats and humans. *Proc. Natl. Acad. Sci. U. S. A.* **103**, 15558–63 (2006).
23. D., D. & A.B., G. Are neuroendocrine tumours a feature of tuberous sclerosis? A systematic review. *Endocr. Relat. Cancer* (2009). doi:10.1677/ERC-08-0142
24. Crona, J. & Skogseid, B. GEP- NETS UPDATE: Genetics of neuroendocrine tumors. *Eur. J. Endocrinol.* (2016). doi:10.1530/EJE-15-0972

25. Scarpa, A. *et al.* Whole-genome landscape of pancreatic neuroendocrine tumours. *Nature* **543**, 65–71 (2017).
26. Raj, N. *et al.* Real-Time Genomic Characterization of Metastatic Pancreatic Neuroendocrine Tumors Has Prognostic Implications and Identifies Potential Germline Actionability. *JCO Precis. Oncol.* (2018). doi:10.1200/po.17.00267
27. Nagano, Y. *et al.* Allelic alterations in pancreatic endocrine tumors identified by genome-wide single nucleotide polymorphism analysis. *Endocr. Relat. Cancer* (2007). doi:10.1677/ERC-06-0090
28. Zhuang, Z. *et al.* Somatic mutations of the MEN1 tumor suppressor gene in sporadic gastrinomas and insulinomas. *Cancer Res.* (1997).
29. Missiaglia, E. *et al.* Pancreatic endocrine tumors: expression profiling evidences a role for AKT-mTOR pathway. *J Clin Oncol* **28**, 245–255 (2010).
30. Lawrence, B. *et al.* Recurrent loss of heterozygosity correlates with clinical outcome in pancreatic neuroendocrine cancer. *npj Genomic Med.* (2018). doi:10.1038/s41525-018-0058-3
31. Cao, Y. *et al.* Whole exome sequencing of insulinoma reveals recurrent T372R mutations in YY1. *Nat. Commun.* (2013). doi:10.1038/ncomms3810
32. Cromer, M. K. *et al.* Neomorphic effects of recurrent somatic mutations in Yin Yang 1 in insulin-producing adenomas . *Proc. Natl. Acad. Sci.* (2015). doi:10.1073/pnas.1503696112
33. Lichtenauer, U. D. *et al.* Frequency and clinical correlates of somatic Ying Yang 1 mutations in sporadic insulinomas. *J. Clin. Endocrinol. Metab.* (2015). doi:10.1210/jc.2015-1100
34. Irshad, K. *et al.* T372R Mutation Status in Yin Yang 1 Gene in Insulinoma Patients. *Horm. Metab. Res.* (2017). doi:10.1055/s-0043-107244
35. Wang, H. *et al.* Insights into beta cell regeneration for diabetes via integration of molecular landscapes in human insulinomas. *Nat. Commun.* (2017). doi:10.1038/s41467-017-00992-9
36. Parekh, V. I. *et al.* Frequency and consequence of the recurrent YY1 p.T372R mutation in sporadic insulinomas. *Endocr. Relat. Cancer* (2018). doi:10.1530/erc-17-0311
37. Burrell, R. A., McGranahan, N., Bartek, J. & Swanton, C. The causes and consequences of genetic heterogeneity in cancer evolution. *Nature*

(2013). doi:10.1038/nature12625
38. Vitale, G. *et al.* Synergistic activity of everolimus and 5-aza-2'-deoxycytidine in medullary thyroid carcinoma cell lines. *Mol. Oncol.* (2017). doi:10.1002/1878-0261.12070
39. Pea, A. *et al.* Genetic Analysis of Small Well-differentiated Pancreatic Neuroendocrine Tumors Identifies Subgroups With Differing Risks of Liver Metastases. *Ann. Surg.* (2018). doi:10.1097/sla.0000000000003022
40. Yao, J. *et al.* Genomic profiling of NETs: A comprehensive analysis of the RADIANT trials. *Endocr. Relat. Cancer* (2018). doi:10.1530/ERC-18-0332
41. Marinoni, I. *et al.* Loss of DAXX and ATRX are associated with chromosome instability and reduced survival of patients with pancreatic neuroendocrine tumors. *Gastroenterology* **146**, 453–60 e5 (2014).
42. Hechtman, J. F. *et al.* Performance of DAXX Immunohistochemistry as a Screen for DAXX Mutations in Pancreatic Neuroendocrine Tumors. *Pancreas* (2019). doi:10.1097/MPA.0000000000001256
43. Lewis, P. W., Elsaesser, S. J., Noh, K. M., Stadler, S. C. & Allis, C. D. Daxx is an H3.3-specific histone chaperone and cooperates with ATRX in replication-independent chromatin assembly at telomeres. *Proc Natl Acad Sci U S A* **107**, 14075–14080 (2010).
44. Heaphy, C. M. *et al.* Prevalence of the alternative lengthening of telomeres telomere maintenance mechanism in human cancer subtypes. *Am. J. Pathol.* (2011). doi:10.1016/j.ajpath.2011.06.018
45. Heaphy, C. M. *et al.* Altered telomeres in tumors with ATRX and DAXX mutations. *Science* (2011). doi:10.1126/science.1207313
46. Kim, J. Y. *et al.* Alternative lengthening of telomeres in primary pancreatic neuroendocrine tumors is associated with aggressive clinical behavior and poor survival. *Clin. Cancer Res.* (2017). doi:10.1158/1078-0432.CCR-16-1147
47. Singhi, A. D. *et al.* Alternative lengthening of telomeres and loss of DAXX/ATRX expression predicts metastatic disease and poor survival in patients with pancreatic neuroendocrine tumors. *Clin. Cancer Res.* **23**, (2017).
48. De Wilde, R. F. *et al.* Loss of ATRX or DAXX expression and concomitant acquisition of the alternative lengthening of telomeres phenotype are late

events in a small subset of MEN-1 syndrome pancreatic neuroendocrine tumors. *Mod. Pathol.* (2012). doi:10.1038/modpathol.2012.53

49. Sato, S. *et al.* Impact of the tumor microenvironment in predicting postoperative hepatic recurrence of pancreatic neuroendocrine tumors. *Oncol. Rep.* (2014). doi:10.3892/or.2014.3530
50. Yuan, F. *et al.* KRAS and DAXX/ATRX gene mutations are correlated with the clinicopathological features, advanced diseases, And poor prognosis in Chinese patients with pancreatic neuroendocrine tumors. *Int. J. Biol. Sci.* **10**, 957–965 (2014).
51. Karpathakis, A. *et al.* Prognostic impact of novel molecular subtypes of small intestinal neuroendocrine tumor. *Clin. Cancer Res.* (2016). doi:10.1158/1078-0432.CCR-15-0373
52. Park, J. K. *et al.* DAXX/ATRX and MEN1 genes are strong prognostic markers in pancreatic neuroendocrine tumor. *Pancreatology* (2013). doi:10.1016/j.pan.2013.07.072
53. Chou, A. *et al.* ATRX loss is an independent predictor of poor survival in pancreatic neuroendocrine tumors. *Hum. Pathol.* (2018). doi:10.1016/j.humpath.2018.07.032
54. Cives, M. *et al.* Analysis of potential response predictors to capecitabine/temozolomide in metastatic pancreatic neuroendocrine tumors. *Endocr. Relat. Cancer* (2016). doi:10.1530/ERC-16-0147
55. Roy, S. *et al.* Loss of Chromatin-Remodeling Proteins and/or CDKN2A Associates With Metastasis of Pancreatic Neuroendocrine Tumors and Reduced Patient Survival Times. *Gastroenterology* (2018). doi:10.1053/j.gastro.2018.02.026
56. Thompson, S. L., Bakhoum, S. F. & Compton, D. A. Mechanisms of Chromosomal Instability. *Current Biology* (2010). doi:10.1016/j.cub.2010.01.034
57. Fruman, D. A. & Rommel, C. PI3K and cancer: Lessons, challenges and opportunities. *Nat. Rev. Drug Discov.* **13**, 140–156 (2014).
58. Thorpe, L. M., Yuzugullu, H. & Zhao, J. J. PI3K in cancer: Divergent roles of isoforms, modes of activation and therapeutic targeting. *Nature Reviews Cancer* **15**, 7–24 (2015).
59. Vanhaesebroeck, B., Stephens, L. & Hawkins, P. PI3K signalling: The path

to discovery and understanding. *Nature Reviews Molecular Cell Biology* **13**, 195–203 (2012).

60. Stokoe, D. *et al.* Dual role of phosphatidylinositol-3,4,5-trisphosphate in the activation of protein kinase B. *Science* **277**, 567–570 (1997).
61. Datta, S. R. *et al.* Akt phosphorylation of BAD couples survival signals to the cell- intrinsic death machinery. *Cell* **91**, 231–241 (1997).
62. Cross, D. a, Alessi, D. R., Cohen, P., Andjelkovich, M. & Hemmings, B. a. Inhibition of glycogen synthase kinase-3 by insulin mediated by protein kinase B. *Nature* **378**, 785–9 (1995).
63. Brunet, A. *et al.* Akt promotes cell survival by phosphorylating and inhibiting a forkhead transcription factor. *Cell* **96**, 857–868 (1999).
64. Zhou, B. P. *et al.* Cytoplasmic localization of p21 CIP1/WAF1 by Akt-induced phosphorylation in HER-2/neu-overexpressing cells. *Nat. Cell Biol.* **3**, 245–252 (2001).
65. Shin, I. *et al.* PKB/Akt mediates cell-cycle progression by phosphorylation of p27Kip1at threonine 157 and modulation of its cellular localization. *Nat. Med.* **8**, 1145–1152 (2002).
66. Gingras, A. C. *et al.* Hierarchical phosphorylation of the translation inhibitor 4E-BP1. *Genes Dev.* **15**, 2852–2864 (2001).
67. Ma, X. M. & Blenis, J. Molecular mechanisms of mTOR-mediated translational control. *Nature Reviews Molecular Cell Biology* **10**, 307–318 (2009).
68. Yang, Q., Inoki, K., Kim, E. & Guan, K.-L. TSC1/TSC2 and Rheb have different effects on TORC1 and TORC2 activity. *Proc. Natl. Acad. Sci.* **103**, 6811–6816 (2006).
69. Sarbassov, D. D., Guertin, D. A., Ali, S. M. & Sabatini, D. M. Phosphorylation and regulation of Akt/PKB by the rictor-mTOR complex. *Science (80-.).* **307**, 1098–1101 (2005).
70. Mori, S. *et al.* The mTOR pathway controls cell proliferation by regulating the FoxO3a transcription factor via SGK1 kinase. *PLoS One* **9**, (2014).
71. Sarbassov, D. D. *et al.* Rictor, a Novel Binding Partner of mTOR, Defines aRapamycin-Insensitive andRaptor-Independent Pathway that Regulates the Cytoskeleton. *Curr. Biol.* **14**, 1296–1302 (2004).
72. Arias, E. *et al.* Lysosomal mTORC2/PHLPP1/Akt Regulate Chaperone-

Mediated Autophagy. *Mol. Cell* **59**, 270–284 (2015).
73. Guri, Y. *et al.* mTORC2 Promotes Tumorigenesis via Lipid Synthesis. *Cancer Cell* **32**, 807-823.e12 (2017).
74. Vandamme, T. *et al.* Hotspot DAXX, PTCH2 and CYFIP2 mutations in pancreatic neuroendocrine neoplasms. *Endocr. Relat. Cancer* (2019). doi:10.1530/ERC-18-0120
75. Kawase, T. *et al.* PH Domain-Only Protein PHLDA3 Is a p53-Regulated Repressor of Akt. *Cell* **136**, 535–550 (2009).
76. Ohki, R. *et al.* PHLDA3 is a novel tumor suppressor of pancreatic neuroendocrine tumors. *Proc. Natl. Acad. Sci. U. S. A.* **111**, E2404-13 (2014).
77. Lindahl, M. *et al.* Human Glial Cell Line-derived Neurotrophic Factor Receptor α4 is the Receptor for Persephin and is Predominantly Expressed in Normal and Malignant Thyroid Medullary Cells. *J. Biol. Chem.* **276**, 9344–9351 (2001).
78. Capdevila, J. & Tabernero, J. A shining light in the darkness for the treatment of pancreatic neuroendocrine tumors. *Cancer Discovery* **1**, 213–221 (2011).
79. Ghayouri, M. *et al.* Activation of the serine/theronine protein kinase akt in enteropancreatic neuroendocrine tumors. *Anticancer Res.* **30**, 5063–5068 (2010).
80. Shida, T. *et al.* Expression of an activated mammalian target of rapamycin (mTOR) in gastroenteropancreatic neuroendocrine tumors. *Cancer Chemother. Pharmacol.* **65**, 889–893 (2010).
81. Perren, A. *et al.* Mutation and expression analyses reveal differential subcellular compartmentalization of PTEN in endocrine pancreatic tumors compared to normal islet cells. *Am. J. Pathol.* **157**, 1097–1103 (2000).
82. Lamberti, G. *et al.* Determination of Mammalian Target of Rapamycin Hyperactivation as Prognostic Factor in Well-Differentiated Neuroendocrine Tumors. *Gastroenterol. Res. Pract.* **2017**, (2017).
83. Faivre, S., Kroemer, G. & Raymond, E. Current development of mTOR inhibitors as anticancer agents. *Nat. Rev. Drug Discov.* **5**, 671–688 (2006).
84. Choi, J., Chen, J., Schreiber, S. L. & Clardy, J. Structure of the FKBP12-

Rapamycin Complex Interacting with Binding Domain of Human FRAP. *Science (80-.).* **273**, 239–242 (1996).

85. Chen, J., Zheng, X. F., Brown, E. J. & Schreiber, S. L. Identification of an 11-kDa FKBP12-rapamycin-binding domain within the 289-kDa FKBP12-rapamycin-associated protein and characterization of a critical serine residue. *Proc. Natl. Acad. Sci.* **92**, 4947–4951 (1995).
86. Oshiro, N. *et al.* Dissociation of raptor from mTOR is a mechanism of rapamycin-induced inhibition of mTOR function. *Genes to Cells* **9**, 359–366 (2004).
87. Choo, A. Y., Yoon, S.-O., Kim, S. G., Roux, P. P. & Blenis, J. Rapamycin differentially inhibits S6Ks and 4E-BP1 to mediate cell-type-specific repression of mRNA translation. *Proc. Natl. Acad. Sci.* **105**, 17414–17419 (2008).
88. Soliman, G. A. *et al.* mTOR Ser-2481 autophosphorylation monitors mTORC-specific catalytic activity and clarifies rapamycin mechanism of action. *J. Biol. Chem.* **285**, 7866–7879 (2010).
89. Jacinto, E. *et al.* Mammalian TOR complex 2 controls the actin cytoskeleton and is rapamycin insensitive. *Nat. Cell Biol.* **6**, 1122–1128 (2004).
90. Rosner, M. & Hengstschläger, M. Cytoplasmic and nuclear distribution of the protein complexes mTORC1 and mTORC2: Rapamycin triggers dephosphorylation and delocalization of the mTORC2 components rictor and sin1. *Hum. Mol. Genet.* **17**, 2934–2948 (2008).
91. Schreiber, K. H. *et al.* Rapamycin-mediated mTORC2 inhibition is determined by the relative expression of FK506-binding proteins. *Aging Cell* **14**, 265–273 (2015).
92. Inoki, K., Li, Y., Zhu, T., Wu, J. & Guan, K. L. TSC2 is phosphorylated and inhibited by Akt and suppresses mTOR signalling. *Nat. Cell Biol.* **4**, 648–657 (2002).
93. Dibble, C. C. *et al.* TBC1D7 Is a Third Subunit of the TSC1-TSC2 Complex Upstream of mTORC1. *Mol. Cell* **47**, 535–546 (2012).
94. Wang, H. *et al.* Proline-rich Akt substrate of 40kDa (PRAS40): A novel downstream target of PI3k/Akt signaling pathway. *Cellular Signalling* **24**, 17–24 (2012).

95. Ma, L., Chen, Z., Erdjument-Bromage, H., Tempst, P. & Pandolfi, P. P. Phosphorylation and functional inactivation of TSC2 by Erk: Implications for tuberous sclerosis and cancer pathogenesis. *Cell* **121**, 179–193 (2005).
96. Roux, P. P., Ballif, B. A., Anjum, R., Gygi, S. P. & Blenis, J. Tumor-promoting phorbol esters and activated Ras inactivate the tuberous sclerosis tumor suppressor complex via p90 ribosomal S6 kinase. *Proc. Natl. Acad. Sci.* **101**, 13489–13494 (2004).
97. Hsu, P. P. *et al.* The mTOR-regulated phosphoproteome reveals a mechanism of mTORC1-mediated inhibition of growth factor signaling. *Science (80-.).* **332**, 1317–1322 (2011).
98. Yu, Y. *et al.* Phosphoproteomic analysis identifies Grb10 as an mTORC1 substrate that negatively regulates insulin signaling. *Science* **332**, 1322–6 (2011).
99. Harrington, L. S. *et al.* The TSC1-2 tumor suppressor controls insulin-PI3K signaling via regulation of IRS proteins. *J. Cell Biol.* **166**, 213–223 (2004).
100. Shah, O. J., Wang, Z. & Hunter, T. Inappropriate activation of the TSC/Rheb/mTOR/S6K cassette induces IRS1/2 depletion, insulin resistance, and cell survival deficiencies. *Curr. Biol.* **14**, 1650–1656 (2004).
101. O'Donnell, A. *et al.* Phase I pharmacokinetic and pharmacodynamic study of the oral mammalian target of rapamycin inhibitor everolimus in patients with advanced solid tumors. *J. Clin. Oncol. Off. J. Am. Soc. Clin. Oncol.* **26**, 1588–1595 (2008).
102. Yao, J. C. *et al.* Efficacy of RAD001 (everolimus) and octreotide LAR in advanced low- to intermediate-grade neuroendocrine tumors: Results of a phase II study. *J. Clin. Oncol.* **26**, 4311–4318 (2008).
103. Yao, J. C. *et al.* Daily oral everolimus activity in patients with metastatic pancreatic neuroendocrine tumors after failure of cytotoxic chemotherapy: a phase II trial. *J. Clin. Oncol.* **28**, 69–76 (2010).
104. Yao, J. C. *et al.* Everolimus for advanced pancreatic neuroendocrine tumors. *N. Engl. J. Med.* **364**, 514–23 (2011).
105. Yao, J. C. *et al.* Everolimus for the treatment of advanced, non-functional neuroendocrine tumours of the lung or gastrointestinal tract (RADIANT-4): A randomised, placebo-controlled, phase 3 study. *Lancet*

387, 968–977 (2016).
106. Vandamme, T. *et al.* Long-term acquired everolimus resistance in pancreatic neuroendocrine tumours can be overcome with novel PI3K-AKT-mTOR inhibitors. *Br. J. Cancer* **114**, (2016).
107. Yao, J. C., Phan, A. T., Jehl, V., Shah, G. & Meric-Bernstam, F. Everolimus in advanced pancreatic neuroendocrine tumors: The clinical experience. *Cancer Research* **73**, 1449–1453 (2013).
108. Yao, J. C. *et al.* Everolimus for the treatment of advanced pancreatic neuroendocrine tumors: Overall survival and circulating biomarkers from the randomized, Phase III RADIANT-3 study. *J. Clin. Oncol.* (2016). doi:10.1200/JCO.2016.68.0702
109. van Adrichem, R. C. S. *et al.* Serum neuron-specific enolase level is an independent predictor of overall survival in patients with gastroenteropancreatic neuroendocrine tumors. *Ann. Oncol.* **27**, (2016).
110. Yao, J. C. *et al.* Everolimus for advanced pancreatic neuroendocrine tumors. *N Engl J Med* **364**, 514–523 (2011).
111. Yao, J. C. *et al.* Chromogranin A and neuron-specific enolase as prognostic markers in patients with advanced pNET treated with everolimus. *J Clin Endocrinol Metab* **96**, 3741–3749 (2011).
112. Vandamme, T. *et al.* Whole exome characterization of pancreatic neuroendocrine tumor cell lines BON-1 and QGP-1. *J. Mol. Endocrinol.* 1–37 (2015). doi:10.1530/JME-14-0304
113. Zitzmann, K. *et al.* Compensatory activation of Akt in response to mTOR and Raf inhibitors - A rationale for dual-targeted therapy approaches in neuroendocrine tumor disease. *Cancer Lett.* **295**, 100–109 (2010).
114. Arany, I., Rady, P., Evers, B. M., Tyring, S. K. & Townsend, C. M. Analysis of multiple molecular changes in human endocrine tumours. *Surg. Oncol.* **3**, 153–159 (1994).
115. Townsend Jr., C. M., Ishizuka, J. & Thompson, J. C. Studies of growth regulation in a neuroendocrine cell line. *Acta Oncol* **32**, 125–130 (1993).
116. Kaku, M., Nishiyama, T., Yagawa, K. & Abe, M. Establishment of a carcinoembryonic antigen-producing cell line from human pancreatic carcinoma. *Gann* **71**, 596–601 (1980).
117. Hofving, T. *et al.* The neuroendocrine phenotype, genomic profile and

therapeutic sensitivity of GEPNET cell lines. *Endocr. Relat. Cancer* (2018). doi:10.1530/ERC-17-0445

118. Parekh, D. *et al.* Characterization of a human pancreatic carcinoid in vitro: morphology, amine and peptide storage, and secretion. *Pancreas* **9**, 83–90 (1994).
119. Doihara, H. *et al.* QGP-1 cells release 5-HT via TRPA1 activation; a model of human enterochromaffin cells. *Mol Cell Biochem* **331**, 239–245 (2009).
120. Iguchi, H., Hayashi, I. & Kono, A. A somatostatin-secreting cell line established from a human pancreatic islet cell carcinoma (somatostatinoma): release experiment and immunohistochemical study. *Cancer Res* **50**, 3691–3693 (1990).
121. Hanahan, D. Heritable formation of pancreatic β-cell tumours in transgenic mice expressing recombinant insulin/simian virus 40 oncogenes. *Nature* (1985). doi:10.1038/315115a0
122. Power, R. F. *et al.* Transgenic mouse model: A new approach for the investigation of endocrine pancreatic B-cell growth. *Gut* (1987). doi:10.1136/gut.28.Suppl.121
123. Adams, T. E., Alpert, S. & Hanahan, D. Non-tolerance and autoantibodies to a transgenic self antigen expressed in pancreatic β cells. *Nature* (1987). doi:10.1038/325223a0
124. Onrust, S. V., Hartl, P. M., Rosen, S. D. & Hanahan, D. Modulation of L-selectin ligand expression during an immune response accompanying tumorigenesis in transgenic mice. *J. Clin. Invest.* (1996). doi:10.1172/JCI118406
125. Daniel, V. C. *et al.* A primary xenograft model of small-cell lung cancer reveals irreversible changes in gene expression imposed by culture in vitro. *Cancer Res.* (2009). doi:10.1158/0008-5472.CAN-08-4210
126. Ter Brugge, P. *et al.* Mechanisms of therapy resistance in patient-derived xenograft models of brca1-deficient breast cancer. *J. Natl. Cancer Inst.* (2016). doi:10.1093/jnci/djw148
127. Cottu, P. *et al.* Acquired resistance to endocrine treatments is associated with tumor-specific molecular changes in patient-derived luminal breast cancer xenografts. *Clin. Cancer Res.* (2014). doi:10.1158/1078-0432.CCR-13-3230

128. Tehrani, Z. & Lin, S. Endocrine pancreas development in zebrafish. *Cell Cycle* (2011). doi:10.4161/cc.10.20.17764
129. Hesselson, D., Anderson, R. M., Beinat, M. & Stainier, D. Y. R. Distinct populations of quiescent and proliferative pancreatic -cells identified by HOTcre mediated labeling. *Proc. Natl. Acad. Sci.* (2009). doi:10.1073/pnas.0906348106
130. Rovira, M. *et al.* Chemical screen identifies FDA-approved drugs and target pathways that induce precocious pancreatic endocrine differentiation. *Proc. Natl. Acad. Sci.* (2011). doi:10.1073/pnas.1113081108
131. Tobia, C., Gariano, G., De Sena, G. & Presta, M. Zebrafish embryo as a tool to study tumor/endothelial cell cross-talk. *Biochimica et Biophysica Acta - Molecular Basis of Disease* (2013). doi:10.1016/j.bbadis.2013.01.016
132. Vitale, G. *et al.* Zebrafish as an innovative model for neuroendocrine tumors. *Endocrine-Related Cancer* **21**, (2014).
133. Gaudenzi, G. *et al.* Patient-derived xenograft in zebrafish embryos: a new platform for translational research in neuroendocrine tumors. *Endocrine* **57**, 214–219 (2017).
134. Domcke, S., Sinha, R., Levine, D. A., Sander, C. & Schultz, N. Evaluating cell lines as tumour models by comparison of genomic profiles. *Nat. Commun.* (2013). doi:10.1038/ncomms3126
135. Gillet, J.-P., Varma, S. & Gottesman, M. M. The clinical relevance of cancer cell lines. *J. Natl. Cancer Inst.* (2013). doi:10.1093/jnci/djt007
136. Lopez, J. R. *et al.* Spectral karyotypic and comparative genomic analysis of the endocrine pancreatic tumor cell line BON-1. *Neuroendocrinology* **91**, 131–141 (2010).

Whole exome characterization of pancreatic neuroendocrine tumor cell lines BON-1 and QGP-1

Timon Vandamme[1,2,3], Marc Peeters[1], Fadime Dogan[2], Patrick Pauwels[4], Elvire Van Assche[3], Matthias Beyens[1,3], Geert Mortier[3], Geert Vandeweyer[3], Wouter de Herder[2], Guy Van Camp[3], Leo J. Hofland[2], Ken Op de Beeck[1,3].

[1]Department of Oncology, University of Antwerp, Universiteitsplein 1, 2610 Antwerp, Belgium
[2]Section of Endocrinology, Department of Internal Medicine, Erasmus Medical Center, Dr. Molenwaterplein 50, 3015GE Rotterdam, The Netherlands
[3]Center of Medical Genetics, University of Antwerp, Universiteitsplein 1, 2610 Antwerp, Belgium
[4]Department of Pathology, University of Antwerp, Universiteitsplein 1, 2610 Antwerp, Belgium

This chapter is based on the research article published in:

Journal of Molecular Endocrinology, 2015; 54(2):137-47. doi: 10.1530/JME-14-0304

I. ABSTRACT

The human BON-1 and QGP-1 cell lines are two frequently used models in pancreatic neuroendocrine tumor (PNET) research. Data on the whole-exome genetic constitution of these cell lines is largely lacking. This study presents the first whole-exome profile of the BON-1 and QGP-1 cell lines. Cell line identity was confirmed by short tandem repeat profiling. Using GTG-banding and CytoSNP-12v2 Beadchip array, cell line ploidy and chromosomal alterations were determined in BON-1 and QGP-1. The exome of both cell lines was sequenced on Ilumina's HiSeq next-generation sequencing (NGS) platform. Single nucleotide variants (SNVs) and insertions and deletions (indels) were called using the Genome Analysis ToolKit. SNVs were validated with Sanger sequencing. Ploidy of BON-1 and QGP-1 was 3 and 4 respectively, with long stretches of loss of heterozygosity across multiple chromosomes, which is associated with aggressive tumor behavior. In BON-1, 57 frameshift indels and 1725 possible protein-altering SNVs were called in the NGS data. In the QGP-1 cell line, 56 frameshift indels and 1095 SNVs were identified. ATRX, a PNET-associated gene, was mutated in both cell lines, while TSC2 contained a mutation in BON-1. NRAS showed a mutation in BON-1, while KRAS was mutated in QGP-1, implicating aberrations in the RAS pathway in both cell lines. Homozygous mutations in TP53 with possible loss of function were identified in both cell lines. Various MUC genes, implicated in cell signaling, lubrication and chemical barriers, which are frequently expressed in PNET tissue samples, showed

homozygous protein-altering SNVs in the BON-1 and QGP-1 cell lines.

II. INTRODUCTION

Pancreatic neuroendocrine tumors (PNETs) are malignant tumors likely arising from islet cells of the pancreas[1]. PNETs can secrete a variety of hormones including somatostatin, insulin, glucagon, serotonin and pancreatic polypeptide. The majority of PNETs however are non-secreting[2]. In the United States, the age-adjusted annual incidence of PNET is 0,32/100000 and the standardized prevalence is 5/100000, according to the Surveillance Epidemiology and End Results (SEER) data[2]. In PNET, surgical resection alone is often curative in early-stage disease, but 40% to 50% of PNET patients have advanced disease at the time of initial diagnosis or present with synchronous tumors[2]. Patients with advanced disease may suffer from complications of uncontrolled hormone secretion and usually succumb from these complications or tumor progression[3]. PNETs are associated with a number of inherited syndromes that are characterized by mutations in well-studied proto-oncogenes or tumor-suppressor genes. These include Multiple Endocrine Neoplasia types 1 and 2 (MEN1 & MEN2), von Hippel-Lindau disease (VHL) and tuberous sclerosis (TSC). However, the majority of PNETs occurs as sporadic tumors[4]. To allow *in vitro* study of PNET, the BON-1, QGP-1 and CM human cell lines have been developed. In 1980, Kaku et al. established the QGP-1 cell line from primary PNET tumor tissue

obtained from a 61-year-old male[5]. The BON-1 cell line was established by Townsend et al. in 1986 from a peripancreatic lymph node metastasis of a 28-year-old male with PNET[6]. In 1987, the CM cell line was established from the peritoneal ascites of a patient with pancreatic insuloma[7]. The BON-1 cell line secretes neurotensin, pancreastatin, chromogranin A, serotonin (5-HT), 5-hydroxytryptophan (5-HTP) and 5-hydroxyindoleactic acid (5-HIAA)[8]. The QGP-1 cell line is a 5HT-, somatatostatin- and carcinoembryonic antigen (CEA)-secreting cell line[9,10]. Although BON-1 and CM have been karyotyped[11,12], high-resolution whole exome genetic information on PNET cell lines is currently lacking. In this study, we present genetic profiles of two frequently used PNET cell line models, BON-1 and QGP-1, obtained using genome-wide single nucleotide polymorphisms (SNP) arrays and whole exome sequencing. These data could lead to better insights in PNET tumorigenesis and identification of interesting new targets for therapy.

III. MATERIAL AND METHODS

1. CELL CULTURE AND DNA ISOLATION

The QGP-1 cell line was purchased from the Japanese Collection of Research Bioresources Cell Bank (JRCB, Osaka, Japan). The BON-1 cell line was a kind gift from Dr. Townsend (University of Texas Medical Branch, Galveston, USA). Both cell lines were confirmed

as *Mycoplasma*-free using MycoAlert (Lonza, Verviers, Belgium). The BON-1 cell line was cultured in 1:1 mixture of Dulbecco`s Modified Eagle Medium (DMEM) and Ham's F-12K (Kaighn's) medium, supplemented with 10% (v/v) fetal calf serum (FCS), penicillin (1×10^5 units/L), fungizone (0,5 mg/L), and L-glutamine (2 mmol/L). The QGP-1 cell line was cultured in Roswell Park Memorial Institute (RPMI) 1640 medium, supplemented with 10% (v/v) FCS and penicillin-streptomycin (1×10^5 units/L). All cell lines were cultured in a humidified incubator at 5% CO_2 and 37º C. Media and supplements were obtained from Life Technologies (Invitrogen, Carlsbad, USA). DNA from BON-1 (passage number 9) and from QGP-1 (passage number 14) was isolated using the QIAamp DNA mini kit (Qiagen, Hilden, Germany), following manufacturer's instructions. The concentration of the isolated DNA was quantified using the Qubit 2.0 fluorometer with the dsDNA Broad Range Assay (Thermo Scientific, Waltham, MA, USA). A high molecular weight band was visible on DNA gel electrophoresis, excluding DNA degradation. Short tandem repeat profiling using the Powerplex kit (Promega, USA) of BON-1 and QGP-1 matched with data of the original group[13] and the JRCB database, respectively, thus confirming the cell lines' identity.

2. SNP ARRAY

BON-1 and QGP-1 DNA was hybridized on the CytoSNP-12v2 Beadchip array (Illumina, San Diego, USA), after whole genome amplification with the Infinium HD assay (Illumina, San Diego, USA) using 200 ng input DNA, according to manufacturer's

protocol. The array was scanned using the Illumina iScan (Illumina, San Diego, USA). Resulting scan data was imported, mapped and clustered in Illumina GenomeStudio software v2011.1 equipped with the genotyping module (version 1.9.4)(Illumina, San Diego, USA), before being exported for further analysis using allele-specific copy number analysis tumors (ASCAT)[14] with default parameters. ASCAT takes both aneuploidy of the tumor cells and non-aberrant cell infiltration into account when analyzing SNP array data. This allows identification of copy number variants, copy-number neutral events and loss of heterozygosity in non-diploid tumor samples, which cannot be picked up by non-corrected SNP array analysis algorithms.

3. PREPARATION OF METAPHASE SPREADS AND GTG-BANDING

Growth of BON-1 and QGP-1 cells in their respective medium was synchronized adding 100 nM 5-fluor-2-deoxyuridin and 4 µM uridine overnight followed by 10 µM thymidine after 15 hours. To prepare metaphase spreads, the synchronized cultures were arrested in mitosis by adding demecolcine (1 µg/ml) during 10 minutes at 37ºC. By incubating the cells in 75 µM KCl at 37ºC during 20 minutes, a hypotonic shock was applied after which the cells were fixed in methanol/acetic acid (3:1, v/v) and washed twice. Metaphase spreads on uncoated glass slides were air-dried and thermally aged during 1 hour at a temperature of 80-100 ºC. Giemsa-banding (GTG-banding) was executed using trypsin and eosin-polychromic-methylene blue solution (Leishman solution)

according to standard protocol[15]. Chromosomal abnormalities identified by GTG-banding in 20 metaphases were described according to the guidelines of the International System for Human Cytogenetic Nomenclature[16].

4. WHOLE EXOME SEQUENCING

Two micrograms of isolated BON-1 and QGP-1 DNA were fragmented using a focused-ultrasonicator (Covaris M220, Covaris, Woburn, USA) running following program: duty factor of 20%, peak power of 50 with 200 cycles per burst during 120 seconds. Next, all samples were prepared for exome sequencing using a TruSeq DNA Sample Preparation kit (Illumina, San Diego, USA) following the low-throughput, gel-free protocol according to manufacture's instructions. DNA exonic sequences were enriched using the Truseq Exome Enrichment Kit (Illumina, San Diego, USA) according to manufacturer's instructions. The enriched samples were hybridized and amplified on three lanes of a paired-end flow cell using Illumina's cBot (Illumina, San Diego, USA). Next, all samples were exome sequenced on Illumina's HiSeq 1500 (Illumina, San Diego, USA) platform.

5. QUALITY CONTROL AND DATA ANALYSIS OF WHOLE EXOME DATA

Raw sequencing reads were analyzed using an in-house developed Perl-based workflow. First, FastQC software (version 1.0) was used to assess quality of the raw data. Adapters and low quality bases

were trimmed using Cutadapt (version 1.2.1) and an in-house developed quality trimmer[17], respectively. Paired-end reads were then aligned to the human reference genome (hg19, NCBI Build 37) using Burrows-Wheeler Aligner (BWA mem, version 0.7.4)[18]. Picard (version 1.88) was used to mark and remove duplicates. Using the Genome Analysis ToolKit (GATK version 2.8.1)[19], insertions and deletions (indels) were realigned and recalibrated. Single nucleotide variants (SNVs) and insertions-deletions (indels) were called using GATK, annotated with ANNOVAR[20] and filtered using VariantDB[21] according to different criteria (Results section). Integrative Genomics Viewer (IGV, version 2.2.5) was used to visualize the reads[22]. Data were visualized using Circos software (version 0.66)[23] and made publicly available through European Nucleotide Archive (http://www.ebi.ac.uk/ena/data/view/PRJEB8223).

IV. RESULTS

1. DETERMINATION OF PLOIDY AND CHROMOSOMAL ABERRATIONS

The genotyping results of the CytoSNP-12v2 Beadchip array were analyzed using the ASCAT algorithm, allowing correction for non-diploidy in both cell lines samples. ASCAT estimated an average overall ploidy of 3 in BON-1 and 4 in QGP-1 (figure 1A-B). ASCAT analysis showed multiple allelic duplications and deletions across

the BON-1 and QGP-1 genome, resulting in frequent copy number variants (CNVs) and regions with loss of heterozygosity (LOH) (figure 1C-D). Long stretches of LOH were seen in chromosomes 1, 3, 4, 6, 9, 11, 17, 18, 22 and X in BON-1, while in QGP-1, LOH of nearly total chromosomes was observed in chromosomes 7, 8, 9, 13, 17, 21, 22 and X. These LOH stretches were also seen in our NGS data (see below). In the NGS data, LOH was defined as an average allelic fraction (AF) above 0,66 in BON-1 and above 0,75 in QGP-1, corresponding to the respective ploidy of 3 and 4 (figure 2). In order to confirm the ploidy calculations of ASCAT, we karyotyped both cell lines. GTG-banding results of BON-1 and QGP-1 were consistent with the results of the CytoSNP-12v2 Beadchip array. The BON-1 GTG-banding showed a near-triploïd karyotype with a modal chromosome number of 63. Extensive chromosomal rearrangements and multiple derivative chromosomes were observed (supplemental figure S1). This was in accordance with previous literature[12]. GTG-banding of the QGP-1 cell line, revealed a near-tetraploid karyotype with a modal chromosome number of 90 to 92, including multiple derivative chromosomes, thus confirming the ASCAT profile (supplemental figure S2).

2. DETECTION AND FILTERING OF SNVS

Whole exome resequencing of BON-1 generated 91,5 million reads, while sequencing of QGP-1 generated 107,6 million reads, Of these, 57,9% of the BON-1 reads and 59,1% of the QGP-1 reads were mapped by BWA on targets enriched by the TruSeq Exome Enrichment kit. The average base coverage for the target regions

was 68x and 81x for BON-1 and QGP-1 respectively, with 92,9% of these nucleotides in BON-1 and 93,9% in QGP-1 covered at least 10 times (figure 2). After indel realignment, the GATK Unified Genotyper was used for variant calling with adapted settings for polyploidic samples. Based upon the SNP array and GTG-banding result, a ploidy of 3 for BON-1 and 4 for QGP-1 was selected as input for the GATK Unified Genotyper. GATK Unified Genotyper detected 65.886 SNVs in BON-1 and 60.979 SNVs in QGP-1 before filtering steps were applied (figure 3). Using VariantDB, we filtered these SNVs for a combination of criteria to reduce the likelihood of false positive results (figure 3). All SNVs in snpEff non-coding regions were removed from further analysis[24]. To remove common SNPs, all variants present in the dbSNP137[25] and 1000 Genomes Project databases[26](Genomes Project, et al. 2010) with a minor allele frequency (MAF) higher than 0,05 were excluded. Filtering for RefSeq stoploss, stopgain and non-synonymous SNV[27] using VariantDB, led to the identification of 1725 potentially protein-altering SNVs in BON-1 and 1095 in QGP-1 (table 1).

Figure 1 | ASCAT profiles and their calculation.

ASCAT first determines the ploidy of the tumor cells and the fraction of aberrant cells (A-B, sunrise plots). This procedure evaluates the goodness of fit for a grid of possible values for both parameters (blue, good solutions; red, bad solutions). On the basis of this goodness of fit, the optimal solution is selected (green cross). The selected ploidy was 3 for BON-1 (A) and 4 for QGP-1 (B). Using the resulting tumor ploidy and aberrant cell fraction, an ASCAT profile was calculated (C-D, upper band), containing the allele-specific copy number of all assayed loci. Copy number is shown on the y axis vs. the genomic location on the x axis (green, allele with lowest copy number; red, allele with highest copy number). For illustrative purposes only, both lines are slightly shifted (red, down; green, up) such that they do not overlap. Only heterozygous SNPs are shown. Finally, for all aberrations found, an aberration reliability score was calculated (C-D, lower band).

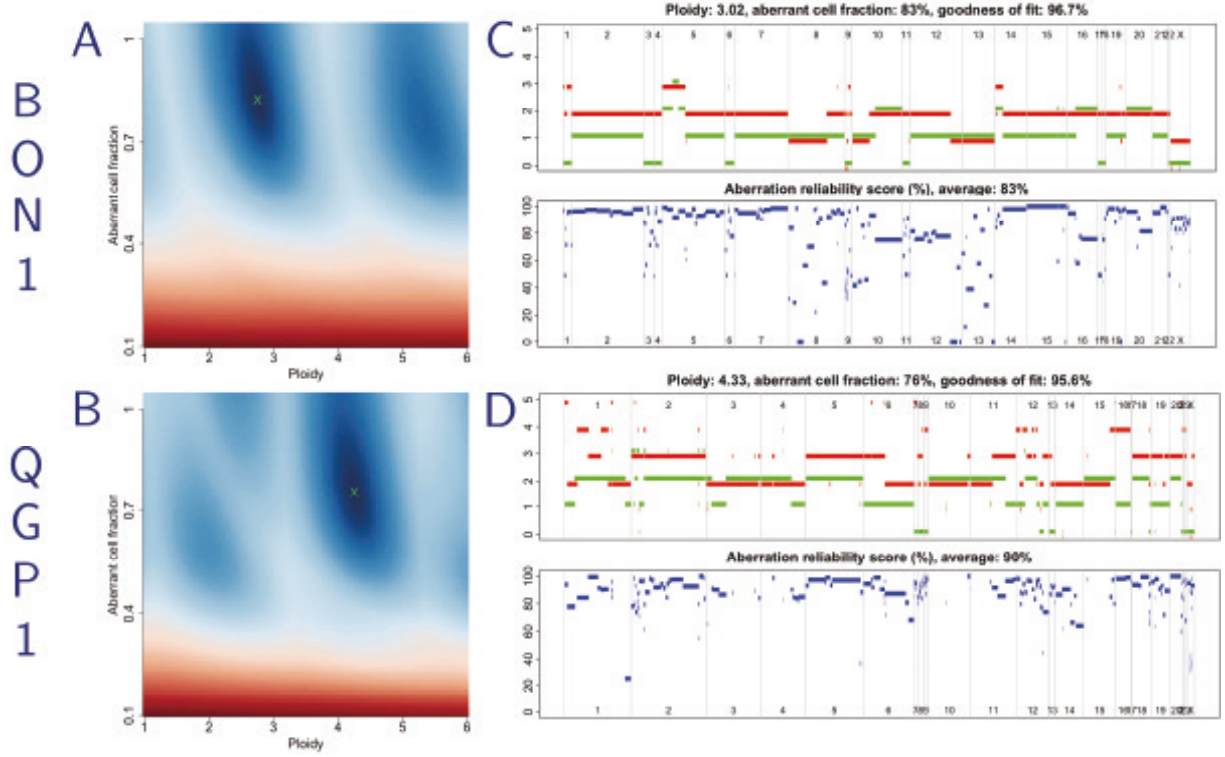
BON1
QGP1
A
B
C
D
Aberrant cell fraction
Ploidy
Ploidy: 3.02, aberrant cell fraction: 83%, goodness of fit: 96.7%
Aberration reliability score (%), average: 83%
Ploidy: 4.33, aberrant cell fraction: 76%, goodness of fit: 95.6%
Aberration reliability score (%), average: 90%

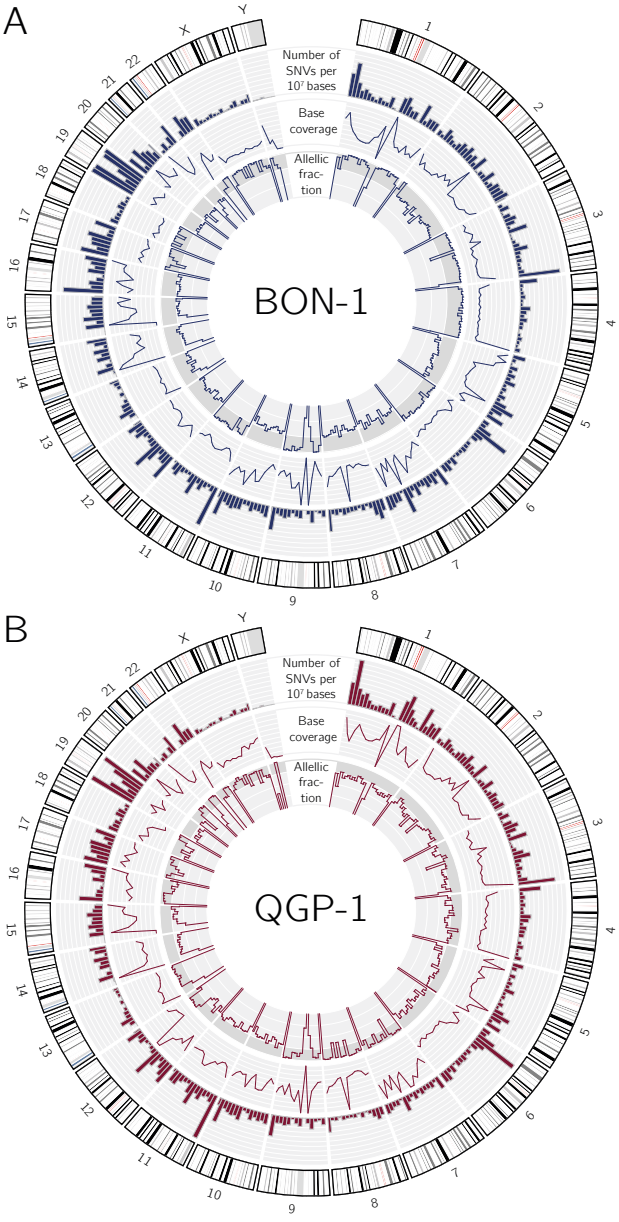
A
Number of SNVs per 10^7 bases
Base coverage
Allelic fraction
BON-1
B
Number of SNVs per 10^7 bases
Base coverage
Allelic fraction
QGP-1

Figure 2 | Circos plot of BON-1 and QGP-1.

Circos plot showing number of predicted SNVs per 10^7 bases (outer band, range 0-1000 SNVs/10^7 bases), base coverage (middle band, range 0-200 average base coverage over 10^7 bases) and allelic fraction of the found SNVs (inner band, range 0-100% of reads show SNV, darker grey background denotes homozygosity) across the genome in BON-1 (A) and QGP-1 (B).

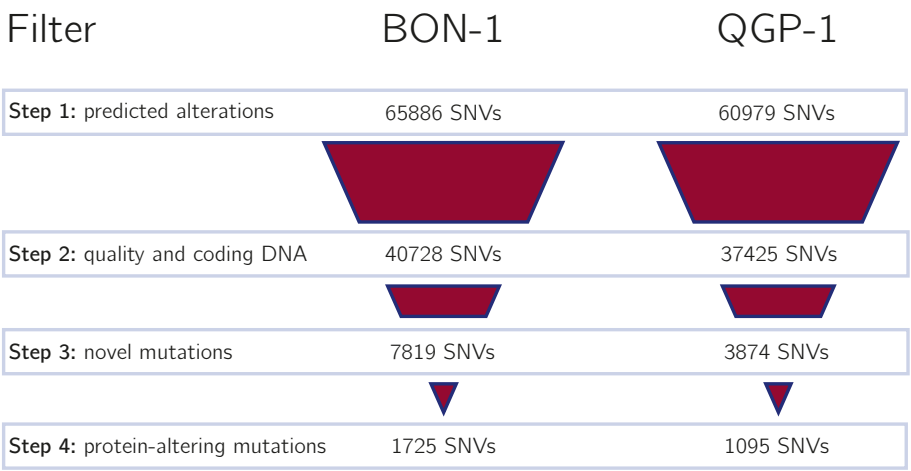

Figure 3 | Number of single nucleotide variants (SNVs) per filter step.

Quality and coding DNA: total reading depth ≥ 10, mapping quality ≥ 50, Fisher-Scaled Strand Bias ≤ 20, allelic ratio ≥ 0,1, Alternative allele-depth ≥ 2, snpEff annotation ≠ non-coding; Novel mutations: only SNVs with a MAF in NCBI dbSNP137 database < 0,05 and in the 1000 genomes 2012 < 0,05; Protein-altering mutations: RefSeq stopgain, stoploss and non-synonymous SNVs.

Table 1 | RefSeq variant type of filtered SNVs in BON-1 and QGP-1

Variant-type filtered SNVs	BON-1 (% of total)	QGP-1 (% of total)
Stopgain SNVs	33 (1,9)	26 (2,4)
Stoploss SNVs	3 (0,2)	1 (0,1)
Non-synonymous SNVs	1689 (97,9)	1068 (97,5)
All filtered SNVs	1725 *(100)*	1095 *(100)*

3. NUCLEOTIDE SUBSTITUTION FREQUENCIES

Both in BON-1 and QGP-1 the most frequent nucleotide substitutions are A <-> G or C <-> T transitions (figure 4). In BON-1, transitions made up 66,8% of the filtered SNVs, resulting in a two-fold overrepresentation of transitions compared to transversions. In QGP-1, transitions accounted for 64,7% of the filtered SNVs. The ratio of transitions to transversions was 1,8 for the filtered SNVs in QGP-1. Overall, the ratio of transitions to transversions is similar in BON-1 and QGP-1 and is higher than the average transitions to transversion rate of 1,7 that is usually seen in human germline samples[28]. A mutation spectrum with a predominant C to T/G to A transition pattern is seen in many adult cancers, including melanoma, breast, lung, colorectal, ovarian and pancreas adenocarcinoma[29,30]. However, in PNETs a more even distribution of transversions and transitions has been reported previously[31].

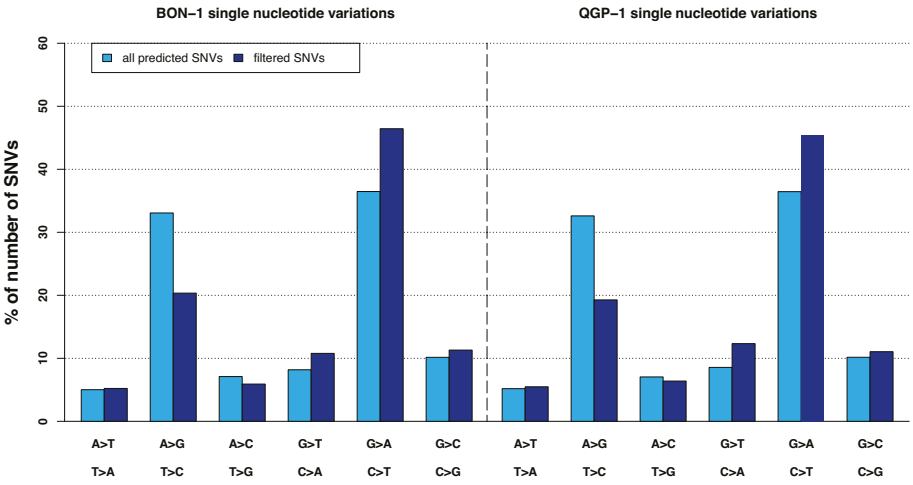

Figure 4 | Transition and transversion diagram.

Mutation spectrum of single nucleotide substitutions (SNVs) in BON-1 (left) and QGP-1 (right). Percentages of total number of predicted SNVs (light blue) and filtered SNVs (dark blue) in each of the six possible mutation classes.

4. DETECTION OF SMALL INSERTIONS AND DELETIONS

On the indel-realigned and BWA-mapped reads, insertions and deletions were called using the GATK Unified Genotyper with the ploidy-settings adjusted to 3 for BON-1 and 4 for QGP-1. Quality filtering was executed with VariantDB using similar criteria as for SNV filtering (figure 5). In BON-1, from the initial 2.923 predicted insertions and 3.194 predicted deletions, 20 insertions and 37 deletions were, after quality filtering, identified as RefSeq frameshift alterations, possibly leading to protein alterations. Of the initial 2.749 predicted insertions and 2.903 predicted deletions in QGP-1, 21 RefSeq frameshift insertions and 35 RefSeq

frameshift deletions remained after quality filtering.

5. PREDICTION OF PROTEIN FUNCTION IMPACT

To further identify SNVs with impact on protein function and a possible role in oncogenesis, an *in silico* prediction of the impact of protein function and structure was made by four different software packages: PolyPhen2, MutationTaster, SIFT and PROVEAN[32-35]. 61,5% of the filtered SNVs (1.061 SNVs) in BON-1 had a predicted impact on protein function by at least 1 of the 4 methods. In QGP-1, 67,2% of all filtered SNVs (736 SNVs) were predicted to be deleterious for protein function by at least 1 of

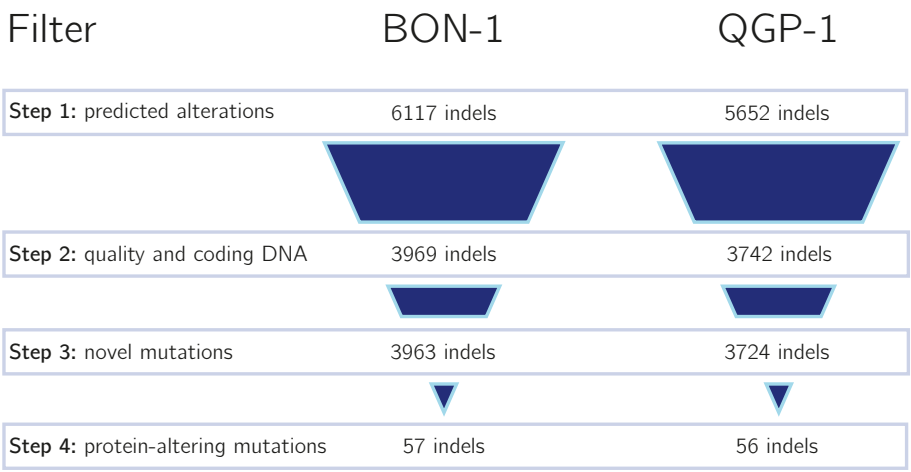

Figure 5 | Number of insertion-deletions (indels) per filter step.

Quality and coding DNA: total reading depth ≥ 10, mapping quality ≥ 50, Fisher-Scaled Strand Bias ≤ 20, allelic ratio ≥ 0,1, snpEff annotation ≠ non-coding, Alternative allele-depth ≥ 2; Novel mutations: only SNVs and indels with a MAF in NCBI dbSNP137 database > 0,05 and in the 1000 genomes 2012 >0,05; Protein-altering mutations: RefSeq frameshift indels.

the 4 used packages. However, only 137 SNVs (7,9% of all filtered SNVs) were predicted as deleterious by all four packages in BON-1, while 119 SNVs (10,8% of all filtered SNVs) in QGP-1 were predicted by all packages to have a deleterious impact on protein function. MutationTaster was used for protein impact prediction of frameshift indels in BON-1 and QGP-1. In BON-1 this resulted in 34 indels (59,6% of identified indels) with a predicted deleterious impact on protein function. In QGP-1 23 indels (41,0% of identified indels) were predicted to be deleterious for protein translation.

6. COMPARISON OF BON-1 AND QGP-1 EXOMES

When comparing the genomic positions of the identified SNVs and indels in BON-1 and QGP-1, 221 positions showed alterations in both QGP-1 and BON-1. On these 221 genomic positions, QGP-1 and BON-1 showed the same nucleotide alterations in 216 positions (97,7%) while on 5 positions a different nucleotide substitution, insertion or deletion in BON-1 and QGP-1 was seen. Of all the alterations found on these 221 genomic positions, 24 alterations were predicted by all four protein prediction programs to be damaging in QGP-1; while in BON-1, 25 alterations were predicted as protein-damaging. We aimed at elucidating underlying PNET pathways and mechanisms by comparing BON-1 and QGP-1, looking at alterations on different genomic positions but within the same gene in BON-1 and QGP-1. First a list of genes, containing SNVs or indels with a predicted damaging impact on protein function was created for BON-1 and QGP-1 separately. This resulted in a gene list containing 134 genes for BON-1 and

119 genes for QGP-1. When both list were combined, thirteen genes were identified that contained one or more mutations in both BON-1 and in QGP-1, including cancer-associated TP53 and CTBP2[36] (supplementary table 1).

7. GENETIC VALIDATION OF SNVS

Artifacts in next generation whole exome sequencing data could arise from different sources such as PCR-amplification-based enrichment, sequencing technology proper or even sample mix-up. As we used a stringent filtering strategy, the risk was minimized; although not fully excluded. Therefore, using Sanger sequencing, we validated a subset of twenty-two SNVs and four indels from genes that came up as mutated in BON-1 and QGP-1 (**table 2**). All SNVs and indels were confirmed by this technique. Although this represents only a small portion of all identified SNVs and indels, it illustrates the low level of sequencing artifacts in our filtered datasets.

V. DISCUSSION

1. OVERVIEW OF GENETIC ALTERATIONS

The presented extensive genetic analysis of the neuroendocrine tumor cell lines BON-1 and QGP-1 is the first study to combine karyotyping, SNP array and NGS whole exome data. In a previous study BON-1 was characterized using GTG-banding,

comparative genomic hybridization (CGH) and fluorescence in situ hybridization (FISH)[12]. These low-resolution methods only allowed studying large structural chromosomal alterations and copy number variations in a limited set of selected genes. SNVs cannot be identified by the methods applied in these studies. No data on the genetic constitution of QGP-1 is present in literature. Our study not only confirms previous findings in BON-1, but also adds new genotypic data using high-resolution methods. SNP array and NGS allow identification of small structural variations such as gene copy number variations and nucleotide changes such as SNVs and indels throughout the genome. For both BON-1 and QGP-1, this is the first time the genome is studied in this detail, leading to insights into the genetic origins of both cell lines and their neuroendocrine tumor characteristics. An important characteristic is the non-diploid nature of both cell lines. By using GTG-banding and a specialized ASCAT-algorithm for non-diploid SNP array data analysis, BON-1 could be accurately determined to be mainly triploid, which is in accordance to previous literature[12], and QGP to be mainly tetraploid. Adapting NGS variant calling algorithms to account for the non-diploidy made it possible to detect variants that were present in only one allele of the tri-allelic BON-1 or tetra-allelic QGP-1 cell line. The first whole exome data set of BON-1 and QGP-1 reveals a set of SNVs and indels that is not commonly present in the general population. This is shown by the fact that 16,1% of all filtered SNVs and indels in BON-1 and 35,7% in QGP-1 are not seen in the publicly available dbSNP137 and 1000 Genomes Project databases. Germline DNA of the originating patients was not available, so it cannot be excluded

that a minority of these variants are in fact rare germline SNPs that are not represented in these databases. However, given their predicted impact on protein function, we believe that the vast majority of filtered SNVs are not rare SNPs and, hence, might contribute to the tumorigenesis of pancreatic neuroendocrine tumors.

2. EXTENSIVE LOSS OF HETEROZYGOSITY IN BON-1 AND QGP-1

In QGP-1 as well as BON-1, the SNP array and NGS data showed an extensive LOH over multiple chromosomes. An increased frequency of LOH has been observed in 60 Caucasian human cancer cell lines derived from several organs including brain, central nervous system, colon, lung, white blood cell, melanocyte, ovary, prostate and kidney origin when compared with germline DNA of healthy subjects[37]. Additionally, LOH in germline DNA is more frequent in patients with different tumor types in comparison to healthy controls[38]. In a previous study, loss of *CDKN2A* and *CDKN2B* was identified in BON-1 through FISH[12]. The lack of reads in the NGS data at the respective *CDKN2A* and *CDKN2B* locus in BON-1, confirm these findings. *CDKN2A* and *CDKN2B* encode the tumor suppressors $p16^{INK4A}$ and $p14^{ARF}$, respectively and inactivation could lead to unrestrained cell growth[39]. No *CDKN2A* and *CDKN2B* alterations were found in QGP-1. In neuroendocrine tumors, a recent study has shown the importance of LOH of the *PHLDA3* gene on tumor progression and poor prognosis, in addition to existing evidence of the importance

of LOH of the *MEN1* gene on tumorigenesis[40,41]. Previous studies showed that *MEN1* expression was very low in BON-1 and that a reduction in growth was found when BON-1 was transfected with *MEN1*[42]. In the presented study, SNP array and NGS of BON-1 showed LOH of *MEN1*. Additionally, LOH of *PHLDA3* was observed in BON-1. In QGP-1, LOH was observed in *MEN1*, but not in *PHLDA3*. This difference illustrates that both cell lines might have other mechanisms causing their malignant transformation.

3. TP53 SHOWS LOSS OF FUNCTION MUTATIONS IN BON-1 AND QGP-1

p53 and associated proteins are important regulators of the cell cycle. In a previous study, exon 4 to exon 8 of *TP53* was Sanger sequenced in BON-1 and QGP-1. This limited sequencing experiment failed to identify any mutations[43]. However, in our NGS sequencing data, we found a homozygous (AF 99%) stopgain g.7574003A>G mutation (ENSP00000269305 p.R342X) in exon 10 of *TP53* in BON-1 and a homozygous (AF 100%) g.7579394delG frameshift deletion (ENSP00000391127 p.P98Lfs*25) in exon 4 in QGP-1. Both mutations were validated through Sanger sequencing and predicted to be damaging by all four prediction algorithms. The predicted loss of function of p53 in the cell lines is supported by the previously reported lack of p53 mRNA and protein expression on immunohistochemistry[43,44]. These findings imply that both cell lines, at least partially, might rely on inactivation of p53 to escape cell death.

4. MUTATIONS IN ATRX, RAS AND PI3K-AKT-MTOR PATHWAY GENES

Recent exome sequencing efforts of tumor material in sporadic PNET patients show frequent mutations in *ATRX, DAXX* and *MEN1*[31]. ATRX and DAXX form a complex that plays a role in the incorporation of histone variant H3.3 at the telomeres, acting as epigenetic regulators[45]. *MEN1* encodes menin, a nuclear protein important in chromatin remodeling and gene expression through histone acetylation and deacetylation[46]. Conflicting results on impact of ATRX/DAXX alterations have been found. In one study, *ATRX/DAXX* mutations correlated with a better survival in PNET patients with metastatic disease[31]. In other studies, with mainly early stage disease patients, loss of ATRX/DAXX expression was associated with a worse prognosis[47,48]. In BON-1, the *ATRX* gene contains a homozygous (AF 100%) g.77682471C>G missense mutation (ENSP00000362441 p.Q929E) and in QGP-1 a homozygous (AF 100%) g.77682716A>G missense mutation (ENSP00000362441 p.F847S) was seen. The real impact of both mutations on protein function is unknown, but all algorithms predicted them both to be benign. The *DAXX* gene contained no mutations in BON-1 and QGP-1, confirming the mutually exclusive nature of *DAXX/ATRX* mutations. Further functional studies are necessary to elucidate the role of the ATRX/DAXX pathway in BON-1 and QGP-1. Although in previous studies no *MEN1* mutation was identified in BON-1[42], our data showed a missense homozygous (AF 100%) g.64572018T>C *MEN1* SNP (ENSP00000377899 p.T546A) in both BON-1 and QGP-1. However, this SNP is benign according to the

ClinVar database and thus probably does not play a role in the malign transformation of the BON-1 and QGP-1 cells[49].

In a previous study, a homozygous mutation in *NRAS* codon 61 was identified in BON-1[44]. In our BON-1 data, a homozygous (AF 100%) g.114713908T>C mutation (ENSP00000358548 p.Q61R) was found in codon 61 of *NRAS*. Additionally, a heterozygous g.25245350C>A mutation (ENSP00000308495 p.G12V) with an allelic ratio of 0,71 was found in the *KRAS* gene in QGP-1. Both the *NRAS* mutation in BON-1 and the *KRAS* mutation in QGP-1 were predicted damaging by all four used prediction algorithms. A recent study shows that *KRAS* mutations are present in 10% of Chinese PNET patients and correlate with a poorer prognosis[47]. This might indicate a role of the RAS pathway in the oncogenesis of PNET.

The phosphoinositide-3-kinase/AKT/mammalian target of rapamycin (PI3K-AKT-mTOR) signaling pathway has been demonstrated to play a major role in NET by regulating cell growth, proliferation, survival and protein synthesis[50]. Hence, mTOR-inhibiting rapamycin and analogs (rapalogs) such as everolimus, have a role in NET therapy. A phase III trial showed an improved progression-free survival with everolimus in monotherapy in progressive advanced PNET[51]. However, in 15% of sporadic PNET mutations were found in PI3K-AKT-mTOR pathway related genes such as *PTEN*, *PI3KCA* and *TSC2*[31]. PI3K-AKT-mTOR pathway genes *PTEN* and *PI3KCA* showed no mutations in BON-1 and QGP-1. However, *TSC2* showed 3 missense mutations in BON-1, including a g.2083797G>A mutation (AF 0,63; ENSP00000344383 p.R1306H)

predicted to be damaging by SIFT. This pattern of mutations could point to a role of the *TSC2* and, thus, the PI3K-AKT-mTOR pathway in the neoplastic properties of the BON-1 cell line. Additionally, comparing BON-1, a cell line with a *TSC2* gene mutation and QGP-1, a cell line without mutations in the PI3K-AKT-mTOR pathway, could elucidate the importance of these mutations in the efficacy of mTOR-directed drugs. Having a model for PNET with and without PI3K-AKT-mTOR pathway mutations could also be helpful for drug-development of targeted agents.

5. MUCIN AS A POSSIBLE NEW BIOMARKER IN PNET

Mucins are high molecular weight glycoproteins with oligosaccharides attached to serine or threonine residues of the mucin core protein backbone by O-glycosidic linkages, which are produced by various epithelial cells and play a role in cell-cell interaction[52]. *MUC* genes are highly variable in humans and often contain novel and unique SNVs in germline samples. For this reason, *MUC* mutations are sometimes removed from further analysis in NGS data analysis. However, mucin overexpression has frequently been seen in PNET tumor samples[53,54]. Hence, this study looked into the presence and relevance of *MUC* gene alterations in BON-1 and QGP-1. *MUC4*, *MUC6*, *MUC16* and *MUC17* genes showed possible protein-altering mutations in both cell lines. Additionally, the *MUC2*, *MUC5B*, *MUC12* and *MUC13* genes show mutations with possible protein impact in BON-1. Further research is needed to fully understand the mechanisms that underlie the involvement of mucins in PNET.

In conclusion, the first high-resolution genetic profile of the BON-1 and QGP-1 cell lines, based on array-based techniques and next generation whole exome sequencing data, is presented in this article, greatly expanding on previous low-resolution genomic data for BON-1 and QGP-1 in literature. These frequently used PNET models show mutations in accordance with current literature on sporadic PNET in patients. However, further validation of BON-1 and QGP-1 as relevant genetic models for different subtypes of PNET in patients, is needed. We believe that our data could contribute to a better understanding of the pathogenesis of PNET.

VI. REFERENCES

1 Schimmack, S., Svejda, B., Lawrence, B., Kidd, M. & Modlin, I. M. The diversity and commonalities of gastroenteropancreatic neuroendocrine tumors. *Langenbeck's archives of surgery / Deutsche Gesellschaft fur Chirurgie* **396**, 273-298, doi:10.1007/s00423-011-0739-1 (2011).

2 Yao, J. C. *et al.* One hundred years after "carcinoid": epidemiology of and prognostic factors for neuroendocrine tumors in 35,825 cases in the United States. *J Clin Oncol* **26**, 3063-3072, doi:10.1200/JCO.2007.15.4377 (2008).

3 Kulke, M. H. *et al.* Future directions in the treatment of neuroendocrine tumors: consensus report of the National Cancer Institute Neuroendocrine Tumor clinical trials planning meeting. *J Clin Oncol* **29**, 934-943, doi:10.1200/JCO.2010.33.2056 (2011).

4 Leotlela, P. D., Jauch, A., Holtgreve-Grez, H. & Thakker, R. V. Genetics of neuroendocrine and carcinoid tumours. *Endocrine-related cancer* **10**, 437-450 (2003).

5 Kaku, M., Nishiyama, T., Yagawa, K. & Abe, M. Establishment of a carcinoembryonic antigen-producing cell line from human pancreatic carcinoma. *Gann* **71**, 596-601 (1980).

6 Townsend, C. M., Jr., Ishizuka, J. & Thompson, J. C. Studies of growth regulation in a neuroendocrine cell line. *Acta oncologica* **32**, 125-130 (1993).

7 Baroni, M. G. *et al.* Beta-cell gene expression and functional characterisation of the human insulinoma cell line CM. *The Journal of endocrinology* **161**, 59-68 (1999).

8 Parekh, D. *et al.* Characterization of a human pancreatic carcinoid in vitro: morphology, amine and peptide storage, and secretion. *Pancreas* **9**, 83-90 (1994).

9 Doihara, H. *et al.* QGP-1 cells release 5-HT via TRPA1 activation; a model of human enterochromaffin cells. *Molecular and cellular biochemistry* **331**, 239-245, doi:10.1007/s11010-009-0165-7 (2009).

10 Iguchi, H., Hayashi, I. & Kono, A. A somatostatin-secreting cell

line established from a human pancreatic islet cell carcinoma (somatostatinoma): release experiment and immunohistochemical study. *Cancer Res* **50**, 3691-3693 (1990).

11 Jonnakuty, C. & Gragnoli, C. Karyotype of the human insulinoma CM cell line--beta cell model in vitro? *Journal of cellular physiology* **213**, 661-662, doi:10.1002/jcp.21135 (2007).

12 Lopez, J. R. *et al.* Spectral karyotypic and comparative genomic analysis of the endocrine pancreatic tumor cell line BON-1. *Neuroendocrinology* **91**, 131-141, doi:10.1159/000254483 (2010).

13 Silva, S. R. *et al.* VEGFR-2 expression in carcinoid cancer cells and its role in tumor growth and metastasis. *International journal of cancer. Journal international du cancer* **128**, 1045-1056, doi:10.1002/ijc.25441 (2011).

14 Van Loo, P. *et al.* Allele-specific copy number analysis of tumors. *Proceedings of the National Academy of Sciences of the United States of America* **107**, 16910-16915, doi:10.1073/pnas.1009843107 (2010).

15 Seabright, M. A rapid banding technique for human chromosomes. *Lancet* **2**, 971-972 (1971).

16 Shaffer, L. G., McGowan-Jordan, J. & Schmid, M. *ISCN2013: An International System for Human Cytogenetic Nomenclature (2009): Recommendations of the International Standing Committee on Human Cytogenetic Nomenclature*. (Karger AG, 2009).

17 Helsmoortel, C. *et al.* Challenges and opportunities in the investigation of unexplained intellectual disability using family-based whole-exome sequencing. *Clinical genetics*, doi:10.1111/cge.12470 (2014).

18 Li, H. & Durbin, R. Fast and accurate short read alignment with Burrows-Wheeler transform. *Bioinformatics* **25**, 1754-1760, doi:10.1093/bioinformatics/btp324 (2009).

19 McKenna, A. *et al.* The Genome Analysis Toolkit: a MapReduce framework for analyzing next-generation DNA sequencing data. *Genome research* **20**, 1297-1303, doi:10.1101/gr.107524.110 (2010).

20 Wang, K., Li, M. & Hakonarson, H. ANNOVAR: functional annotation of genetic variants from high-throughput sequencing data. *Nucleic acids research* **38**, e164, doi:10.1093/nar/gkq603 (2010).

21 Vandeweyer, G., Van Laer, L., Loeys, B., Van Den Bulcke, T. & Kooy, R. F.

VariantDB: A flexible annotation and filtering portal for next generation sequencing data. (in press).

22 Thorvaldsdottir, H., Robinson, J. T. & Mesirov, J. P. Integrative Genomics Viewer (IGV): high-performance genomics data visualization and exploration. *Briefings in bioinformatics*, doi:10.1093/bib/bbs017 (2012).

23 Krzywinski, M. *et al.* Circos: an information aesthetic for comparative genomics. *Genome research* **19**, 1639-1645, doi:10.1101/gr.092759.109 (2009).

24 Cingolani, P. *et al.* A program for annotating and predicting the effects of single nucleotide polymorphisms, SnpEff: SNPs in the genome of Drosophila melanogaster strain w1118; iso-2; iso-3. *Fly* **6**, 80-92, doi:10.4161/fly.19695 (2012).

25 Sherry, S. T. *et al.* dbSNP: the NCBI database of genetic variation. *Nucleic acids research* **29**, 308-311 (2001).

26 Genomes Project, C. *et al.* A map of human genome variation from population-scale sequencing. *Nature* **467**, 1061-1073, doi:10.1038/nature09534 (2010).

27 Pruitt, K. D. *et al.* RefSeq: an update on mammalian reference sequences. *Nucleic acids research* **42**, D756-763, doi:10.1093/nar/gkt1114 (2014).

28 Lynch, M. Rate, molecular spectrum, and consequences of human mutation. *Proceedings of the National Academy of Sciences of the United States of America* **107**, 961-968, doi:10.1073/pnas.0912629107 (2010).

29 Jones, S. *et al.* Core signaling pathways in human pancreatic cancers revealed by global genomic analyses. *Science* **321**, 1801-1806, doi:10.1126/science.1164368 (2008).

30 Greenman, C. *et al.* Patterns of somatic mutation in human cancer genomes. *Nature* **446**, 153-158, doi:10.1038/nature05610 (2007).

31 Jiao, Y. *et al.* DAXX/ATRX, MEN1, and mTOR pathway genes are frequently altered in pancreatic neuroendocrine tumors. *Science* **331**, 1199-1203, doi:10.1126/science.1200609 (2011).

32 Adzhubei, I. A. *et al.* A method and server for predicting damaging missense mutations. *Nature methods* **7**, 248-249, doi:10.1038/nmeth0410-248 (2010).

33 Schwarz, J. M., Cooper, D. N., Schuelke, M. & Seelow, D. MutationTaster2: mutation prediction for the deep-sequencing age. *Nature methods* **11**, 361-362, doi:10.1038/nmeth.2890 (2014).

34 Choi, Y., Sims, G. E., Murphy, S., Miller, J. R. & Chan, A. P. Predicting the functional effect of amino acid substitutions and indels. *PloS one* **7**,

e46688, doi:10.1371/journal.pone.0046688 (2012).

35 Kumar, P., Henikoff, S. & Ng, P. C. Predicting the effects of coding non-synonymous variants on protein function using the SIFT algorithm. *Nature protocols* **4**, 1073-1081, doi:10.1038/nprot.2009.86 (2009).

36 Takayama, K. *et al.* CtBP2 modulates the androgen receptor to promote prostate cancer progression. *Cancer Res*, doi:10.1158/0008-5472.CAN-14-1030 (2014).

37 Ruan, X., Kocher, J. P., Pommier, Y., Liu, H. & Reinhold, W. C. Mass homozygotes accumulation in the NCI-60 cancer cell lines as compared to HapMap Trios, and relation to fragile site location. *PloS one* **7**, e31628, doi:10.1371/journal.pone.0031628 (2012).

38 Assie, G., LaFramboise, T., Platzer, P. & Eng, C. Frequency of germline genomic homozygosity associated with cancer cases. *JAMA : the journal of the American Medical Association* **299**, 1437-1445, doi:10.1001/jama.299.12.1437 (2008).

39 Rocco, J. W. & Sidransky, D. p16(MTS-1/CDKN2/INK4a) in cancer progression. *Experimental cell research* **264**, 42-55, doi:10.1006/excr.2000.5149 (2001).

40 Ohki, R. *et al.* PHLDA3 is a novel tumor suppressor of pancreatic neuroendocrine tumors. *Proceedings of the National Academy of Sciences of the United States of America* **111**, E2404-2413, doi:10.1073/pnas.1319962111 (2014).

41 Corbo, V. *et al.* MEN1 in pancreatic endocrine tumors: analysis of gene and protein status in 169 sporadic neoplasms reveals alterations in the vast majority of cases. *Endocrine-related cancer* **17**, 771-783, doi:10.1677/ERC-10-0028 (2010).

42 Stalberg, P. *et al.* Transfection of the multiple endocrine neoplasia type 1 gene to a human endocrine pancreatic tumor cell line inhibits cell growth and affects expression of JunD, delta-like protein 1/preadipocyte factor-1, proliferating cell nuclear antigen, and QM/Jif-1. *The Journal of clinical endocrinology and metabolism* **89**, 2326-2337, doi:10.1210/jc.2003-031228 (2004).

43 Bartz, C., Ziske, C., Wiedenmann, B. & Moelling, K. p53 tumour suppressor gene expression in pancreatic neuroendocrine tumour cells.

Gut **38**, 403-409 (1996).

44 Arany, I., Rady, P., Evers, B. M., Tyring, S. K. & Townsend, C. M., Jr. Analysis of multiple molecular changes in human endocrine tumours. *Surgical oncology* **3**, 153-159 (1994).

45 Lewis, P. W., Elsaesser, S. J., Noh, K. M., Stadler, S. C. & Allis, C. D. Daxx is an H3.3-specific histone chaperone and cooperates with ATRX in replication-independent chromatin assembly at telomeres. *Proceedings of the National Academy of Sciences of the United States of America* **107**, 14075-14080, doi:10.1073/pnas.1008850107 (2010).

46 Kim, H., Lee, J. E., Cho, E. J., Liu, J. O. & Youn, H. D. Menin, a tumor suppressor, represses JunD-mediated transcriptional activity by association with an mSin3A-histone deacetylase complex. *Cancer Res* **63**, 6135-6139 (2003).

47 Yuan, F. *et al.* KRAS and DAXX/ATRX Gene Mutations Are Correlated with the Clinicopathological Features, Advanced Diseases, and Poor Prognosis in Chinese Patients with Pancreatic Neuroendocrine Tumors. *International journal of biological sciences* **10**, 957-965, doi:10.7150/ijbs.9773 (2014).

48 Marinoni, I. *et al.* Loss of DAXX and ATRX are associated with chromosome instability and reduced survival of patients with pancreatic neuroendocrine tumors. *Gastroenterology* **146**, 453-460 e455, doi:10.1053/j.gastro.2013.10.020 (2014).

49 Landrum, M. J. *et al.* ClinVar: public archive of relationships among sequence variation and human phenotype. *Nucleic acids research* **42**, D980-985, doi:10.1093/nar/gkt1113 (2014).

50 Kasajima, A. *et al.* mTOR expression and activity patterns in gastroenteropancreatic neuroendocrine tumours. *Endocrine-related cancer* **18**, 181-192, doi:10.1677/ERC-10-0126 (2011).

51 Yao, J. C. *et al.* Everolimus for advanced pancreatic neuroendocrine tumors. *The New England journal of medicine* **364**, 514-523, doi:10.1056/NEJMoa1009290 (2011).

52 Yonezawa, S., Goto, M., Yamada, N., Higashi, M. & Nomoto, M. Expression profiles of MUC1, MUC2, and MUC4 mucins in human neoplasms and their relationship with biological behavior. *Proteomics* **8**, 3329-3341,

doi:10.1002/pmic.200800040 (2008).

53 Carrara, S. *et al.* Mucin expression pattern in pancreatic diseases: findings from EUS-guided fine-needle aspiration biopsies. *The American journal of gastroenterology* **106**, 1359-1363, doi:10.1038/ajg.2011.22 (2011).

54 Carr, J. C. *et al.* Overexpression of membrane proteins in primary and metastatic gastrointestinal neuroendocrine tumors. *Ann Surg Oncol* **20 Suppl 3**, S739-746, doi:10.1245/s10434-013-3318-6 (2013).

1. SUPPLEMENTARY TABLE 1 GENES MUTATED IN BOTH BON-1 AND QGP-1

Gene	Mutations in BON-1	Mutations in QGP-1
CNN2	g.1037781A>C	g.1037645delC
CROCC	g.17266395G>C	g.17250856T>C
CTBP2	g.126681824A>G	g.126686574T>G
	g.126683243T>C	g.126686577A>C
	g.126683244G>C	g.126686593C>G
	g.126686574T>G	g.126686646G>C
	g.126686577A>C	g.126686649C>G
	g.126686593C>G	g.126686656C>T
	g.126691926A>G	g.126686659A>G
	g.126692017C>G	g.126692017C>G
	g.126692019A>G	g.126692019A>G
	g.126692029T>G	
	g.126692039T>G	
FAM135A	g.71187020C>A	g.71187020C>A
FBXL14	g.1703090C>A	g.1703090C>A
HERC2	g.28501300A>C	g.28518046A>G
	g.28518046A>G	
HYDIN	g.70894087C>T	g.70894087C>T
	g.71098649C>T	g.70989335A>G
		g.71098649C>T
PABPC1	g.101717819G>A	g.101724924A>G
	g.101724924A>G	g.101724941T>C
	g.101724941T>C	g.101730335A>C
PABPC3	g.25672073A>G	g.25672073A>G
PIF1	g.65108864T>C	g.65113687G>A
TP53	g.7574003A>G	g.7579393delG
GPATCH4	g.156565049insAC	g.156565049insAC
CYFIP2	g.156721863insC	g.156721863insC

Supplementary figure 1 Short tandem repeat profile of BON-1

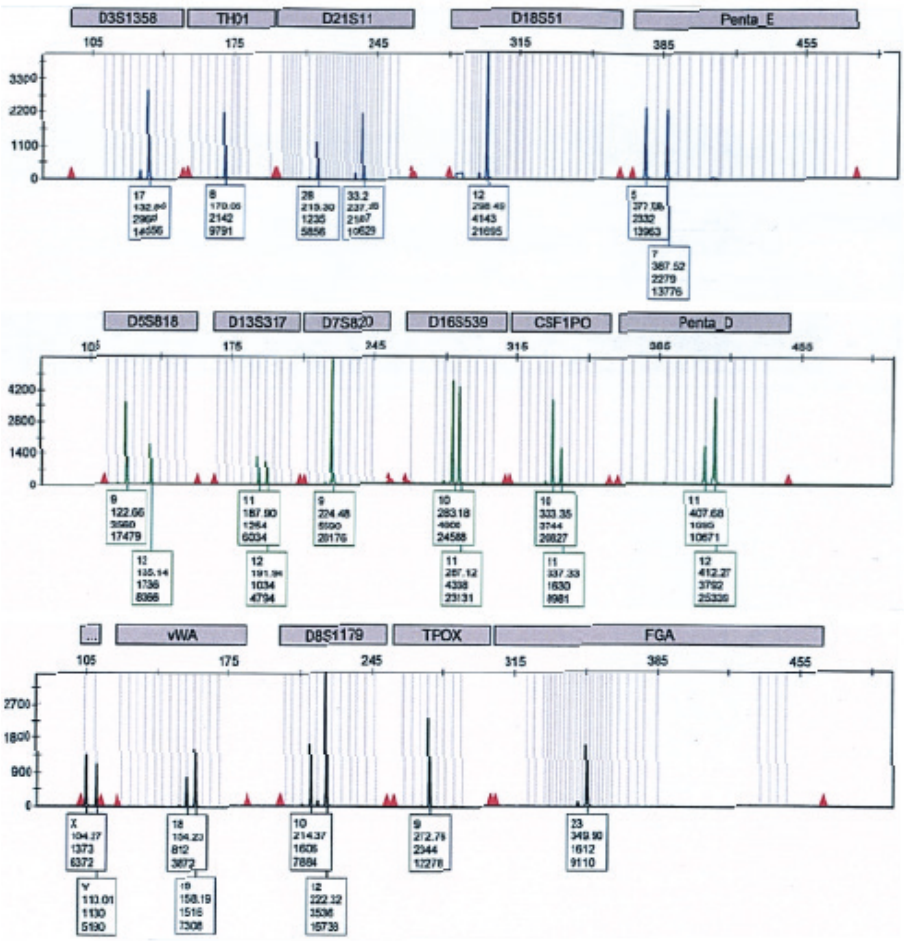

Supplementary figure 2 Short tandem repeat profile of QGP-1

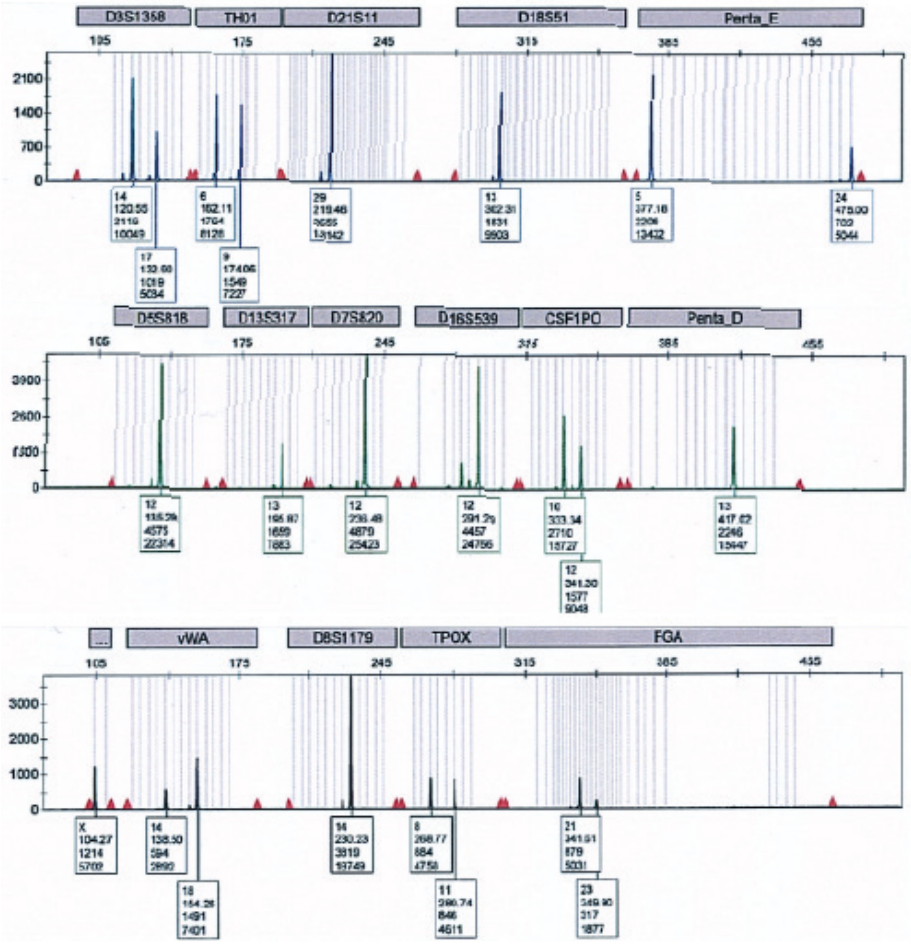

Hotspot DAXX, PTCH2 and CYFIP2 mutations in pancreatic neuroendocrine neoplasms

Timon Vandamme[1,2,*], Matthias Beyens[1,*], Boons Gitta[1], Anne Schepers[3], Kimberly Kamp[2], K Biermann[4], Patrick Pauwels[5], Wouter W. De Herder[2], Leo J. Hofland[2], Marc Peeters[1], Guy Van Camp[3] and Ken Op de Beeck[1]

[1]Department of Oncology, University of Antwerp, Antwerp, Belgium
[2]Section of Endocrinology, Department of Internal Medicine, Section of Endocrinology, Erasmus Medical Center, Rotterdam, The Netherlands
[3]Center of Medical Genetics, University of Antwerp, Belgium
[4]Department of Pathology, Erasmus Medical Center, Rotterdam, The Netherlands
[5]Department of Pathology, University of Antwerp, Belgium
* Equal contributing authors

This chapter is based on the research article published in:

Endocrine-Related Cancer 2019 Jan 1;26(1):1-12. doi: 10.1530/ERC-18-0120

I. ABSTRACT

Mutations in *DAXX/ATRX*, *MEN1*, and genes involved in the phosphoinositide-3-kinase/Akt/mammalian target of rapamycin (PI3K/Akt/mTOR) pathway have been implicated in pancreatic neuroendocrine neoplasms (pNENs). However, mainly mutations present in the majority of tumor cells have been identified, while proliferation-driving and therapy resistance-causing mutations could be present only in small fractions of the tumor. Formalin-fixed paraffin-embedded matched tumor-normal tissue of 38 well-differentiated neuroendocrine neoplasms was sequenced using a HaloPlex targeted resequencing panel. Novel amplicon-based algorithms were used to identify single nucleotide variants (SNVs) and insertion-deletions (Indels) both present >10% of reads (high-abundance) and in <10% of reads (low-abundance). Found variants were validated by Sanger sequencing. Sequencing resulted in 416,711,794 reads with an average target base coverage of 2663±1476. Across all samples, 32 high-abundance somatic, 3 germline and 30 low-abundance mutations were withheld after filtering and validation. Overall, 92% of high-abundance and 84% of low-abundance mutations were predicted protein-damaging. Frequently mutated genes were *MEN1*, *DAXX*, *ATRX*, *TSC2*, PI3K/Akt/mTOR and MAPK-ERK pathway-related genes. Additionally, recurrent alterations on same genomic position, so-called hotspot mutations, were found in *DAXX*, *PTCH2* and *CYFIP2*. This first ultra-deep sequencing study highlighted genetic intra-tumor heterogeneity in pNEN, by the presence of

low-abundance mutations. The importance of the *ATRX/DAXX* pathway was confirmed by the first-ever pNEN-specific protein-damaging hotspot mutation in *DAXX*. In this study, both novel genes, including the pro-apoptotic *CYFIP2* gene and hedgehog-signaling *PTCH2*, and novel pathways, such as the MAPK-ERK pathway, were implicated in pNEN.

II. INTRODUCTION

Neuroendocrine neoplasms of the pancreas (pNENs), originating from the islet cells, are considered rare, although incidence is increasing[1]. pNENs can occur as part of genetic syndromes, such as multiple neuroendocrine neoplasia 1 (MEN1), Von-Hippel Lindau (VHL) and tuberous sclerosis complex (TSC). However, most pNENs are sporadic tumors without familial history of NENs. Recently, non-familial pNENs haven been genetically characterized using whole-exome and whole-genome sequencing in large cohorts of 40 to 102 patients[2–4]. These studies identified *MEN1* as most frequently mutated gene, in frequencies ranging from 37% to 44% of all sequenced tumors. Additionally, *DAXX* was found to be mutated in 22% to 25% of all tumor samples, while *ATRX* was mutated in 10% to 17% of all tumors. Menin (the *MEN1* protein), DAXX, and ATRX are epigenetic regulators. Menin is involved in histone modification, while ATRX and DAXX play a role in alternative telomere lengthening and chromatin remodeling[5,6]. Additionally, mutations in genes involved in the phosphoinositide-3-kinase/Akt/mammalian target of rapamycin

(PI3K/Akt/mTOR) pathway were found in 12% to 14% of tumors[2,4]. In the pivotal Radiant-3 trial, treatment with everolimus, an mTOR inhibitor, has demonstrated an improved progression-free survival in advanced pNENs[7]. Hence, alterations in the PI3K/Akt/mTOR pathway, such as mutations in *PTEN*, could have clinical implications. However, no molecular predictive biomarker for everolimus treatment has yet been identified. Frequent tumor-specific copy number alterations in *MEN1*, *ATRX*, *DAXX* an PI3K/Akt/mTOR genes implicate these core pathways further[4]. Recent efforts to describe molecular subtypes, have led to the identification of five mutational signatures in pNEN, including the novel *MUTYH* signature[4]. However, in more than 50% of all tumors no dominant mutational signature could be identified[4]. RNA expression analysis revealed three expression subtypes, respectively the insulinoma, MEN-1-like/intermediate and metastasis-like (MLP) subtype[3,4]. Clinical utility of these expression subtypes is subject of further study, as expression subtypes show a variable association with tumor grade, mainly in WHO 2010 grade 1 and 2 tumors[3]. Moreover, within-patient and within-tumor heterogeneity in proliferation have been demonstrated in neuroendocrine neoplasm models and patients[8–10]. In recent pNEN sequencing studies, average sequencing depth was 61 to 102-fold[3,4]. Although covering all of the genome, these studies might lack sequencing power to reliably detect mutations present in a fraction of the cells, as these rare alleles might be present in less than 1 out of 61 to 102 averaged sequencing reads on a given genomic position. Therefore, current studies lack information on mutational heterogeneity. By increasing sequencing depth,

mutations, present in a fraction of cells, can be reliably identified[11]. This study is the first to use an ultra-deep targeted resequencing approach in pNENs to elucidate mutations, present in less than 10% of sequencing reads.

III. MATERIAL AND METHODS

1. SAMPLE COLLECTION AND CLINICAL DATA

Patients, diagnosed between 1997 and 2013 with a reported WHO 2010 grade 1 or 2 pancreatic neuroendocrine neoplasm were retrospectively included in this study[12]. Patients with a familial syndrome were excluded. Formalin-fixed paraffin-embedded (FFPE) samples of tumor and matched distant normal tissue, if available, of all patients was collected at the Erasmus Medical Center (Rotterdam, the Netherlands) and the Antwerp University Hospital (Antwerp, Belgium). All samples were reviewed by a dedicated pathologist for histology, Ki67 index, mitoses per high power field and tumor purity. Only samples with estimated tumor purity >60% on hematoxylin and eosin (H&E) stained histological slide, after macro-dissection, were included. Data on age, sex, TNM stage, age at diagnosis, secretion status, received treatments, disease-free survival and overall survival was collected. The study was approved by the institutional human ethics review board of the Antwerp University Hospital. Based on the opt-out registry to document the objection of patients to use excess tissue materials

for scientific research, none of the included patients had opposed ((as specified in Belgian and Dutch law).

2. TARGETED GENE PANEL DEVELOPMENT

A custom HaloPlex enrichment panel (Agilent Technologies, Santa Clara, CA, VS) was developed to sequence all exons of 20 genes (Table 1**)**. Genes were selected based upon patient and cell line sequencing results[2,13]. PI3K/Akt/mTOR pathway-related genes *MTOR, PTEN, PIK3CA* and *TSC2* mutations have been found in pNEN patients and could have therapeutic implications[2,4,14]. The gene panel was extended with the PI3K-related *PIK3C2A* gene, as it was found mutated in pNEN cell line data[10]. Epigenetic modifiers could play a role in pNEN, as demonstrated by *MEN1*, *ATRX* and *DAXX* mutations identified previously in pNEN[2,4]. Next to these genes, *KANSL1* and *PIF1*, two epigenetic modifiers found in pNEN cell line data, were included in the panel[10]. As pre-clinical data suggests a role for the MAPK/ERK pathway in pNEN, *KRAS, MAP4K2*, *MAPK9* and *MAPKBP1* were added to the panel[9,15]. The *SMAD4* gene has been found mutated in neuroendocrine neoplasms, both in patient material and in cell lines[10,16]. *TP53* and *CYFIP2* are two genes involved in apoptosis that are frequently implicated in oncogenesis. Both genes were found mutated in pNEN cell line data and were hence added to the panel[10]. Finally, the panel was extended with three genes (*KISS1, PTCH2, WNT1)* in known cancer-related pathways. All genes contained mutations in pNEN cell line data[10]. In our custom HaloPlex primer design, 99.59% of the 70,715 target kilobases of selected genes were covered by

RefSeq gene id	Encoded protein	Chromosomal position	Exons	Size (bp)	Coverage (%)
PI3K/AKT/mTOR pathway					
MTOR	Mechanistic target of rapamycin	chr1:11166651-11319476	60	9217	99.75
PIK3C2A	Phosphatidylinositol-4-phosphate 3-kinase catalytic subunit type 2 alpha	chr11:17111274-17191298	32	5705	100
PIK3CA	Phosphatidylinositol-4,5-bisphosphate 3-kinase catalytic subunit alpha	chr3:178916603-178952162	20	3609	99.5
PTEN	Phosphatase and tensin homolog	chr10:89624216-89725239	9	1392	100
TSC2	Tuberous sclerosis 2	chr16:2098260-2138621	43	6592	98.07
Transcription/chromatin remodeling					
ATRX	ATRX, chromatin remodeler	chrX:76763818-77041497	37	8299	99.92
*DAXX**	Death domain associated protein	chr6:33286509-33290701	8	2436	100
KANSL1	KAT8 regulatory NSL complex subunit 1	chr17:44108831-44249519	14	3598	100
MEN1	Menin 1	chr11:64571795-64577591	9	2028	100
PIF1	PIF1 5'-to-3' DNA helicase	chr15:65107879-65116544	13	2444	100
MAPK/ERK pathway					
KRAS	KRAS proto-oncogene, GTPase	chr12:25362718-25398328	6	828	100
MAP4K2	Mitogen-activated protein kinase kinase kinase 2	chr11:64556998-64570631	32	3103	100
MAPK9	Mitogen-activated protein kinase 9	chr5:179663373-179707571	14	1943	100
MAPKBP1	Mitogen-activated protein kinase binding protein 1	chr15:42067463-42117644	32	5461	100
p53 pathway					
CYFIP2	Cytoplasmic FMR1 Interacting Protein 2	chr5:156712361-156820018	34	4543	99.89
TP53	Tumor protein p53	chr17:7565246-7579922	14	1697	97.88
G protein–coupled receptor (GPCR) signaling pathway					
KISS1	KiSS-1 metastasis-suppressor	chr1:204159601-204162014	2	457	100
Hedgehog signaling pathway					
PTCH2	Patched 2	chr1:45286350-45308614	24	4171	100
TGF-β signaling pathway					
SMAD4	SMAD family member 4	chr18:48573406-48604847	13	1999	100
Wnt signaling pathway					
WNT1	Wnt family member 1	chr12:49372423-49375433	4	1193	100

developed primers. The primer design was optimized for use with FFPE material and for sequencing on Illumina technology with a read length of 150 base pairs by increasing the number of amplicons to 19,838.

Table 1.

List of genes (including encoded protein, chromosomal positions and number of exons) and the calculated coverage of the custom HaloPlex enrichment panel. * Multifunctional protein also associated with FAS signaling pathway.

3. DNA ISOLATION, HALOPLEX ENRICHMENT AND SEQUENCING

After macro-dissection, 10 slides of 5 µm of both tumor and normal tissue were used as input for DNA isolation using the QIAamp DNA FFPE Tissue Kit (Qiagen, Hilden, Germany), following manufacturer's instructions. The concentration of the isolated DNA was quantified using the Qubit 2.0 fluorometer with the dsDNA Broad Range Assay (Thermo Scientific, Wilmington, USA). To determine the amount of input DNA for HaloPlex enrichment, quality and degradation of the DNA were checked following the FFPE-Derived DNA Quality Assessment-protocol (Agilent Technologies, Santa Clara, CA, VS) using the LabChip GX (PerkinElmer, Waltham, MA, VS) with a High Sensitivity DNA kit (PerkinElmer, Waltham, MA, VS). Next, all tumor samples and three representative normal samples were prepared for targeted resequencing using a custom HaloPlex Design enrichment, optimized for FFPE sample enrichment, following the FFPE-optimized protocol according to manufacturer's instructions. The enriched samples were hybridized, amplified and sequenced on two lanes of a paired-end flow cell using HiSeq 1500 (Illumina, San Diego, USA) platform in rapid run mode.

4. READ ALIGNMENT, VARIANT CALLING AND FILTERING

Raw sequencing reads were analyzed using an in-house developed Perl-based workflow. First, FastQC software (version 1.0) was used to assess quality of the raw data[17]. Adapters and low-quality

bases were trimmed using Cutadapt (version 1.2.1) and an in-house developed paired-end read quality trimmer[18], respectively. Paired-end reads were then aligned to the human reference genome (hg19, NCBI Build 37) using Burrows-Wheeler Aligner (BWA mem, version 0.7.3a)[19]. Picard (version 1.88) was used to mark and remove duplicates[20]. Afterwards, the three aligned normals were merged using Samtools (version 0.1.18)[21]. After merging, somatic variant calling was performed on the tumor aligned data with VarScan2 (version 2.3.9) using the three merged normals as one merged normal[22]. Alignments with mapping quality lower than 17 or nucleotides with base quality lower than 17 were ignored. The max per-BAM depth was set on 30,000 avoiding excessive memory usage. No correction for tumor purity was set during the somatic calling, purities were kept on default (100%). The variant calling files were first filtered using pyAmpli to eliminate false positive variants introduced by amplicon-based enrichment[23]. All variants were annotated with ANNOVAR[24], and filtered using VariantDB[25] according to different criteria (Results section). Identified variants were validated in tumor and its matching normal tissue, if available, with Sanger sequencing on the 3130xl Genetic Analyser (Applied Biosystems Inc., Foster City, VS) platform and analyzed using CLC DNA Workbench v5 software (CLC Bio, Aarhus, Denmark). Data were visualized using the Maftools package[26] in R (version 3.3.3)[27]. Survival statistics were generated using the survival and survminer package for R (version 3.3.3)[27].

IV. RESULTS

1. PATIENT CHARACTERISTICS

Thirty-eight pNEN patients were included, of which 51% were male. Of the 38 included patients, 13 patients had a functional tumor (11 insulinomas, one gastrinoma and one glucagonoma). Mean age at diagnosis was 53 ± 14 years. Of all patients, 9 (16%) had metastatic disease at diagnosis (Supplementary Table S1). Tumor tissue was available for all included patients, while matched normal tissue was collected in 27 patients (71%). Twenty-four patients were diagnosed with WHO grade 1 disease, while 13 patients had a WHO grade 2 tumor. Upon central pathology review, one patient was reclassified as a WHO 2010 grade 3 tumor, given the Ki67 index of 30%. Median follow-up time was 6.3 years (range: 1.9-19.2 years). Median overall survival was 13 years [95% confidence interval 11 years – not reached].

2. GENETIC ALTERATIONS IN PANCREATIC NEUROENDOCRINE NEOPLASMS

Targeted resequencing of the selected HaloPlex enrichment 20-gene panel (see materials and methods) resulted in a total of 416,711,794 reads, passing quality filtering, across 38 tumor samples and three normal samples. Of all reads, an average 80.4 ± 5.0% mapped on target regions. Average target base coverage was 2663 ± 1476 and 94.7 ± 1.9% of all target bases was covered at

least 30 times. Using VarScan2, variants in the tumor were called against three merged normal samples. Afterwards, the amplicon-based filtering method pyAmpli was deployed to withhold only alterations present in more than one amplicon (if more than one amplicon was in the enrichment design)[23]. Additionally, all variants that were marked as "somatic" by VarScan2 were withheld. By this combined elimination, genetic alterations that are inherent to the enrichment with the HaloPlex-panel and, hence, appear in all amplicons across all samples, are removed as false-positive. Additionally, genetic alterations that are present in all three sequenced normal samples will most likely not be oncogenic driver mutations. Hence, these mutations can be discarded as common polymorphisms or artefacts when they are seen in the tumor samples. After this combined filtering, 17 indels and 2270 SNVs were withheld in the 38 tumors. The resulting median mutation burden of 0.80 per Megabase (Mb, range 0.51-1.54) within the 20 selected genes, with a genomic length of 70.71 Mb, is in line with the previously reported genome-wide mutation burden of 0.82 per Mb in pNEN and is low in comparison to other tumor types[4]. Given the similar mutation burden between the targeted sequencing panel and the previously reported whole-genome data, the 20 selected genes in our panel showed no enrichment for mutations in comparison to other genomic regions. Before further filtering, the median number of genetic alterations per tumor was 56 with the *MTOR* gene containing the most alterations (Figure 1). The most frequent nucleotide substitutions were C <-> T transitions (Figure 1). Across all samples, transitions made up 63.4% ± 2.3% of the filtered SNVs, resulting in a ratio of transitions to transversions

of 1.74 ± 0.18 in the presented gene panel. In human germline samples, an average transitions to transversion rate of 1.7 is usually seen genome-wide[28]. A genome-wide mutation spectrum with a predominant C to T/G to A transition pattern is seen in many adult cancers, including melanoma, breast, lung, colorectal, ovarian and pancreas adenocarcinoma[29,30]. However, in pNENs a more even distribution of transversions and transitions has been reported previously, in line with the data in this study[2].

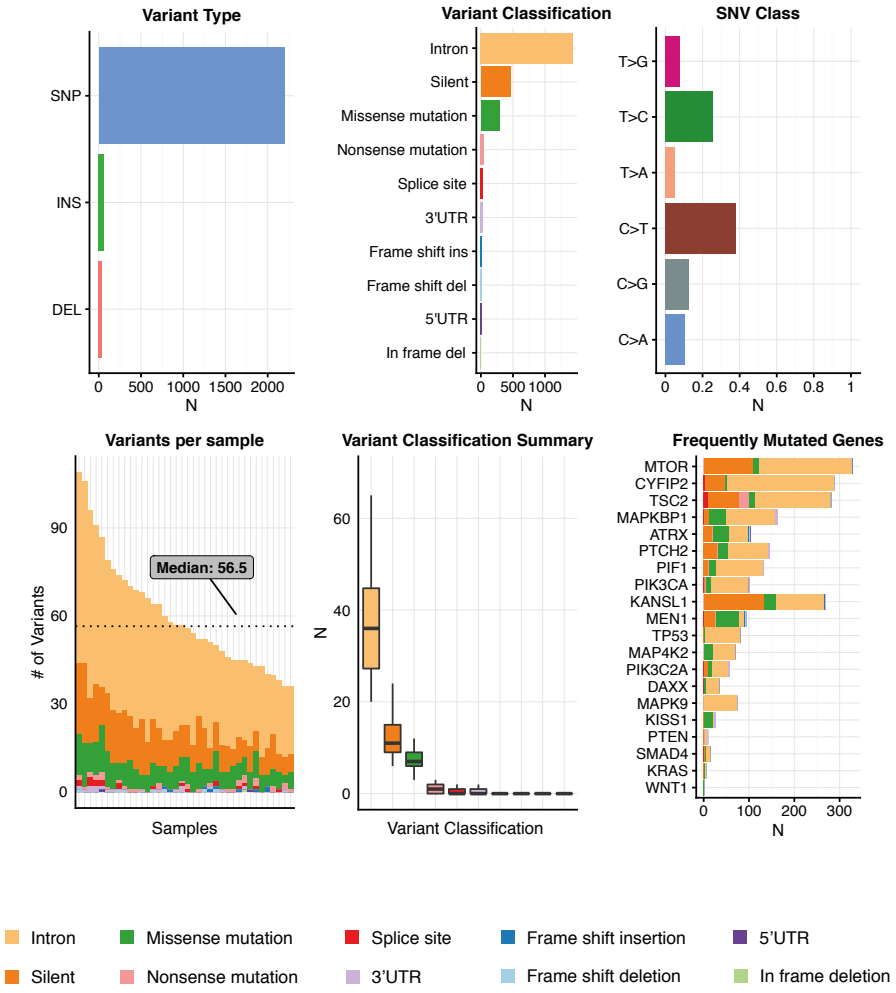

Figure 1 | Summary plot.

SNVs (N=2270), insertions (N=9) and deletions (N=8) of all 38 samples, after amplicon-based filtering.

3. IDENTIFICATION AND VALIDATION OF SOMATIC AND GERMLINE MUTATIONS

To identify mutations with possible functional impact, RefSeq synonymous as well as intronic SNVs and intronic indels were first removed from further analysis[31]. To eliminate common single nucleotide polymorphisms (SNPs), only variants with a minor allele frequency (MAF) smaller than 0.05 in the dbSNP v142, ESP65000 and 1000 Genomes databases were withheld[32,33]. Final visual inspection of all remaining variants in Integrative Genomics Viewer (IGV version 2.2.5), led to the identification of 72 mutations with possible functional impact (Figure 2)[34]. Of these 72 mutations, 42 alterations were identified in more than 10% of sequencing reads at that genomic position and were considered high-abundance alterations. These 42 alterations were Sanger sequenced in tumor tissue. Additionally, of 27 patients (71%) corresponding normal tissue was available, allowing Sanger sequencing of normal tissue for 22 mutations. Out of the 42 high-abundant variants, 35 were validated through Sanger sequencing, while 6 variants could not be detected in the Sanger electropherogram traces. For one variant, PCR amplification of the tumor DNA region containing the variant was unsuccessful, despite successful amplification in control DNA and use of different primers. Overall, 83.3% of all high-abundant variants could be validated (Supplementary Table S2). The 35 validated mutations contained three germline RefSeq non-synonymous variants, one in *MAPKBP1* and two in *PIF1* respectively, all unique in three different tumors. None of the mutations were

present in the cancer somatic mutation COSMIC v70 database (accession date: 12th April 2017), while two SNVs were reported in the dbSNP142 database with unknown clinical significance, respectively dbSNP142 rs139868280 (*PIF1*) and rs201725344 (*MAPKBP1*)[33,35]. The other *PIF1* chr15:g.65108822C>T mutation was not found in any of the queried databases, including ExAc (version 03), 1000 Genomes Project (October 2014), dbSNP142 and COSMIC v70[32,33,35,36].

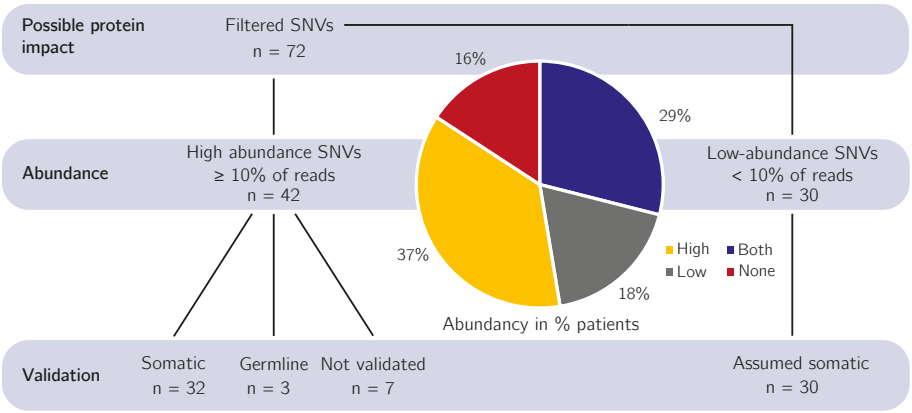

Figure 2 | Filter strategy and abundancy of mutations across tumors.

Filtered variants are SNVs or indels that are not RefSeq synonymous or intronic and have a minor allele frequency (MAF) ≤ 0.05 in dbSNP v142, ESP65000 and 1000 Genomes. Abundance is considered low for alterations found in <10% of targeted resequencing reads in tumor tissue and high when an alteration is present in ≥10% of targeted resequencing reads. Mutation are validated somatic when mutation is present in Sanger sequencing of tumor but not in normal (if available). Germline mutations are present in Sanger sequencing traces of both tumor and normal tissue. Not validated SNVs are those SNVs with absent Sanger traces or inconclusive results. All low-abundance SNVs or indels are assumed to be somatic. Pie-chart shows the percentage of patients whose tumors contained only low-abundance mutations (grey), only high-abundance mutations (yellow), both (red) or no mutations (blue).

4. ABUNDANT MUTATIONS INCLUDE A DAXX AND CYFIP2 HOTSPOT MUTATION

Of the 32 validated high-abundant somatic mutations, 21 SNVs were annotated as non-synonymous by RefSeq, 6 as frameshift indels, 3 as stopgain SNVs, 1 as SNV in the 3'-UTR and 1 as nonframeshift indel. The most commonly mutated genes were *MEN1*, *TSC2*, *DAXX*, *MAP4K2* and *PTCH2*, with four high-abundance mutations each, while three mutations were found in *ATRX*, *KANSL1* and *MAPKBP1*. These 8 genes accounted for 80% of all validated high-abundance mutations. No high-abundance mutations were found in *PIF1*, *PIK3CA*, *PTEN*, *MAPK9*, *KRAS* and *TP53*. Using variantDB, all variants were annotated for functional impact prediction using the MutationAssesor, MutationTaster, Provean and PolyPhen algorithms[25]. Of all variants, 92.0% was predicted damaging by at least one algorithm, while 36.0% was predicted damaging by at least 3 algorithms. Three mutations were also seen in other tumor types, according the COSMIC database[35]. Two recurrent, so-called hotspot, mutations were found, one in *CYFIP2* and one in *DAXX*. The *CYFIP2* non-synonymous variant g.156766140G>A (NM_001037333, p.D820N) was found in two pNEN tumors. This variant had previously been identified in skin squamous cell carcinoma, according to COSMIC, and was predicted to be damaging by MutationTaster and PROVEAN[37,38]. Within the *DAXX* gene, one genomic position was altered differently in two tumors, yielding the non-synonymous g.33289247G>A (NM_001141970.1, p.S102L) and the stopgain g.33289247G>T (NM_001141970.1, p.S102X) mutations. Both mutations were predicted damaging

by all used prediction algorithms, pointing towards a very likely *DAXX* loss-of-function in these tumors. The non-synonymous g.33289247G>A *DAXX* mutations has previously been found as a somatic mutation in one lung squamous cell carcinoma, according to COSMIC.

5. LOW-ABUNDANCE MUTATIONS CONTAIN A HOTSPOT MUTATION IN PTCH2

Next to high-abundance mutations, 30 mutations were found in less than 10% of targeted resequencing reads in tumor tissue. These mutations are considered low-abundance mutations. As the detection limit of Sanger sequencing is around 10%, these low-abundant alterations could not be Sanger sequenced[39]. However, the Sanger sequencing validation rate of 83% in the high-abundant mutations demonstrates that the used combined filtering strategy (see above) yields mainly true positives. Additionally, only 9% of validated mutations was present in corresponding normal samples, illustrating that the employed filtering strategy selects for somatic variants. Hence, we assume that most of the low-abundance mutations are also both valid and somatic. RefSeq annotated 21 of these 30 low-abundance mutations as non-synonymous SNVs, 4 as frameshift indels, 3 as stopgain SNVs, 1 as splicing SNV and 1 as SNV in the 3'-UTR. The 3'-UTR *PIK3C2A* g.17111197_17111198del was found in 3 tumors. In addition, 2 intronic variants were found, the *DAXX* g.33286734A>C which was seen in 8 pNENs, and the TSC2 g.2124481_2124482insG, identified in 5 tumors. However, functional impact of these intronic mutations remains

unclear. When predicting protein impact on the 30 exonic mutations with the MutationAssesor, MutationTaster, Provean and PolyPhen algorithms using variantDB, 84.0% of all SNVs was predicted damaging by at least one algorithm, while 52.0% was predicted damaging by three or more prediction algorithms[25]. After inclusion of the frameshift indels, which can be considered to have a deleterious impact on protein function, 86.6% of all mutations have a likely protein impact. Three mutations were previously found in cancer samples, according to the COSMIC database, including the non-synonymous *TP53* g.7578457C>T mutation (NM_001276695.1, p.R158H) which was identified in 36 tumors of various origin[35]. Two tumors contained the same stopgain g.45292871C>A mutation (NM_001166292, p.G828X) in *PTCH2*, predicted to be damaging by MutationTaster, PROVEAN and SIFT. This protein-damaging *PTCH2* mutation is hence a novel low-abundance hotspot mutation within pNEN.

6. MUTATIONAL SIGNATURES IN PNEN

In total, 32 tumors contained mutations while 6 tumors had no mutations that survived filtering (Figure 3). Both low-abundance and high-abundance mutations were seen in 11 tumors (29%). High-abundance mutations were seen exclusively in 14 tumors (37%), while 7 tumors (18%) only contained low-abundance mutations (Figure 2). *MEN1* was mutated most frequently in 8 out of 38 tumors (21%). *DAXX* and *ATRX* were both mutated in 5 out of 38 tumors (13%). The PI3K/Akt/mTOR-related gene *TSC2* was mutated in 7 out of 38 tumors (18%). Overall, mutations in

PI3K/Akt/mTOR-related genes were seen in 29% of the tumors, including a validated non-synonymous g.1308007C>T mutation in *MTOR* (NM_004958, p.A329T, rs35903812) not previously reported in pNEN. The mitogen-activated kinase and extracellular signal-regulated kinase (MAPK-ERK pathway) genes *MAP4K2* and *MAPKBP1* were each mutated in three tumors.

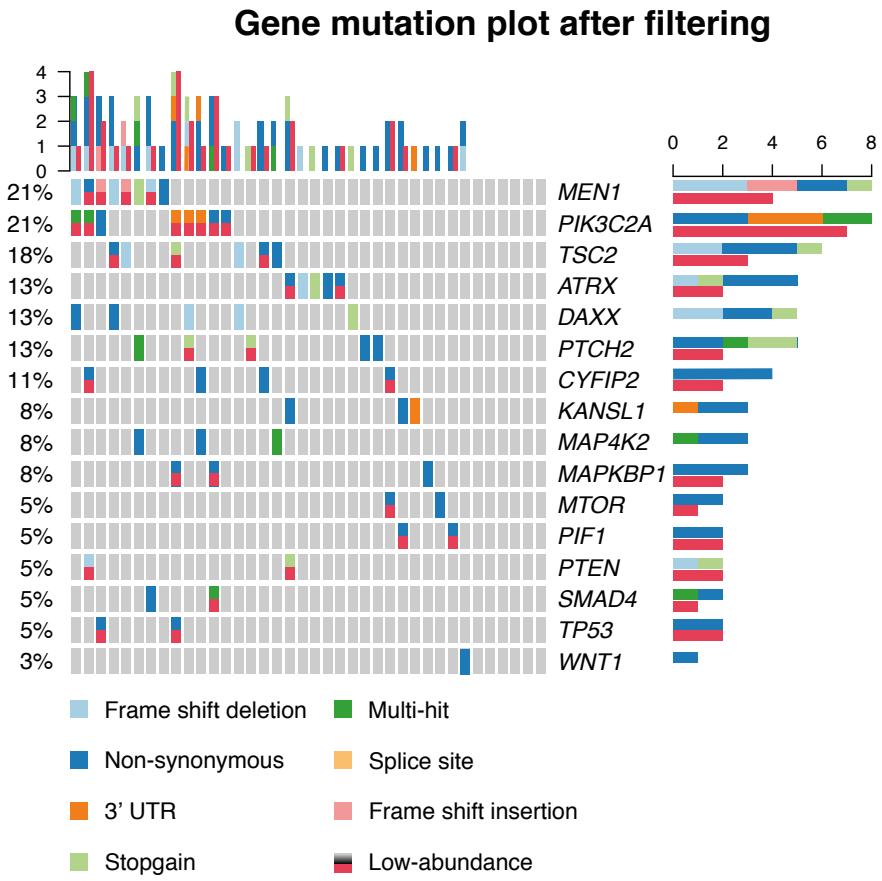

Figure 3 | Gene mutation plot after filtering.

Plot showing frequency, type of mutations, abundancy and mutational distribution of genetic alterations across 38 included tumors, after filtering and validation (if executed), including both high-abundance (N=32) and low-abundance (N=30) mutations. Low-abundance mutations are marked with red, in addition to color-coded mutation type.

V. DISCUSSION

This study presents the first ultra-deep targeted resequencing of pNENs in archival tissue. The relative rarity of pNENs has led to only a limited number of large-scale studies on the genetic constitution of pNENs[2,3,40]. Additionally, these studies focus on a broad overview of frequent genetic alterations in pNEN and report high-abundance mutations. These high-abundance mutations are present in the majority of tumors cells. However, various studies have demonstrated that the genetic make-up of primary tumors evolves dynamically in time[41,42]. This time-dependent change of the genetic alterations present in a tumor reflects the appearance and disappearance of subsets of tumor cells, so-called subclones, within one tumor[41,42]. In our study, the use of ultra-deep sequencing allowed for the identification of genetic alterations that are present in a low fraction of the tumoral tissue, so-called low-abundance mutations. These low-abundance mutations are indicative for the genetic heterogeneity within a single tumor. Recent genetic studies have identified the insulinoma, MEN-1-like/intermediate and metastasis-like (MLP) RNA expression subtype in pNENs[3]. Although the MEN-1-like tumors frequently contains *MEN1* mutations, the mutational burden of high-abundance mutations in other core pathways seems to be more variable across subtypes[3]. Additionally, DNA damage repair, chromatin modification, alternated telomere length and the PI3K/Akt/mTOR pathways have been highlighted as core altered pathways in pNEN[40,43]. In this study, we demonstrate

that low-abundance mutations are found in these pathways. Hence, low-abundance mutations might help to better classify tumors. However, validation of these low-abundance mutations remains complex and its lack forms a limitation of our study. The gene with the most high-abundance mutations within our study was the tumor suppressor gene *DAXX*. ATRX and DAXX form a complex facilitating the incorporation of histone variant H3.3 at the telomeres and, consequently, play a role in alternative lengthening of telomeres[5,6]. In many cancer types, it has been demonstrated that alternative telomere lengthening (ATL) leads to a prolonged cell survival, which is a hallmark of cancer[44]. In pNEN, ATL has been associated with a reduced disease-free survival[45]. Additionally, loss of ATRX and DAXX on immunohistochemistry (IHC) staining, caused by inactivating mutations or copy number loss, is associated with increased occurrence of metastasis and reduced disease-free survival[40,45]. Both high- and low-abundance mutations in *DAXX* and *ATRX* were identified in this study, including the first-ever validated recurrent, hotspot, mutation in *DAXX*, with likely loss-of-function on protein level. In line with other studies, exonic (transcript coding or protein encoding) mutations in *DAXX* and *ATRX* were mutually exclusive[2,40]. As this is the first study to demonstrate the existence of low-abundance mutations in *ATRX* and *DAXX*, conclusions on clinical impact are limited. Nonetheless, detection of low-abundance mutations might lead to the identification of DAXX and ATRX loss before this is apparent on IHC and, thus, an earlier identification of high-risk patients. Given the low number of events in the studied population (both in disease-recurrence

and in mortality), this study is not adequately powered to evaluate prognostic relevance of these low-abundance mutations. Hence, further studies are needed. Menin, the nuclear protein encoded by *MEN1*, impacts ATL by negatively regulating hTERT[46]. Additionally, it plays a key role in chromatin remodeling and gene expression through histone acetylation and deacetylation[47]. *MEN1* mutations have been implicated in pNEN oncogenesis, both as part of the familial MEN1 syndrome, and in sporadic tumors[2,40,48,49]. In 12-14% of all pNEN patients, a mutation in PI3K/Akt/mTOR-related genes is reported, including mutations in *PTEN*, *MTOR*, *DEPDC5*, *TSC1*, *TSC2* and *PIK3CA*[2,40,50]. In this study, PI3K/Akt/mTOR-related mutations could be identified in 29% of all tumors, including a novel p.A329T mutation in *MTOR* in pNEN. This increased frequency of mutations in the PI3K/Akt/mTOR-related genes is due to the detection of low-abundance mutations in these tumor samples. The relation of everolimus efficacy and PI3K/Akt/mTOR pathway-related mutations remains the subject of study in pNEN. However, in other cancer types, mutations of the PI3K/Akt/mTOR pathways seems to confer everolimus sensitivity[14,51]. In neuroendocrine neoplasms and other cancer types, cross-talk activation between the PI3K/Akt/mTOR pathway and the mitogen-activated kinase and extracellular signal-regulated kinase (MAPK-ERK pathway) through PI3K has been described[15,52,53]. Until now, no mutations in MAPK-ERK pathway-related genes have been reported in pNEN. In this study, mutations in *MAP4K2* and *MAPKBP1* were identified, further implicating this pathway in pNEN and providing additional rationale for the use of MEK-inhibitors in pNEN, either in combination with mTOR inhibitors

or alone. Although *TP53* is frequently mutated in other cancers, *TP53* mutation frequency is low in pNEN, as demonstrated by only two low-abundance *TP53* mutations being present in our cohort[2,40]. Additionally, the pro-apoptotic gene *CYFIP2* was mutated in four tumors. In two tumors, the exact same mutation was present, a so-called hotspot mutation. This validated mutation has never been reported before in pNEN and is predicted to be protein-damaging, warranting further studies into the role of *CYFIP2* in pNEN. Three mutations (one high-abundance and two low-abundance) were found in *SMAD4*. Unlike in small intestinal neuroendocrine neoplasms, where *SMAD4* loss is relatively common, the frequency of *SMAD4* mutations in pNEN has been the matter of debate[16,54,55]. Multiple low-abundance recurrent mutations were identified, including a hotspot mutation in *PTCH2*. *PTCH2* encodes the Patched 2 protein, which is involved in hedgehog signaling[56,57]. *PTCH2* mutations haven been found in basal cell carcinoma, medulloblastoma and rhabdomyosarcoma and myeloproliferative neoplasms[57–59]. However, this is the first time that hedgehog signaling has been implicated in pNENs. As the technical limitations of Sanger sequencing didn't allow validation of this low-abundance mutation, further studies in replication cohorts are needed to confirm hedgehog signaling as a novel pathway in pNENs. Given that various hedgehog signaling inhibitors have been approved for use in basal cell carcinoma, confirmatory studies on the role of hedgehog signaling could open new therapeutic options for pNENs, harboring *PTCH2* mutations[60]. Finally, the limited availability of fresh-frozen tissue in pNEN could hinder the implementation of next-generation

sequencing technology in pNEN diagnostics. In contrast, archival tissue, necessary for histological diagnosis of pNEN, is frequently available and can be easily manipulated and stored in a cost-effective manner. A possible limitation of the use of FFPE, is the induction of false-positive mutations by formalin fixation[61]. These mutations often follow a deamination pattern, resulting in transitions (C>T or G>A). Hence, when formalin fixation would result in a considerable number of additional induced mutations, there would be an increase in the number of transitions (C>T or G>A) in comparison to transversions (A>C or G>T). However, the ratio of transitions to transversion in this study is similar to transition-transversion ratios seen in normal human (germline) samples and in pancreatic neuroendocrine neoplasm samples from fresh-frozen tissue[2]. Therefore, the impact of formalin-fixation can be considered to be relatively limited. To further reduce any potential impact, the in-house developed pyAmpli tool filters specifically for mutations present in more than one amplicon and, thus, amplified DNA fragment[23]. As fixation-induced "deamination" is stochastic and happens randomly in all DNA strands, the chance that two different DNA molecules have exactly the same formalin fixation-induced is very limited. Hence, our study demonstrates that by using this approach archival FFPE tissue can be used reliably in genetic analysis of pNENs.

In conclusion, this study adds to the growing body of evidence on the broad genetic constitution of pNENs by demonstrating the presence of low-abundance mutations and genetic heterogeneity in pNENs. We highlight the importance of the *ATRX/DAXX*

pathway by reporting the first-ever pNEN-specific protein-damaging hotspot mutation in *DAXX*, and uncover novel genes and pathways involved in pNENs, including pro-apoptotic *CYFIP2*, hedgehog signaling and the MAPK-ERK pathway.

VI. REFERENCES

1. Dasari, A. *et al.* Trends in the Incidence, Prevalence, and Survival Outcomes in Patients With Neuroendocrine Tumors in the United States. *JAMA Oncol.* **3,** 1335–1342 (2017).
2. Jiao, Y. *et al.* DAXX/ATRX, MEN1, and mTOR pathway genes are frequently altered in pancreatic neuroendocrine tumors. *Science (80-.).* **331,** 1199–1203 (2011).
3. Sadanandam, A. *et al.* A cross-species analysis in pancreatic neuroendocrine tumors reveals molecular subtypes with distinctive clinical, metastatic, developmental, and metabolic characteristics. *Cancer Discov.* (2015). doi:10.1158/2159-8290.CD-15-0068
4. Scarpa, A. *et al.* Whole-genome landscape of pancreatic neuroendocrine tumours. *Nature* **543,** 65–71 (2017).
5. Elsässer, S. J., Allis, C. D. & Lewis, P. W. New epigenetic drivers of cancers. *Science* **331,** 1145–1146 (2011).
6. Heaphy, C. M. *et al.* Altered telomeres in tumors with ATRX and DAXX mutations. *Science* **333,** 425 (2011).
7. Yao, J. C. *et al.* Efficacy of RAD001 (everolimus) and octreotide LAR in advanced low- to intermediate-grade neuroendocrine tumors: Results of a phase II study. *J. Clin. Oncol.* **26,** 4311–4318 (2008).
8. Yuan, F. *et al.* KRAS and DAXX/ATRX gene mutations are correlated with the clinicopathological features, advanced diseases, And poor prognosis in Chinese patients with pancreatic neuroendocrine tumors. *Int. J. Biol. Sci.* **10,** 957–965 (2014).
9. Vandamme, T. *et al.* Long-term acquired everolimus resistance in pancreatic neuroendocrine tumours can be overcome with novel PI3K-AKT-mTOR inhibitors. *Br. J. Cancer* **114,** 650–658 (2016).
10. Vandamme, T. *et al.* Whole-exome characterization of pancreatic neuroendocrine tumor cell lines BON-1 and QGP-1. *J. Mol. Endocrinol.* **54,** (2015).
11. Gerstung, M. *et al.* Reliable detection of subclonal single-nucleotide variants in tumour cell populations. *Nat. Commun.* **3,** (2012).

12. Bosman, F. T., Carneiro, F., Hruban, R. H. & Theise, N. D. WHO Classification of Tumours of the Digestive System, Fourth Edition. in *International Agency for Research on Cancer* **3,** 417 (2010).
13. Vandamme, T., Beyens, M., Peeters, M., Van Camp, G. & de Beeck, K. O. Next generation exome sequencing of pancreatic neuroendocrine tumor cell lines BON-1 and QGP-1 reveals different lineages. *Cancer Genetics* **208,** 523 (2015).
14. Wagle, N. *et al.* Activating mTOR mutations in a patient with an extraordinary response on a phase I trial of everolimus and pazopanib. *Cancer Discov.* **4,** 546–553 (2014).
15. Valentino, J. D. *et al.* Cotargeting the PI3K and RAS pathways for the treatment of neuroendocrine tumors. *Clin. Cancer Res.* **20,** 1212–1222 (2014).
16. Bartsch, D. *et al.* Mutations of the DPC4/Smad4 gene in neuroendocrine pancreatic tumors. *Oncogene* **18,** 2367–2371 (1999).
17. Andrews, S. FastQC: A quality control tool for high throughput sequence data. *Http://Www.Bioinformatics.Babraham.Ac.Uk/Projects/Fastqc/* http://www.bioinformatics.babraham.ac.uk/projects/ (2010). doi:citeulike-article-id:11583827
18. Martin, M. Cutadapt removes adapter sequences from high-throughput sequencing reads. *EMBnet.journal* **17,** 10 (2011).
19. Li, H. Aligning new-sequencing reads by BWA BWA : Burrows-Wheeler Aligner. *PPT* (2010).
20. Broad Institute. Picard tools. *https://broadinstitute.github.io/picard/* (2016). Available at: https://broadinstitute.github.io/picard/%5Cnhttp://broadinstitute.github.io/picard/.
21. Li, H. *et al.* The Sequence Alignment / Map format and SAMtools. *Bioinformatics* **25,** 2078–2079 (2009).
22. Koboldt, D. C. *et al.* VarScan 2: Somatic mutation and copy number alteration discovery in cancer by exome sequencing. *Genome Res.* **22,** 568–576 (2012).
23. Beyens, M., Boeckx, N., Van Camp, G., Op de Beeck, K. & Vandeweyer, G. pyAmpli: An amplicon-based variant filter pipeline for targeted resequencing data. *BMC Bioinformatics* **18,** (2017).

24. Wang, K., Li, M. & Hakonarson, H. ANNOVAR: Functional annotation of genetic variants from high-throughput sequencing data. *Nucleic Acids Res.* **38,** (2010).
25. Vandeweyer, G., Van Laer, L., Loeys, B., Van den Bulcke, T. & Kooy, R. F. VariantDB: A flexible annotation and filtering portal for next generation sequencing data. *Genome Med.* **6,** (2014).
26. Mayakonda, A. & Koeffler, H. P. Maftools: Efficient analysis, visualization and summarization of MAF files from large-scale cohort based cancer studies. *bioRxiv* 052662 (2016). doi:10.1101/052662
27. R Core Team. R. *R Core Team* (2017). doi:3-900051-14-3
28. Lynch, M. Rate, molecular spectrum, and consequences of human mutation. *Proc. Natl. Acad. Sci. U. S. A.* **107,** 961–8 (2010).
29. Greenman, C. *et al.* Patterns of somatic mutation in human cancer genomes. *Nature* **446,** 153–158 (2007).
30. Jones, S. *et al.* Core signaling pathways in human pancreatic cancers revealed by global genomic analyses. *Science* **321,** 1801–6 (2008).
31. Pruitt, K. D. *et al.* RefSeq: An update on mammalian reference sequences. *Nucleic Acids Res.* **42,** (2014).
32. 1000 genome project consortium. A map of human genome variation from population-scale sequencing. *Nature* **467,** 1061–73 (2010).
33. Sherry, S. T. dbSNP: the NCBI database of genetic variation. *Nucleic Acids Res.* **29,** 308–311 (2001).
34. IGV (Integrative Genomic Viewer). Integrative Genomics Viewer. *Broad Inst.* **29,** 24–26 (2013).
35. Forbes, S. A. *et al.* COSMIC: Somatic cancer genetics at high-resolution. *Nucleic Acids Res.* **45,** D777–D783 (2017).
36. Lek, M. *et al.* Analysis of protein-coding genetic variation in 60,706 humans. *Nature* **536,** 285–291 (2016).
37. Choi, Y., Sims, G. E., Murphy, S., Miller, J. R. & Chan, A. P. Predicting the Functional Effect of Amino Acid Substitutions and Indels. *PLoS One* **7,** (2012).
38. Schwarz, J. M., Cooper, D. N., Schuelke, M. & Seelow, D. Mutationtaster2: Mutation prediction for the deep-sequencing age. *Nature Methods* **11,** 361–362 (2014).

39. Tsiatis, A. C. *et al.* Comparison of Sanger sequencing, pyrosequencing, and melting curve analysis for the detection of KRAS mutations: diagnostic and clinical implications. *J. Mol. Diagn.* **12,** 425–32 (2010).
40. Scarpa, A. *et al.* Whole-genome landscape of pancreatic neuroendocrine tumours. *Nature* **543,** 65–71 (2017).
41. Burrell, R. A., McGranahan, N., Bartek, J. & Swanton, C. The causes and consequences of genetic heterogeneity in cancer evolution. *Nature* **501,** 338–345 (2013).
42. Stratton, M., Campbell, P. & Futreal, P. The cancer genome. *Nature* **458,** 719–724 (2009).
43. Jiao, Y. *et al.* DAXX/ATRX, MEN1, and mTOR pathway genes are frequently altered in pancreatic neuroendocrine tumors. *Science (80-.).* **331,** 1199–1203 (2011).
44. Cesare, A. J. & Reddel, R. R. Alternative lengthening of telomeres: Models, mechanisms and implications. *Nature Reviews Genetics* **11,** 319–330 (2010).
45. Singhi, A. D. *et al.* Alternative lengthening of telomeres and loss of DAXX/ATRX expression predicts metastatic disease and poor survival in patients with pancreatic neuroendocrine tumors. *Clin. Cancer Res.* **23,** 600–609 (2017).
46. Lin, S. Y. & Elledge, S. J. Multiple tumor suppressor pathways negatively regulate telomerase. *Cell* **113,** 881–889 (2003).
47. Kim, H., Lee, J. E., Cho, E. J., Liu, J. O. & Youn, H. D. Menin, a tumor suppressor, represses JunD-mediated transcriptional activity by association with an mSin3A-histone deacetylase complex. *Cancer Res.* **63,** 6135–6139 (2003).
48. Corbo, V. *et al.* MEN1 in pancreatic endocrine tumors: Analysis of gene and protein status in 169 sporadic neoplasms reveals alterations in the vast majority of cases. *Endocr. Relat. Cancer* **17,** 771–783 (2010).
49. Crona, J. & Skogseid, B. GEP- NETS UPDATE: Genetics of neuroendocrine tumors. *Eur. J. Endocrinol.* **174,** R275–R290 (2016).
50. Chou, W. C. *et al.* Genes involved in angiogenesis and mTOR pathways are frequently mutated in Asian patients with pancreatic neuroendocrine tumors. *Int. J. Biol. Sci.* **12,** 1523–1532 (2016).
51. Grabiner, B. C. *et al.* A diverse array of cancer-associated MTOR mutations are hyperactivating and can predict rapamycin sensitivity.

Cancer Discov. **4,** 554–563 (2014).
52. Carracedo, A. *et al.* Inhibition of mTORC1 leads to MAPK pathway activation through a PI3K-dependent feedback loop in human cancer. *J. Clin. Invest.* **118,** 3065–3074 (2008).
53. Zitzmann, K. *et al.* Compensatory activation of Akt in response to mTOR and Raf inhibitors - A rationale for dual-targeted therapy approaches in neuroendocrine tumor disease. *Cancer Lett.* **295,** 100–109 (2010).
54. Francis, J. M. *et al.* Somatic mutation of CDKN1B in small intestine neuroendocrine tumors. *Nat. Genet.* **45,** 1483–1486 (2013).
55. Perren, A. *et al.* DPC4/Smad4: No Mutations, Rare Allelic Imbalances, and Retained Protein Expression in Pancreatic Endocrine Tumors. *Diagnostic Mol. Pathol.* (2003). doi:10.1097/00019606-200312000-00001
56. Rahnama, F., Toftgård, R. & Zaphiropoulos, P. G. Distinct roles of PTCH2 splice variants in Hedgehog signalling. *Biochem. J.* **378,** 325–334 (2004).
57. Smyth, I. *et al.* Isolation and characterization of human Patched 2 (PTCH2), a putative tumour suppressor gene in basal cell carcinoma and medulloblastoma on chromosome 1p32. *Hum. Mol. Genet.* **8,** 291–297 (1999).
58. Klein, C. *et al.* Ptch2 loss drives myeloproliferation and myeloproliferative neoplasm progression. *J. Exp. Med.* **213,** 273–290 (2016).
59. Taeubner, J. *et al.* Congenital embryonal rhabdomyosarcoma caused by heterozygous concomitant PTCH1 and PTCH2 germline mutations. *Eur. J. Hum. Genet.* **26,** 137–142 (2018).
60. Lacouture, M. E. *et al.* Characterization and Management of Hedgehog Pathway Inhibitor-Related Adverse Events in Patients With Advanced Basal Cell Carcinoma. *Oncologist* **21,** 1218–1229 (2016).
61. Williams, C. *et al.* A high frequency of sequence alterations is due to formalin fixation of archival specimens. *Am. J. Pathol.* **155,** 1467–1471 (1999).

1. SUPPLEMENTARY TABLE 1

Patient id	WHO 2010 grade	ENETS TNM	Months follow-up	Clinical status
1	1	T3N0M0	175	Disease-free
2	1	T2N0M0	95	Disease-free
3	1	T1N0M0	130	Disease-free
4	1	T3N0M0	52	Disease-free
5	1	T2N0M0	68	Disease-free
6	2	T2N0M0	72	Disease-free
7	1	T2N0M0	53	Disease-free
8	1	TxNxMx	153	Deceased
9	1	T1N0M0	22	Deceased (not disease-related)
10	1	T2N0M0	65	Disease-free
11	1	T1N0M0	48	Disease-free
12	2	T3N1M0	73	Disease-free
13	2	T4N1M0	39	Active disease
14	2	T3N1M0	50	Disease-free
15	2	T3N0M0	71	Disease-free
16	1	T3N1M1	53	Disease-free
17	2	T3N1M0	52	Disease-free
18	2	T4N0M1	40	Deceased
19	1	T1N1M0	88	Disease-free
20	1	T3N1M1	118	Active disease
21	1	T2N0M0	75	Disease-free
22	1	T2N1M0	134	Active disease
23	2	T4NxM1	98	Active disease
24	2	T3N0M1	69	Disease-free

Patient id	WHO 2010 grade	ENETS TNM	Months follow-up	Clinical status
25	2	T4N0M1	144	Active disease
26	2	T4N1M1	90	Disease-free
27	1	TxN0M0	79	Disease-free
28	1	T3N0M1	69	Deceased
29	1	T2 N1M0/1	112	Active disease
30	2	TxN0M0	229	Disease-free
31	1	T1N0M0	45	Disease-free
32	1	T2N0M0	94	Disease-free
33	1	T1mN0M0	132	Deceased
34	2	T2N0M0	93	Deceased
35	3	TxN1M1	105	Deceased
36	1	T1N0M0	69	Disease-free
37	1	T2N0M0	140	Disease-free
38	1	T2N0M0	135	Disease-free

2. SUPPLEMENTARY TABLE 2

N	Gene	CHR:POS	Reference	Alt	Patient id	Somatic state	RefSeq Variant-Type
1	MTOR	chr1:11187828	C	A	20	Low-abundance	nonsynonymous SNV
2	MTOR	chr1:1308007	C	T	19	Somatic	nonsynonymous SNV
3	PTCH2	chr1:45292324	C	T	11	Somatic	nonsynonymous SNV
4	PTCH2	chr1:45292871	C	A	25;22	Low-abundance	stopgain
5	PTCH2	chr1:45295296	C	T	4	Somatic	nonsynonymous SNV
6	PTCH2	chr1:45295689	G	A	5	Somatic	nonsynonymous SNV
7	PTCH2	chr1:45297396	C	G	4	Somatic	nonsynonymous SNV
8	PTEN	chr10:89692856	G	T	28	Low-abundance	stopgain
9	PTEN	chr10:89711892	TC	T	38	Low-abundance	frameshift deletion
10	PIK3C2A	chr11:17111197	AGT	A	27;24;25	Low-abundance	UTR3
11	PIK3C2A	chr11:17118687	T	C	10	Low-abundance	nonsynonymous SNV
12	PIK3C2A	chr11:17124314	C	T	21	Somatic	nonsynonymous SNV
13	PIK3C2A	chr11:17158120	C	T	14	Low-abundance	nonsynonymous SNV
14	PIK3C2A	chr11:17158152	A	C	18	Low-abundance	nonsynonymous SNV
15	PIK3C2A	chr11:17170212	AC	A	38	Low-abundance	splicing

N	Gene	CHR:POS	Reference	Alt	Patient id	Somatic state	RefSeq Variant-Type
16	PIK3C2A	chr11:17190548	C	A	18	Low-abundance	nonsynonymous SNV
17	PIK3C2A	chr11:17190844	G	T	38	Low-abundance	nonsynonymous SNV
18	MAP4K2	chr11:64563757	C	T	7	Somatic	nonsynonymous SNV
19	MAP4K2	chr11:64564655	G	T	27	Somatic	nonsynonymous SNV
20	MAP4K2	chr11:64569546	C	A	7	Somatic	nonsynonymous SNV
21	MAP4K2	chr11:64569572	C	G	4	Somatic	nonsynonymous SNV
22	MEN1	chr11:64571820	G	A	38	Low-abundance	nonsynonymous SNV
23	MEN1	chr11:64572092	C	CG	21	Low-abundance	frameshift insertion
24	MEN1	chr11:64572133	CT	C	29	Somatic	frameshift deletion
25	MEN1	chr11:64575559	T	A	35	Somatic	nonsynonymous SNV
26	MEN1	chr11:64577274	AG	A	14	Somatic	frameshift deletion
27	MEN1	chr11:64577329	TAGAC	T	17	Low-abundance	frameshift deletion
28	MEN1	chr11:64577380	C	CG	34	Low-abundance	frameshift insertion
29	MEN1	chr11:64577392	G	A	4	Somatic	stopgain
30	WNT1	chr12:49373410	T	A	1	Somatic	nonsynonymous SNV

N	Gene	CHR:POS	Reference	Alt	Patient id	Somatic state	RefSeq VariantType
31	MAPKBP1	chr15:42111514	G	A	26	Germline	nonsynonymous SNV
32	MAPKBP1	chr15:4213067	C	A	24	Low-abundance	nonsynonymous SNV
33	MAPKBP1	chr15:4213196	C	T	18	Low-abundance	nonsynonymous SNV
34	MAPKBP1	chr15:42114423	A	C	9	Somatic	nonsynonymous SNV
35	PIF1	chr15:65108822	C	T	35	Germline	nonsynonymous SNV
36	PIF1	chr15:65114563	C	T	26	Low-abundance	nonsynonymous SNV
37	PIF1	chr15:65114700	C	G	12	Germline	nonsynonymous SNV
38	PIF1	chr15:65116156	C	T	6	Low-abundance	nonsynonymous SNV
39	TSC2	chr16:2103404	AGGCCCGGCACGC	A	34	Somatic	frameshift deletion
40	TSC2	chr16:2105442	C	A	24	Low-abundance	stopgain
41	TSC2	chr16:2129285	T	C	7	Somatic	nonsynonymous SNV

N	Gene	CHR:POS	Reference	Alt	Patient id	Somatic state	RefSeq VariantType
42	TSC2	chr16:2135287	CCACAAGATCGCCGTCCTGTATG	C	13	Somatic	frameshift deletion
43	TSC2	chr16:2136365	G	A	37	Low-abundance	nonsynonymous SNV
44	TSC2	chr16:2136376	G	T	29	Low-abundance	nonsynonymous SNV
45	KANSL1	chr17:44108804	CAATA	C	8	Somatic	UTR3
46	KANSL1	chr17:44108993	G	A	28	Somatic	nonsynonymous SNV
47	KANSL1	chr17:44249388	T	C	6	Somatic	nonsynonymous SNV
48	TP53	chr17:7576541	G	A	24	Low-abundance	nonsynonymous SNV
49	TP53	chr17:7578457	C	T	21	Low-abundance	nonsynonymous SNV
50	SMAD4	chr18:48573420	G	T	18	Low-abundance	nonsynonymous SNV
51	SMAD4	chr18:48593557	G	T	17	Somatic	nonsynonymous SNV

N	Gene	CHR:POS	Reference	Alt	Patient id	Somatic state	RefSeq VariantType
52	SMAD4	chr18:48604710	C	T	18	Low-abundance	nonsynonymous SNV
53	CYFIP2	chr5:156742061	C	T	38	Low-abundance	nonsynonymous SNV
54	CYFIP2	chr5:156746776	G	A	20	Low-abundance	nonsynonymous SNV
55	CYFIP2	chr5:156766140	G	A	27;37	Somatic	nonsynonymous SNV
56	DAXX	chr6:33287999	GC	G	13	Somatic	frameshift deletion
57	DAXX	chr6:33288323	C	T	29	Somatic	nonsynonymous SNV
58	DAXX	chr6:33289247	G	A	14	Somatic	nonsynonymous SNV
59	DAXX	chr6:33289247	G	T	23	Somatic	stopgain
60	DAXX	chr6:33289258	CAG	C	25	Somatic	frameshift deletion
61	ATRX	chrX:76909614	G	A	16	Somatic	stopgain
62	ATRX	chrX:76937108	TC	T	2	Somatic	frameshift deletion
63	ATRX	chrX:76938853	T	C	28	Low-abundance	nonsynonymous SNV

N	Gene	CHR:POS	Reference	Alt	Patient id	Somatic state	RefSeq VariantType
64	ATRX	chrX:76939097	C	T	36	Low-abundance	nonsynonymous SNV
65	ATRX	chrX:76939301	G	C	33	Somatic	nonsynonymous SNV

Long-term acquired everolimus resistance in pancreatic neuroendocrine tumors can be overcome with novel PI3K–AKT–mTOR inhibitors

Timon Vandamme[1,2,*], Matthias Beyens[1,3,*], Ken Op de Beeck[1,3], Fadime Dogan[2], Peter M van Koetsveld[2], Patrick Pauwels[4], Geert Mortier[3], Christel Vangestel[5], Wouter W. de Herder[1], Guy Van Camp[3], Marc Peeters[1] and Leo J. Hofland[2]

[1]Center of Oncological Research (CORE), University of Antwerp, Antwerp, Belgium
[2]Section of Endocrinology, Department of Internal Medicine, Erasmus Medical Center, Rotterdam, The Netherlands
[3]Center of Medical Genetics, University of Antwerp, Belgium
[4]Department of Pathology, University of Antwerp, Antwerp, Belgium
[5]Department of Molecular Imaging, University of Antwerp, Antwerp, Belgium
*Equal contributing authors

This chapter is based on the research article published in:

British Journal of Cancer, 2016; 114(6):650-8. doi: 10.1038/bjc.2016.25

I. ABSTRACT

1. BACKGROUND

The mTOR-inhibitor everolimus improves progression-free survival in advanced pancreatic neuroendocrine tumours (PNETs). However, adaptive resistance to mTOR inhibition is described.

2. METHODS

QGP-1 and BON-1, two human PNET cell lines, were cultured with increasing concentrations of everolimus up to 22 weeks to reach a dose of 1 µM everolimus, respectively, 1000-fold and 250-fold initial IC50. Using total DNA content as a measure of cell number, growth inhibitory dose-response curves of everolimus were determined at the end of resistance induction and over time after everolimus withdrawal. Response to ATP-competitive mTOR inhibitors OSI-027 and AZD2014, and PI3K-mTOR inhibitor NVP-BEZ235 was studied. Gene expression of 10 PI3K-Akt-mTOR pathway-related genes was evaluated using quantitative real-time PCR (RT-qPCR).

3. RESULTS

Long-term everolimus-treated BON-1/R and QGP-1/R showed a significant reduction in everolimus sensitivity. During a drug

holiday, gradual return of everolimus sensitivity in BON-1/R and QGP-1/R led to complete reversal of resistance after 10-12 weeks. Treatment with AZD2014, OSI-027 and NVP-BEZ235 had an inhibitory effect on cell proliferation in both sensitive and resistant cell lines. Gene expression in BON-1/R revealed downregulation of MTOR, RICTOR, RAPTOR, AKT and HIF1A, whereas 4EBP1 was upregulated. In QGP-1/R, a downregulation of HIF1A and an upregulation of ERK2 were observed.

4. CONCLUSIONS

Long-term everolimus resistance was induced in two human PNET cell lines. Novel PI3K-AKT-mTOR pathway-targeting drugs can overcome everolimus resistance. Differential gene expression profiles suggest different mechanisms of everolimus resistance in BON-1 and QGP-1.

II. INTRODUCTION

Neuroendocrine tumors (NETs) are a diverse group of neoplasms, mainly found in the gastro-intestinal tract, lung and pancreas. Pancreas NETs (PNETs) are relatively rare, with an incidence of 0,43 per 100.000 according to the Surveillance, Epidemiology, and End Results (SEER) registry[1]. However, this rate has doubled during the last 20 years[2,3]. Primary therapy for localized PNET remains surgical excision. However, up to 60% of all patients present with unresectable disease[4]. In these patients, systemic treatment has an essential role in controlling the disease[5]. The role of traditional cytotoxic therapies in PNET remains a matter of debate, with only non-randomized series showing response to streptozocin-based chemotherapy[6–8]. Newer chemotherapy regimens with temozolomide alone[9], or in combination with capecitabine[10], show promise. The low response rate for streptozocin-based chemotherapy and the associated side effects underscore the need for targeted drugs.

The phosphoinositide-3-kinase/Akt/mammalian target of rapamycin (PI3K-Akt-mTOR) signaling pathway plays a major role in NET by regulating cell growth, proliferation, survival and protein synthesis (Figure 1A). Furthermore, elevated mTOR expression and activity is associated with a higher proliferative capacity and worse prognosis[11]. Recently, exome sequencing of primary PNET tumor samples revealed mTOR pathway genes to be mutated in 16% of all PNETs, in addition to highlighting mutations in other genes, including *MEN1* (44% of all patients),

DAXX (25%) and *ATRX* (18%)[12]. mTOR acts as the catalytic subunit of two functionally distinct complexes, named mTOR complex 1 (mTORC1) and mTOR complex 2 (mTORC2)[13]. mTOR proves to be an interesting target for therapy of PNET with mTOR-inhibiting rapamycin and analogs (rapalogues) such as everolimus (RAD001). Rapamycin, everolimus and other rapalogues form a complex with the 12 kD FK506-binding protein FKBP12[14,15]. This rapalog-FKBP12 complex allosterically inhibits mTOR when it is part of mTORC1. However, rapalogues only have limited effect on mTOR when mTOR is part of mTORC2 because of steric hindrance by the Rictor mTORC2-subunit[16]. A phase III trial with everolimus was conducted in 410 patients with well- and moderately-differentiated PNETs and showed an improvement in median progression-free survival (PFS) in the everolimus treated group compared to the placebo group[17]. Similar results were seen in the phase III trial with sunitinib, a pan-tyrosine kinase inhibitor[18]. Based on these results everolimus and sunitinib became the first FDA and EMA approved drugs in 30 years for the treatment of locally advanced, unresectable or metastatic PNETs. However, an objective partial response was only seen in 5% of the patients receiving everolimus or sunitinib. The significant effect on PFS was thus mainly due to disease stabilization and minor reductions in tumor growth. As PFS in phase III study with everolimus is still limited to 11 months, adaptive resistance to mTOR inhibition with rapalogues was described[19]. To overcome this resistance, novel PI3K-AKT-mTOR targeting drugs have been developed, such as NVP-BEZ235, OSI-027 and AZD2014. Exploiting the homology between the kinase domain of mTOR and PI3K,

NVP-BEZ235 docks in the active pocket of both molecules and reduces kinase activity of PI3K and mTOR by competing with ATP-binding. The selective mTOR inhibitors AZD2014 & OSI-027 target the kinase domain of mTOR, blocking both mTORC1 and mTORC2 in an ATP-competitive manner, without blocking PI3K kinase activity[20,21]. Although the efficacy of novel drugs in PNET cell line model of short-term adaptive resistance to everolimus has been studied[22], no data is currently available about long-term adaptive resistance in everolimus-treated PNET. A better understanding of the mechanisms underlying resistance to rapalogues is thus necessary for a predictive biomarker for everolimus resistance to be identified.

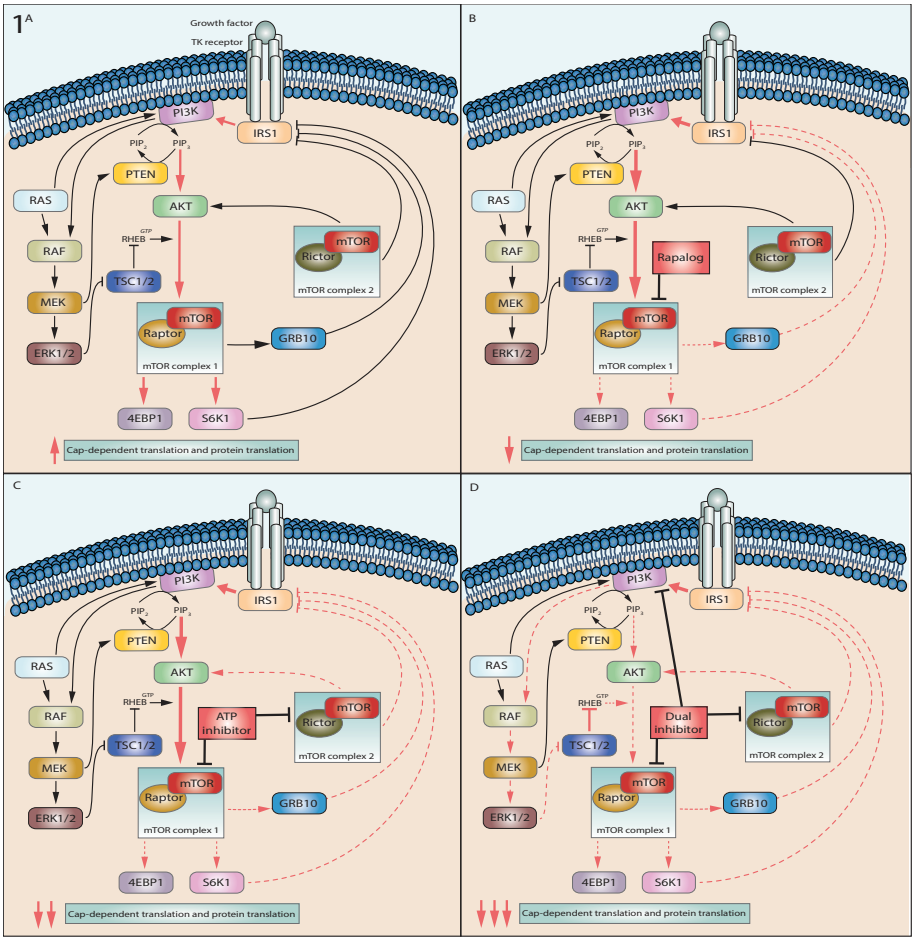

Figure 1 | Simplified representation of the PI3K-AKT-mTOR pathway.

PI3K-AKT-mTOR pathway in pancreatic neuroendocrine tumors (A) and its response to rapalogues (B), ATP-competitive inhibitors (C) and dual PI3K-mTOR inhibitors (D). Red full lines describe an increase and red dashed lines show a decrease of feedback under different conditions. A detailed description can be found in the text.

III. METHODS

1. CELL LINES AND CULTURE CONDITIONS

BON-1 and QGP-1, two human PNET cell line models, were used in this study. The BON-1 cell line was a kind gift from Dr. Townsend (University of Texas Medical Brachn, Galveston, USA)[23]. The QGP-1 cell line was purchased from the Japanese Collection of Research Bioresources Cell Bank (JRCB, Osaka, Japan)[24]. BON-1 and QGP-1 cell line identity was confirmed using short tandem repeat profiling[25]. The BON-1 cell line was cultured in 1:1 mixture of Dulbecco's modified Eagle medium (DMEM) and F12 medium, supplemented with 10% fetal calf serum (FCS), penicillin (1×10^5 units/L), fungizone (0.5 mg/L), and L-glutamine (2 mmol/L). The QGP-1 cell line was cultured in Roswell Park Memorial Institute (RPMI) 1640 medium, supplemented with 10% FCS and penicillin-streptomycin (1×10^5 units/L penicillin and 1×10^5 units/L streptomycin). All cell lines were incubated in an atmosphere of 95% humidity and 5% CO_2 at 37 º C. Media and supplements were obtained from Life Technologies Bio-cult Europe (Invitrogen, Breda, The Netherlands).

2. DRUGS AND REAGENTS

Everolimus (RAD001), AZD2014, OSI-27 and NVP-BEZ23 were purchased from Selleckchem (Selleck Chemicals, Houston, USA). Rapamycin was purchased from LG Laboratories (Woburn, USA).

All inhibitors were dissolved in 100% dimethylsulfoxide (DMSO) to a 1 mM concentration and stored in -20ºC. All drugs were diluted to working concentrations in 40% DMSO before use. In all the experiments, controls were treated with a vehicle DMSO concentration equivalent to the 0.4% final DMSO concentration in the treatment dilutions.

3. CELL PROLIFERATION ASSAY USING TOTAL DNA CONTENT

Cells were plated in 1 mL medium in 24-well plates at the density necessary to obtain a 70-80% cell confluence in the control groups at the end of the experiment. Medium was refreshed and the tested compounds were added to wells in quadruplicate after twenty-four hours for QGP-1 and seventy-two hours for BON-1. Time points where chosen to reduce inter- and intra-experiment variability. The concentrations of compounds tested ranged between 0,1 nM and 1 μM for everolimus, rapamycin and NVP-BEZ235. Given the narrow therapeutic margin of AZD2014 and OSI-027, the used concentrations ranged from 1 nM to 1 μM with an added 50 nM concentration. Every 3 days, the cells were supplied with fresh medium and compounds. After 7 days of treatment, the cells were harvested for DNA measurement. Measurement of total DNA content, as a measure of cell number, was performed with the bisbenzimide DNA-intercalating fluorescent dye (Hoechst 33258; Boehring Diagnostics, La Jolla, CA, USA) as previously described[26].

4. QUANTITATIVE REAL-TIME PCR OF PI3K-AKT-MTOR PATHWAY GENES

The tested cell line conditions were plated in 3 mL medium in six-well plates at the density required to obtain 70-80% cell confluence at the end of the experiment. Twenty-four hours later for QGP-1 cell line conditions and seventy-two hours later for BON-1 cell line conditions, medium was replaced, and cells were incubated for seventy-two hours with vehicle. One-step reverse transcription quantitative PCR (RT-qPCR) was performed on total RNA from six biological replicates in a single reaction using the Power SYBR Green RNA-To-CT 1-Step kit (Life Technologies, USA) on a LightCycler 480 instrument (Roche Applied Science, Penzberg, Germany). Primers were designed using QuantPrime software[27] and RTPrimerDB (http://www.rtprimerdb.org) and have been obtained from Integrated DNA Technologies (Leuven, Belgium) (Supplementary Table 1). All reactions have been performed in triplicates in 384-well plates with 2 µL total RNA (prediluted to 15 ng/µL) as input in a total reaction volume of 10 µL, further comprising 5 µL Power SYBR Green RT-PCR Mix (2x) (Life Technologies, Carlsbad, USA), 0.08 µL RT Enzyme Mix (125x) (Life Technologies, Carlsbad, USA) and 200 nM of each primer (final concentration).

5. STATISTICAL ANALYSIS

All cell proliferation assays were performed at least twice at different times. The repeated experiments gave comparable

results. The comparative statistical evaluations between the different cell line conditions were performed by two-way ANOVA with treatment concentration and cell line condition as variables. For post-hoc testing, a multiple comparative test with Dunn–Šidák correction was used. For RT-qPCR experiments, normalized relative gene expression values were calculated using qBasePLUS software version 1.5 (Biogazelle, Zwijnaarde, Belgium). mRNA expression was normalized to household gene expression (*GAPDH* and *RPL13A* for BON-1; *HPRT* and *YWAZ* for QGP-1) according to the geNorm algorithm[28]. Comparison between gene expression levels was done by Student's t-test and adjusted for multiple testing using Holm-Bonferroni correction. All statistical analyses were done using GraphPad Prism 5.0 for Windows (GraphPad Software, La Jolla, USA).

IV. RESULTS

1. INDUCING EVEROLIMUS RESISTANCE

In untreated human PNET cell lines BON-1 and QGP-1, the everolimus concentration that reduces growth by 50% (IC_{50}) after 7 days of treatment was 1 nM and 4 nM, respectively (data not shown). Starting from this IC_{50} concentration, QGP-1 and BON-1 were continuously cultured in increasing concentrations of everolimus. The everolimus concentration was progressively doubled every 14 days during 8-10 dose doublings until a final

concentration 1 μM was reached. In parallel, clonal BON-1 and QGP-1 cells were long-term vehicle-treated. The established long-term everolimus-treated cell lines (BON-1/R and QGP-1/R) were maintained in the maximally achieved everolimus concentration. No morphological changes were seen between the long-term vehicle-treated cell lines and the long-term everolimus-treated cell lines (Supplementary Figure 2). After the establishment of the long-term everolimus-treated BON-1/R and QGP-1/R, both showed a statistically significant reduced growth inhibitory response to everolimus in comparison with long-term vehicle-treated BON-1 and QGP-1 at everolimus concentrations between 10nM and 1μM for BON-1/R and at 1nM and 1μM for QGP-1/R, respectively (Figure 2A-B). Additionally, BON-1/R and QGP-1/R had a significantly reduced sensitivity to rapamycin in concentrations ranging from 1 nM to 1 μM when compared with their long-term vehicle-treated BON-1 and QGP-1 counterparts (Figure 2C-D).

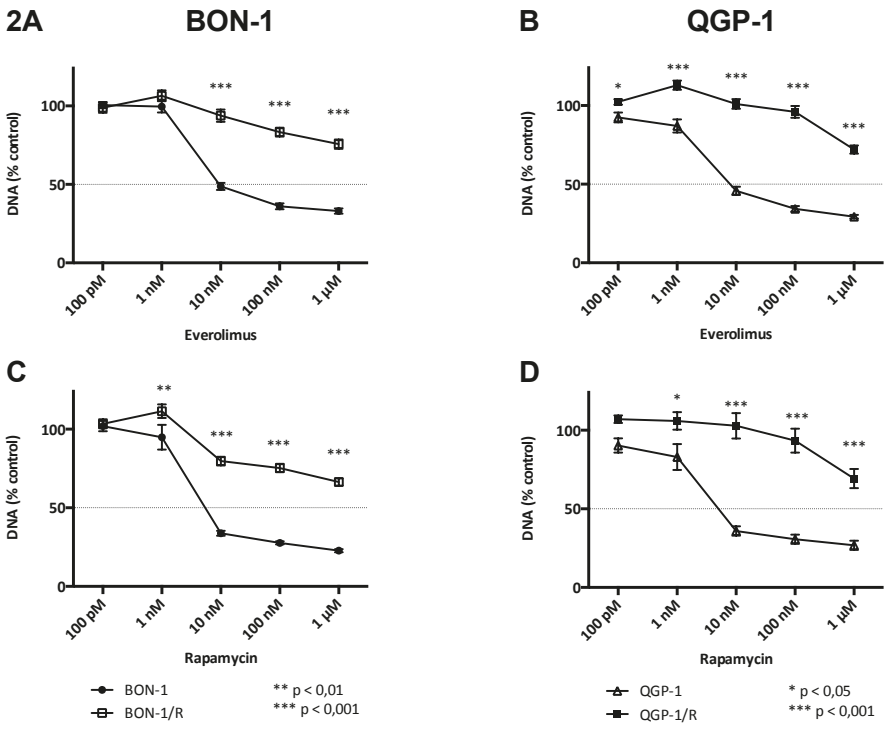

Figure 2 | Dose-response curves of everolimus and rapamycin treatment.

Dose-response curves of QGP-1/R & long-term vehicle-treated QGP-1 and BON-1/R & long-term vehicle-treated BON-1, respectively, after 7 days of treatment with increasing concentrations of everolimus (A-B) or rapamycin (C-D). Growth inhibitory response is expressed as the percentage of vehicle-treated control (± S.E.M). Control is normalized at 100%.

2. EVOLUTION OF EVEROLIMUS-RESISTANCE OVER TIME

In order to study reversibility of everolimus-resistance, the BON-1/R and QGP-1/R cell lines were cultured without everolimus maintenance treatment during 10 and 12 weeks, respectively,

showing a gradual return of everolimus sensitivity (data not shown). After 10-12 weeks, this resulted in the BON-1/R STOP and QGP-1/R STOP cell line conditions. When comparing these cell line conditions with BON-1/R and QGP-1/R, maintained during 10-12 weeks at maximum 1 μM everolimus concentration, and vehicle-treated BON-1 and QGP-1, a return of BON-1/R STOP and QGP-1/R STOP to the sensitivity levels of BON-1 and QGP-1 was observed (Figure 3A-B).

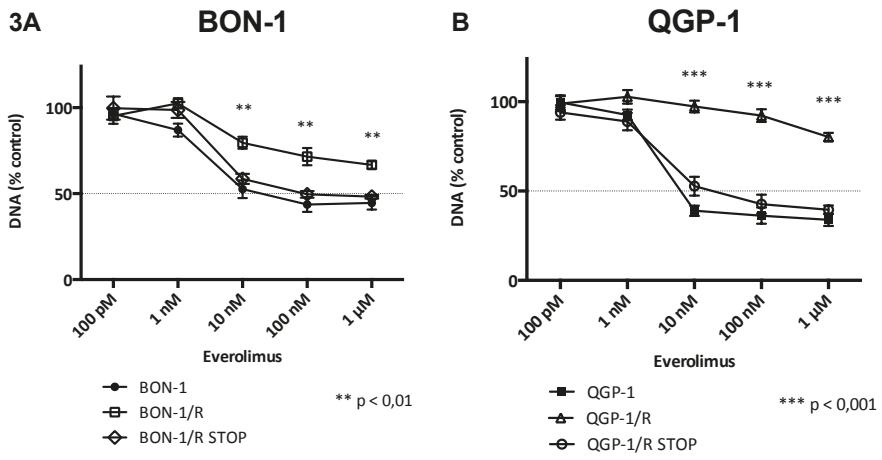

Figure 3 | Dose-response curves of cell lines after wash-out period.

Dose-response curves after 7 days of treatment with increasing concentrations of everolimus in BON-1/R, long-term vehicle-treated BON-1, and BON-1/R after an everolimus wash-out period of 12 weeks (BON-1/R STOP) (A) and QGP-1/R, and in long-term vehicle-treated QGP-1/DMSO and QGP-1/R after an everolimus wash-out period of 10 weeks (QGP-1/R STOP) (B). Growth inhibitory response is expressed as the percentage of vehicle-treated control (± S.E.M). Control is normalized at 100%. P-values shown are for Dunn–Šidák post-hoc comparison after two-way ANOVA between BON-1/R and QGP-1/R and BON-1/R STOP and QGP-1/R STOP, respectively.

3. OVERCOMING EVEROLIMUS-RESISTANCE

A dose response study in both everolimus resistant- and sensitive BON-1 and QGP-1 cells to the growth inhibitory effect of AZD2014, OSI-027 and NVP-BEZ235 was executed in parallel. After a 7-day-treatment with AZD2014, cell proliferation was significantly less reduced at the 250 nM and 500 nM concentration of AZD2014 in BON-1/R when compared to long-term vehicle-treated BON-1. When exposing QGP-1/R and QGP-1 to AZD2014 for 7 days, growth reduction was significantly more pronounced in long-term vehicle-treated QGP-1 when compared to QGP-1/R in all tested AZD2014 concentrations above 100 nM. A maximal inhibition of >80% of cell proliferation was obtained at 1 μM of AZD2014 in all cell lines tested (Figure 4A-B). BON-1/R and long-term vehicle-treated BON-1 didn't respond significantly different to OSI-027, while QGP-1/R was more resistant to OSI-27 than QGP-1 in all concentrations tested above 100 nM. The maximum inhibition with OSI-027 reached in BON-1/R, BON-1 and QGP-1 cells was a 50% reduction of cell proliferation (Figure 4C-D). No statistically significant difference in the inhibition of cell proliferation was observed after 7 days of treatment with NVP-BEZ235 in BON-1/R when compared to long-term vehicle-treated BON-1 in the 1 nM to 1 μM NVP-BEZ235 concentration range. In both everolimus-sensitive and -resistant BON-1 cells, a maximum inhibition of >92% of control cell proliferation was reached at 100 nM of NVP-BEZ23. When comparing the QGP-1/R and QGP-1, NVP-BEZ235 was less potent at 10nM, compared to QGP-1/R cells. Maximal cell growth inhibition was achieved a 100nM in both QGP-1/R and

long-term vehicle-treated QGP-1 (Figure 4E-F).

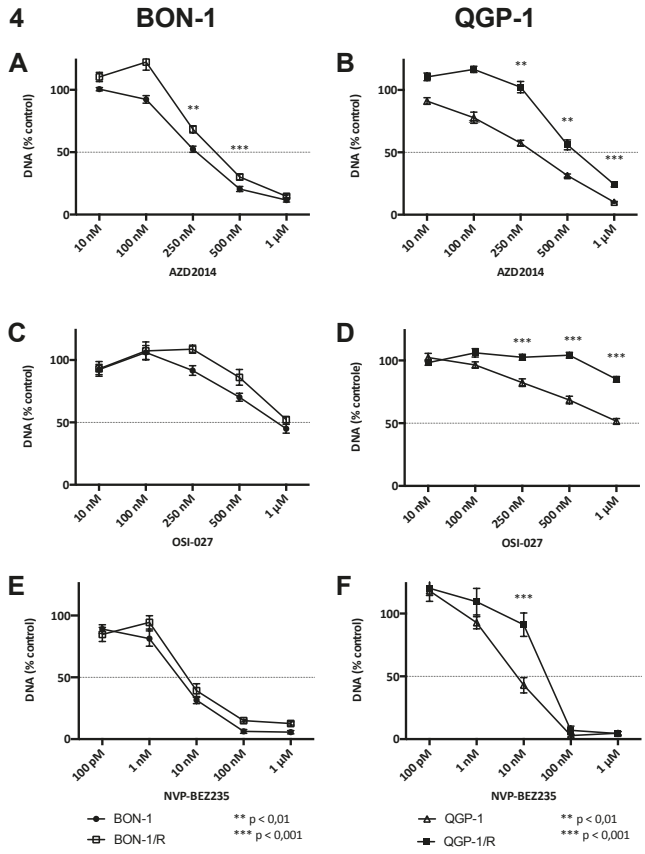

Figure 4 | Dose-response curves of AZD2014, OSI-027 and NVP-BEZ235 treatment.

Dose-response curves in BON-1/R & long-term vehicle-treated BON-1 and QGP-1/R & long-term vehicle-treated QGP-1, respectively, after 7 days of treatment with AZD2014 (A-B), OSI-027 (C-D) and NVP-BEZ235 (E-F). Response is expressed as the percentage of vehicle-treated control (± S.E.M). Control is normalized at 100%.

4. GENE EXPRESSION CHANGES IN EVEROLIMUS RESISTANCE

Differential gene expression of *MTOR, RAPTOR, RICTOR, AKT, S6K1, 4EBP1, ERK1, ERK2, BCL2* and *HIF1A* between BON-1/R and long-term vehicle-treated BON-1 showed a significant downregulation of *MTOR, RICTOR, RAPTOR, AKT* and *HIF1A*, while *4EBP1* was significantly upregulated ($p<0.05$) (Figure 5). When comparing QGP-1/R and QGP-1, a significant downregulation of *HIF1A* and a significant upregulation of *ERK2* were observed ($p<0.05$).

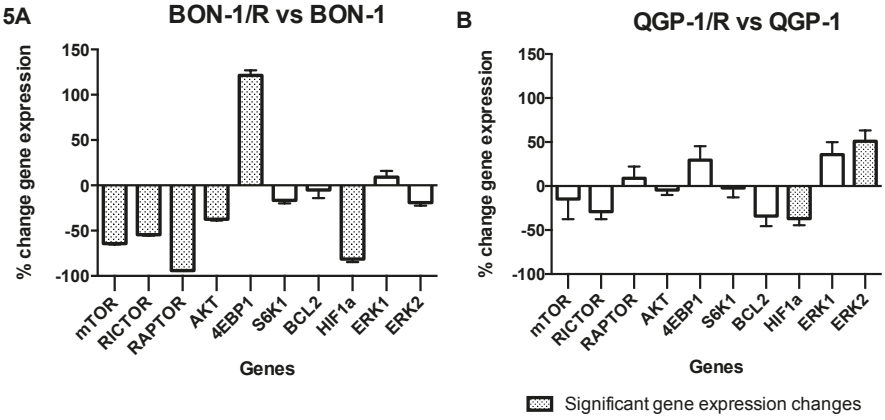

Figure 5 | Gene expression levels.

Changes in mRNA expression (mean percentage ± SEM) between BON-1/R & BON-1/DMSO and QGP-1/R (A) and QGP/DMSO (B). In addition to MTOR, mTORC1 component RAPTOR and mTORC2 component RICTOR expression was studied. Moreover, gene expression of AKT, encoding the mTOR upstream AKT, S6K1 and 4EBP1, encoding the mTOR downstream p70 ribosomal kinase 1 (S6K1) and eukaryotic translation initiation factor 4E binding protein 1 (4E-BP1), respectively, was determined. Additionally, BCL2, a gene encoding for anti-apoptotic protein B-cell leukemia 2 (Bcl-2), and HIF1A, encoding the hypoxia-inducible factor 1-alpha protein (HIF-1 alpha) was used to study the overall effect on apoptosis and proliferation in the cell. Finally, expression of ERK1 and ERK2, two components of the MAPK-ERK pathway was determined. Differences were tested using Student's t-test. P-value <0,05, after Bonferroni correction for multiple testing, was considered significant (hatched bars).

V. DISCUSSION

In this study, to the best of our knowledge, the first two PNET models for long-term acquired everolimus resistance were established. Both QGP-1 and BON-1 were cultured during more then 20 weeks in increasing concentrations of everolimus and continued to grow under a 250 and 1000-fold IC_{50} growth inhibitory concentration of everolimus, respectively. Corresponding *in vivo* concentrations are not reachable in patients[29]. Continued cell growth under these high everolimus concentrations, unreachable in patients, hence indicates an everolimus resistance with possible clinical implications. Both the resulting BON-1/R and QGP-1/R show a significantly decreased response to everolimus in comparison to long-term vehicle-treated BON-1 and QGP-1, even in the highest concentrations tested (1 μM). Similar results were seen when comparing BON-1/R and QGP-1/R and its vehicle-treated counterparts for response to rapamycin. This indicates that BON-1/R and QGP-1/R are not only everolimus-resistant but are also resistant to other rapalogues. A previous study looked at everolimus-resistance in BON-1[22]. However, this study treated BON-1 cells during 8 weeks with a dose of 10nM, which is a much shorter period and a lower dose than used in this study. Additionally, the authors didn't perform a resistance induction experiment with QGP-1. Given the long duration of treatment, the resulting BON-1/R and QGP-1/R cell lines in our study could be considered as a representative model for rapalogue resistance seen in PNET patients, where median time to treatment failure

and, thus, acquired everolimus resistance is 11 months[30].

Various mechanisms have been proposed for the limited response to everolimus in PNET (Figure 1B). Not all phosphorylation sites of mTORC1 downstream proteins such as p70 ribosomal S6 kinase 1 (S6K1), growth factor receptor bound protein 10 (GRB10) and eukaryotic translation initiation factor 4E binding protein 1 (4E-BP1) respond to the same extent to allosteric inhibition of mTORC1 by rapalogues[31], thereby diminishing rapalog efficacy. Adaptive resistance may also be caused by induction of activated phosphorylation of AKT. This occurs through the lifting of negative feedback of the mTORC1 downstream p70 ribosomal S6 kinase 1 (S6K1) on the PI3K-AKT-mTOR pathway[32–34]. S6K1 effects this negative feedback on insulin receptor substrate-1 (IRS-1), which regulates insulin-like growth factor I (IGF-1)[33]. Furthermore, mTORC1 activates GRB10, which negatively regulates IGF-1 signaling. When mTORC1 is inhibited by rapalogues, this negative feedback loop of IGF-1 is suppressed, synergistically adding to the effect of mTOR inhibition of the S6K1 feedback loop[35]. Since rapalogues effectively block mTORC1 but only have a limited, dose-dependent action on the mTORC2, the effect of rapalogues on mTOR signaling may be circumvented through increased activity of mTORC2[32,33]. Furthermore, a direct role of S6K1 on mTORC2-mediated AKT phosphorylation has been described since S6K1 might be instrumental in the inhibitory phosphorylation of Rictor, the rapalog-insensitive component of mTORC2[32]. Novel mTOR inhibitors, blocking both mTORC1 and mTORC2 by competitively binding the ATP-binding mTOR kinase pocket, have

been developed to overcome these escape mechanisms. AZD2014 is an ATP-competitive mTOR inhibitor, currently undergoing phase II evaluation in different tumor types[36,37] (Figure 1C). In our study, AZD2014 effectively reduces cell proliferation both in the everolimus-sensitive QGP-1 and BON-1, as well as in the everolimus-resistant BON-1/R and QGP-1/R. This is the first time that AZD2014 shows efficacy in PNET models. Additionally, these results indicate that AZD2014 overcomes everolimus resistance in PNET in concentrations reachable in patients[36]. Further development of this drug in PNET could hence benefit PNET patients. Additionally, OSI-027, a drug from the same ATP-competitive mTOR inhibiting class was tested. In contrast with the other tested compounds, the growth inhibitory effect of OSI-027 in the concentration ranges tested reaches growth inhibition by only 50% at 1μM in vehicle-treated BON-1 and QGP-1 cell lines. In a xenograft mouse model, concentrations of up to 2 μM could be reached, but further studies on pharmacokinetics in humans are needed[38]. Although resistant and sensitive BON-1 responded equally to OSI-027 treatment, only limited efficacy in overcoming everolimus resistance with OSI-027 was observed in the QGP-1 cell line. This difference in response to OSI-027 between BON-1/R and QGP-1/R suggests two distinct molecular mechanisms of resistance. NVP-BEZ235 is dual blocker of mTOR, blocking both mTORC1 and mTORC2, and the upstream PI3K[39] (Figure 1D). NVP-BEZ235 has proven efficacy in *in vitro* and *in vivo* PNET models[39,40]. Dual inhibition of PI3K-mTOR pathway could prevent cross talk activation of the mitogen-activated kinase and extracellular signal-regulated kinase (MAPK-ERK pathway) through PI3K-mediated

feedback loop[14,40–43]. This cross talk could lead to an escape of mTORC1 inhibition and, hence, to rapalog resistance. Although NVP-BEZ235 has completed phase II studies, clinical development of this drug might not progress to phase III because of the drug's safety profile[44]. However, our current study demonstrates that dual blocking of PI3K and mTOR could be an attractive strategy as well to overcome long-term acquired everolimus resistance. Additionally, maximum inhibition in both resistant and sensitive cell lines was reached with NVP-BEZ235 concentrations more than 10-fold lower than dose-limiting plasma concentrations obtained in phase I studies[45]. As this is in line with previously reported *in vitro* results and an *in vivo* study with lower dose NVP-BEZ235 in a glioblastoma model demonstrated efficacy, it could hence be interesting to evaluate low-dose NVP-BEZ235 in PNET[20,22].

Another possible mechanism for everolimus resistance is tumor heterogeneity. Within-patient and within-tumor heterogeneity in proliferation, genomic alterations and functional imaging characteristics have been demonstrated in neuroendocrine tumor patients[36,46,47]. This heterogeneity could be caused by tumoral subclones with different phenotypes and responses to treatment[48]. By treating a patient with everolimus, selection of everolimus-resistant subclones could occur, leading to resistance. While short-term everolimus resistance is mainly driven by phosphorylation changes in PI3K-AKT-mTOR pathway proteins[33], a shift in clonal population could be a driving force in long-term everolimus resistance. This is illustrated by the gradual reversal of everolimus resistance in BON-1/R and QGP-1/R, with

a complete return of everolimus sensitivity only after more than two months of culturing without everolimus. If this resistance would only be caused by phosphorylation and dephosphorylation of proteins, a faster reversal of everolimus resistance could be expected. Long-term treatment with everolimus might hence select or induce subclones with a different genetic, epigenetic or transcriptional make-up that makes them more resistant to everolimus. Future studies using next generation sequencing would be a good strategy to identify these resistant subclones and yield biomarkers for everolimus resistance. Given the long timeframe of sustained resistance, alterations in gene expression were studied to elucidate possible resistance mechanisms. In BON-1/R, the main components of both mTORC1 and mTORC2 and the important upstream protein AKT were down-regulated, while effector protein 4EBP1 expression was upregulated, hinting at a compensatory mechanism in which 4EBP1 is less dependent on mTORC1 and mTORC2. On the other hand, the main upregulated gene in QGP-1/R was ERK2, part of the MAPK-ERK pathway, illustrating a possible escape through this pathway. Interestingly, both cell lines seem to have a differential gene expression profile after developing resistance to everolimus. This is corroborated by their different response to novel PI3K-AKT-mTOR pathway targeting drugs. QGP-1/R is more resistant to treatment to the two tested ATP-competitive mTOR inhibitors, AZD2014 and OSI-027, than BON-1/R. Similarly, although full inhibition of proliferation with NVP-BEZ235 could be reached in both BON-1/R and QGP-1/R, a higher concentration of NVP-BEZ235 is needed to overcome resistance in QGP-1/R. Hence, we could conclude that

the underlying mechanisms of everolimus resistance in BON-1/R and QGP-1/R might be different. If our data can be extrapolated to PNET patients, our study could provide an insight in the mechanisms determining resistance to mTOR inhibition in the clinic. Ultimately, this might lead to a better selection of patients and true personalized medicine.

In conclusion, the first PNET models for long-term everolimus treatment, resulting in acquired rapalog-resistance, are presented here. Both the ATP-competitive mTOR blocker, AZD2014, as the dual PI3K-mTOR blocker NVP-BEZ235 are able to overcome this rapalog resistance. Further evaluation of both drugs in *in vivo* and patients' studies, targeted at overcoming everolimus resistance, could hence be challenging. Additionally, both models allow the study of the detailed mechanisms of acquired resistance in PNET. Expanding these studies with advanced genetic and genomic techniques, such as next generation sequencing, could lead to the identification of biomarkers for everolimus resistance.

VI. ACKNOWLEDGEMENTS

The BON-1 cell line was a kind gift from J.C. Thompson, Department of Surgery, University of Texas Medical Branch, Galveston, Texas, USA to Leo J. Hofland, Section of Endocrinology, Department of Internal Medicine, Erasmus Medical Center, Rotterdam, the Netherlands for research purposes. This work was supported by the Flemish Agency of Scientific Research (FWO grant G.0327.13N)

and the ENETS-Ipsen 2013 Translational Research Fellowship.

VII. REFERENCES

1. Yao, J. C. *et al.* One hundred years after 'carcinoid': Epidemiology of and prognostic factors for neuroendocrine tumors in 35,825 cases in the United States. *J. Clin. Oncol.* **26,** 3063–3072 (2008).
2. Lawrence, B. *et al.* The Epidemiology of Gastroenteropancreatic Neuroendocrine Tumors. *Endocrinology and Metabolism Clinics of North America* **40,** 1–18 (2011).
3. Fraenkel, M., Kim, M. K., Faggiano, A. & Valk, G. D. Epidemiology of gastroenteropancreatic neuroendocrine tumours. *Best Pract. Res. Clin. Gastroenterol.* **26,** 691–703 (2012).
4. Halfdanarson, T. R., Rubin, J., Farnell, M. B., Grant, C. S. & Petersen, G. M. Pancreatic endocrine neoplasms: Epidemiology and prognosis of pancreatic endocrine tumors. *Endocrine-Related Cancer* **15,** 409–427 (2008).
5. Corbo, V. *et al.* Pancreatic endocrine tumours: Mutational and immunohistochemical survey of protein kinases reveals alterations in targetable kinases in cancer cell lines and rare primaries. *Ann. Oncol.* **23,** 127–134 (2012).
6. Calender, A. [Recent data on molecular genetics of neuroendocrine tumors]. *Ann Endocrinol* **58,** 113–123 (1997).
7. Hansel, D. E. *et al.* Expression of neuropilin-1 in high-grade dysplasia, invasive cancer, and metastases of the human gastrointestinal tract. *Am. J. Surg. Pathol.* **28,** 347–56 (2004).
8. Schonhoff, S. E., Giel-Moloney, M. & Leiter, A. B. Minireview: Development and differentiation of gut endocrine cells. *Endocrinology* **145,** 2639–2644 (2004).
9. Ekeblad, S. *et al.* Temozolomide as monotherapy is effective in treatment of advanced malignant neuroendocrine tumors. *Clin. Cancer Res.* **13,** 2986–2991 (2007).
10. Strosberg, J. R. *et al.* First-line chemotherapy with capecitabine and temozolomide in patients with metastatic pancreatic endocrine carcinomas. *Cancer* **117,** 268–275 (2011).

11. Missiaglia, E. *et al.* Pancreatic endocrine tumors: expression profiling evidences a role for AKT-mTOR pathway. *J Clin Oncol* **28,** 245–255 (2010).
12. Jiao, Y. *et al.* DAXX/ATRX, MEN1, and mTOR pathway genes are frequently altered in pancreatic neuroendocrine tumors. *Science (80-.).* **331,** 1199–1203 (2011).
13. Capdevila, J., Salazar, R., Halperín, I., Abad, A. & Yao, J. C. Innovations therapy: mammalian target of rapamycin (mTOR) inhibitors for the treatment of neuroendocrine tumors. *Cancer Metastasis Rev.* **30 Suppl 1,** 27–34 (2011).
14. Helpap, B. & Köllermann, J. Undifferentiated carcinoma of the prostate with small cell features: Immunohistochemical subtyping and reflections on histogenesis. *Virchows Arch.* **434,** 385–391 (1999).
15. Lach, B., Gregor, A., Rippstein, P. & Omulecka, A. Angiogenic histogenesis of stromal cells in hemangioblastoma: Ultrastructural and immunohistochemical study. *Ultrastruct. Pathol.* **23,** 299–310 (1999).
16. Goto, K. *et al.* Clinicopathologic and DNA cytometric analysis of carcinoid tumors of the thymus. *Mod. Pathol.* **14,** 985–994 (2001).
17. Yao, J. C. *et al.* Everolimus for advanced pancreatic neuroendocrine tumors. *N. Engl. J. Med.* **364,** 514–23 (2011).
18. Raymond, E. *et al.* Sunitinib malate for the treatment of pancreatic neuroendocrine tumors. *N. Engl. J. Med.* **364,** 501–13 (2011).
19. Yao, J. C., Phan, A. T., Jehl, V., Shah, G. & Meric-Bernstam, F. Everolimus in advanced pancreatic neuroendocrine tumors: The clinical experience. *Cancer Research* **73,** 1449–1453 (2013).
20. Maira, S.-M. *et al.* Identification and characterization of NVP-BEZ235, a new orally available dual phosphatidylinositol 3-kinase/mammalian target of rapamycin inhibitor with potent in vivo antitumor activity. *Mol. Cancer Ther.* **7,** 1851–1863 (2008).
21. Yu, K. *et al.* Biochemical, cellular, and in vivo activity of novel ATP-competitive and selective inhibitors of the mammalian target of rapamycin. *Cancer Res.* **69,** 6232–40 (2009).
22. Passacantilli, I. *et al.* Combined therapy with RAD001 e BEZ235 overcomes resistance of PET immortalized cell lines to mTOR inhibition. *Oncotarget* **5,** 5381–91 (2014).

23. Townsend Jr., C. M., Ishizuka, J. & Thompson, J. C. Studies of growth regulation in a neuroendocrine cell line. *Acta Oncol* **32,** 125–130 (1993).
24. Kaku, M., Nishiyama, T., Yagawa, K. & Abe, M. Establishment of a carcinoembryonic antigen-producing cell line from human pancreatic carcinoma. *Gann* **71,** 596–601 (1980).
25. Vandamme, T. *et al.* Whole-exome characterization of pancreatic neuroendocrine tumor cell lines BON-1 and QGP-1. *J. Mol. Endocrinol.* **54,** (2015).
26. Barrett, P. *et al.* Endocrine cells of the human gastrointestinal tract have no proliferative capacity. *Histochem. J.* **27,** 482–486 (1995).
27. Arvidsson, S., Kwasniewski, M., Riaño-Pachón, D. M. & Mueller-Roeber, B. QuantPrime - A flexible tool for reliable high-throughput primer design for quantitative PCR. *BMC Bioinformatics* **9,** (2008).
28. Mestdagh, P. *et al.* A novel and universal method for microRNA RT- qPCR data normalization . Genome Biol 10 : R64 normalization. *Genome Biol.* **10,** R64 (2009).
29. O'Donnell, A. *et al.* Phase I pharmacokinetic and pharmacodynamic study of the oral mammalian target of rapamycin inhibitor everolimus in patients with advanced solid tumors. *J. Clin. Oncol. Off. J. Am. Soc. Clin. Oncol.* **26,** 1588–1595 (2008).
30. Yao, J. C. *et al.* Everolimus for advanced pancreatic neuroendocrine tumors. *N Engl J Med* **364,** 514–523 (2011).
31. Kang, S. A. *et al.* mTORC1 phosphorylation sites encode their sensitivity to starvation and rapamycin. *Science (80-.).* **341,** 1–16 (2013).
32. Julien, L.-A., Carriere, A., Moreau, J. & Roux, P. P. mTORC1-Activated S6K1 Phosphorylates Rictor on Threonine 1135 and Regulates mTORC2 Signaling. *Mol. Cell. Biol.* **30,** 908–921 (2010).
33. O 'reilly, K. E. *et al.* Kinase Signaling and Activates Akt mTOR Inhibition Induces Upstream Receptor Tyrosine mTOR Inhibition Induces Upstream Receptor Tyrosine Kinase Signaling and Activates Akt. *Cancer ResCancer Res* **66,** 1500–1508 (2006).
34. Ohike, N., Jürgensen, a, Pipeleers-Marichal, M. & Klöppel, G. Mixed ductal-endocrine carcinomas of the pancreas and ductal adenocarcinomas with scattered endocrine cells: characterization of the endocrine cells.

Virchows Arch. **442,** 258–65 (2003).
35. Emerling, B. M. & Akcakanat, A. Targeting PI3K/mTOR signaling in cancer. in *Cancer Research* **71,** 7351–7359 (2011).
36. Basu, B. *et al.* First-in-human pharmacokinetic and pharmacodynamic study of the dual m-TORC 1/2 inhibitor AZD2014. *Clin. Cancer Res.* **21,** 3412–3419 (2015).
37. Pike, K. G. *et al.* Optimization of potent and selective dual mTORC1 and mTORC2 inhibitors: The discovery of AZD8055 and AZD2014. *Bioorganic Med. Chem. Lett.* **23,** 1212–1216 (2013).
38. Bhagwat, S. V. *et al.* Preclinical Characterization of OSI-027, a Potent and Selective Inhibitor of mTORC1 and mTORC2: Distinct from Rapamycin. *Mol. Cancer Ther.* **10,** 1394–1406 (2011).
39. Doglioni, C. *et al.* Cyclin D3 expression in normal, reactive and neoplastic tissues. *J. Pathol.* **185,** 159–166 (1998).
40. Paireder, S. *et al.* Comparison of protocols for DNA extraction from long-term preserved formalin fixed tissues. *Anal. Biochem.* **439,** 152–160 (2013).
41. Carracedo, A. *et al.* Inhibition of mTORC1 leads to MAPK pathway activation through a PI3K-dependent feedback loop in human cancer. *J. Clin. Invest.* **118,** 3065–3074 (2008).
42. Svejda, B. *et al.* Limitations in small intestinal neuroendocrine tumor therapy by mTor kinase inhibition reflect growth factor-mediated PI3K feedback loop activation via ERK1/2 and AKT. *Cancer* **117,** 4141–4154 (2011).
43. Zitzmann, K. *et al.* Compensatory activation of Akt in response to mTOR and Raf inhibitors - A rationale for dual-targeted therapy approaches in neuroendocrine tumor disease. *Cancer Lett.* **295,** 100–109 (2010).
44. Fazio, N. *et al.* A phase II study of BEZ235 in patients with everolimusresistant, advanced pancreatic neuroendocrine tumours. *Anticancer Res.* **36,** 713–720 (2016).
45. Bendell, J. C. *et al.* A phase 1 study of the sachet formulation of the oral dual PI3K/mTOR inhibitor BEZ235 given twice daily (BID) in patients with advanced solid tumors. *Invest. New Drugs* **33,** 463–471 (2015).
46. Gebauer, N. *et al.* Genomic landscape of pancreatic neuroendocrine

tumors. *World J. Gastroenterol.* **20,** 17498–17506 (2014).
47. Yang, L. *et al.* Comprehensive lipid profiling of plasma in patients with benign breast tumor and breast cancer reveals novel biomarkers. *Anal. Bioanal. Chem.* **407,** 5065–5077 (2015).
48. Marusyk, A. *et al.* Non-cell autonomous tumor-growth driving supports sub-clonal heterogeneity. *Nature* **514,** 54–58 (2014).

1. SUPPLEMENTARY TABLE 1

Gene name	Forward primer	Reverse primer
RICTOR	5'-ACAGCTCACGGTTGTAG-GTTGC-3'	5'-TCTAAGTAGCCTTGC-CCATCCTC-3'
S6K1	5'-GGGAGTTGGACCATAT-GAACTTGG-3'	5'-GCCCTCTGTTCA-CACTAGTTTCTG-3'
4EBP1	5'-GGCGGTGAAGAGTCA-CAGTTTG-3'	5'-TTGGTAGTGCTCCACACGAT-GG-3'
HIF1A	5'-AGCCGCTGGAGACACAAT-CATATC-3'	5'-TGCTGGTCATCAGTTTCTGT-GTCG-3'
MTOR	5'-ATGTGGGCAGCAT-CACTCTTGC-3'	5'-ATTGGGTCAGAGAGTGG-CCTTC-3'
BCL2	5'-CTGGGATGCCTTTGTG-GAACTG-3'	5'-AGTCTTCAGAGACAGCCAG-GAG-3'
RAPTOR	5'-AGCTGGAGGATGAAGGATC-GGATG-3'	5'-AGGGTCCACACCAACAT-TCAGG-3'
ERK1	5'-GCAGGACCTGATGGAGACT-GAC-3'	5'-CCAGAATGCAGCCCA-CAGAC-3'
ERK2	5'-GCGCTACACCAACCTCTCGT-3'	5'-CACGGTGCAGAACGT-TAGCTG-3'

2. SUPPLEMENTARY FIGURE 2

Figure 2 | Cell line morphology.

No morphological changes were seen between the long-term vehicle-treated cell lines (A: BON-1; C: QGP-1) and the long-term everolimus-treated cell lines (B: BON-1/R; D: QGP-1/R)

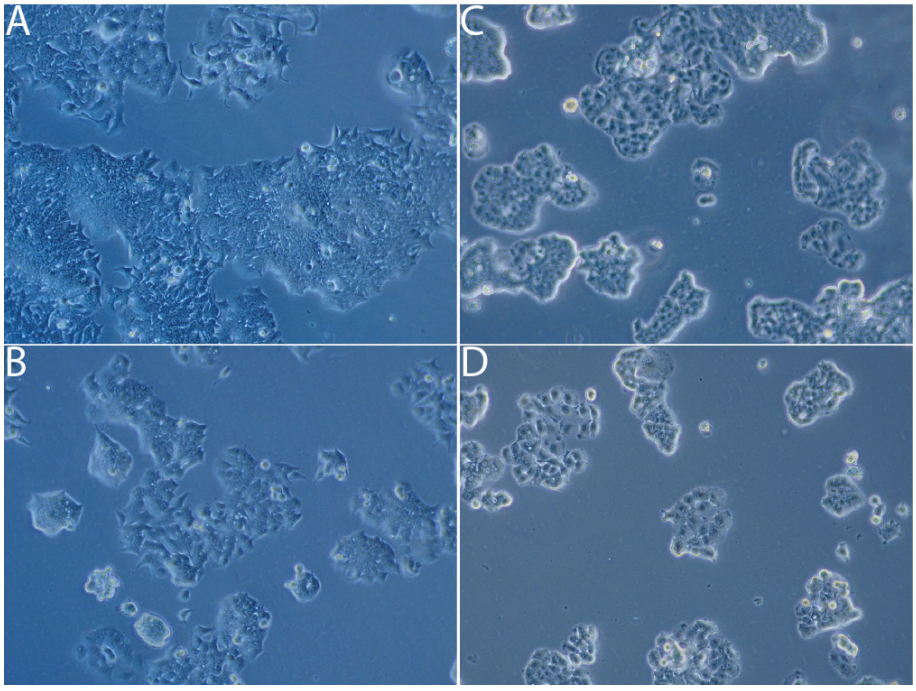

CDK4 amplification and CDKN1B (p27) deletion in acquired rapalogue resistant neuroendocrine neoplasm cells

Matthias Beyens*[1,2], Timon Vandamme*[1,2,3], Gitta Boons[1,2], Anne Schepers[1], Geert Vandeweyer[1], Wouter de Herder[3], Leo Hofland[3], Marc Peeters[2], Guy Van Camp[1,2] and Ken Op de Beeck[1,2]

[1]Center of Medical Genetics Antwerp, University of Antwerp, Edegem, Belgium
[2]Center of Oncological Research (CORE), University of Antwerp, Antwerp, Belgium
[3]Department of Internal Medicine, Section of Endocrinology, Erasmus Medical Center, Rotterdam, The Netherlands
[4]Department of Oncology, Antwerp University Hospital, Antwerp, Belgium
* Equal contributing authors

Submitted for publication

I. ABSTRACT

1. BACKGROUND

Rapalogues improve progression-free survival in advanced neuroendocrine neoplasms (NEN). However, acquired resistance to rapalogues is described in cell line models and in two phase-III trials. To the best of our knowledge, no genetic mechanism for acquired rapalogue resistance in NEN has been identified.

2. METHODS

Rapalogue resistance was previously induced in BON-1 and QGP-1 through continuous culture in increasing doses of everolimus, resulting in resistant cell lines. Copy number analysis was performed on the sensitive and resistant cell lines. Gene expression analysis was performed on differentially regulated genes.

3. RESULTS

Pathway analysis showed significant enrichments in the cell cycle pathway in rapalogue-resistant cell lines. We found a *CDK4* amplification and *CDKN1B* (p27) deletion. These copy number alterations significantly impact the cell cycle gene RNA expression levels.

4. CONCLUSIONS

The association of *CDK4* and *CDKN1B* (p27) copy number alterations with rapalogue, and thus everolimus sensitivity is demonstrated for the first time in NENs, in line with studies in other cancer types. This study highlights the potential use of CDK4 and p27 as biomarkers for the efficacy of rapalogues in NENs. Additionally, it provides rationale for the use of cell cycle inhibitors in the treatment of rapalogue resistant NENs. These findings contribute to the understanding of rapalogue resistance in NENs and other cancer types.

II. INTRODUCTION

The phosphoinositide-3-kinase/Akt/mammalian target of rapamycin (PI3K-Akt-mTOR) signaling pathway plays a vital role in the integration of environmental cues, regulating growth and homeostasis[1]. Upregulation of the PI3K-Akt-mTOR pathway has been observed in different cancers, including breast cancer, renal cell carcinoma and neuroendocrine neoplasms (NENs)[1]. NENs are tumors derived from the neuroendocrine cells throughout the body. Although considered rare, recent data shows a rising incidence of NENs in the pancreas, lung and small intestine[2].

Genetic studies in NEN have identified PI3K-Akt-mTOR pathway alterations in NEN cell lines and patients, making it an attractive therapeutic target[3–5]. Rapamycin and analogues, so-called rapalogues, are non-ATP-competitive mTOR complex-1 (mTORC1) inhibitors. mTORC1 incorporates the rapamycin-sensitive accessory protein Raptor. Rapalogues, such as everolimus, bind to intracellular receptor FKBP12, hereby inhibiting complexation with Raptor[1]. By blocking mTORC1 formation, rapalogues effectively circumvent the highly conserved serine/threonine-specific protein kinase activity of mTORC1. Hence, everolimus and other rapalogues deregulate the translation initiation control mechanism through inhibition of factor 4E (eIF4E) and S6 kinase 1 (S6K1), downstream of mTORC1[6]. Two phase-III trials with everolimus were conducted, respectively, in 410 patients with well- and moderately differentiated pNENs and in 302 patients with lung and gastrointestinal NENs. Both trials showed an improvement in

median progression-free survival (PFS) in the everolimus-treated group compared with the placebo group[7]. However, PFS in both phase-III studies with everolimus was still limited to 11 months and acquired resistance to mTOR inhibition with rapalogues was described[8].

To study this acquired resistance, we previously induced rapalogue resistance using the drug everolimus in two well-established human pancreatic NEN cell lines[9]. In this study, we aimed to detect structural genetic variations between rapalogue-sensitive parental cell lines, BON-1 and QGP-1, and rapalogue-resistant cell lines BON-1/R and QGP-1/R using low-pass whole-genome sequencing (LP-WGS). Ultimately, this study could lead to the identification of interesting new therapeutic targets and combinations to prevent and/or overcome resistance to rapalogues.

III. MATERIALS AND METHODS

1. CELL LINES AND CULTURE CONDITIONS

BON-1 and QGP-1, two human pNEN cell line models, were used in this study. The BON-1 cell line was a kind gift from Dr Townsend (University of Texas Medical Brachn, Galveston, TX, USA; Townsend et al, 1993). The QGP-1 cell line was purchased from the Japanese Collection of Research Bioresources Cell Bank (JRCB, Osaka, Japan)[10]. BON-1 and QGP-1 cell line identity was confirmed using short tandem repeat profiling[4,11]. The BON-1 cell line

was cultured in 1:1 mixture of Dulbecco's modified Eagle medium (DMEM) and F12 medium, supplemented with 10% fetal calf serum (FCS), penicillin (1 × 105 units per l), fungizone (0.5 mg/l), and L-glutamine (2 mmol/l). The QGP-1 cell line was cultured in Roswell Park Memorial Institute (RPMI) 1640 medium, supplemented with 10% FCS and penicillin-streptomycin (1 × 105 units per l penicillin and 1 × 105 units per l streptomycin). All cell lines were incubated in an atmosphere of 95% humidity and 5% CO_2 at 37 °C. Media and supplements were obtained from Life Technologies Bio-cult Europe (Invitrogen, Breda, The Netherlands). In previous published research, we developed two acquired rapalogue-resistant cell lines by step-wise increase of everolimus concentrations for a period of 20 and 22 weeks to reach a dose of 1 μM everolimus, 1000-fold and 250-fold initial IC_{50}, BON-1 and QGP-1 respectively[9]. Applying this cell culture method, we established rapalogue(rapamycin/everolimus)-sensitive parental cell lines, BON-1 and QGP-1, and rapalogue(rapamycin/everolimus)-resistant cell lines, BON-1/R and QGP-1/R.

2. DRUGS AND REAGENTS

Everolimus (RAD001, 40-O [2-hydroxyethyl] rapamycin) was purchased from Selleckchem (Selleck Chemicals, Houston, TX, USA). Everolimus was dissolved in 100% dimethylsulfoxide (DMSO) to a 1 mM concentration and stored at −20 °C. Upon use, everolimus was diluted to a 1 μM working concentration in 40% DMSO before use. Rapalogue-sensitive parental cell lines were continuously cultured in medium containing 0.4% DMSO. Rapalogue-resistant

cell lines were continuously cultured in medium containing 1 μM everolimus-enriched.

3. LOW-PASS WHOLE-GENOME SEQUENCING AND COPY NUMBER ANALYSIS

Genomic DNA of everolimus-sensitive parental cell, BON-1 and QGP-1, and everolimus-resistant cell lines, BON-1/R and QGP-1/R, was isolated using a QIAamp DNA Mini Kit (Qiagen), following the manufacturer's instructions. Concentration of isolated DNA was quantified using a Qubit 2.0 fluorometer using dsDNA Broad Range Assay (Thermo Scientific, Waltham, MA, USA). DNA gel electrophoresis was performed for exclusion of DNA degradation.

Two micrograms of isolated BON-1, BON-1/R, QGP-1 and QGP-1/R high-quality DNA were fragmented using a focused-ultrasonicator (Covaris M220, Covaris, Woburn, MA, USA) running the following program: duty factor of 20%, peak power of 50 with 200 cycles/burst during 120 s. Next, all samples were prepared for whole-genome sequencing using a TruSeq DNA Sample Preparation Kit (Illumina Inc., San Diego, CA, USA) following the low-throughput, gel-free protocol according to the manufacturer's instructions. Paired-end libraries of each parental and resistant cell line were 2x100 bp sequenced on an Illumina HiSeq1500 instrument (Illumina Inc., San Diego, CA, USA).

Sequencing reads were adaptor trimmed with CutAdapt (v1.12) and mapped to the human genome build 19 (hg19) with Burrows Wheeler Aligner (BWA v0.7.15). The presence of CNVs in the

samples was analyzed using in-house developed analysis pipelines. The algorithm divides the genome into non-overlapping 50 kb-bins and counts all mapped sequencing reads for each rapalogue-sensitive parental cell line and rapalogue-resistant cell line within each bin. Next, $\log_2$-ratios were calculated for every parental and resistant cell line pair.

The circular binary segmentation (CBS) algorithm from DNACopy was used to normalize and subsequent log profile the $\log_2$-ratios[12]. The segmentation algorithm calls rapalogue-resistant cell line 50-kb amplifications and deletions. As a $\log_2$-ratio threshold we used -0.25 for deletions and 0.25 for amplifications. GC normalization was performed on the read counts to reduce biases introduced by differences in GC content between bins.

4. PATHWAY ENRICHMENT ANALYSIS

Pathway enrichment analysis was performed on copy number altered gene-set with the hypergeometric model available from the Reactome Pathway Knowledgebase to assess whether the number of altered genes in the resistant cell lines associates with any pathway[13]. Adjusted P-values were calculated on the hypergeometric model.

5. QUANTITATIVE REAL-TIME PCR OF CELL CYCLE REGULATORY GENES

The rapalogue-sensitive parental and rapalogue-resistant cell lines were plated in 3 ml medium in six-well plates at the density

required to obtain 70–80% cell confluence at the end of the experiment. Twenty-four hours later for QGP-1 cells and 72 h later for BON-1 cells, medium was replaced and cells were incubated for 72 h with vehicle. Quantitative PCR (qPCR) was performed on cDNA from three biological replicates using the Power SYBR Green kit (Life Technologies, Thermo Fisher Scientific, Waltham, MA, USA) on a LightCycler 480 instrument (Roche Applied Science, Penzberg, Germany). Primers provided by RTPrimerDB (http://www.rtprimerdb.org) have been obtained from Integrated DNA Technologies (Leuven, Belgium) (Supplementary Material 1). All reactions have been performed in triplicates in 384-well plates with 2 µl total RNA (pre-diluted to 15 ng/µl) as input in a total reaction volume of 10 µl, further comprising 5 µl Power SYBR Green RT-PCR Mix (2×; Life Technologies, Thermo Fisher Scientific), 0.08 µl RT Enzyme Mix (125×; Life Technologies, Thermo Fisher Scientific) and 200 nM of each primer (final concentration).

Normalized relative *CCND1*, *CCNE1*, *CDK2*, *CDK4*, *CDK6*, *CDKN1A*, *CDKN1B*, *E2F1* and *RB1* transcript expression values were calculated using qBasePLUS software version 1.6 (Biogazelle, Zwijnaarde, Belgium). Messenger RNA expression was normalized to household gene expression (*GAPDH* and *RPL13A* for BON-1; *HPRT* and *YWAZ* for QGP-1) according to the geNorm algorithm and our previous cell line paper[9,14]. Comparison between gene expression levels was done by Student's t-test. All statistical analyses were performed using GraphPad Prism 6.0 for Mac (GraphPad Software, La Jolla, CA, USA).

IV. RESULTS

1. LOW-PASS WHOLE-GENOME SEQUENCING DATA

We performed low-pass whole-genome sequencing (LP-WGS) on everolimus-sensitive parental cell lines BON-1 and QGP-1, and on everolimus-resistant cell lines BON-1/R and QGP-1/R. LP-WGS allows a highly specific detection of subchromosomal amplifications and deletions. LP-WGS reads were trimmed and mapped to version 19 of the human genome. Coverages ranged from 1.97× and 2.08×, BON-1 and BON-1/R respectively, and 2.09× and 1.86×, QGP-1 and QGP-1/R respectively. Next, average read depths in 50 kb-bin windows were calculated for each cell line. Subsequently, everolimus-resistant cell lines were compared with their everolimus-sensitive parental counterparts and logarithmically transformed to obtain $\log_2$-ratio copy number values.

2. MULTIPLE SUBCHROMOSOMAL AMPLIFICATIONS AND DELETIONS IN RAPALOGUE-RESISTANCE BON-1/R AND QGP-1/R

We identified (sub)chromosomal numeric alterations in BON-1/R and QGP-1/R. For BON-1/R, in total, 4 and 6 chromosomal regions were amplified or deleted, respectively (Figure 1A, Supplementary Material 2). For QGP-1/R, in total, 8 and 9 chromosomal regions were amplified or deleted, respectively (Figure 1B, Supplementary Material 2). At the gene level, we observed 1008 and 773 genes that were amplified and deleted, respectively, in BON-1/R, while

in QGP-1/R, we detected 643 and 1675 genes that were amplified and deleted, respectively.

Within these amplifications and deletions across BON-1/R and QGP-1/R, we evaluated whether known oncogenes and tumor suppressor genes were altered. This allows identification of genes with potential relation to growth advantages, e.g. acquired resistance to continuously everolimus treatment. First, we compared the resulting amplification and deletion CNV lists from our *in vitro* study with the COSMIC database (12th April 2017). Secondly, we evaluated whether known COSMIC cancer genes were oncogenes and/or tumor suppressor genes (TSGs) (Supplementary Material 3). For BON-1/R amplified genes, 36 genes were present in the COSMIC database. Of the 36 amplified genes, 36% were oncogenes and 39% were tumor suppressor genes, 6% had a dual annotation, and 19% could not be assigned to any of these categories. For BON-1/R deleted genes, 14 genes were found in COSMIC. Of the 14 deleted genes, 29% were oncogenes and 36% were tumor suppressor genes, 7% had a dual annotation, and 29% could not be assigned to the latter categories. Next, we analyzed the QGP-1/R amplified genes of which 24 genes were known in COSMIC. Of the 24 amplified genes, 38% were oncogenes and 46% were tumor suppressor genes and 17% could not be assigned to the latter categories. Investigation of the QGP-1/R deleted genes, indicated 38 genes as present in COSMIC. Of the 38 deleted genes, 21% were oncogenes and 45% were tumor suppressor genes, 5% had a dual annotation, and 29% could not be assigned to the latter categories.

3. SHARED SUBCHROMOSOMAL AMPLIFICATIONS AND DELETIONS ACROSS RAPALOG-RESISTANT CELL LINES

While the overall genome structures were cell line-specific, we observed regions of shared copy number changes between the resistant cell lines. These similarities in genome structure might be suggestive for a shared mechanism of action. In total, we detected 34 recurrent amplified genes and 37 recurrent deleted genes (Supplementary Material 4). All these genes were located on chromosome 8 and chromosome 20.

4. CELL CYCLE REGULATORY COMPONENTS ARE ALTERED IN RAPALOGUE-RESISTANT BON-1/R AND QGP-1/R

Pathway enrichment analysis on copy number altered gene-sets revealed significant enrichment of several cell cycle associated GO identifiers in BON-1/R (GO:0044770: FDR = $2.88e^{-3}$; GO:0045787: FDR = $1.66e^{-2}$; GO0045786: FDR = $1.87e^{-2}$; GO:0045931: FDR = $2.20e^{-2}$; GO:0007050: FDR = $2.34e^{-2}$; GO:0051726: FDR = $2.43e^{-2}$) and in QGP-1/R (GO:0045786: FDR = $2.55e^{-4}$; GO:0007050: FDR = $2.71e^{-2}$) in comparison to its sensitive counterparts. For this reason, we focused on the alterations in cell cycle components.

In the current study, we found *CDK4* to be amplified and *CDKN1B*, coding for p27, to be deleted, in BON-1/R and QGP-1/R respectively compared to their sensitive comparators. Both genes are present and functionally annotated in the COSMIC database (Supplementary Material 3). The oncogene *CDK4* promotes cell cycle progression through G_1-S phase stimulation, and consequently induces

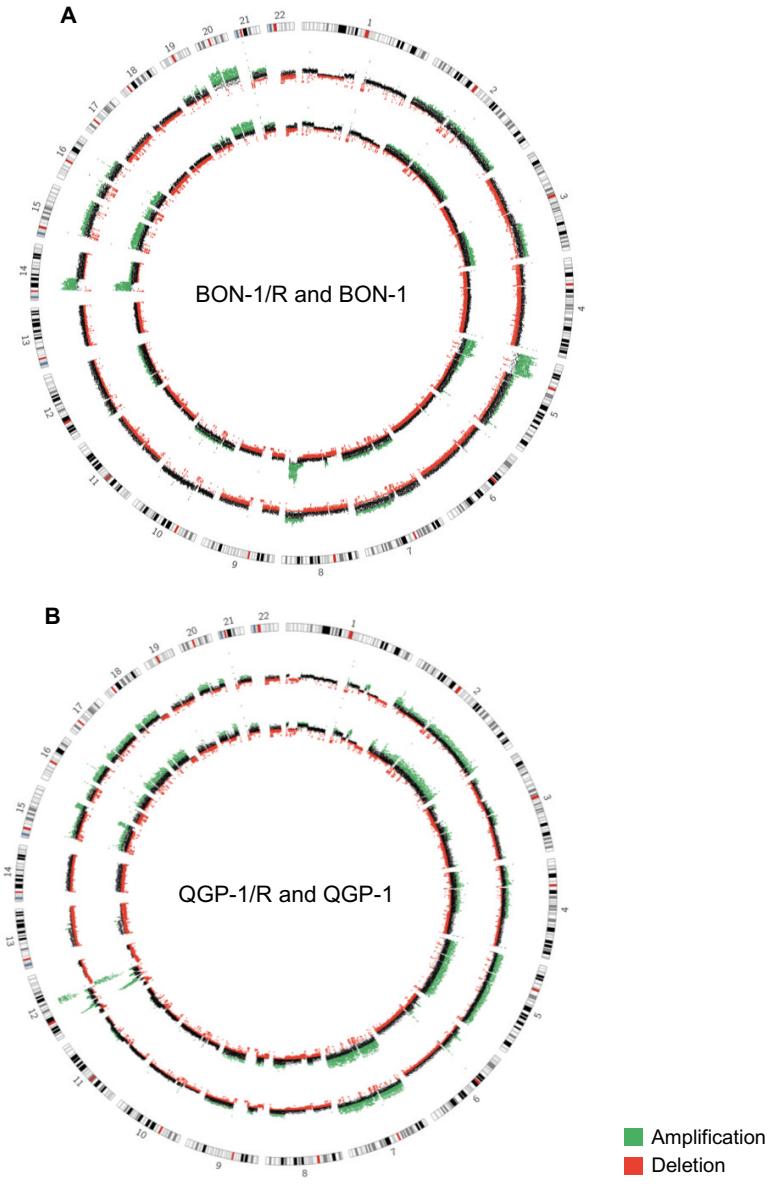
A
BON-1/R and BON-1
B
QGP-1/R and QGP-1
Amplification
Deletion

DNA synthesis. On the other hand, the tumor suppressor gene *CDKN1B* regulates and inhibits G_1-S phase transition.

Therefore, we investigated the impact of these alterations on the gene expression of the G_1-S cell cycle regulatory components. Comparison of gene expression of *CCND1*, *CCNE1*, *CDKN1A*, *CDKN1B*, *CDK2*, *CDK4*, *CDK6*, *E2F1* and *RB1* between BON-1/R and parental everolimus-sensitive BON-1 showed a significant upregulation of *CCND1*, *CDK4* and *CDK6*, whereas *CDKN1A* was significantly downregulated (P<0.05) (Figure 2A). When comparing QGP-1/R and QGP-1, a significant upregulation of *CCND1* and *CDK6*, and a significant downregulation of *CDKN1B* and *E2F1* were observed (P<0.05) (Figure 2B).

Figure 1 | Circos plot summarizing copy number changes in resistant and sensitive cell lines.

Copy number changes are summarized in a Circos plot for BON-1/R and BON-1 (A), and QGP-1/R and QGP-1 (B). From outer to inner ring: 1) chromosomal ideogram 2) copy number changes of sensitive cell line 3) copy number changes of rapalogue-resistant cell line. Read depths of aligned low-pass whole genome sequencing data are plotted per chromosome against the genomic coordinates (in Mb). Deletions and amplifications are colored red and green, respectively.

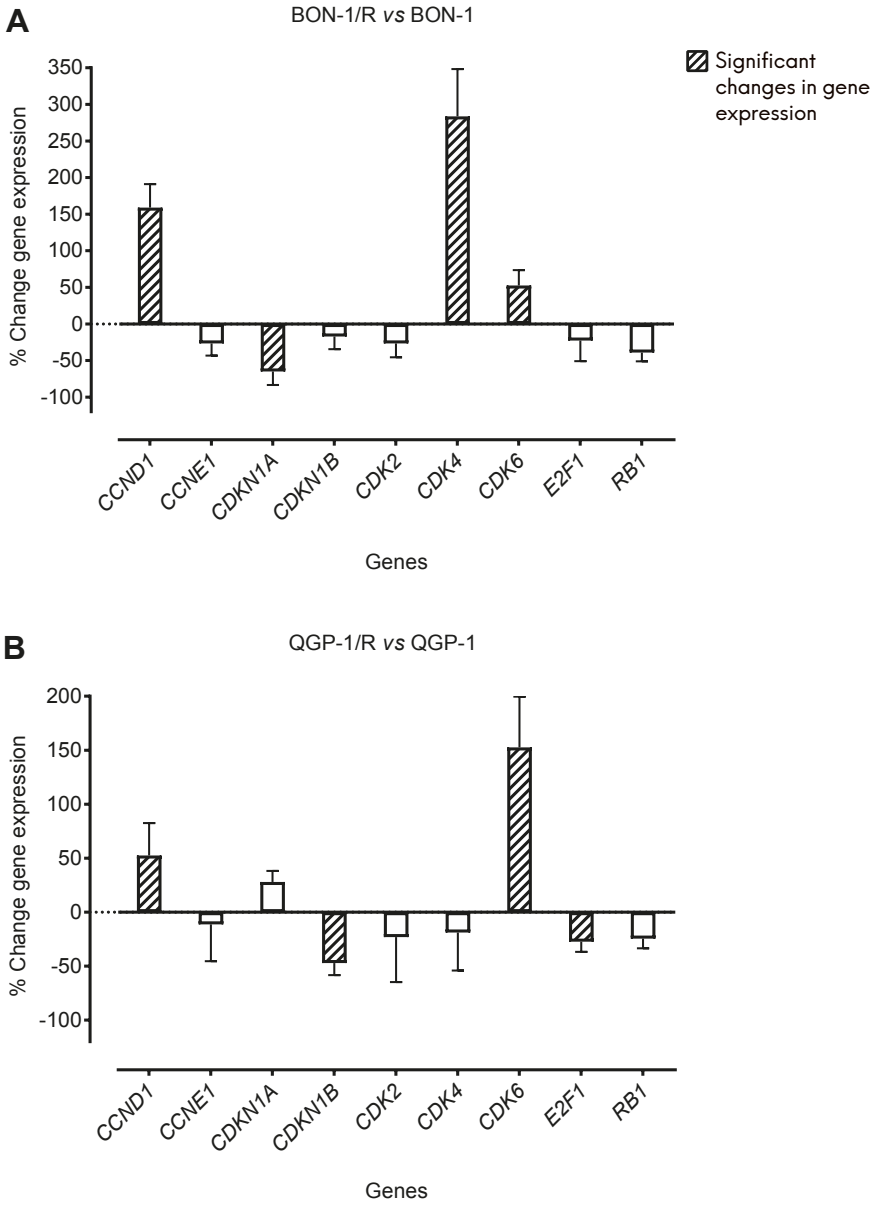
A
BON-1/R vs BON-1
Significant changes in gene expression
% Change gene expression
350
300
250
200
150
100
50
0
-50
-100
CCND1
CCNE1
CDKN1A
CDKN1B
CDK2
CDK4
CDK6
E2F1
RB1
Genes
B
QGP-1/R vs QGP-1
% Change gene expression
200
150
100
50
0
-50
-100
CCND1
CCNE1
CDKN1A
CDKN1B
CDK2
CDK4
CDK6
E2F1
RB1
Genes

Figure 2 | Changes in mRNA expression between resistant and sensitive cell lines.

Changes are expressed in mean percentage ± s.e.m. between BON-1/R and BON-1 (A), and QGP-1/R and QGP-1 (B). The expression of CCND1 (encoding cyclin D1), CCNE1 (cyclin E1), CDKN1A (p21), CDKN1B (p27), CDK2 (CDK2), CDK4 (CDK4), CDK6 (CDK6) E2F1 (E2F1) and RB1 (RB1) was determined. Differences were tested using Student's t-test. $P<0.05$ was considered significant (hatched bars).

V. DISCUSSION

In the pivotal Radiant trials, treatment with everolimus demonstrated an improved progression-free survival in advanced NENs[8]. However, no molecular biomarkers for everolimus efficacy in NEN have been identified yet. In our previous publication, we show that the two *in vitro* pNEN models, BON-1 and QGP-1, are sensitive for everolimus treatment at baseline[9]. The study shows that sensitivity to rapamycin and rapalogues, such as everolimus, is not an intrinsic trait of the sensitive cell lines, and that the efficacy is not the same in both cell lines[9]. Subsequently, everolimus resistance was induced in BON-1 and QGP-1[9], resulting in two everolimus resistant cell lines, BON-1/R and QGP-1/R. Since genetic aberrations were shown to have major contributions in acquired resistance in other tumor types[15], we investigated copy number alterations in both resistant cell lines. Previously, we have characterized the copy number alterations of the everolimus sensitive BON-1 and QGP-1 in detail and showed the validity of these models as research tools for pNEN[16].

In this study, we used low-pass whole-genome sequencing, a technique that is able to detect copy number variations but does

not allow detection of small nucleotide variations due to the low coverage. Most of the detected copy number alterations in BON-1/R and QGP-1/R do not affect oncogenes or TSGs, nor alter the mechanism of action of rapalogues on the PI3K/Akt/mTOR pathway or any downstream effectors (Supplementary Material 2 and 3). The conclusion is that the majority of these subchromosomal copy number changes probably do not drive everolimus resistance. However, pathway enrichment analysis pointed towards structural variations in cell cycle pathways as possible drivers for everolimus resistance in both everolimus-resistant cell lines. For this reason, we focused on the alterations in cell cycle components.

Recently, the importance of alterations in cell cycle regulatory components in NEN and in the efficacy of rapalogue treatment in different tumor types has been made clear in previous studies[17–21]. Through an Akt-feedback loop, mTOR complex-2 (mTORC2) inhibits Forkhead box class O (FOXO), leading to a decrease of pro-apoptotic stimuli through suppression of *CDKN1B* (p27) promotor activity and, thus, activation of CDK4[22]. p27 predominantly binds the cyclin D – CDK4 complex and subsequently sequesters itself from cyclin E – CDK2 complex and drives the cell to the S-phase entry by loss of inhibition of the cyclin E – CDK2 complex. The multiprotein mTORC2 contains the rapamycin-insensitive companion Rictor, however prolonged rapamycin-exposure does inhibits its formation[23]. Therefore, in the current study, we specifically explored structural variations in cell cycle regulatory component in BON-1/R and QGP-1/R.

1. CYCLIN-DEPENDENT KINASE CDK4 AMPLIFICATION AND UPREGULATION IN BON-1/R

In this study, we have shown that *CDK4* amplification correlates with significant upregulation of *CDK4* in BON-1/R (Figure 2A). Previous experiments in mice have linked the retinoblastoma pathway, and in particular Cdk4, to pNEN tumourigenesis[24]. Indeed, Tang and colleagues demonstrated via immunohistochemistry staining in 92 cases of well-differentiated pNENs, high expression of CDK4 (58% of patients), its substrate phosphorylated RB (68%), and of cyclin D1 (68%)[25]. They found a significant correlation between CDK4 and Cyclin D1 protein levels with phosphorylation status of RB. Additionally, Guo *et al.* described upregulation of cyclin D1 in 20 out of 31 sporadic pNENs[26].

We hypothesize that *CDK4* amplification and its corresponding significant upregulation in everolimus-resistant BON-1/R might increase the cyclin D1 and CDK4 complexation. The latter complex will phosphorylate RB and promote G_1-S-phase transition (Figure 3). We show a significant upregulation of *CCND1*, which might be translated in increased levels of cyclin D1. Shi and colleagues show in *in vitro* experiments that low Akt activity induces resistance towards rapamycin treatment by allowing continued cap-independent protein synthesis of cyclin D1[27]. In our previous study, we show that *Akt*, *mTOR*, *Rictor* and *Raptor* are significantly downregulated in BON-1/R, directly circumventing any Akt activation[9]. Further, Chen and colleagues indicate that high-doses of rapamycin silences the Rictor component formation, which subsequently leads to the inhibition of mTORC2-activating

phosphorylation of Akt[28]. Consequently, this stimulates the cap-independent protein synthesis of cyclin D1. Further, a significant upregulation of *CDK6*, encoding CDK6, and significant downregulation of *CDKN1A*, encoding p21, might support this hypothesis of increased RB phosphorylation (Figure 3).

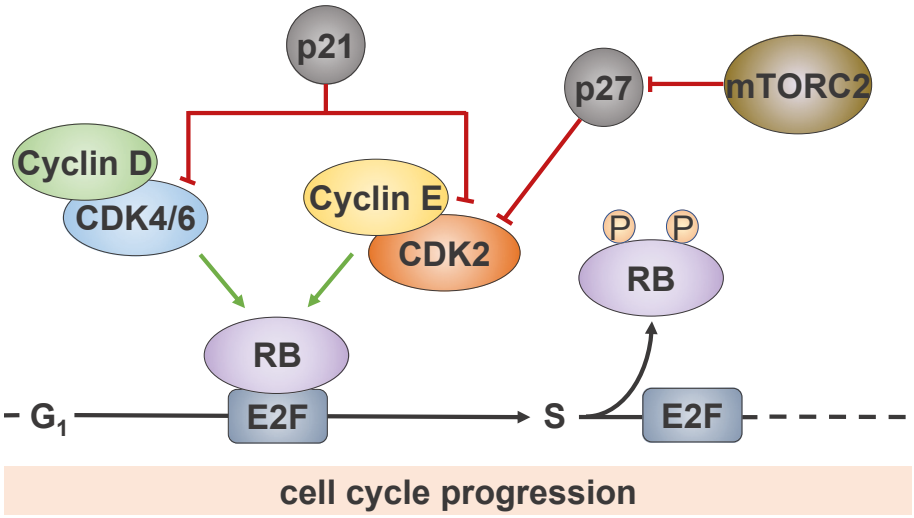

Figure 3 | Overview of cell-cycle regulatory components.

G1-S cell cycle transition acts as a restriction point ensuring controlled cell cycle progression. CDK4 gain and upregulation might promote cell cycle progression in BON-1/R. p27 (CDKN1B) loss and downregulation might result in diminished inhibition and therefore promote cell cycle progression in QGP-1/R. Quiescent cells (G0) enter a gap phase (G1) during which factors, necessary for subsequent DNA synthesis (S) phase, are assembled. G1-S transition is a restriction point that ensures a controlled cell cycle progression. Accumulation of Cyclin D-cyclin-dependent kinase 4 (CDK4) complex regulates this restriction point. Additionally, cell cycle progression is regulated by cyclin-dependent kinase inhibitors (CKIs) such as CDKN1B (p27) and CDKN1A (p21). Upon binding, CKI prevents Cyclin-CDK activation. In G0 and early G1, p27 levels are maximal and it inhibits cyclin E-CDK2. Progressive decrease in p27 during G1-phase allows cyclin E-CDK2 to exert its activity. Cyclin E-CDK2 hyperphosphorylates RB, which subsequently dissociates from transcription factor E2F. E2F activates genes and other transcription factors that are required for G1-S transition and initiation of DNA replication.

2. CYCLIN-DEPENDENT KINASE INHIBITOR CDKN1B DELETION AND DOWNREGULATION IN QGP-1/R

Next to the *CDK4* amplification in BON-1/R, we found a *CDKN1B* ($p27^{Kip1}$) deletion in QGP-1/R that correlates with a significant downregulation of *CDKN1B* expression in QGP-1/R (Figure 2B). Although *CDKN1B* expression is not fully diminished, this may still result in loss of its inhibitory function on Cyclin E-CDK2. First, $p27^{Kip1}$ levels act as an 'all-or-nothing' threshold for G_1-S phase transition (Figure 3). Nourse and colleagues have shown in proliferating cells that cyclin E-Cdk2 still has a significant kinase activity, despite the presence of basal levels of $p27^{Kip1}$[29]. Second, Liang and Slingerland show that upregulation of the MAPK pathway facilitates Ras-driven p27 proteolysis[30]. In our previous publication, we report a significant upregulation of *ERK2* in QGP-1/R, a key component in the MAPK signaling[9].

Further, $p27^{Kip1-/-}$ mice develop islet cell hyperplasia and tumors, including pNENs[24] and upregulation of CDK2 has shown to increase the islet cell proliferation[31,32]. Rapamycin prevents PI3K-Akt-mTOR stimulated downregulation of $p27^{Kip1}$ in rapalogue-sensitive cells[33]. Nevertheless, prolonged rapamycin exposure of sensitive murine BC3H1 fibroblast and T lymphocyte cells results in rapamycin-resistant clones with low p27 levels[34]. Chen and colleagues correlated rapalogue activities and gene expression patterns in the NCI-60 cell lines[35]. They discovered that *CDKN1B* was the most highly positively correlated gene. Cells expressing low levels of p27 exhibited resistance to rapalogues. This correlation has been confirmed in human breast cancer cells and human

cancer xenografts[35].

Furthermore, Diersch *et al*. have shown that p27 levels are predictive for the responsiveness of the dual PI3K/mTOR inhibitor BEZ235 in pancreatic cancer cells and Cho *et al.* found that dual PI3K/mTOR inhibition was more effective than rapamycin both *in vitro* and *in vivo* renal cell carcinoma models[36,37]. In our previous publication, BEZ235 is proven to be a more potent inhibitor and is able to overcome rapalogue resistance. BEZ235 has shown to promote the nuclear accumulation of p27[37]. The re-localization mechanism is the key element in overcoming the rapalogue resistance, as nuclear absence or cytoplasmic localization of p27 has been linked to drug resistance in many *in vitro* cellular studies[38–40].

Noteworthy, frequent somatic mutations, such as protein-inactivating frameshift and hemizygous deletions, encompassing *CDKN1B* were observed in small intestinal NEN, breast and prostate cancer[41–43]. Also, *CDKN1B* is known as *MEN4*, a gene involved in familial MEN syndromes without an identifiable *MEN1* mutation[44].

3. CELL CYCLE REGULATORY COMPONENT ALTERATION AS POTENTIAL NEW THERAPEUTIC TARGET IN OVERCOMING RAPALOGUE RESISTANCE

CDK4 nor p27 have yet been therapeutically targeted in pNENs. CDK4/6 inhibition could be an alternative treatment strategy in overcoming acquired rapalogue resistance. Palbociclib (PD0332991), a CDK4/6 inhibitor, significantly improves progres-

sion-free survival in estrogen receptor-positive (ER+) breast cancer[45]. CDK4/6 inhibition prevents phosphorylation of RB and reactivates binding of RB with E2F. However, acquired resistance towards Palbociclib is not uncommon. It has been shown that a cross-talk between CDK4/6 and other endocrine signaling in breast cancer such as the PI3K/Akt/mTOR pathway drive an alternative mitogen activation[46]. Further, Tang *et al.* have shown that QGP-1 parental cell line, with high levels of CDK4, is less sensitive for rapalogues and responds particularly well to Palbociclib treatment.

4. CDK4 AND CDKN1B AS POTENTIAL BIOMARKERS FOR RAPALOGUE EFFICACY IN PNEN

In vitro experiments could further elucidate the role of p27 and CDK4 in rapalogue sensitivity and could demonstrate whether the latter treatments overcome rapalogue resistance. Another possible follow-up study might focus on the effects of rapalogue treatment on the p27 localization in sensitive and resistant cell lines and tumors. p27 has been extensively studied in various human cancers that show low levels of p27 and its mislocation is associated with poor prognosis[47,48]. In parallel, CDK4 and p27 phosphorylation status would be evaluated. Finally, validity as candidate biomarkers for rapalogue efficacy in NEN can be confirmed in retro- and prospective randomized clinical trials. In this strategy, patients are biopsied before and after treatment with rapalogues. These studies will provide *in vivo* insights on CDK4 and p27 protein levels, localization and phosphorylation status.

In conclusion, multiple copy number amplifications and deletions have been identified in everolimus resistant pNEN cell lines QGP-1/R and BON-1/R. Focusing on recurrent alterations in tumor suppressor and oncogenes, led to the identification of copy number alterations in two cell cycle regulatory components: a CDK4 amplification and CDKN1B deletion, respectively. These copy number alterations lead to expression changes of CDK4, p27 and other cell cycle components. This study is the first to demonstrate a role of CDK4 and p27 in acquired everolimus resistance in NENs, which is in line with recent studies in other tumor types[35,49]. Both CDK4 and p27 might be pivotal for everolimus resistance and could be a potential biomarker for the efficacy of everolimus treatment in NEN patients. Additionally, it provides a rationale for the use of cell cycle inhibitors in the treatment of rapalogue resistant in NEN. Hence, further in vitro and in vivo follow-up studies need to be planned to investigate CDK4 and p27 protein levels, localization and phosphorylation status in correlation with everolimus resistance in patients.

VI. REFERENCES

1. Laplante, M. & Sabatini, D. M. MTOR signaling in growth control and disease. *Cell* **149,** 274–293 (2012).
2. Dasari, A. *et al.* Trends in the Incidence, Prevalence, and Survival Outcomes in Patients With Neuroendocrine Tumors in the United States. *JAMA Oncol.* **3,** 1335–1342 (2017).
3. Scarpa, A. *et al.* Whole-genome landscape of pancreatic neuroendocrine tumours. *Nature* **543,** 65–71 (2017).
4. Vandamme, T. *et al.* Whole exome characterization of pancreatic neuroendocrine tumor cell lines BON-1 and QGP-1. *J. Mol. Endocrinol.* 1–37 (2015). doi:10.1530/JME-14-0304
5. Gagliano, T. *et al.* MTOR, p70S6K, AKT, and ERK1/2 levels predict sensitivity to mTOR and PI3K/mTOR inhibitors in human bronchial carcinoids. *Endocr. Relat. Cancer* **20,** 463–475 (2013).
6. Kang, S. A. *et al.* mTORC1 phosphorylation sites encode their sensitivity to starvation and rapamycin. *Science (80-.).* **341,** 1–16 (2013).
7. Sun, S. Y. *et al.* Activation of Akt and eIF4E survival pathways by rapamycin-mediated mammalian target of rapamycin inhibition. *Cancer Res.* **65,** 7052–7058 (2005).
8. Yao, J. C. *et al.* Everolimus for advanced pancreatic neuroendocrine tumors. *N. Engl. J. Med.* **364,** 514–23 (2011).
9. Vandamme, T. *et al.* Long-term acquired everolimus resistance in pancreatic neuroendocrine tumours can be overcome with novel PI3K-AKT-mTOR inhibitors. *Br. J. Cancer* **114,** 650–658 (2016).
10. Kaku, M., Nishiyama, T., Yagawa, K. & Abe, M. Establishment of a carcinoembryonic antigen-producing cell line from human pancreatic carcinoma. *Gann* **71,** 596–601 (1980).
11. Vandamme, T., Beyens, M., Peeters, M., Van Camp, G. & de Beeck, K. O. Next generation exome sequencing of pancreatic neuroendocrine tumor cell lines BON-1 and QGP-1 reveals different lineages. *Cancer Genetics* **208,** 523 (2015).
12. Seshan, V. E. & Olshen, A. B. DNAcopy : A Package for Analyzing DNA

Copy Data. *Bioconductor Vignette* 1–7 (2014).
13. Fabregat, A. *et al.* The reactome pathway knowledgebase. *Nucleic Acids Res.* **44,** D481–D487 (2016).
14. Mestdagh, P. *et al.* A novel and universal method for microRNA RT-qPCR data normalization. *Genome Biol.* **10,** R64 (2009).
15. Yeung, Y. *et al.* K-Ras mutation and amplification status is predictive of resistance and high basal pAKT is predictive of sensitivity to everolimus in biliary tract cancer cell lines. *Mol. Oncol.* **11,** 1130–1142 (2017).
16. Vandamme, T. *et al.* Whole-exome characterization of pancreatic neuroendocrine tumor cell lines BON-1 and QGP-1. *J. Mol. Endocrinol.* **54,** (2015).
17. Harada, K., Miyake, H., Kumano, M. & Fujisawa, M. Acquired resistance to temsirolimus in human renal cell carcinoma cells is mediated by the constitutive activation of signal transduction pathways through mTORC2. *Br. J. Cancer* **109,** 2389–2395 (2013).
18. Yao, J. C., Phan, A. T., Jehl, V., Shah, G. & Meric-Bernstam, F. Everolimus in advanced pancreatic neuroendocrine tumors: The clinical experience. *Cancer Research* **73,** 1449–1453 (2013).
19. Breuleux, M. *et al.* Increased AKT S473 phosphorylation after mTORC1 inhibition is rictor dependent and does not predict tumor cell response to PI3K/mTOR inhibition. *Mol. Cancer Ther.* **8,** 742–753 (2009).
20. McDonald, P. C. *et al.* Rictor and integrin-linked kinase interact and regulate Akt phosphorylation and cancer cell survival. *Cancer Res.* **68,** 1618–1624 (2008).
21. Tenkerian, C. *et al.* mTORC2 Balances AKT Activation and eIF2 Serine 51 Phosphorylation to Promote Survival under Stress. *Mol. Cancer Res.* **13,** 1377–1388 (2015).
22. Li, C. J., Chang, J. K., Chou, C. H., Wang, G. J. & Ho, M. L. The PI3K/Akt/FOXO3a/p27Kip1 signaling contributes to anti-inflammatory drug-suppressed proliferation of human osteoblasts. *Biochem. Pharmacol.* **79,** 926–937 (2010).
23. Sarbassov, D. D. *et al.* Prolonged Rapamycin Treatment Inhibits mTORC2 Assembly and Akt/PKB. *Mol. Cell* **22,** 159–168 (2006).
24. Sotillo, R. *et al.* Wide spectrum of tumors in knock-in mice carrying

a Cdk4 protein insensitive to INK4 inhibitors. *EMBO J.* **20,** 6637–6647 (2001).

25. Tang, L. H. *et al.* Attenuation of the retinoblastoma pathway in pancreatic neuroendocrine tumors due to increased Cdk4/Cdk6. *Clin. Cancer Res.* **18,** 4612–4620 (2012).
26. Guo, S. S. *et al.* Frequent overexpression of cyclin D1 in sporadic pancreatic endocrine tumours. *J. Endocrinol.* **179,** 73–79 (2003).
27. Shi, Y. J., Sharma, A., Wu, H., Lichtenstein, A. & Gera, J. Cyclin D1 and c-myc internal ribosome entry site (IRES)-dependent translation is regulated by AKT activity and enhanced by rapamycin through a p38 MAPK- and ERK-dependent pathway. *J. Biol. Chem.* **280,** 10964–10973 (2005).
28. Chen, X. G. *et al.* Rapamycin regulates Akt and ERK phosphorylation through mTORC1 and mTORC2 signaling pathways. *Mol. Carcinog.* **49,** 603–610 (2010).
29. Nourse, J. *et al.* Interleukin-2-mediated elimination of the p27Kip1 cyclin-dependent kinase inhibitor prevented by rapamycin. *Nature* **372,** 570–3 (1994).
30. Liang, J. & Slingerland, J. M. Multiple roles of the PI3K/PKB (Akt) pathway in cell cycle progression. *Cell cycle (Georgetown, Tex.)* **2,** 339–345 (2003).
31. Milne, T. A. *et al.* Menin and MLL cooperatively regulate expression of cyclin-dependent kinase inhibitors. *Proc Natl Acad Sci U S A* **102,** 749–754 (2005).
32. Karnik, S. K. *et al.* Menin regulates pancreatic islet growth by promoting histone methylation and expression of genes encoding p27Kip1 and p18INK4c. *Proc. Natl. Acad. Sci. U. S. A.* **102,** 14659–64 (2005).
33. Moss, S. C., Lightell, D. J., Marx, S. O., Marks, A. R. & Woods, T. C. Rapamycin regulates endothelial cell migration through regulation of the cyclin-dependent kinase inhibitor p27Kip1. *J. Biol. Chem.* **285,** 11991–7 (2010).
34. Luo, Y. *et al.* Rapamycin resistance tied to defective regulation of p27Kip1. *Mol. Cell. Biol.* **16,** 6744–6751 (1996).
35. Chen, G. *et al.* Identification of p27/KIP1 expression level as a candidate biomarker of response to rapalogs therapy in human cancer. *J. Mol. Med.*

88, 941–952 (2010).
36. Diersch, S. *et al.* Efemp1 and p27(Kip1) modulate responsiveness of pancreatic cancer cells towards a dual PI3K/mTOR inhibitor in preclinical models. *Oncotarget* **4,** 277–88 (2013).
37. Cho, D. C. *et al.* The efficacy of the novel dual PI3-kinase/mTOR inhibitor NVP-BEZ235 compared with rapamycin in renal cell carcinoma. *Clin. Cancer Res.* **16,** 3628–3638 (2010).
38. Cariou, S. *et al.* Down-regulation of p21WAF1/CIP1 or p27Kip1 abrogates antiestrogen-mediated cell cycle arrest in human breast cancer cells. *Proc. Natl. Acad. Sci. U. S. A.* **97,** 9042–9046 (2000).
39. Schmidt, M. & Fan, Z. Protection against chemotherapy-induced cytotoxicity by cyclin-dependent kinase inhibitors (CKI) in CKI-responsive cells compared with CKI-unresponsive cells. *Oncogene* **20,** 6164–71 (2001).
40. Ciarallo, S. *et al.* Altered p27(Kip1) phosphorylation, localization, and function in human epithelial cells resistant to transforming growth factor beta-mediated G(1) arrest. *Mol. Cell. Biol.* **22,** 2993–3002 (2002).
41. Francis, J. M. *et al.* Somatic mutation of CDKN1B in small intestine neuroendocrine tumors. *Nat. Genet.* **45,** 1483–1486 (2013).
42. Barbieri, C. E. *et al.* Exome sequencing identifies recurrent SPOP, FOXA1 and MED12 mutations in prostate cancer. *Nat. Genet.* **44,** 685–689 (2012).
43. Stephens, P. J. *et al.* The landscape of cancer genes and mutational processes in breast cancer. *Nature* **486,** 400–404 (2012).
44. Pellegata, N. S. *et al.* Germ-line mutations in p27Kip1 cause a multiple endocrine neoplasia syndrome in rats and humans. *Proc. Natl. Acad. Sci. U. S. A.* **103,** 15558–63 (2006).
45. Turner, N. C. *et al.* Palbociclib in Hormone-Receptor–Positive Advanced Breast Cancer. *N. Engl. J. Med.* **373,** 209–219 (2015).
46. Finn, R. S., Aleshin, A. & Slamon, D. J. Targeting the cyclin-dependent kinases (CDK) 4/6 in estrogen receptor-positive breast cancers. *Breast Cancer Res.* **18,** (2016).
47. Tigli, H., Buyru, N. & Dalay, N. Molecular analysis of the P27/Kip1 gene in breast cancer. *Mol. Diagnosis* **9,** (2005).
48. Chu, I. M., Hengst, L. & Slingerland, J. M. The Cdk inhibitor p27 in human

cancer: Prognostic potential and relevance to anticancer therapy. *Nat. Rev. Cancer* **8,** 253–267 (2008).

49. Atkins, M. B., Yasothan, U. & Kirkpatrick, P. Everolimus. *Nat. Rev. Drug Discov.* **8,** 535–536 (2009).

VII. SUPPLEMENTARY MATERIALS

Supplementary Material 1 | Gene expression qPCR primers.

Gene expression quantification primers were provided by RTPrimerDB. Primer transcript targets are given as RefSeq transcript identifiers.

Gene	RefSeq transcript	Forward	Reverse
CCND1	NM_053056.2	CGCCCCACCCCTCCAG	CCGCCCAGACCCTCAGACT
CCNE1	NM_001238.1	CCACACCTGACAAAGAAGATGATGAC	GAGCCTCTGGATGGTGCAATAAT
CDK2	NM_001798.3	GCTAGCAGACTTTGGACTAGCCAG	AGCTCGGTACCACAGGGTCA
CDK4	NM_000075.2	ATGTTGTCCGGCTGATGGA	CACCAGGGTTACCTTGATCTCC
CDK6	NM_001145306.1	CTGAATGCTCTTGCTCCTTT	AAAGTTTTGGTGGTCCTTGA
CDKN1A	NM_000389.4	CTGTCTTGTACCCTTGTGCC	GGTAGAAATCTGTCATGCTGG
CDKN1B	NM_004064.3	CGCCATATTGGGCCACTAA	CGCAGAGCCGTGAGCAA
E2F1	NM_005225.2	CACAGATCCCAGCCAGTCTCTA	GAGAAGTCCTCCCGCACATG
RB1	NM_000321.2	GCTTGGTTAACTTGGGAGAA	AGGTCAACTGCTGCAATAAA

Supplementary Material 2 | Summary of BON-1/R and QGP-1/R amplifications and deletions.

Karyotype notation of amplifications and deletions in BON-1/R (left panel) and QGP-1/R (right panel).

BON-1/R		QGP-1/R	
Amplifications	**Deletions**	**Amplifications**	**Deletions**
3q11.1-3q13.33	1q25.3-1q44	1p36.33-1p36.11	2p25.1-p22.2
8p12-8p11.22	5p15.33	7q11.23	6p24.3-p21.32
8q24.12-8q24.3	5p15.31-5p15.2	8p21.2-8p11.11	10q11.22
12q11-12q24.33	5p14.1-5p11	9p24.3-9p23	12p13.31-p12.3
	8p23.3-8p12	10p15.3-10p14	12q21.2
	20p11.23-20p11.1	10p12.33-10q11.21	16p13.3-16q21
		12p12.1	16q23.1-16q23.2
		12p11.23-12p11.21	19q13.32-19q13.43
			20p13-20q11.22

Supplementary Material 3 | Amplifications and deletions of COSMIC cancer census genes in BON-1/R and QGP-1/R.

COSMIC annotated amplified and deleted genes in BON-1/R (left panel) and QGP-1/R (right panel). Blue marked genes are known oncogenes, green marked genes are known tumor suppressor genes, orange marked genes are known to exert both oncogenic and tumor suppressor functions, and non-marked genes cannot be assigned to one of the latter categories.

BON-1/R				QGP-1/R			
Amplifications		**Deletions**		**Amplifications**		**Deletions**	
ALDH2	MYC	CDC73	PCM1	ABI1	MLLT10	ALK	GRIN2A
ARID2	NAB2	ELK4	PTPRC	CAMTA1	NRG1	ASXL1	HERPUD1
ATF1	NACA	FH	SDHA	CD274	PAX7	AXIN1	HIST1H3B
BCL7A	NCOR2	H3F3A	SLC45A3	FGFR1	PDCD1LG2	BCL3	HIST1H4I
BTG1	NDRG1	IL7R	TERT	HIP1	PPFIBP1	C2orf44	IL21R
CBLB	NRG1	LIFR	TPR	HOOK3	PRDM16	CBFB	KLK2
CDK4	POLE	MDM4	WRN	IKBKB	RPL22	CBLC	MAF
CLIP1	*PTPN11*			*JAK2*	*SDHB*	*CDH11*	*MYCN*
COL2A1	*PTPRB*			*KIF5B*	*SPEN*	*CDKN1B*	*MYH11*
DDIT3	*RECQL4*			KLF6	*TNFRSF14*	*CIITA*	*NCOA1*
ERBB3	*SH2B3*			*KRAS*	*WHSC1L1*	*CREBBP*	*PALB2*
FGFR1	*SMARCD1*			MDS2	WRN	CYLD	PPP2R1A
HMGA2	*STAT6*					*DAXX*	*RUNDC2A*
HNF1A	*TBX3*					*DEK*	*SOCS1*
HOXC11	*TFG*					*DN-MT3A*	*STRN*
HOXC13	*WHSC1L1*					*ERCC2*	*TNFRSF17*
LRIG3	*WIF1*					*ERCC4*	*TRAF7*
MDM2	*ZCCHC8*					*ETV6*	*TSC2*
						FUS	*ZNF331*

Supplementary Material 4 | Recurrent amplified and deleted genes in BON-1/R and QGP-1/R.

Recurrent amplified and deleted genes in everolimus-resistant BON-1/R and QGP-1/R cell lines. Blue marked genes are known oncogenes, green marked genes are known tumour suppressor genes and non-marked genes cannot be assigned to one of the latter categorie

BON-1/R and QGP-1/R

Amplifications		Deletions	
ADAM32	*HTRA4*	*ABHD12*	*FAM182B*
ADAM5P	*LETM2*	*ACSS1*	*FOXA2*
ADAM9	*LSM1*	*C20orf191*	*GGTLC1*
ADRB3	*MAK16*	*C20orf3*	*GINS1*
ASH2L	*NRG1*	*C20orf39*	*GZF1*
BAG4	*PLEKHA2*	*CD93*	*NANP*
BRF2	*PPAPDC1B*	*CST1*	*NAPB*
C8orf41	PROSC	CST11	NCRNA00153
C8orf86	RAB11FIP1	CST2	NKX2-2
DDHD2	RNF122	CST3	NKX2-4
DUSP26	RPL10AP3	CST4	NXT1
EIF4EBP1	STAR	CST5	PAX1
ERLIN2	TACC1	CST7	PYGB
FGFR1	TM2D2	CST8	SSTR4
FUT10	UNC5D	CST9	THBD
GOT1L1	WHSC1L1	CST9L	VSX1
GPR124	ZNF703	CSTL1	XRN2
		ENTPD6	ZNF337
		FAM182A	

Transcriptomic analysis of everolimus sensitive and resistant pancreatic neuroendocrine cell lines reveal everolimus escape mechanisms

Matthias Beyens[1,2*], Timon Vandamme[1,2,3*], Leo Hofland[3], Gitta Boons[1,2], Wouter De Herder[3], Marc Peeters[1], Guy Van Camp[1,2] en Ken Op de Beeck[1,2].

[1]Centre for Oncological Research (CORE), University of Antwerp, Universiteitsplein 1, 2610 Antwerp, Belgium
[2] Center of Medical Genetics, University of Antwerp and Antwerp University Hospital, Prins Boudewijnlaan 43, 2650 Antwerp, Belgium
[3] Department of Internal Medicine, Division of Endocrinology, Erasmus Medical Center, Dr. Molewaterplein 50, 3015GE Rotterdam, The Netherlands
*Equal contributing authors

Submitted for publication

I. ABSTRACT

1. PURPOSE

The mTOR inhibitor everolimus is a main treatment modality for advanced pancreatic neuroendocrine neoplasms (pNENs). BON-1 and QGP-1, two human pNEN cell lines, have been used extensively to understand the effects of short-term everolimus exposure and long-term everolimus resistance. Recently, the genetic constitution of these cell lines has been unraveled using whole-exome sequencing. However, only limited data is currently available on RNA expression in everolimus sensitive and acquired everolimus resistant BON-1 and QGP-1 cell lines.

2. METHODS

Strand-specific total RNA sequencing (RNA-seq) and low-pass whole-genome sequencing were executed on everolimus-sensitive BON-1 and QGP-1 and on acquired everolimus-resistant BON-1/R and QGP-1/R, at baseline and after 24 hours of everolimus treatment, on an Illumina HiSeq1500 platform. Differential gene expression analysis and pathway analysis on differentially expressed genes (DEGs) were performed. In parallel, results were validated using RNA microarray. Additionally, transcriptome profiles were hierarchically clustered with 217 cell lines of the Cancer Cell Line Encyclopedia (CCLE). Finally, copy number variants (CNVs) were correlated with gene expression changes.

3. RESULTS

BON-1 and QGP-1 transcriptomes clustered separately from pancreatic adenocarcinoma cell lines in CCLE and closely to different human cancer cell lines with known (neuro)endocrine phenotype characteristics. Pathway analysis of BON-1 and QGP-1 after everolimus exposure showed significant changes in MAPK/ERK signaling, Ras GTPase binding, translation initiation machinery and cell cycle regulation, including *SKP2* downregulation. In BON-1/R and QGP-1/R, downregulation of protein phosphatase 2A regulatory B55β subunit (*PPP2R2B*), as well as upregulation of the eukaryotic translation elongation factor 1 delta (*EEF1D*) and eukaryotic translation initiation factor 4E-binding protein (*EIF4EBP1*), was observed. Pathway analysis of BON-1/R and QGP-1/R DEGs showed shared enrichment of genes involved in cell membrane maintenance, including multiple S100 and annexin family genes, as well as involvement of MAPK/ERK signaling. Generally, observed alterations in gene expression correlated well with CNVs in the cell lines.

4. CONCLUSIONS

Full transcriptome data of BON-1 and QGP-1 cell lines, both at baseline and after everolimus exposure, aids the understanding of these pNEN models. In addition, genome-wide gene expression data of BON-1/R and QGP-1/R, two everolimus-resistant cell lines, yields new insights into expression of genes involved in everolimus resistance.

II. INTRODUCTION

Neuroendocrine neoplasms (NENs) are tumors that arise from endocrine cells and are mainly found in the pancreas, lung and small intestine[1]. Many insights in the pathophysiology of these rare tumors originate from research on pre-clinical models of this disease, such as human cell lines[2,3]. However, only a few patient-derived cell lines exist[4]. Two of the most frequently used patient-derived cell lines for the study of pancreatic NEN (pNEN) are BON-1 and QGP-1[2,3]. The BON-1 cell line was established in 1986 from a peripancreatic lymph node metastasis of a 28-year-old male with a pNEN[5]. In 1980, the QGP-1 cell line was developed from pancreatic NEN tumor tissue obtained from a 61-year-old male[6]. Both cell lines have been used extensively to study novel therapeutic strategies in pNEN[7–11]. However, the validity of cell lines as models for different cancers has been a matter of debate[12,13]. The advent of large-scale genomics techniques has made it possible to better understand the genetic make-up of clinical tumor samples and the corresponding pre-clinical cell line models for many cancer types[13,14]. Recently, the genetic constitution of BON-1 and QGP-1 was determined using whole-exome sequencing by our group and others[9,15,16]. In addition, whole-exome and whole-genome sequencing analysis of large cohorts of pNEN tumor samples has been reported in recent studies[17,18]. Although the genetic make-up of BON-1 and QGP-1 shows similarities with patient samples, the BON-1 and QGP-1 genomes contain unique mutations, likely as a result of the

immortalization needed to survive in vitro[9,15,16,19]. Both cell lines retain expression of typical neuroendocrine tumor markers, such as synaptophysin and neuron-specific enolase[9]. Additionally, both cell lines secrete hormones, a pathognomonic characteristic of NENs. The BON-1 cell line secretes neurotensin, pancreastatin, chromogranin A, serotonin (5-HT), 5-hydroxytryptophan (5-HTP) and 5-hydroxyindoleactic acid (5-HIAA)[20]. The QGP-1 cell line is a 5HT-, somatostatin- and carcinoembryonic antigen (CEA)-secreting cell line[21,22]. Although the full genetic background of BON-1 and QGP-1 has been extensively studied, only limited data is available on the RNA expression profile in both cell lines. A whole transcriptome analysis may elucidate the role of BON-1 and QGP-1 as pNEN disease models. Gene expression and sequencing data of pNEN patient samples have identified phosphoinositide-3-kinase (PI3K)/protein kinase B (Akt)/mammalian target of rapamycin (mTOR) as a driving pathway in pNENs[17,18,23,24]. This has led to the development of everolimus, an mTOR inhibitor, in pNENs. A phase-III trial has demonstrated a significant survival benefit of everolimus in advanced pNENs when compared to placebo[25,26]. Although everolimus is currently the main treatment modality for many pNEN patients, its efficacy is limited by primary and acquired drug resistance[27]. To study this everolimus resistance, cell lines have been used extensively, to understand both the effects of short-term everolimus exposure and long-term everolimus resistance[7,10,28–30]. An *in vitro* and *in vivo* study using BON-1 and QGP-1 demonstrated that pNEN could escape the effects of short-term everolimus through the mitogen activated kinase and extracellular signal-regulated kinase

(MAPK/ERK) pathway and that this could be overcome by dual inhibition of both pathways[10]. These results were confirmed in models for long-term, acquired everolimus resistance, including the everolimus-resistant BON-1/R and everolimus-resistant QGP-1/R cell lines, which were established by our group through sequential culturing in increasing concentrations of everolimus during 22 and 24 weeks, respectively[7,28]. Additionally, a recent study has highlighted the involvement of cell cycle components in everolimus resistance[29]. Despite the identification of the role of both the cell cycle and MAPK/ERK pathway, a thorough overview of the expression changes in everolimus resistance in pNEN is currently lacking.

Hence, this study presents transcriptome sequencing data of everolimus-sensitive BON-1 and QGP-1 and its everolimus-resistant counterparts BON-1/R and QGP-1/R. The comparison of the resistant cell lines with their sensitive counterparts could lead to a better understanding of the mechanisms of everolimus resistance.

III. MATERIAL AND METHODS

1. CELL LINES AND CULTURE CONDITIONS

BON-1 and QGP-1, two human pancreatic neuroendocrine neoplasm cell lines were used in this study (Figure 1). The BON-1 cell line was cultured in 1:1 mixture of Dulbecco's modified

Eagle medium (DMEM) and F12 medium, supplemented with 10% fetal calf serum (FCS), penicillin (1 × 105 units per l), fungizone (0.5 mg/l), and L-glutamine (2 mmol/l). The QGP-1 cell line was cultured in Roswell Park Memorial Institute (RPMI) 1640 medium, supplemented with 10% FCS and penicillin-streptomycin (1×10^5 units per l penicillin and 1×10^5 units per l streptomycin). All cell lines were incubated in an atmosphere of 95% humidity and 5% CO_2 at 37 °C. Media and supplements were obtained from Life Technologies Bio-cult Europe (Invitrogen, Breda, The Netherlands). Previously, we induced everolimus-resistance in BON-1 and QGP-1 through sequential culturing in increasing concentrations of everolimus during 22 and 24 weeks, respectively[31]. This resulted in two everolimus-sensitive parental cell lines, BON-1 and QGP-1, and two everolimus-resistant cell lines, BON-1/R and QGP-1/R (Figure 1).

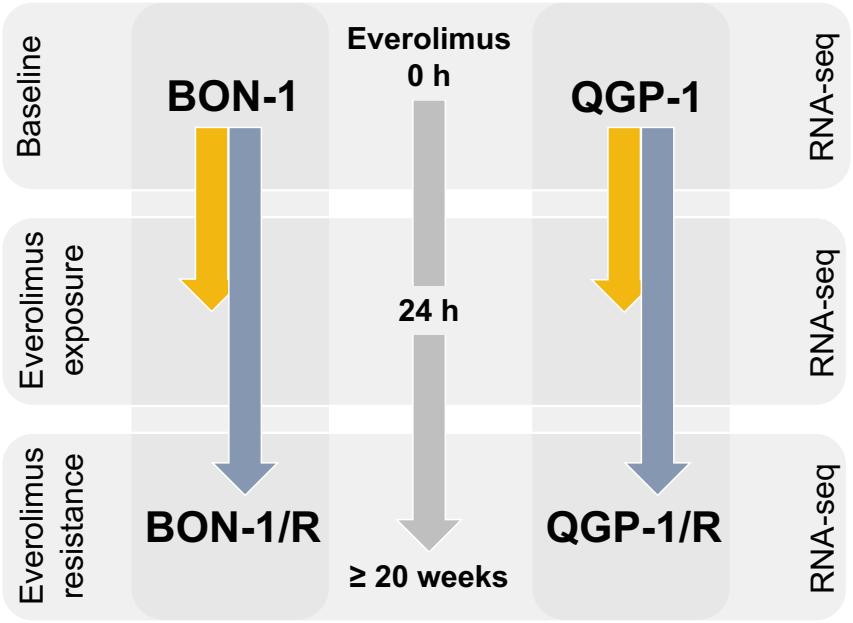

Figure 1 | Study design and workflow

BON-1 and QGP-1 were exposed to 0,4% DMSO vehicle for 24 hours (baseline), to 1 µM everolimus for 24 hours (everolimus-exposure) and to increasing concentrations of everolimus up to 1 µM over 20 to 22 weeks (everolimus-resistant cell lines BON-1/R and QGP-1/R). Next, strand-specific total RNA sequencing was performed on biological triplicates of every cell line condition and differential expression analysis was accomplished by comparing everolimus-exposure and everolimus-resistant cell lines with baseline cell lines.

2. DRUGS AND REAGENTS

Everolimus (RAD001, 40-O [2-hydroxyethyl] rapamycin) was purchased from Selleckchem (Selleck Chemicals, Houston, TX, USA). Everolimus was dissolved in 100% dimethylsulfoxide

(DMSO) to a 1 mM concentration and stored at −20 °C. Upon use, everolimus was diluted to a 1 μM working concentration in 40% DMSO.

3. TRANSCRIPTOME EXTRACTION, LIBRARY CONSTRUCTION, RNA SEQUENCING AND ALIGNMENT

Three biological replicates of the everolimus-sensitive BON-1 and QGP-1, both after 24-hour exposure to vehicle (0.4% DMSO) and after 24-hour exposure to 1 μM everolimus, and everolimus-resistant BON-1/R and QGP-1/R, were lysed in 350 μl buffer RLT (Qiagen, Germany) with added β-mercaptoethanol (1%) (Figure 1). Total RNA was isolated using an RNeasy® Mini kit (Qiagen, Germany) according to the manufacturer's protocol. An RNase-free DNase set (Qiagen, Germany) was used according to the manufacturer's instructions to ensure complete genomic DNA elimination. Purity of isolated RNA was determined by measuring the optical density (OD) of the samples at 260 and 280 nm. OD_{260}/OD_{280} ratio ranged from 1.9 to 2.2 for all samples. The RNA integrity number (RIN) was measured using the Experion RNA Analysis kit and the Experion automated electrophoresis station (Bio-Rad, USA). To ensure high quality RNA, a RIN equal to or greater than 8 was required to proceed with the RNA-seq. Samples were stored at -80°C.

RNA-seq libraries were generated using the Illumina TruSeq Stranded Total RNA LT sample preparation kit (with Ribo-Zero Gold) (Illumina, USA) according to the standard manufacturer's

protocol (Part no. 15031048 Rev. D April 2013). A ribosomal depletion step was performed on 1 µg of total RNA using Ribo-Zero Gold, followed by a heat fragmentation step to produce libraries with an insert size between 120 basepairs (bp) and 200 bp. cDNA was synthesized from the enriched and fragmented RNA using SuperScript II Reverse Transcriptase (Invitrogen, USA) and random primers. The cDNA library was converted into double-stranded DNA in the presence of dUTP to prevent subsequent amplification of the second strand and to maintain the strand-specificity of the library. Following 3'-adenylation and adaptor ligation, libraries were subjected to 15 cycles of PCR to produce libraries ready for sequencing. Prior to sequencing, libraries were quality checked using the LabChip GX (PerkinElmer, USA) with a High Sensitivity DNA kit (PerkinElmer, USA). Quantification of libraries for clustering on the sequencing flow-cell was performed using the KAPA Library Quantification Kit - Illumina/Universal (KAPA Biosystems, USA) in combination with a real-time PCR instrument. Next, the sequencing libraries were loaded on the flow-cells of a HiSeq1500 platform (Illumina, USA) for 2 × 100 bp length sequencing. Replicates were dispersed on different flow-cell lanes to correct for lane biases. Reads were mapped with HISAT2 v2.1.0 to the human reference genome build 19 (hg19)[32]. Aligned files are sorted with samtools v1.6 and indexed with sambamba v0.6.6[33,34]. Quality reports are generated with multiQC v0.11 and in-house scripts[35]. Count data was generated using featureCounts v1.4.4[36].

4. DIFFERENTIAL GENE EXPRESSION ANALYSIS

Euclidean distances between everolimus-sensitive BON-1 and QGP-1 and everolimus-resistant BON-1/R and QGP-1/R were assessed. The Euclidean distance matrix was created by calculating correlations using average linkage as clustering algorithm. Triplicates had to cluster in the same leaflet node upon differential statistical testing, otherwise samples were removed from the downstream analysis.

First, low-abundance transcripts were removed from the analysis by removing all transcripts with a variance across parental and everolimus-resistant cell lines with less than one. Next, Sailfish v0.10.1 performed a quasi-mapping-based estimation of transcript abundances[37]. Subsequently, the generated transcript count data was normalized by equi-variance transformation based on the negative binomial distribution algorithm DESeq2 v1.20.0[38]. Finally, we applied the DESeq2 algorithm to identify differentially expressed genes (DEGs) using the following criteria: 1) fold change (FC) $\geq |0.5|$ for up- or downregulation and 2) false discovery rate (FDR) ≤ 0.05.

To validate RNA-seq determined gene expression values, an additional RNA microarray HumanHT-12 v4.0 gene expression BeadChip (Illumina, USA) experiment was performed on three replicates of all three conditions of the BON-1 and QGP-1 cell lines. We correlated the different expression levels gene-wise after they were transformed into $\log_2$ Transcripts Per Kilobase Million (TMP) (RNA-seq) and $\log_2$ quantile normalized expression value

(RNA microarray). The correlation between RNA-seq and RNA microarray gene expressions profiles was calculated by fitting a linear regression on the intersection of significant RNA-seq and RNA microarray DEGs.

5. GENE ONTOLOGY AND PATHWAY ANALYSIS

Gene ontology (GO) and pathway analysis were performed to assist in the interpretation of the biological implications of DEGs. Database for Annotation, Visualization and Integrated Discovery (DAVID) v6.8 tool was used for this gene-set enrichment[39]. DAVID provides a comprehensive set of functional annotation tools. On the collection of DEGs, two separate functional annotation clustering analysis were carried out: 1) gene-set enrichment analysis using the three GO sub-ontologies biological process, cellular component and molecular function, and 2) pathway analysis using KEGG pathway as annotation source. Only significant (FDR $\leq$ 0.05) GOs and pathways were investigated further.

6. HIERARCHICAL CLUSTER ANALYSIS OF CANCER CELL LINE ENCYCLOPEDIA TRANSCRIPTOMES

The transcriptomes of 947 human cancer cell lines have previously been investigated by the European Bioinformatics Institute and are publicly available in the Cancer Cell Line Encyclopedia[40]. In order to compare the public datasets with our pNEN cell line data: 1) TPM count matrices were calculated, 2) only genes

with >1 read were kept. Next, row (gene feature) and column (sample) correlation were calculated with the Euclidean distance algorithm. Finally, cluster analysis using the Ward's hierarchical agglomerative method allowed identification of similar clusters in the data[41]. In addition, optimal numbers of clusters were estimated using the gap statistic method[42]. The outcome of this analysis was plotted as a dendrogram in R v3.5.

7. INFLUENCE OF COPY NUMBER VARIATIONS ON TRANSCRIPTOME EXPRESSION PROFILE

Copy number variation (CNV) analysis was performed through whole-genome sequencing of everolimus-sensitive, parental BON-1 and QGP-1 and everolimus-resistant BON-1/R and QGP-1/R. After isolation of genomic DNA using the QIAamp DNA Mini Kit (Qiagen), quality control using gel electrophoresis and fragmentation using a focused-ultrasonicator (Covaris M220, Covaris, Woburn, MA, USA), all samples were prepared for whole-genome sequencing using the TruSeq DNA Sample Preparation Kit (Illumina Inc., San Diego, CA, USA). Paired-end libraries of each parental and resistant cell line were 2x100 bp sequenced on an Illumina HiSeq1500 instrument (Illumina Inc., San Diego, CA, USA). Sequencing reads were adaptor trimmed with CutAdapt (v1.12) and mapped to the human genome build 19 (hg19) with Burrows Wheeler Aligner (BWA v0.7.15). Subsequently, we integrated the CNV data with the transcriptome data. RNA-seq data of the cell lines was transformed to a combined normalized feature count matrix originating from the DESeq2 algorithm. Subsequently,

genome-wide read ratios of all cell lines were log-transformed (log_2-ratio). Next, we labelled genes with CNV analysis log_2-ratio > 0.25 as amplified genes in our transcriptome data matrix, genes with log_2-ratio < -0.25 as deleted genes, and residual genes as being non CNV-affected, 'neutral' genes. To statistically test whether the identified CNVs influenced transcriptome expression profiles, we performed the non-parametric Unpaired Two-Samples Wilcoxon test for comparing the CNV category group means.

IV. RESULTS

1. STUDY DESIGN AND QUALITY ANALYSIS

To better understand the gene expression profile of pNEN cell lines of human origin, a strand-specific total RNA sequencing (RNA-seq) experiment was completed on BON-1 and QGP-1 after short-term vehicle exposure, which was considered to reflect the baseline gene expression profile. In addition, the immediate effect of everolimus on the everolimus-sensitive BON-1 and QGP-1 transcriptome was evaluated by sequencing BON-1 and QGP-1 after 24 hours of 1μM everolimus exposure. Next to sequencing of everolimus-sensitive BON-1 and QGP-1, full transcriptome analysis of the induced long-term everolimus-resistant BON-1/R and QGP-1/R cell lines was performed. This resulted in three conditions for both cell lines: everolimus-sensitive at baseline, everolimus-sensitive after 24 hours of everolimus exposure and

everolimus-resistant (Figure 1). For each of the cell line conditions, three biological replicates were sequenced. No significant differences between the biological replicates within the same conditions were observed, with the exception of one everolimus-sensitive baseline QGP-1 replicate. This sample showed deviating values in the distance matrix and principal component analysis. Accordingly, the replicate was removed and further analysis on baseline QGP-1 was performed using the mean of two replicates. In all other cell line conditions, three replicates were used for downstream analysis. To validate RNA-seq determined gene expression values, an additional RNA microarray experiment was performed and correlated gene-wise based on expression levels after counting. The correlation between RNA-seq and RNA microarray gene expression profiles for BON-1 and QGP-1 was 0.86 and 0.91. This demonstrates that RNA expression profiles can be replicated across different platforms.

2. TRANSCRIPTOME PROFILE OF EVEROLIMUS-SENSITIVE BON-1 AND QGP-1 CLUSTERS WITH ENDOCRINE CELL LINES AND CHANGES IN RESPONSE TO EVEROLIMUS EXPOSURE

To position BON-1 and QGP-1 in the landscape of existing cell lines, their baseline transcriptome was compared with RNA-seq data from the Cancer Cell Line Encyclopedia (CCLE)[40]. Of the 947 human cell lines available in the CCLE, a general cell line compendium consisting of the NCI-60 cell lines and all cell lines with known endocrine or small cell characteristics were selected,

resulting in 217 cell line datasets. Gene expression TPM counts were calculated. The 217 selected cell lines were clustered with the RNA-seq data of BON-1 and QGP-1 cell lines. The Ward's hierarchical agglomerative clustering method resulted in 4 optimal clusters and a distance matrix plotted as a dendrogram (Figure 2). Interestingly, the BON-1 and QGP-1 transcriptomes clustered separately from pancreatic adenocarcinoma cell lines, including several PANC-cell lines[43]. In contrast, BON-1 and QGP-1 clustered closely to different human cancer cell lines with known (neuro)endocrine phenotype characteristics, such as lung NEN cells NCI-H727, gastric neuroendocrine carcinoma cell line ECC12, and medullary thyroid carcinoma TT cell line[44–46].

To study short-term everolimus-induced RNA expression changes, differential transcriptome expression and pathway analysis were performed, comparing baseline BON-1 and QGP-1 with everolimus-exposed BON-1 and QGP-1. The differential expression analysis that compared the BON-1 and QGP-1 with their short-term everolimus-exposed counterparts resulted in 841 DEGs (461 upregulated and 380 downregulated) and 302 DEGs (165 upregulated and 137 downregulated), respectively in BON-1 and QGP-1. Pathway analysis on the DEGs of BON-1 and QGP-1 after everolimus exposure showed significant enrichment of genes involved in the regulation of MAPK/ERK signaling, Ras GTPase binding, endocrine pancreas development, cell cycle regulation and translation initiation machinery. Next, we identified the shared DEGs in the sensitive cell lines after everolimus exposure. This might provide insight into the molecular mechanistic actions

of everolimus in neuroendocrine neoplasms. Intersection of BON-1 and QGP-1 DEGs resulted in 67 shared genes of which 37 were uniformly upregulated and 30 were uniformly downregulated in both cell lines. Common upregulated genes included pro-apototic genes (such as *BMF*), fibroblast growth factor 3 (*FGFR3*), and Neuropilin 1 (*NPY1*). In both cell lines, downregulation of different heat shock proteins, apoptosis-related genes (such as *AIFM1* and *GDF15*), genes involved in fatty acid metabolism, and tryptophan hydroxylase 1 (*TPH1*) was observed. Additionally, we identified a downregulation of *SKP2* in the both cell lines under everolimus-treatment. mTOR inhibitors are known to downregulate *SKP2* expression in mTOR-inhibitor sensitive cells[47].

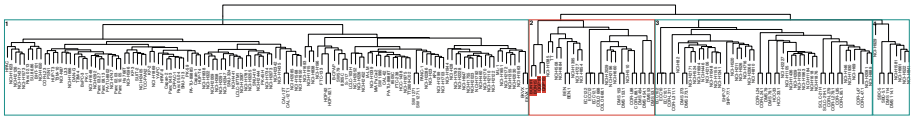

Figure 2 | Cancer Cell Line Encyclopedia cluster analysis.

Ward's hierarchical agglomerative clustering of RNA-seq data of everolimus-sensitive BON-1 and QGP-1, and everolimus-resistant BON-1/R and QGP-1/R with the RNA expression profiles of 217 Cancer Cell Line Encyclopedia (CCLE) cell lines resulted in 4 optimal clusters (colored lines). Cluster 2 (red) contains BON-1, QGP-1, BON-1/R and QGP-1/R (highlighted in red).

3. TRANSCRIPTOME PROFILE OF EVEROLIMUS-RESISTANT BON-1/R AND QGP-1/R

The transcriptomes of the induced long-term everolimus-resistant BON-1/R and QGP-1/R cell lines were clustered together with the human cancer cell lines originating from the Cancer Cell Line Encyclopedia[40]. This allows identification of similar clusters in the data based on their tissue origin. The transcriptome profile of resistant BON-1/R and QGP-1/R clusters together with everolimus-sensitive BON-1 and QGP-1, indicating that resistance-induced changes might be everolimus-specific and are not caused by overall dedifferentiation (Figure 2). Hence, comparison of BON-1/R and QGP-1/R with their baseline, sensitive counterparts, BON-1 and QGP-1, might identify changes in gene expression that are caused by long-term acquired everolimus resistance and could help unravelling the transcriptomic mechanisms that confer everolimus resistance.In total, this analysis identified 939 DEGs (397 upregulated and 542 downregulated) and 1008 DEGs (490 upregulated and 518 downregulated), respectively in BON-1/R and QGP-1/R. To study shared transcriptome changes between BON-1/R and QGP-1/R, which could mediate everolimus-resistance, we intersected the DEGs of both cell lines. Intersection resulted in 148 shared DEGs of which 83 were upregulated and 65 were downregulated, including a shared downregulation of protein phosphatase 2A regulatory B55β subunit (*PPP2R2B*). Protein phosphatase 2A plays an essential role in controlling the phosphoinositide-dependent kinase-1 (PDK1) pathway and mediating a potential escape of mTOR inhibition in cancer[48].

Furthermore, we discovered an upregulation of two components of the eukaryotic translation elongation machinery in BON-1/R and QGP-1/R; the eukaryotic translation elongation factor 1 delta (*EEF1D*) and eukaryotic translation initiation factor 4E-binding protein (*EIF4EBP1*). The eukaryotic translation elongation signaling is one of the effectors of the PI3K/Akt/mTOR pathway and is known to stimulate the pNEN cells to proliferate[49–52]. Pathway analysis of BON-1/R and QGP-1/R DEGs showed shared enrichments of genes involved in the PI3K/Akt/mTOR pathway, genes involved in cell membrane maintenance, including multiple S100 and annexin family genes, as well as involvement of MAPK/ERK signaling including genes that negatively regulate ERK1 and ERK2 (Figure 3).

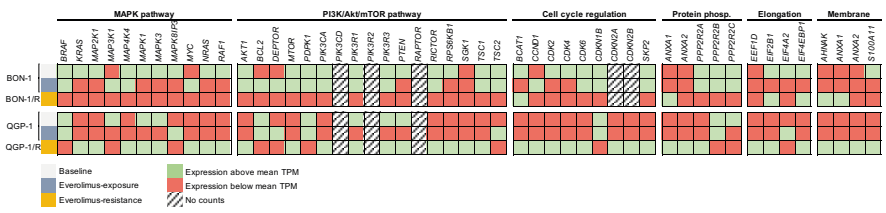

Figure 3 | Expression changes in key pathway genes in pNET cell lines at baseline, after everolimus exposure and after everolimus resistance.

Gene expression, based upon transcript counts per million (TPM), of key components of selected pathways in the baseline BON-1 and QGP-1, BON-1 and QGP-1 after 24 hours of everolimus exposure and in everolimus-resistant BON-1/R and QGP-1/R are shown. When the TPM was above the mean TPM within the cell line condition, genes were color-coded as green, while genes are color-coded as red when TPM was below mean TPM of the cell line condition. When no counts were detected, respective boxes were shaded.

4. INTEGRATION OF COPY-NUMBER ALTERATIONS AND EXPRESSION PROFILES

Using low-pass whole-genome sequencing data, the effects of CNVs on the gene expression profiles of the resistant BON-1/R and QGP-1/R were investigated. Genes were categorized into three categories; amplified, deleted or non CNV-affected (neutral) genes (Figure 4). In the everolimus-resistant BON-1/R, we observed an increase in gene expression of amplified regions (N = 646; mean = 0.4581; $P < 2.2^{-16}$) compared to non CNV-affected, neutral genes (N = 13,757; mean = -0.0007). Furthermore, we detected a decrease in gene expression in deleted regions (N = 417; mean = -0.6857; $P < 2.2^{-16}$) in comparison with CNV neutral genes. In the everolimus-resistant QGP-1/R, we observed an overall increase in expression of amplified genes (N = 370; mean = 0.5419; $P < 2.2^{-16}$) compared to neutral genes (N = 13,647; mean = 0.0209). Moreover, we found a decrease in gene expression in deleted regions (N = 977; mean = -0.4972; $P < 2.2^{-16}$). In contrast, we observed several genes that were expressed in the opposite direction to the copy number change. This was the case for 39.56% and 17.57% of amplifications and 53.94% and 23.44% of deletions, in BON-1/R and QGP-1/R respectively. Next, we evaluated whether CNV-affected oncogenes and tumor suppressor genes were differentially expressed. This allows the identification of genes with a potential relationship to growth advantages, e.g. acquired resistance to continuously everolimus treatment. First, we compared the resulting upregulated amplified and downregulated deleted genes from our *in vitro* study with the COSMIC database (12th April 2017). Secondly, we evaluated

whether known COSMIC cancer genes were oncogenes and/or tumor suppressor genes. For BON-1/R upregulated amplified genes, 32 genes were present in the COSMIC database. Of the 32 genes, 44% were oncogenes and 50% were tumor suppressor genes and 6% had a dual annotation. For BON-1/R downregulated deleted genes, 15 genes were found in COSMIC. Of the 15 genes, 40% were oncogenes and 53% were tumor suppressor genes and 7% had a dual annotation. Next, we analyzed the QGP-1/R upregulated amplified genes of which 27 genes were known in COSMIC. Of the 27 genes, 41% were oncogenes and 59% were tumor suppressor genes. Investigation of the QGP-1/R downregulated deleted genes, indicated 36 genes as present in COSMIC. Of the 36 genes, 25% were oncogenes, 67% were tumor suppressor genes and 8% had a dual annotation. Interestingly, we found important cell cycle regulators of the G1/S transition to be altered in both CNV status and gene expression level. We found *CDK4* to be amplified and upregulated and *CDKN1B* (p27) to be deleted and downregulated in BON-1/R and QGP-1/R, respectively.

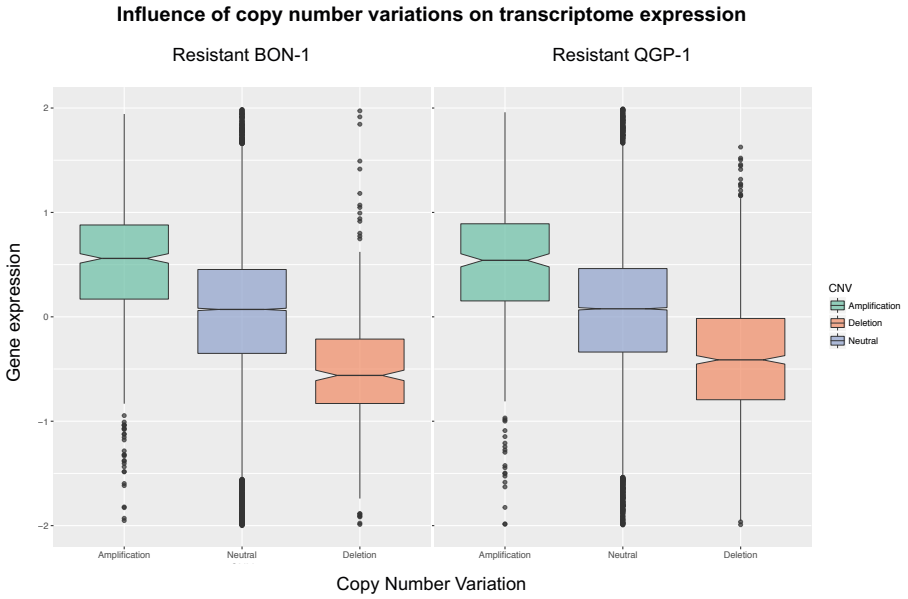

Figure 4 | Influence of copy number variations on transcriptome expression.

Gene expression split on copy number status is shown as box plots. Copy number variation (CNV) calls present in the everolimus-resistant cell lines in comparison with their everolimus-sensitive counterparts of BON-1 (left panel) and QGP-1 (right panel). Filled green color = amplification; filled blue color = neutral; and filled orange color = deletion.

V. DISCUSSION

1. NEUROENDOCRINE CELL LINES CLUSTER PHENOTYPICALLY WITHIN A HUMAN CANCER CELL LINE PANEL

This study presents the first full strand-specific transcriptomic profile of BON-1. Additionally, it adds to existing expression profile data of QGP-1 in The Cancer Cell Line Encyclopedia (CCLE). The CCLE project is an effort to conduct a detailed genetic characterization of a large panel of human cancer cell lines, including copy number, variant data and mRNA profiles. We present a unique extension of the pNEN cell lines transcriptome compendium to the CCLE data by not only sequencing baseline BON-1 and QGP-1, but also by providing a trancriptome profile of both cell lines after 24 hours of everolimus exposure. In addition, the first full transcriptome analysis of the BON-1/R and QGP-1/R cell lines, an established model for acquired everolimus resistance in pNEN, was performed[31]. This transcriptome data extension could serve as an attractive starting point for the study of gene expression and oncogenesis driving pathways in the two most frequently studied pNEN cell line models, BON-1 and QGP-1. Within the CCLE data set, gene expression profiles of BON-1 and QGP-1 noticeably cluster with human cancer cell lines with known (neuro)endocrine phenotype resemblance, such as lung NEN cell lines NCI-H727, gastric neuroendocrine carcinoma cells ECC10 and ECC12, and the medullary thyroid carcinoma TT cell line[44–

[46]. The QGP-1 and BON-1 cell lines have been under increasing scrutiny, as their doubling time of less than 48 hours might not be reflective of slow-growing neuroendocrine neoplasms[9,53]. In addition, somatostatin receptors, the target for somatostatin analogues, are expressed to a lesser extent in BON-1 and QGP-1 than in patient tissues[9,53]. To overcome these limitations, the well-differentiated pNEN cell line NT-3 has recently been established[53]. Although this cell line retains somatostatin receptor expression, the doubling time of 10.9 days might limit its usability for experiments[53]. In addition, NT-3 is an insulin-secreting cell line from an insulinoma background. As different pathways, such as IGF-1, are upregulated in insulinomas when compared with other pNENs, results from this cell line might not be extrapolated to all pNENs[54]. Hence, the use of multiple cell lines, including BON-1 and QGP-1, remains necessary to obtain results that are valid across different subtypes of pNEN. Moreover, it appears that the underlying physiological neuroendocrine phenotype is preserved throughout the carcinogenic transformation of BON-1 and QGP-1. The hierarchical cluster analysis indicates that BON-1 and QGP-1 are useful tools to investigate physiological and pathophysiological differentiation, carcinogenic transformation, and can be exploited to identify molecular targets for novel therapeutics[53]. However, it is clear that biological differences between pNENs from patients and pNEN-derived cell cultures must be carefully considered when experimental systems are used as models for human cancer[55].

2. SKP2 IS DOWNREGULATED IN PANCREATIC NEUROENDOCRINE CELLS AFTER EVEROLIMUS EXPOSURE

The frequent upregulation of the PI3K/Akt/mTOR pathway in human neuroendocrine cancer cells promotes uncontrolled cell proliferation and survival[56]. In the differential gene expression analysis of the everolimus-sensitive BON-1 and QGP-1 after short-term everolimus exposure, we investigated everolimus-induced transcriptomic changes. In both cell lines, everolimus exposure leads to expression changes that favor apoptosis in both cell lines, while at the same time reducing expression of genes involved in cell metabolism pathways, such as fatty acid metabolism. Cells adapt to exposure to everolimus by upregulation of neuropelin-1 (NPY1) and fibroblast growth factor receptor 3 (FGFR3). A recent study in pNEN tumor samples showed that NPY1 expression levels are significantly correlated with tumor grade, lymph node metastasis, and TNM stage and that knock-down of NPY1 reduced migration of BON-1 cells[57]. FGFR3 has been implicated in bladder and FGFR inhibitors are currently being explored in this setting[58]. Interestingly, a crosstalk between FGFR3 and the MAPK/ERK pathway has recently been discovered[59]. In addition, downregulation of *SKP2* was identified in BON-1 and QGP-1. SKP2 is a subunit of the ubiquitin protein ligase complex, which regulates the turnover of proteins involved in cell cycle regulation, including p27. Totary-Jain and colleagues investigated the role of SKP2 in the response of tumor cells to the mTOR inhibitor rapamycin and showed an important downregulation

of SKP2 in rapamycin-sensitive cells[47]. Moreover, they showed that shRNA-mediated SKP2-silencing in rapamycin-resistant cells was sufficient to increase sensitivity in xenografts. As reported by our group, BON-1 and QGP-1 are rapamycin and everolimus sensitive cell lines, and thus evaluation of *SKP2* expression could provide a potential everolimus response marker in pNEN[7].

3. ANNEXINS, CELL CYCLE PROTEINS AND MAPK/ERK COULD MEDIATE EVEROLIMUS RESISTANCE

Besides the full transcriptomic data of BON-1 and QGP-1, the current study describes full gene expression data of BON-1/R and QGP-1/R, two everolimus-resistant cell lines. Full genomic and transcriptomic datasets across different cell lines and conditions allowed the investigation of everolimus resistance. As differential gene expression contributes to acquired resistance in other tumor types, we performed pathway analysis on the DEGs in BON-1/R and QGP-1/R[60–62]. This analysis showed enrichment of genes involved in the regulation of cell membranes, such as S100 and annexin members. S100 and annexin proteins are among the most frequently dysregulated proteins in neoplasia and are overexpressed in various cancers[63,64]. More importantly, changes in annexin expression have been associated with chemotherapeutic resistance to cisplatin and prednisolone, in ovarian cancer and acute lymphoblastic leukemia[65,66]. Increased expression of annexin proteins prevents uptake or accumulation of these drugs in the cancer cells. Hence, annexins may affect the transmembrane transportation of everolimus. Our group

and other researchers have suggested that everolimus resistance might be mediated by cross-talk activation of the MAPK/ERK signaling through a PI3K-mediated feedback loop[7,67–71] . In the current gene expression study, pathway analysis further substantiates this hypothesis. Hence, there could be a rationale for mTOR and MAPK/ERK inhibitor combination therapy in the treatment of everolimus-resistant pNEN patients, as these agents could act in a synergistic manner[10]. Recently, the importance of alterations in cell cycle regulatory components in NEN and in the efficacy of rapalog treatment in different tumor types has been demonstrated[27,61,72–74]. Genes involved in the regulation of the cell cycle were enriched in everolimus-resistant BON-1/R and QGP-1/R. Altered expression of cell cycle regulatory components has been associated with the development of islet cell hyperplasia and pNENs[75–77]. Furthermore, Chen and colleagues correlated rapalog activities and gene expression patterns in the NCI-60 cell lines[78]. For instance, they discovered that *CDKN1B* (p27), a differentially expressed transcript in our resistant QGP-1/R, was strongly correlated to everolimus resistance. Cells expressing low levels of p27 exhibited resistance to rapalogs. This correlation has been confirmed in human breast cancer cells and human cancer xenografts[78].

4. PPP2R2B AND EFFECTORS OF PI3K-AKT-MTOR ARE ALTERED IN EVEROLIMUS-RESISTANT CELLS

In this transcriptome study, we showed a downregulation of protein phosphatase 2A (PP2A) regulatory B55β subunit, *PPP2R2B*.

PP2A acts as a tumor suppressor[79]. PP2A can be inactivated by the downregulation of the regulatory subunits. Tan and colleagues found that decreased *PPP2R2B* expression induced PDK-1-dependent MYC phosphorylation at Ser62 by rapamycin, resulting in rapamycin resistance[48]. Furthermore, they demonstrated that inhibition of PDK1 and Myc, but not PIK3CA and Akt, sensitizes the therapeutic response of rapamycin. This suggests that inhibition of PDK1 may have therapeutic potential. In addition, they highlighted the use of *PPP2R2B* as a biomarker for rapamycin efficacy in colorectal cancer patients[48]. Besides altered expression of *PPP2R2B*, we identified multiple DEGs of the eukaryotic translation elongation machinery, in particular, the eukaryotic translation elongation factor 1 delta (*EEF1D*) and eukaryotic translation initiation factor 4E-binding protein (*EIF4EBP1*). Both genes are effectors of PI3K/Akt/mTOR signaling[52]. These effectors regulate translation of mRNAs involved in oncogenic processes[52,80,81]. Phosphorylated EIF4EBP1 has an oncogenic activity and is associated with poor survival and therapy resistance in several cancers[82–85]. On the other hand, *EIF4EBP1* overexpression is associated with poor prognosis in several cancers, including pNEN[86–88]. EEF1D plays a tumor promoting role. Accordingly, EEF1D overexpression has been associated with increased proliferation rates of multiple tumors[49–51,89,90]. Recently, Cheng and colleagues demonstrated that overexpression of EEF1D modulates PI3K/Akt/mTOR signaling. In their experiment, EEF1D overexpression increased the phosphorylation of Akt, mTOR and B-cell lymphoma 2 (Bcl-2)-associated death promoter (BAD), and thus enhanced cell proliferation[50].

5. GENE COPY NUMBER STATUS IS CORRELATED WITH GENE EXPRESSION LEVEL

We investigated the effects of CNVs from the low-pass whole-genome sequencing study on gene expression in the resistant BON-1/R and QGP-1/R. We observed that, in general, gene expression was increased in genes found in higher copy CNVs and decreased in genes found in lower copy CNVs. However, some genes showed expression changes in the opposite direction of the copy number change. This could be due to additional regulators or transcription factors controlling gene expression in *trans*. Alternatively, gene expression may be disrupted if regulatory regions are affected by the CNV or by epigenetic mechanisms, such as DNA methylation, causing transcriptional silencing.

6. FUTURE PERSPECTIVES AND CONCLUSION

As for any model system, there are also limitations associated with these cell lines. The microenvironment and drug pharmacokinetic effects on clinical responses cannot be assessed[91]. Gene expression profiles in cell line models are not identical to those from primary tissues[92]. Culturing of the cells might also introduce new mutations and alter the cell line characteristics. Therefore, further functional validation, such as knockout/knock-in of specific genes/alleles, and clinical confirmation of biomarkers discovered using *in vitro* models will be required. Due to the difficulty of access to clinical samples, *in vitro* human models will remain an important resource for cancer pharmacogenomic research in spite of their

limitations. Therefore, future models might include the use of 3D culture with incorporation of patient-specific tumor-infiltrating lymphocytes to better simulate the *in vivo* microenvironment and, thus, could further optimize *in vitro* cell line models to improve their predictive validity.

In conclusion, the current study improves the understanding of the BON-1 and QGP-1 cell lines as models for pNEN by presenting full transcriptome data, both at baseline and after everolimus exposure. In addition, genome-wide gene expression data of BON-1/R and QGP-1/R, two everolimus-resistant cell lines, is presented. Various studies have investigated only single genes of interest to unravel the mechanisms that confer everolimus-resistance. The current study shows that systems biology-based computational approaches may complement conventional gene-centered methods and, as such, may provide novel insights into everolimus resistance in pNENs.

VI. REFERENCES

1. Dasari, A. *et al.* Trends in the Incidence, Prevalence, and Survival Outcomes in Patients With Neuroendocrine Tumors in the United States. *JAMA Oncol.* **3,** 1335–1342 (2017).
2. Grozinsky-Glasberg, S., Shimon, I. & Rubinfeld, H. The role of cell lines in the study of neuroendocrine tumors. *Neuroendocrinology* (2012). doi:10.1159/000338793
3. Babu, V., Paul, N. & Yu, R. Animal models and cell lines of pancreatic neuroendocrine tumors. *Pancreas* (2013). doi:10.1097/MPA.0b013e31827ae993
4. Modlin, I. M., Moss, S. F., Chung, D. C., Jensen, R. T. & Snyderwine, E. Priorities for improving the management of gastroenteropancreatic neuroendocrine tumors. *Journal of the National Cancer Institute* (2008). doi:10.1093/jnci/djn275
5. Townsend Jr., C. M., Ishizuka, J. & Thompson, J. C. Studies of growth regulation in a neuroendocrine cell line. *Acta Oncol* **32,** 125–130 (1993).
6. Kaku, M., Nishiyama, T., Yagawa, K. & Abe, M. Establishment of a carcinoembryonic antigen-producing cell line from human pancreatic carcinoma. *Gann* **71,** 596–601 (1980).
7. Vandamme, T. *et al.* Long-term acquired everolimus resistance in pancreatic neuroendocrine tumours can be overcome with novel PI3K-AKT-mTOR inhibitors. *Br. J. Cancer* **114,** 650–658 (2016).
8. Van Adrichem, R. C. S. *et al.* Effects of Somatostatin Analogs and Dopamine Agonists on Insulin-Like Growth Factor 2-Induced Insulin Receptor Isoform A Activation by Gastroenteropancreatic Neuroendocrine Tumor Cells. *Neuroendocrinology* (2016). doi:10.1159/000444280
9. Hofving, T. *et al.* The neuroendocrine phenotype, genomic profile and therapeutic sensitivity of GEPNET cell lines. *Endocr. Relat. Cancer* (2018). doi:10.1530/ERC-17-0445
10. Valentino, J. D. *et al.* Cotargeting the PI3K and RAS pathways for the treatment of neuroendocrine tumors. *Clin. Cancer Res.* (2014). doi:10.1158/1078-0432.CCR-13-1897

11. Veenstra, M. J. *et al.* Epidrug-induced upregulation of functional somatostatin type 2 receptors in human pancreatic neuroendocrine tumor cells. *Oncotarget* (2016). doi:10.18632/oncotarget.9462
12. Wilding, J. L. & Bodmer, W. F. Cancer cell lines for drug discovery and development. *Cancer Research* (2014). doi:10.1158/0008-5472.CAN-13-2971
13. Domcke, S., Sinha, R., Levine, D. A., Sander, C. & Schultz, N. Evaluating cell lines as tumour models by comparison of genomic profiles. *Nat. Commun.* (2013). doi:10.1038/ncomms3126
14. Gillet, J.-P., Varma, S. & Gottesman, M. M. The clinical relevance of cancer cell lines. *J. Natl. Cancer Inst.* (2013). doi:10.1093/jnci/djt007
15. Vandamme, T. *et al.* Whole-exome characterization of pancreatic neuroendocrine tumor cell lines BON-1 and QGP-1. *J. Mol. Endocrinol.* **54,** (2015).
16. Boora, G. K. *et al.* Exome-level comparison of primary well-differentiated neuroendocrine tumors and their cell lines. *Cancer Genet.* (2015). doi:10.1016/j.cancergen.2015.04.002
17. Scarpa, A. *et al.* Whole-genome landscape of pancreatic neuroendocrine tumours. *Nature* **543,** 65–71 (2017).
18. Jiao, Y. *et al.* DAXX/ATRX, MEN1, and mTOR pathway genes are frequently altered in pancreatic neuroendocrine tumors. *Science (80-.).* **331,** 1199–1203 (2011).
19. Vandamme, T., Beyens, M., Peeters, M., Van Camp, G. & de Beeck, K. O. Next generation exome sequencing of pancreatic neuroendocrine tumor cell lines BON-1 and QGP-1 reveals different lineages. *Cancer Genet.* **208,** (2015).
20. Parekh, D. *et al.* Characterization of a human pancreatic carcinoid in vitro: morphology, amine and peptide storage, and secretion. *Pancreas* **9,** 83–90 (1994).
21. Doihara, H. *et al.* QGP-1 cells release 5-HT via TRPA1 activation; a model of human enterochromaffin cells. *Mol Cell Biochem* **331,** 239–245 (2009).
22. Iguchi, H., Hayashi, I. & Kono, A. A somatostatin-secreting cell line established from a human pancreatic islet cell carcinoma (somatostatinoma): release experiment and immunohistochemical

study. *Cancer Res* **50,** 3691–3693 (1990).
23. Missiaglia, E. *et al.* Pancreatic endocrine tumors: Expression profiling evidences a role for AKT-mTOR pathway. *J. Clin. Oncol.* **28,** 245–255 (2010).
24. Vandamme, T. *et al.* Hotspot DAXX, PTCH2 and CYFIP2 mutations in pancreatic neuroendocrine neoplasms. *Endocr. Relat. Cancer* 1–13 (2018). doi:10.1530/ERC-18-0120
25. Yao, J. C. *et al.* Everolimus for advanced pancreatic neuroendocrine tumors. *N. Engl. J. Med.* **364,** 514–23 (2011).
26. Yao, J. C. *et al.* Everolimus for the treatment of advanced pancreatic neuroendocrine tumors: Overall survival and circulating biomarkers from the randomized, Phase III RADIANT-3 study. *J. Clin. Oncol.* (2016). doi:10.1200/JCO.2016.68.0702
27. Yao, J. C., Phan, A. T., Jehl, V., Shah, G. & Meric-Bernstam, F. Everolimus in advanced pancreatic neuroendocrine tumors: The clinical experience. *Cancer Research* **73,** 1449–1453 (2013).
28. Passacantilli, I. *et al.* Combined therapy with RAD001 e BEZ235 overcomes resistance of PET immortalized cell lines to mTOR inhibition. *Oncotarget* (2014). doi:10.18632/oncotarget.2111
29. Aristizabal Prada, E. T. *et al.* The role of GSK3 and its reversal with GSK3 antagonism in everolimus resistance. *Endocr. Relat. Cancer* **25,** 893–908 (2018).
30. Zitzmann, K. *et al.* Compensatory activation of Akt in response to mTOR and Raf inhibitors - a rationale for dual-targeted therapy approaches in neuroendocrine tumor disease. *Cancer Lett* **295,** 100–109 (2010).
31. Vandamme, T. *et al.* Long-term acquired everolimus resistance in pancreatic neuroendocrine tumours can be overcome with novel PI3K-AKT-mTOR inhibitors. *Br. J. Cancer* **114,** (2016).
32. Sirén, J., Välimäki, N. & Mäkinen, V. HISAT2 - Fast and sensitive alignment against general human population. *IEEE/ACM Trans. Comput. Biol. Bioinforma.* **11,** 375–388 (2014).
33. Li, H. *et al.* The Sequence Alignment / Map format and SAMtools. *Bioinformatics* **25,** 2078–2079 (2009).
34. Tarasov, A., Vilella, A. J., Cuppen, E., Nijman, I. J. & Prins, P. Sambamba:

Fast processing of NGS alignment formats. *Bioinformatics* **31,** 2032–2034 (2015).

35. Ewels, P., Magnusson, M., Lundin, S. & Käller, M. MultiQC: Summarize analysis results for multiple tools and samples in a single report. *Bioinformatics* **32,** 3047–3048 (2016).
36. Liao, Y., Smyth, G. K. & Shi, W. FeatureCounts: An efficient general purpose program for assigning sequence reads to genomic features. *Bioinformatics* **30,** 923–930 (2014).
37. Patro, R., Mount, S. M. & Kingsford, C. Sailfish enables alignment-free isoform quantification from RNA-seq reads using lightweight algorithms. *Nat. Biotechnol.* (2014). doi:10.1038/nbt.2862
38. Love, M. I., Huber, W. & Anders, S. Moderated estimation of fold change and dispersion for RNA-seq data with DESeq2. *Genome Biol.* **15,** (2014).
39. Dennis, G. *et al.* DAVID: Database for Annotation, Visualization, and Integrated Discovery. *Genome Biol.* (2003). doi:10.1186/gb-2003-4-9-r60
40. Barretina, J. *et al.* The Cancer Cell Line Encyclopedia enables predictive modelling of anticancer drug sensitivity. *Nature* (2012). doi:10.1038/nature11003
41. Murtagh, F. & Legendre, P. Ward's Hierarchical Agglomerative Clustering Method: Which Algorithms Implement Ward's Criterion? *J. Classif.* (2014). doi:10.1007/s00357-014-9161-z
42. Tibshirani, R., Walther, G. & Hastie, T. Estimating the number of clusters in a data set via the gap statistic. *J. R. Stat. Soc. Ser. B Stat. Methodol.* (2001). doi:10.1111/1467-9868.00293
43. Lieber, M., Mazzetta, J., Nelson-Rees, W., Kaplan, M. & Todaro, G. Establishment of a continuous tumor-cell line (PANC-1) from a human carcinoma of the exocrine pancreas. *Int. J. Cancer* (1975). doi:10.1002/ijc.2910150505
44. Fujiwara, T. *et al.* Characterization of four new cell lines derived from small-cell gastrointestinal carcinoma. *Int J Cancer* (1993).
45. Giaccone, G. *et al.* Neuromedin B is present in lung cancer cell lines. in *Cancer Research* (1992).
46. Molè, D. *et al.* The expression of the truncated isoform of somatostatin receptor subtype 5 associates with aggressiveness in medullary thyroid

carcinoma cells. *Endocrine* (2015). doi:10.1007/s12020-015-0594-x

47. Totary-Jain, H. *et al.* Rapamycin resistance is linked to defective regulation of Skp2. *Cancer Res.* (2012). doi:10.1158/0008-5472.CAN-11-2195
48. Tan, J. *et al.* B55β-Associated PP2A Complex Controls PDK1-Directed Myc signaling and modulates rapamycin sensitivity in colorectal cancer. *Cancer Cell* **18,** 459–471 (2010).
49. Flores, I. L. *et al.* EEF1D modulates proliferation and epithelial-mesenchymal transition in oral squamous cell carcinoma. *Clin. Sci.* (2016). doi:10.1042/CS20150646
50. Cheng, D. D., Li, S. J., Zhu, B., Zhou, S. M. & Yang, Q. C. EEF1D overexpression promotes osteosarcoma cell proliferation by facilitating Akt-mTOR and Akt-bad signaling. *J. Exp. Clin. Cancer Res.* (2018). doi:10.1186/s13046-018-0715-5
51. Shuda, M. *et al.* Enhanced expression of translation factor mRNAs in hepatocellular carcinoma. *Anticancer Res.* (2000).
52. Laplante, M. & Sabatini, D. M. MTOR signaling in growth control and disease. *Cell* **149,** 274–293 (2012).
53. Benten, D. *et al.* Establishment of the First Well-differentiated Human Pancreatic Neuroendocrine Tumor Model. *Mol. Cancer Res.* (2018). doi:10.1158/1541-7786.MCR-17-0163
54. Henfling, M. *et al.* The IGF pathway is activated in insulinomas but downregulated in metastatic disease. *Endocr. Relat. Cancer* 1–35 (2018). doi:10.1530/ERC-18-0222
55. Rockwell, S. In vivo-in vitro tumour cell lines: characteristics and limitations as models for human cancer. *Br. J. Cancer. Suppl.* (1980).
56. Massironi, S. *et al.* Neuroendocrine tumors of the gastro-entero-pancreatic system. *World Journal of Gastroenterology* (2008). doi:10.3748/wjg.14.5377
57. Yang, Y., Yang, L. & Li, Y. Neuropilin-1 (NRP-1) upregulated by IL-6/STAT3 signaling contributes to invasion in pancreatic neuroendocrine neoplasms. *Hum. Pathol.* **81,** 192–200 (2018).
58. Pal, S. K. *et al.* Efficacy of BGJ398, a fibroblast growth factor receptor 1–3 inhibitor, in patients with previously treated advanced

urothelial carcinoma with FGFR3 alterations. *Cancer Discov.* (2018). doi:10.1158/2159-8290.CD-18-0229

59. Byeon, H. K. *et al.* Fibroblast growth factor receptor 3-mediated reactivation of ERK signaling promotes head and neck squamous cancer cell insensitivity to MEK inhibition. *Cancer Sci.* **109,** 3816–3825 (2018).
60. Misale, S., Di Nicolantonio, F., Sartore-Bianchi, A., Siena, S. & Bardelli, A. Resistance to Anti-EGFR therapy in colorectal cancer: From heterogeneity to convergent evolution. *Cancer Discovery* **4,** 1269–1280 (2014).
61. Harada, K., Miyake, H., Kumano, M. & Fujisawa, M. Acquired resistance to temsirolimus in human renal cell carcinoma cells is mediated by the constitutive activation of signal transduction pathways through mTORC2. *Br. J. Cancer* **109,** 2389–2395 (2013).
62. Kurmasheva, R. T., Huang, S. & Houghton, P. J. Predicted mechanisms of resistance to mTOR inhibitors. *Br. J. Cancer* **95,** 955–960 (2006).
63. Jaiswal, J. K. & Nylandsted, J. S100 and annexin proteins identify cell membrane damage as the achilles heel of metastatic cancer cells. *Cell Cycle* (2015). doi:10.1080/15384101.2014.995495
64. Mussunoor, S. & Murray, G. I. The role of annexins in tumour development and progression. *Journal of Pathology* (2008). doi:10.1002/path.2400
65. Yan, X. *et al.* Increased expression of annexin A3 is a mechanism of platinum resistance in ovarian cancer. *Cancer Res.* (2010). doi:10.1158/0008-5472.CAN-09-3215
66. Kim, A., Serada, S., Enomoto, T. & Naka, T. Targeting annexin A4 to counteract chemoresistance in clear cell carcinoma of the ovary. *Expert Opin. Ther. Targets* (2010). doi:10.1517/14728222.2010.511180
67. Carracedo, A. *et al.* Inhibition of mTORC1 leads to MAPK pathway activation through a PI3K-dependent feedback loop in human cancer. *J. Clin. Invest.* **118,** 3065–3074 (2008).
68. Helpap, B. & Köllermann, J. Undifferentiated carcinoma of the prostate with small cell features: Immunohistochemical subtyping and reflections on histogenesis. *Virchows Arch.* **434,** 385–391 (1999).
69. Paireder, S. *et al.* Comparison of protocols for DNA extraction from long-term preserved formalin fixed tissues. *Anal. Biochem.* **439,** 152–160

(2013).
70. Svejda, B. *et al.* Limitations in small intestinal neuroendocrine tumor therapy by mTor kinase inhibition reflect growth factor-mediated PI3K feedback loop activation via ERK1/2 and AKT. *Cancer* **117,** 4141–4154 (2011).
71. Zitzmann, K. *et al.* Compensatory activation of Akt in response to mTOR and Raf inhibitors - A rationale for dual-targeted therapy approaches in neuroendocrine tumor disease. *Cancer Lett.* **295,** 100–109 (2010).
72. Breuleux, M. *et al.* Increased AKT S473 phosphorylation after mTORC1 inhibition is rictor dependent and does not predict tumor cell response to PI3K/mTOR inhibition. *Mol. Cancer Ther.* **8,** 742–753 (2009).
73. McDonald, P. C. *et al.* Rictor and integrin-linked kinase interact and regulate Akt phosphorylation and cancer cell survival. *Cancer Res.* **68,** 1618–1624 (2008).
74. Tenkerian, C. *et al.* mTORC2 Balances AKT Activation and eIF2 Serine 51 Phosphorylation to Promote Survival under Stress. *Mol. Cancer Res.* **13,** 1377–1388 (2015).
75. Sotillo, R. *et al.* Wide spectrum of tumors in knock-in mice carrying a Cdk4 protein insensitive to INK4 inhibitors. *EMBO J.* **20,** 6637–6647 (2001).
76. Milne, T. A. *et al.* Menin and MLL cooperatively regulate expression of cyclin-dependent kinase inhibitors. *Proc Natl Acad Sci U S A* **102,** 749–754 (2005).
77. Karnik, S. K. *et al.* Menin regulates pancreatic islet growth by promoting histone methylation and expression of genes encoding p27Kip1 and p18INK4c. *Proc. Natl. Acad. Sci. U. S. A.* **102,** 14659–64 (2005).
78. Chen, G. *et al.* Identification of p27/KIP1 expression level as a candidate biomarker of response to rapalogs therapy in human cancer. *J. Mol. Med.* **88,** 941–952 (2010).
79. Sangodkar, J. *et al.* All roads lead to PP2A: Exploiting the therapeutic potential of this phosphatase. *FEBS Journal* (2016). doi:10.1111/febs.13573
80. Magnuson, B., Ekim, B. & Fingar, D. C. Regulation and function of ribosomal protein S6 kinase (S6K) within mTOR signalling networks.

Biochem. J. (2012). doi:10.1042/BJ20110892

81. Li, X. *et al.* Overexpression of 4EBP1, p70S6K, Akt1 or Akt2 differentially promotes Coxsackievirus B3-induced apoptosis in HeLa cells. *Cell Death Dis.* (2013). doi:10.1038/cddis.2013.331
82. No, J. H. *et al.* Activation of mTOR signaling pathway associated with adverse prognostic factors of epithelial ovarian cancer. *Gynecol. Oncol.* (2011). doi:10.1016/j.ygyno.2010.12.364
83. Castellvi, J. *et al.* Phosphorylated 4E binding protein 1: A hallmark of cell signaling that correlates with survival in ovarian cancer. *Cancer* (2006). doi:10.1002/cncr.22195
84. Rojo, F. *et al.* 4E-binding protein 1, a cell signaling hallmark in breast cancer that correlates with pathologic grade and prognosis. *Clin. Cancer Res.* (2007). doi:10.1158/1078-0432.CCR-06-1560
85. Karlsson, E. *et al.* The mTOR effectors 4EBP1 and S6K2 are frequently coexpressed, and associated with a poor prognosis and endocrine resistance in breast cancer: A retrospective study including patients from the randomised Stockholm tamoxifen trials. *Breast Cancer Res.* (2013). doi:10.1186/bcr3557
86. Karlsson, E. *et al.* High-resolution genomic analysis of the 11q13 amplicon in breast cancers identifies synergy with 8p12 amplification, involving the mTOR targets S6K2 and 4EBP1. *Genes Chromosom. Cancer* (2011). doi:10.1002/gcc.20900
87. Cha, Y.-L. *et al.* EIF4EBP1 overexpression is associated with poor survival and disease progression in patients with hepatocellular carcinoma. *PLoS One* (2015). doi:10.1371/journal.pone.0117493
88. Qian, Z. R. *et al.* Prognostic significance of MTOR pathway component expression in neuroendocrine tumors. *J. Clin. Oncol.* (2013). doi:10.1200/JCO.2012.46.6946
89. De Bortoli, M. *et al.* Medulloblastoma outcome is adversely associated with overexpression of EEF1D, RPL30, and RPS20 on the long arm of chromosome 8. *BMC Cancer* (2006). doi:10.1186/1471-2407-6-223
90. Liu, Y., Chen, Q. & Zhang, J. T. Tumor suppressor gene 14-3-3sigma is down-regulated whereas the proto-oncogene translation elongation factor 1delta is up-regulated in non-small cell lung cancers as identified

by proteomic profiling. *J. Proteome Res.* (2004).
91. Voskoglou-Nomikos, T., Pater, J. L. & Seymour, L. Clinical predictive value of the in vitro cell line, human xenograft, and mouse allograft preclinical cancer models. in *Clinical Cancer Research* (2003). doi:10.1158/1078-0432.ccr-06-0113
92. Zeeberg, B. R. *et al.* Concordance of gene expression and functional correlation patterns across the NCI-60 cell lines and the Cancer Genome Atlas glioblastoma samples. *PLoS One* (2012). doi:10.1371/journal.pone.0040062

General discussion

Partially based upon

Next-generation exome sequencing of pancreatic neuroendocrine tumor cell lines BON-1 and QGP-1 reveals different lineages

Timon Vandamme[1,2,3], Matthias Beyens[1,2], Marc Peeters[2], Guy Van Camp[1,2], Ken Op de Beeck[1,2]. Cancer Genetics. 2015; 208(10):523. doi: 10.1016/j.cancergen.2015.07.003

Resistance to targeted treatment of gastroenteropancreatic neuroendocrine tumors

Matthias Beyens[1,2], Timon Vandamme[1,2,3], Marc Peeters[2], Guy Van Camp[1,2], Ken Op de Beeck[1,2]. Endocrine-related Cancer, 2019; 25 (3): R109–R130. doi: 10.1530/ERC-18-0420.

Clinical applications of (epi) genetics in gastroenteropancreatic neuroendocrine neoplasms: moving towards liquid biopsies

Boons Gitta[1,2], Vandamme Timon[1,2,3], Peeters Marc[2], Van Camp Guy[1,2], Op de Beeck Ken[1,2]. Reviews in Endocrine and Metabolic Disorders, 2019. doi: 10.1007/s11154-019-09508-w

[1]Center of Medical Genetics Antwerp, University of Antwerp, Universiteitsplein 1, 2610 Antwerp, Belgium
[2]Center for Oncological Research, University of Antwerp, Universiteitsplein 1, 2610 Antwerp, Belgium
[3]Section of Endocrinology, Department of Internal Medicine, Erasmus Medical Center. Dr Molenwaterplein 40, 3015GD Rotterdam, the Netherlands

I. UNDERSTANDING PNEN BIOLOGY REQUIRES MODELS

Pancreatic neuroendocrine neoplasms (pNENs) are very distinct from other pancreatic neoplasms in biology, histology and clinical behavior[1,2]. According to the latest Surveillance, Epidemiology, and End Results (SEER) data, the annual age-adjusted incidence of pNEN is 0.48 per 100,000 person years in the United States[1]. Although there is a clear rise in incidence over the last decades, pNENs remain rare[1]. Hence, pre-clinical models have been extensively used to understand pNEN biology and the development of novel therapeutic strategies. Because of their relative ease of use and their availability, patient-derived cell line models such as BON-1 and QGP-1 have been instrumental in the development of many drugs in pNENs[3,4]. However, knowledge of the genetic background of these cell lines was scarce. In this thesis, the BON-1 and QGP-1 cell lines are extensively characterized at the genetic and genomic level. In **chapter 2**, we demonstrate that BON-1 and QGP-1 share a considerable number of mutated genes with patient samples, including mutations in *ATRX* and the PI3K-Akt-mTOR pathway. However, the BON-1 and QGP-1 genome contains additional mutated genes such as p53, probably as a result of the immortalization needed to survive *in vitro*. Additionally, extensive loss of heterozygosity (LOH) in the triploid BON-1 and tetraploid QGP-1 has been observed. The LOH of *MEN1* and *CDKN2A* and *CDKN2B* genes in our cell line data is in line with recent sequencing data that revealed *MEN1* and *CDKN2B* LOH in patient samples[5].

The full transcriptome profiling of BON-1 and QGP-1, presented in **chapter 6**, shows that both cell lines cluster with other cell lines with neuroendocrine characteristics. In addition, both cell lines retain expression of typical neuroendocrine neoplasm markers, such as synaptophysin and neuron-specific enolase[6].

However, sub-clonality might be of importance in pNEN, both in models and in patients. For instance, Ganesh K. Boora et al. published exome sequencing results of several neuroendocrine neoplasm (NEN) cell lines, including BON-1 and QGP-1[7]. When comparing this dataset with our whole-exome data, a number of mutations were unique to each dataset. As the same Illumina platform and a similar bio-informatics approach were used, it is unlikely that this divergence is caused by different methodology. Therefore, we could be looking at different lineages of the same cell lines. Since both cell lines have an aberrant chromosome number with a ploidy of 3 in BON-1 and tetraploidy in QGP-1, chromosomal instability could result in a higher mutation rate. Although in our studies we used early passages of BON-1 and QGP-1 (passage 9 and 14, respectively), increasing passage number could result in sub-clonality, explaining the difference between both datasets. Sub-clonality in BON-1 and QGP-1 could have important consequences for experiments with these cell lines, since genetic alterations could lead to phenotypic changes. It is hence vital to confirm genetic identity of the used cell lines and perform mutational analysis of genes of interest.

In **chapter 3** sub-clonality in patient samples is demonstrated

through a targeted ultradeep sequencing approach. The identification of low-abundance mutations, present in only a subset of tumor cells, could have important clinical implications. As tumors evolve dynamically over time, mutations that are initially present in a low fraction of cells could become the leading clone, pushing disease progression and metastasis. This observation is supported by a recent pilot study in small intestinal neuroendocrine neoplasms (siNEN), comparing primary tumors and metastasis of 5 patients[8]. In this study, a markedly higher allelic fraction of mutations was seen in metastasis samples compared to the primary tumor, which could point towards a single dominant clone from the primary leading to metastasis. Mutational difference between primary lesions and metastasis ranged from 6% to 100%, which is higher than in other malignancies such as non-small cell lung cancer (<50% mutational difference), endometrial cancer (<45% mutational difference), and head and neck squamous cell carcinoma (<60% mutational difference)[9–11]. As most mutations in known tumor suppressor and oncogenes were shared between primary tumors and metastasis, the impact of this genetic heterogeneity between primary and metastasis on disease progression is the subject of further study. Hence, a more extensive study with multi-region sequencing, including pNEN, could provide additional valuable insights regarding the role of subclonal mutations in NENs.

II. UNDERSTANDING AND OVERCOMING EVEROLIMUS RESISTANCE IN PNEN

Everolimus is frequently used as a targeted therapy for GEP-NENs, but its effects are limited by both primary and acquired resistance. Predictive biomarkers are needed in this respect. In **chapter 4, 5, 6** we have therefore focused on the identification of resistance mechanisms, ways to overcome resistance, and biomarkers related to these treatments. In **chapter 4**, we demonstrate that *ERK2* is upregulated in induced rapalog resistance cell line models, pointing towards cross-talk between the PI3K/Akt/mTOR and Raf/MEK/ERK pathway. Carracedo and colleagues demonstrated an everolimus administration schedule-dependent increase of Raf/MEK/ERK signaling activation in patients with solid tumors in advanced diseases stages[12]. In addition, mTOR inhibition in combination with a MEK1/2 inhibitor was synergistic for anti-proliferative effects in GEP-NEN models[13]. In **chapter 5**, the role of cell cycle regulatory components in everolimus resistance is highlighted. In our resistant cell line model, we found CDK4 upregulated and $p27^{Kip1}$ downregulated. Physiologically, $p27^{Kip1}$, a cyclin-dependent kinase (CDK) inhibitor, inhibits the cyclin D1 - CDK4/6 complex. This inhibition prevents phosphorylation of retinoblastoma (RB) and its dissociation from transcription factors implicated in the G_1-S progression. In addition, transcriptomic analysis of both resistant cell lines in **chapter 6** showed a downregulation of protein phosphatase 2A (PP2A) regulatory B55β subunit, *PPP2R2B*. Protein phosphatase 2A (PP2A) is a multiprotein serine/threonine

phosphatase regulating cell growth, proliferation and survival[14,15]. PP2A regulates PDK1 activity towards MYC phosphorylation. Epigenetic inactivation of *PPP2R2B* in colorectal cancer, encoding the B55β regulatory subunit of the PP2A phosphatase, has been associated with rapamycin resistance[16]. Following rapamycin treatment, downregulated PP2A induces PDK1-dependent phosphorylation of MYC, and thus promotes cell proliferation[16].

To overcome everolimus resistance, various novel PI3K/Akt/mTOR inhibitors have been developed. The second generation of mTOR-inhibitors, so-called small molecule mTOR kinase inhibitors (TORKi's), inhibit the kinase activity of mTORC1 and mTORC2 in a FKBP-12-independent mechanism of action by competitive binding the ATP-binding mTOR kinase pocket[17–19]. Various TORKi's have been developed, including AZD2014 and OSI-027, and their clinical relevance was assessed in clinical trials. In **chapter 4**, we have shown that AZD2014 and OSI-027 are able to overcome everolimus resistance. AZD2014 (with International Nonproprietary Name (INN)-alias vistusertib) effectively reduces cell proliferation in rapalog-resistant BON-1 and QGP-1 cells at concentrations that are reachable in patients[20]. However, AZD2014 efficacy has been proven to be inferior to everolimus in a phase-II study including metastatic renal cell carcinoma with mPFS 1.8 and 4.6 months, in AZD2014 and everolimus stratum respectively[21]. Further development of combination therapies with AZD2014 in relapsed/refractory diffuse large B-cell lymphoma and hormone receptor-positive metastatic breast cancer did not yield clear benefit in comparison to mTORC1 inhibitors such as everolimus[22,23]. In both

trials the maximum tolerated doses were used[22,23]. However, the selected dose might not have been adequate to fully exert its established preclinical activity. The toxic effect–mandated doses of vistusertib might only achieve suboptimal inhibition of the mTORC1 complex, leading to feedback loops and residual 4E-BP1 activity, sufficient to eliminate a significant treatment effect[12,24]. A dose-finding phase-I trial evaluating OSI-027 in advanced solid cancers demonstrated that the effective concentrations of the drug were above the tolerable doses[25]. One of the major adverse effects was the acute onset of renal impairment within few days of treatment. For this reason, the clinical development has been discontinued.

Another approach to overcome everolimus resistance is the use of dual PI3K-mTOR inhibitors such as BEZ235. These inhibitors prevent unwanted feedback activation of PI3K signaling and the mTORC2-dependent Akt activation via phosphorylation. While this broad inhibitory activity is beneficial from a therapeutic point of view, it also causes serious side effects limiting their clinical applicability. BEZ235 showed promise in multiple preclinical studies. High efficacy in inhibiting the PI3K-Akt-mTOR pathway and cell proliferation has been ascribed to its combined PI3K, mTORC1 and mTORC2 inhibition[26,27]. In **chapter 4**, we demonstrate that BEZ235 is able to overcome *in vitro* acquired rapalog resistance. Despite the promising pre-clinical results, two phase-II trials testing BEZ235 in pNENs were terminated prematurely due to limited efficacy and a challenging tolerability profile compared to everolimus[28,29]. The first phase-

II trial evaluating BEZ235 in patients with everolimus-resistant pNENs never reached stage 2 of the trial, which would have been triggered by a 16-week PFS rate of >60% in stage 1. The lower than expected PFS is due to the high rate (72.7% of the patients) of treatment-related grade 3 and 4 side effects[28]. In another phase-II study evaluating everolimus versus BEZ235 in patients with everolimus-sensitive pNENs, BEZ235 treatment showed a limited degree of efficacy with a median PFS of 8.2 months compared to that of the everolimus treated group with a median PFS of 10.8 months[29]. Like in the above mentioned study, the lack of efficacy may be attributed to the poorer tolerability of BEZ235; the adverse effects were twice as frequent in the BEZ235 arm of the study[29]. Although further clinical trials evaluating BEZ235 are halted, other ATP-competitive dual inhibitors could be considered if they show less adverse effects.

Next to overcoming resistance, the identification of a biomarker for everolimus resistance would allow optimizing matching of treatment and patient and, based upon tumor characteristics, lead to a patient-tailored approach of treatment. Additionally, it could help to identify treatment failure earlier, thereby increasing treatment efficacy. A study on 17 pNEN patients by Serra et al. suggested predictive value for everolimus efficacy of the Gly388Arg *FGFR4* polymorphism, with a worse response in *FGFR4-R388* patients, in concordance with preclinical models[30]. However, this polymorphism did not seem to have prognostic or predictive value for everolimus response in a retrospective study on 35 GEP-NENs[31]. Genetic analysis of 191 GEP-NEN patients of the

RADIANT trials could not evaluate the predictive value of PI3K/Akt/mTOR pathway mutations due to a low number of mutations and inequal distribution over treatment and placebo cohorts[32]. In this analysis, no other mutations or CNVs could be identified to be predictive for therapy response. In our pre-clinical resistance model, no clear genetic or genomic biomarker for everolimus resistance was found. In conclusion, there are still no prognostic or predictive molecular markers available for everolimus.

III. FUTURE PERSPECTIVES

The recent advances in the understanding of the genetic constitution have clearly accelerated research in pNENs. However, several gaps remain. Due to their low incidence, many studies are being performed on relatively small sample sizes. This stresses the importance of collaborations for the study of rare diseases, whereby both samples and data should be pooled to achieve larger datasets, like available in The Cancer Genome Atlas (TCGA) for various other tumor types. Furthermore, most studies have only focused on one aspect of the tumor cell, such as the genetic constitution[5,33]. However, to fully understand the molecular mechanisms driving development and progression of pNENs, it would be interesting to apply an integrative approach by combining multi-omics data, including RNA expression and epigenetic dysregulation. The latter could be very relevant, as the most commonly mutated genes in pNEN such as *MEN1*, *ATRX* and *DAXX* are all involved in regulating epigenetic modifications[34]. In

addition, pNENs have a relatively low tumor mutational burden in comparison to other tumor types[35]. Hence, it could be that the pNENs are tumors mainly driven by epigenetic changes rather than by mutations or copy number alterations. The first studies on epigenetics in pNEN are being undertaken, mainly focusing on DNA methylation changes. Genome-wide DNA methylation profiles of 53 and 64 sporadic pNENs, respectively, were shown to be different depending on the mutation status (e.g. *DAXX, ATRX* or *MEN1* mutated)[36,37]. Promotor hypermethylation of tumor suppressor genes is a frequent event in both MEN1-related and sporadic pNENs[38]. In a recent study, clustering of the genome-wide DNA methylation profile of 9 sporadic, 10 VHL-related and 10 MEN1-related PNENs and 4 pancreatic islets resulted in a cluster of VHL PNENs and a cluster containing both sporadic and MEN1-related PNENs[39]. However, the role of these methylation changes in carcinogenesis and tumor progression remains unclear. Only very few studies exist on other forms of epigenetic changes such as histone modifications[40]. Hence, further studies, both exploratory and mechanistic, are needed to improve our understanding of the epigenetics of pNENs.

In addition, the search for prognostic and predictive biomarkers for everolimus resistance has focused on mutations and mRNA expression changes and yielded little results. However, epigenetic modifications might hold the key to uncover a biomarker. To study the impact of these epigenetic modifications, methylation arrays in our *in vitro* cell line models could be used in a first screening phase. In a next step, *in vivo* results in matched biopsies before

everolimus treatment and after everolimus treatment failure could yield interesting results. As these matched biopsies are not easily obtained, an alternative approach would be to use patient-derived xenograft models (PDXs) and compare the effect of everolimus exposure between tissues derived from individual patients. Interestingly, identification of methylation-based biomarker in tissue could be translated to a blood-based assay, as recent studies show that tumor-specific methylation changes are reliably detectable in circulating tumor DNA[41]. Tumor heterogeneity and clonal evolution might play a role in everolimus resistance. Therefore, the collected matched intra-patient samples could be subjected to single-cell sequencing techniques, allowing for spatiotemporal mapping of the appearance and characteristics of everolimus resistance. Finally, as everolimus affects mTORC1 phosphorylation sites through steric hindrance, a proteomics-based approach might be another interesting avenue to pursue. Recent advantages in proteome analysis, including label-free liquid chromatography/mass spectrometry-based methods and genome-wide CRISPR-Cas9 screens, could help elaborate the kinetics involved in everolimus resistance and its associated feedback-loops[42,43].

Next to biomarker discovery, epigenetic modifications seem to be involved in therapy resistance through transcriptional silencing of target components or activation of rescue pathways[44–47]. In prostate cancer cell lines, the histone deacetylase (HDAC) inhibitor valproic acid has been shown to overcome resistance to temsirolimus, a rapalog[48]. Moreover, valproic acid acetylates

histone variants H3 and H4 in temsirolimus-resistant bladder cancer and in everolimus-resistant renal cancer cells[49–51]. Finally, valproic acid increases rapalog sensitivity via regulation of the CDK2/cyclin A cell cycle axis[50,51]. These results have led to multiple phase-I studies with (pan-)HDAC inhibitors panobinostat and vorinostat in combination with rapalogs in cancer, showing promising results[52–55]. A recent study used a RNAseq and Virtual Proteomics by Enriched Regulon analysis (VIPER) on 212 GEP-NEN samples to prioritize drugs targeting master regulators of GEP-NEN tumor growth. In this study, the class I (HDAC1/3) inhibitor entinostat was identified to have strong anti-tumoral effects, both *in vitro* and *in vivo*[56]. Likewise, demethylating compounds such as 5-aza-2-deoxycytidine were effective in combination with everolimus in medullary thyroid cancer[57]. The synergistic effect has been linked to apoptosis induction through Bax and Bcl-2, two downstream effectors of mTOR[58–61]. Hence, targeting epigenetic changes in pNEN could be an interesting strategy to overcome everolimus resistance and should be studied further.

IV. REFERENCES

1. Dasari, A. *et al.* Trends in the Incidence, Prevalence, and Survival Outcomes in Patients With Neuroendocrine Tumors in the United States. *JAMA Oncol.* **3**, 1335–1342 (2017).
2. Rindi, G. *et al.* A common classification framework for neuroendocrine neoplasms: an International Agency for Research on Cancer (IARC) and World Health Organization (WHO) expert consensus proposal. *Modern Pathology* (2018). doi:10.1038/s41379-018-0110-y
3. Grozinsky-Glasberg, S., Shimon, I. & Rubinfeld, H. The role of cell lines in the study of neuroendocrine tumors. *Neuroendocrinology* (2012). doi:10.1159/000338793
4. Babu, V., Paul, N. & Yu, R. Animal models and cell lines of pancreatic neuroendocrine tumors. *Pancreas* (2013). doi:10.1097/MPA.0b013e31827ae993
5. Scarpa, A. *et al.* Whole-genome landscape of pancreatic neuroendocrine tumours. *Nature* **543**, 65–71 (2017).
6. Hofving, T. *et al.* The neuroendocrine phenotype, genomic profile and therapeutic sensitivity of GEPNET cell lines. *Endocr. Relat. Cancer* (2018). doi:10.1530/ERC-17-0445
7. Boora, G. K. *et al.* Exome-level comparison of primary well-differentiated neuroendocrine tumors and their cell lines. *Cancer Genet.* (2015). doi:10.1016/j.cancergen.2015.04.002
8. Walter, D. *et al.* Genetic heterogeneity of primary lesion and metastasis in small intestine neuroendocrine tumors. *Sci. Rep.* (2018). doi:10.1038/s41598-018-22115-0
9. Saber, A. *et al.* Mutation patterns in small cell and non-small cell lung cancer patients suggest a different level of heterogeneity between primary and metastatic tumors. *Carcinogenesis* (2017). doi:10.1093/carcin/bgw128
10. Gibson, W. J. *et al.* The genomic landscape and evolution of endometrial carcinoma progression and abdominopelvic metastasis. *Nat. Genet.* (2016). doi:10.1038/ng.3602

11. Hedberg, M. L. *et al.* Genetic landscape of metastatic and recurrent head and neck squamous cell carcinoma. *J. Clin. Invest.* (2016). doi:10.1172/JCI82066
12. Carracedo, A. *et al.* Inhibition of mTORC1 leads to MAPK pathway activation through a PI3K-dependent feedback loop in human cancer. *J. Clin. Invest.* **118**, 3065–3074 (2008).
13. Valentino, J. D. *et al.* Cotargeting the PI3K and RAS pathways for the treatment of neuroendocrine tumors. *Clin. Cancer Res.* (2014). doi:10.1158/1078-0432.CCR-13-1897
14. Chen, W. *et al.* Identification of specific PP2A complexes involved in human cell transformation. *Cancer Cell* **5**, 127–136 (2004).
15. Wlodarchak, N. & Xing, Y. PP2A as a master regulator of the cell cycle. *Critical Reviews in Biochemistry and Molecular Biology* **51**, 162–184 (2016).
16. Tan, J. *et al.* B55β-Associated PP2A Complex Controls PDK1-Directed Myc signaling and modulates rapamycin sensitivity in colorectal cancer. *Cancer Cell* **18**, 459–471 (2010).
17. Feldman, M. E. *et al.* Active-site inhibitors of mTOR target rapamycin-resistant outputs of mTORC1 and mTORC2. *PLoS Biol.* **7**, 0371–0383 (2009).
18. Thoreen, C. C. *et al.* An ATP-competitive mammalian target of rapamycin inhibitor reveals rapamycin-resistant functions of mTORC1. *J. Biol. Chem.* **284**, 8023–8032 (2009).
19. Yu, K. *et al.* Biochemical, cellular, and in vivo activity of novel ATP-competitive and selective inhibitors of the mammalian target of rapamycin. *Cancer Res.* **69**, 6232–40 (2009).
20. Basu, B. *et al.* First-in-human pharmacokinetic and pharmacodynamic study of the dual m-TORC 1/2 inhibitor AZD2014. *Clin. Cancer Res.* **21**, 3412–3419 (2015).
21. Powles, T. *et al.* A Randomised Phase 2 Study of AZD2014 Versus Everolimus in Patients with VEGF-Refractory Metastatic Clear Cell Renal Cancer. *Eur. Urol.* **69**, 450–456 (2016).
22. Eyre, T. A. *et al.* A phase II study to assess the safety and efficacy of the dual mTORC1/2 inhibitor vistusertib in relapsed, refractory DLBCL.

Hematol. Oncol. **69**, 1–8 (2019).
23. Schmid, P. *et al.* Fulvestrant Plus Vistusertib vs Fulvestrant Plus Everolimus vs Fulvestrant Alone for Women With Hormone Receptor–Positive Metastatic Breast Cancer. *JAMA Oncol.* (2019). doi:10.1001/jamaoncol.2019.2526
24. Kang, S. A. *et al.* mTORC1 phosphorylation sites encode their sensitivity to starvation and rapamycin. *Science (80-.).* **341**, 1–16 (2013).
25. Mateo, J. *et al.* A first in man, dose-finding study of the mTORC1/mTORC2 inhibitor OSI-027 in patients with advanced solid malignancies. *Br. J. Cancer* **114**, 889–896 (2016).
26. Maira, S.-M. *et al.* Identification and characterization of NVP-BEZ235, a new orally available dual phosphatidylinositol 3-kinase/mammalian target of rapamycin inhibitor with potent in vivo antitumor activity. *Mol. Cancer Ther.* **7**, 1851–1863 (2008).
27. Passacantilli, I. *et al.* Combined therapy with RAD001 e BEZ235 overcomes resistance of PET immortalized cell lines to mTOR inhibition. *Oncotarget* (2014). doi:10.18632/oncotarget.2111
28. Fazio, N. *et al.* A phase II study of BEZ235 in patients with everolimusresistant, advanced pancreatic neuroendocrine tumours. *Anticancer Res.* **36**, 713–720 (2016).
29. Salazar, R. *et al.* Phase II Study of BEZ235 versus Everolimus in Patients with Mammalian Target of Rapamycin Inhibitor-Naïve Advanced Pancreatic Neuroendocrine Tumors. *Oncologist* theoncologist.2017-0144 (2017). doi:10.1634/theoncologist.2017-0144
30. Serra, S. *et al.* The FGFR4-G388R single-nucleotide polymorphism alters pancreatic neuroendocrine tumor progression and response to mTOR inhibition therapy. *Cancer Res.* (2012). doi:10.1158/0008-5472.CAN-12-2102
31. Cros, J. *et al.* Gly388Arg FGFR4 polymorphism is not predictive of everolimus efficacy in well-differentiated digestive neuroendocrine tumors. *Neuroendocrinology* (2016). doi:10.1159/000440724
32. Yao, J. *et al.* Genomic profiling of NETs: A comprehensive analysis of the RADIANT trials. *Endocr. Relat. Cancer* (2018). doi:10.1530/ERC-18-0332
33. Jiao, Y. *et al.* DAXX/ATRX, MEN1, and mTOR pathway genes are frequently

altered in pancreatic neuroendocrine tumors. *Science (80-.).* **331**, 1199–1203 (2011).

34. Heaphy, C. M. *et al.* Altered telomeres in tumors with ATRX and DAXX mutations. *Science* (2011). doi:10.1126/science.1207313
35. McKenna, A. *et al.* The Genome Analysis Toolkit: a MapReduce framework for analyzing next-generation DNA sequencing data. *Genome Res* **20**, 1297–1303 (2010).
36. Pipinikas, C. P. *et al.* Epigenetic dysregulation and poorer prognosis in DAXX-deficient pancreatic neuroendocrine tumours. *Endocr. Relat. Cancer* (2015). doi:10.1530/erc-15-0108
37. Chan, C. S. *et al.* ATRX, DAXX or MEN1 mutant pancreatic neuroendocrine tumors are a distinct alpha-cell signature subgroup. *Nat. Commun.* (2018). doi:10.1038/s41467-018-06498-2
38. Conemans, E. B. *et al.* DNA methylation profiling in MEN1-related pancreatic neuroendocrine tumors reveals a potential epigenetic target for treatment. *Eur. J. Endocrinol.* (2018). doi:10.1530/EJE-18-0195
39. Tirosh, A. *et al.* Distinct genome-wide methylation patterns in sporadic and hereditary nonfunctioning pancreatic neuroendocrine tumors. *Cancer* (2019). doi:10.1002/cncr.31930
40. Veenstra, M. J. *et al.* Epidrug-induced upregulation of functional somatostatin type 2 receptors in human pancreatic neuroendocrine tumor cells. *Oncotarget* (2016). doi:10.18632/oncotarget.9462
41. Xu, R. H. *et al.* Circulating tumour DNA methylation markers for diagnosis and prognosis of hepatocellular carcinoma. *Nat. Mater.* (2017). doi:10.1038/NMAT4997
42. Eckert, M. A. *et al.* Proteomics reveals NNMT as a master metabolic regulator of cancer-associated fibroblasts. *Nature* (2019). doi:10.1038/s41586-019-1173-8
43. Phelan, J. D. *et al.* A multiprotein supercomplex controlling oncogenic signalling in lymphoma. *Nature* (2018). doi:10.1038/s41586-018-0290-0
44. Hervouet, E., Cheray, M., Vallette, F. & Cartron, P.-F. DNA Methylation and Apoptosis Resistance in Cancer Cells. *Cells* (2013). doi:10.3390/cells2030545
45. Kelly, T. K., De Carvalho, D. D. & Jones, P. A. Epigenetic modifications as

therapeutic targets. *Nature Biotechnology* (2010). doi:10.1038/nbt.1678
46. Berdasco, M. & Esteller, M. Aberrant Epigenetic Landscape in Cancer: How Cellular Identity Goes Awry. *Developmental Cell* (2010). doi:10.1016/j.devcel.2010.10.005
47. Wilting, R. H. & Dannenberg, J. H. Epigenetic mechanisms in tumorigenesis, tumor cell heterogeneity and drug resistance. *Drug Resistance Updates* (2012). doi:10.1016/j.drup.2012.01.008
48. Makarević, J. *et al.* HDAC Inhibition Counteracts Metastatic Re-Activation of Prostate Cancer Cells Induced by Chronic mTOR Suppression. *Cells* 7, 129 (2018).
49. Juengel, E. *et al.* HDAC inhibition as a treatment concept to combat temsirolimus-resistant bladder cancer cells. *Oncotarget* (2017). doi:10.18632/oncotarget.22454
50. Juengel, E. *et al.* HDAC-inhibition counteracts everolimus resistance in renal cell carcinoma in vitro by diminishing cdk2 and cyclin A. *Mol. Cancer* (2014). doi:10.1186/1476-4598-13-152
51. Juengel, E. *et al.* Acetylation of histone H3 prevents resistance development caused by chronic mTOR inhibition in renal cell carcinoma cells. *Cancer Lett.* (2012). doi:10.1016/j.canlet.2012.05.003
52. Earwaker, P. *et al.* RAPTOR up-regulation contributes to resistance of renal cancer cells to PI3K-mTOR inhibition. *PLoS One* (2018). doi:10.1371/journal.pone.0191890
53. Strickler, J. H. *et al.* Phase I study of bevacizumab, everolimus, and panobinostat (LBH-589) in advanced solid tumors. *Cancer Chemother. Pharmacol.* (2012). doi:10.1007/s00280-012-1911-1
54. Oki, Y. *et al.* Phase i study of panobinostat plus everolimus in patients with relapsed or refractory lymphoma. *Clin. Cancer Res.* (2013). doi:10.1158/1078-0432.CCR-13-1906
55. Zibelman, M. *et al.* Phase i study of the mTOR inhibitor ridaforolimus and the HDAC inhibitor vorinostat in advanced renal cell carcinoma and other solid tumors. *Invest. New Drugs* (2015). doi:10.1007/s10637-015-0261-3
56. Alvarez, M. J. *et al.* A precision oncology approach to the pharmacological targeting of mechanistic dependencies in neuroendocrine tumors. *Nat.*

Genet. (2018). doi:10.1038/s41588-018-0138-4

57. Vitale, G. *et al.* Synergistic activity of everolimus and 5-aza-2'-deoxycytidine in medullary thyroid carcinoma cell lines. *Mol. Oncol.* (2017). doi:10.1002/1878-0261.12070

58. Dimaras, H. & Gallie, B. L. The p75NTRneurotrophin receptor is a tumor suppressor in human and murine retinoblastoma development. *Int. J. Cancer* (2008). doi:10.1002/ijc.23356

59. Jin, H. *et al.* p75 Neurotrophin Receptor Inhibits Invasion and Metastasis of Gastric Cancer. *Mol. Cancer Res.* (2007). doi:10.1158/1541-7786.MCR-06-0407

60. Küchler, J. *et al.* P75NTRinduces apoptosis in medulloblastoma cells. *Int. J. Cancer* (2011). doi:10.1002/ijc.25508

61. Yang, Z. *et al.* Epigenetic Inactivation and Tumor-Suppressor Behavior of NGFR in Human Colorectal Cancer. *Mol. Cancer Res.* (2015). doi:10.1158/1541-7786.MCR-13-0247

Summary

I. SUMMARY

Pancreatic neuroendocrine neoplasms (pNENs) comprise only 1-2% of all pancreatic neoplasms, with an incidence of about 0.48 per 100,000 person years. Recent advances in next-generation sequencing (NGS) has led to a better understanding of the genetic constitution of pNENs, uncovering the role of the phosphoinositide-3-kinase (PI3K)/protein kinase B (Akt)/mTOR signalling in these tumors. Surgical resection is the primary treatment in locoregional pNENs, and the only curative treatment option. However, more than 50% of cases present with unresectable disease at time of diagnosis. For these advanced pNENs, the mTOR-inhibitor everolimus, a so-called rapalog, has demonstrated to improve progression-free survival. However, primary and acquired resistance to everolimus, may limit its efficacy as single treatment modality. In acquired resistance, patients who initially respond to everolimus, later relapse and develop resistance, whereas in primary resistance, patients do not respond at all. To allow *in vitro* study of pNEN, the BON-1 and QGP-1 human cell lines have been developed. In this thesis, we characterize the genetic make-up of both cell lines and compare it to patient samples. In addition, we establish a model for acquired everolimus resistance and use this to uncover everolimus resistance mechanisms.

Chapter 1 provides an overview of the current knowledge of pNENs genetics and highlights the role of the PI3K/Akt/mTOR

signaling in pNEN cancerogenesis. In addition, it summarizes the preclinical and clinical development of everolimus. Chapter 1 ends with an overview of the main aims of this thesis.

Chapter 2 presents the first high-resolution genetic profile of the BON-1 and QGP-1 cell lines, based on array-based techniques and next generation whole exome sequencing data. These frequently used pNEN models show mutations in accordance with sporadic pNEN in patients. This study highlights BON-1 and QGP-1 as relevant genetic models for different subtypes of pNEN in patients, although further validation is needed. The molecular characterization of both frequently used pNEN models contributes to a better understanding of the pathogenesis of pNEN.

Chapter 3 adds to the growing body of evidence on the broad genetic constitution of pNENs by demonstrating the presence of low-abundance mutations and genetic heterogeneity in pNENs. We highlight the importance of the *ATRX/DAXX* pathway by reporting the first-ever pNEN-specific protein-damaging hotspot mutation in *DAXX*, and uncover novel genes and pathways involved in pNENs, including pro-apoptotic *CYFIP2*, hedgehog signaling and the MAPK-ERK pathway.

In **chapter 4** BON-1/R and QGP-1/R, the first pNEN models for acquired rapalog-resistance after long-term everolimus treatment, are presented. Both the ATP-competitive mTOR blocker, AZD2014, and the dual PI3K-mTOR blocker NVP-BEZ235 are able to overcome this rapalog resistance. Additionally, the role of cross-talk between the PI3K/Akt/mTOR pathway and the

MAPK-ERK pathway in everolimus resistance is described. Both models allow the study of the detailed mechanisms of acquired resistance in pNEN.

Chapter 5 describes the low-pass whole genome sequencing of in everolimus resistant pNEN cell lines QGP-1/R and BON-1/R, revealing multiple copy number amplifications and deletions. Focusing on recurrent alterations in tumor suppressor and oncogenes, this study led to the identification of copy number alterations in two cell cycle regulatory components: a *CDK4* amplification and *CDKN1B* deletion, respectively. These copy number alterations lead to expression changes of CDK4, p27 and other cell cycle components. This study is the first to demonstrate a role of CDK4 and p27 in acquired everolimus resistance in NENs, which is in line with recent studies in other tumor types. Both CDK4 and p27 might be pivotal for everolimus resistance and could be a potential biomarker for the efficacy of everolimus treatment in NEN patients. Additionally, it provides a rationale for the use of cell cycle inhibitors in the treatment of rapalog-resistant NENs.

Chapter 6 improves the understanding of the BON-1 and QGP-1 cell lines as models for pNEN by presenting full transcriptome data, both at baseline and after everolimus exposure. In addition, genome-wide gene expression data of BON-1/R and QGP-1/R, two everolimus-resistant cell lines, is presented. The transcriptome profile of BON-1 and QGP-1 clusters with other cell lines with neuroendocrine characteristics, indicating that BON-1 and QGP-1

are useful tools to investigate physiological and pathophysiological differentiation and can be exploited to identify molecular targets for novel therapeutics in pNEN. In the resistant BON-1/R and QGP-1/R, the transcriptomic profile highlights the role of cell cycles proteins in everolimus resistance. In addition, transcriptomic changes further implicate the MAPK-ERK pathway in everolimus resistance and provides a rationale for dual PI3K/Akt/mTOR and MAPK-ERK inhibition in pNEN.

In **chapter** 7 the overall findings of these thesis are discussed in relation to the current body of literature. In addition, future perspectives and possible novel areas of research, such as epigenetics, are put forward.

II. SAMENVATTING

Pancreatische neuroendocriene neoplasieën (pNENs) vormen slecht 1-2% van alle pancreatische gezwellen, met een incidentie rond de 0.48 per 100,000 personenjaren. Recente vooruitgang in de next-generation sequencing (NGS) heeft geleid tot een beter begrip van de genetische constitutie van pNENs en van de rol van de fosfoinositide-3-kinase (PI3K)/proteine kinase B (Akt)/mTOR signaalstransductieweg in deze tumoren. Chirurgische resectie is de voorkeursbehandeling in locoregionale pNENs en de enige curatieve behandeling. Meer dan 50% van de patiënten is echter reeds inoperabel bij diagnose. In deze gevorderde pNENs heeft de mTOR-ihibitor everolimus, een zogenaamde rapaloog, aangetoond dat het de progressievrije overleving kan verlengen in pNEN patienten. Primaire en verworven resistentie tegen everolimus hindert echter de efficaciteit van deze behandeling in monotherapie. Bij verworven resistentie, reageren de patiënten initieel goed op everolimus, maar wordt de ziekte snel progressief door het optreden van resistentie. Bij primaire resistentie heeft de behandeling reeds van bij de start weinig effect. De BON-1 en QGP-1 humane cellijnen zijn ontwikkeld om pNEN *in vitro* te bestuderen. In dit proefschrift karakteriseren we de genetische opmaak van beide cellijnen en vergelijken deze met pNEN weefsels van patiënten. Daarnaast wordt een model voor verworven everolimusresistentie gecreeërd en gebruikt om resistentiemechanismes voor everolimus te onderzoeken.

Hoofdstuk 1 geeft een overzicht van de huidige kennis van de genetica van pNEN en beschrijft de rol van de PI3K/Akt/mTOR signaalstransductieweg in pNEN cancerogenese. Daarnaast geeft het een overzicht van de pre-klinische en klinische ontwikkeling van everolimus. Hoofdstuk 1 eindigt met een overzicht van de belangrijkste doelstellingen van deze thesis.

In **hoofdstuk 2** wordt, met behulp van chip-gebaseerde technnieken en next generation volledige exoomsequenering, het eerste gedetailleerde genetische profiel van de BON-1 en QGP-1 cellijnen gepresenteerd. Deze frequent gebruikte pNEN modellen vertonen gelijkaardige mutaties als tumoren van patiënten. Dit toont aan dat BON-1 en QGP-1 relevante genetische modellen zijn voor verschillende subtypes van pNEN. Verdere validatie blijft echter noodzakelijk. De moleculaire karakterisering van beide frequent gebruikte pNEN modellen draagt bij tot een beter begrip van de pathogenese van pNENs.

Hoofdstuk 3 draagt bij aan de groeiende evidentie rond de bredere genetische samenstelling van pNENs, door aan te tonen dat er mutaties in lage frequenties in pNENs voorkomen. Daarnaast wordt genetische heterogeniteit in pNENs aangetoond. Het belang van de *ATRX/DAXX* signaalstransductieweg in pNENs wordt benadrukt door het rapporteren van de eerste pNEN-specifieke recurrente mutatie, die de functie van het eiwit verhindert, in het *DAXX* gen. Verschillende nieuwe genen en signaalstransductiewegen worden geïmpliceerd in pNENs, waaronder het pro-apoptotische *CYFIP2* gen, hedgehog

signaalstransductie en de MAPK-ERK signaalstransductieweg.

In **hoofdstuk 4** beschrijven we BON-1/R en QGP-1/R, de twee eerste modellen voor verworven rapaloog-resistentie na langdurige everolimusblootstelling. Zowel de ATP-competitieve mTOR-blokker AZD2014, als de duale PI3K-mTOR blokker NVP-BEZ235 kunnen deze rapaloog-resistentie overwinnen. Daarnaast wordt verwevenheid tussen de PI3K/Akt/mTOR signaalstransductieweg en de MAPK-ERK signaalstransductie in everolimusresistentie beschreven. Beide resistentiemodellen laten een gedetailleerde studie van de mechanismen voor verworven resistentie in pNEN toe.

Hoofdstuk 5 beschrijft de volledige genoomsequentie van de everolimus-resistente cellijnen QGP-1/R en BON-1/R. Hierbij worden verschillende copynumberduplicaties en -deleties waargenomen. Het bestuderen van terugkerende copynumbervariaties in tumorsuppressor- en oncogenen leidde tot de identificatie van twee celcyclusregulerende componenten: een *CDK4* amplificatie en een *CDKN1B* deletie. Deze copynumbervariaties vertaalden zich in expressieveranderingen in CDK4, p27 en andere celcycluscomponenten. Deze studie toont als eerste aan dat CDK4 en p27 een rol spelen in verworven everolimusresistentie in NENs, wat in lijn is met recente gegevens in andere typen tumoren. Zowel CDK4 als p27 zijn mogelijk essentieel voor everolimusresistentie en zouden dus als biomerker voor de effectiviteit van everolimus in NEN patiënten kunnen dienen. Daarnaast geeft dit een rationale om celcyclusinhibitoren te gebruiken in de behandeling

van rapaloog-resistente NENs.

Hoofdstuk 6 beschrijft de volledig transcriptoomgegevens van BON-1 en QGP-1, zowel zonder behandeling als na blootstelling aan everolimus. Op deze manier draagt dit hoofdstuk bij aan ons begrip van beide cellijnen als pNEN models. Daarnaast wordt de genoombrede genexpressiedata van BON-1/R en QGP-1/R, twee everolimusresistente cellijnen, beschreven. Het transcriptoom van BON-1 en QGP-1 clustert met andere cellijnen met neuroendocriene kenmerken. Dit duidt erop dat BON-1 en QGP-1 nuttige instrumenten zijn om fysiologisch en pathofysiologische differentatie te bestuderen. Daarnaast kunnen deze cellijnen gebruikt worden om moleculaire doelwitten voor nieuwe behandeling te identificeren in pNENs. Het transcriptoomprofiel van de resistente BON-1/R en QGP-1/R toont de rol van de celcycluseiwitten in everolimusresistentie. Daarnaast wordt de rol van de MAPK-ERK in everolimusresistentie verder uitgediept. Eveneens toont deze studie de rationale aan voor het gebruiken van gecombineerde remming van de PI3K/Akt/mTOR and MAPK-ERK signaaltransductieweg in pNEN.

In **hoofdstuk 7** worden de overkoepelende bevindingen van deze thesis besproken en in geplaatst in de huidige literatuur. Daarnaast worden toekomstperspectieven beschreven en nieuwe onderzoeksgebieden, zoals epigentica, geïdentificeerd.

Appendix

List of publications

I. LIST OF PUBLICATIONS

I. **Vandamme T**, Peeters M, Dogan F, Pauwels P, Van Assche E, Beyens M, Mortier G, Vandeweyer G , de Herder W.W, Van Camp G, Hofland L.J, Op de Beeck K. Whole exome characterization of pancreatic neuroendocrine tumor cell lines BON-1 and QGP-1. Journal of molecular endocrinology. 2015;54(2):137-47.

I. **Vandamme T**, Beyens M, Peeters M, Van Camp G, Op de Beeck K. Next generation exome sequencing of pancreatic neuroendocrine tumor cell lines BON-1 and QGP-1 reveals different lineages. Cancer Genetics. 2015; 208(10):523.

II. **Vandamme T**, Beyens M, Op de Beeck K, Dogan F, van Koetsveld P, Pauwels P, Mortier G, Vangestel C, de Herder W, Van Camp G, Peeters M, Hofland L. J. Long-term acquired everolimus resistance in pancreatic neuroendocrine tumors can be overcome with novel PI3K-AKT-mTOR inhibitors. British Journal of Cancer, 2016;114(6):650-8.

III. **Vandamme T**, Beyens M, Boons G, Schepers A, Kamp K, Biermann K, Pauwels P, De Herder W W, Hofland L J, Peeters M, Van Camp G, Op de Beeck K. Hotspot DAXX, PTCH2 and CYFIP2 mutations in pancreatic neuroendocrine neoplasms. Endocrine-related Cancer, 2019; 26(1):1-12.

IV. Beyens M, **Vandamme T**, Peeters M, Van Camp G, Op de Beeck K. Resistance to targeted treatment of gastroenteropancreatic neuroendocrine tumors. Endocrine-related Cancer, 2019; 25

(3): R109–R130.

V. Boons G, **Vandamme T**, Peeters M, Van Camp G, Op de Beeck K. Clinical applications of (epi)genetics in gastroenteropancreatic neuroendocrine neoplasms: moving towards liquid biopsies. Reviews in Endocrine and Metabolic Disorders, 2019; 20 (3), 333-351.

VI. Beyens M *, **Vandamme T** *, Boons G, Schepers A, Vandeweyer G, de Herder WW, Hofland LJ, Peeters M, Van Camp G, Op de Beeck K. CDK4 amplification and CDKN1B (p27) deletion in acquired rapalogue resistant neuroendocrine tumor cells. *Submitted for publication. (* Shared first authorship)*

VII. Beyens M *, **Vandamme T** *, Hofland LJ, Boons G, De Herder WW, Peeters M, Van Camp G, Op de Beeck K. Transcriptomic analysis of everolimus sensitive and resistant pancreatic neuroendocrine cell lines reveal everolimus escape mechanisms. *Submitted for publication. (* Shared first authorship)*

II. PUBLICATIONS NOT BELONGING TO THIS THESIS

I. **Vandamme T**, Kunnen J, Simoens M. Hyperammonemic encephalopathy in diffuse liver metastasis: is this the end stage? Gastroenterology. 2012;143(1):e9-e10.

II. Hofland LJ, **Vandamme T**, Albertelli M, Ferone D. Hormone and Receptor Candidates for Target and Biotherapy of Neuroendocrine Tumors. Front Horm Res. 2015; 44:216-38.

III. van Adrichem RCS, Kamp K, **Vandamme T**, Peeters M, Feelders RA, de Herder WW. Serum neuron-specific enolase level is an independent predictor of overall survival in patients with gastroenteropancreatic neuroendocrine tumors. Annals of Oncology, 2016; 27(4):746-7.

IV. Boons G, **Vandamme T**, Peeters M, Beyens M, Driessen A, Janssens K, Zwaenepoel K, Roeyen G, Van Camp G, Op de Beeck K. Cell-Free DNA From Metastatic Pancreatic Neuroendocrine Tumor Patients Contains Tumor-Specific Mutations and Copy Number Variations. Frontiers in Oncology, 2018;8:467.

V. Triest L, Debeuckelaere C, **Vandamme T**, Van Den Heuvel B, Van Den Brande J, Papadimitriou K, Rasschaert M, Prenen H, Peeters M. Should Anti-EGFR Agents Be Used in Right-Sided RAS Wild-type Advanced Colorectal Cancer? Curr Colorectal Cancer Rep, 2019; 15:130–134

VI. Boons G, **Vandamme T**, Ibrahim J, Roeyen G, Driessen A, Peeters D, Lawrence B, Print C, Peeters M, Van Camp G, Op de Beeck K. *PDX1* DNA Methylation Distinguishes Two Subtypes of Pancreatic Neuroendocrine Neoplasms with a Different Prognosis. Cancers (Basel). 2020;12(6):1461.

Curriculum Vitae

Timon Vandamme was born on December 31, 1987 in Antwerp, Belgium. After graduating from Sint-Gabrielcollege in Boechout, Belgium, he started his medical studies at the University of Antwerp, Belgium. While studying to become a physician, he completed a semester at the Universidad de Barcelona, Spain and a clinical rotation at the Universidad de Monterrey (UDEM), Mexico. After completion of his medical studies, he gained additional expertise in the treatment of neuroendocrine tumors during a research stay in the Erasmus MC, Rotterdam, the Netherlands, an European Neuroendocrine Tumor Society (ENETS)-certified Center of Excellence.

He pursued a joint PhD at the University of Antwerp and the Erasmus MC on everolimus resistance and pancreatic neuroendocrine tumor genomics. The PhD project is part of an international collaboration between the Center for Oncological Research (CORE) & Human Molecular Genetics group of the University of Antwerp and the laboratory of Experimental Endocrinology of the Erasmus MC.

His research has led to multiple publications in peer-reviewed journals and is funded by The Research Foundation - Flanders (FWO) and Stichting tegen Kanker. He presented his research at national and international conferences, including three oral presentations at ENETS. His research won different awards, including the ENETS-Ipsen Translational Research Fellowship in 2013. He serves as reviewer for various international journals.

During his PhD, he was involved in setting up NETwerk, the first European Neuroendocrine Tumor Society (ENETS) Network of Excellence in Antwerp, Belgium. He is an active member of the Coordination Unit and the Steering Committee.

Upon completion of his post-graduate training in gastro-enterology and digestive oncology at Antwerp University Hospital, ZNA Jan Palfijn and GZA Sint-Vincentius, he started as a consultant in digestive oncology at the Antwerp University Hospital. In his future career, he hopes be able to leverage insights from both research and clinical practice to improve patient care in neuroendocrine tumors and other digestive tract malignancies.

PhD Portfolio

I. SUMMARY OF PHD TRAINING AND TEACHING ACTIVITIES

Name PhD student: Timon Vandamme	**PhD period: 2012-2019**
Erasmus MC Department: Internal Medicine, Division of Endocrinology	**Promotors: Leo J. Hofland, Marc Peeters, Patrick Pauwels, Ken Op de Beeck**
Research School: Molecular Medicine	

1. PhD training		
	Year	**Workload (ECTS)**
General academic skills		
- Workshop Photoshop and Illustrator CS5 for PhD-students and other researchers	2013	0,3
- Laboratory animal science UAntwerpen	2012	12
Research skills		
- R-Workshop	2012	2
- Workshop Next Generation Sequencing	2013	0,2
- The Xth SNP Course & Symposium, Population Genomics of Complex Traits and Diseases Methodology	2013	2
- Survival Analysis in R	2016	2

(Inter)national Presentations

- *NET en NETwerk* Supraregionale MOC digestieve oncologie Zuid-Mid-West-Vlaanderen, Kortrijk, Belgium, **Invited lecture**	2018	2
- *Neuro-endocriene tumoren diagnose, behandeling en follow up?* Vereniging Verpleegkundigen Radiotherapie en Oncologie (VVRO) tweedaagse opleiding Oncologie, Gent, Belgium, **Invited lecture**	2018	2
- *Ultra-deep targeted resequencing reveals recurrent DAXX and CYFIP2 mutations and implicates novel pathways in of pancreatic neuroendocrine tumors.* 15th Annual ENETS Conference, Barcelona, Spain. **Oral**	2018	2
- *Onderzoek binnen NETwerk* NETwerk-symposium rond samenwerking in neuro-endocriene tumorzorg. Antwerp, Belgium. **Invited lecture**	2017	2
- *Exome sequencing in neuroendocrine pancreatic tumor models* 17th Congress of the European Neuroendocrine Association (ENEA 2016), Milan, Italy. **Invited lecture**	2016	2
- *Ultra-deep targeted resequencing of 38 pancreatic neuroendocrine tumors reveals tumor heterogeneity for actionable mutations.* XXXVIIIth Belgian Week of Gastro-enterology, Brussels, Belgium. **Oral**	2016	2
	2015	2

- *Resistance to molecular targeted therapy* Masterclass on Site, Rotterdam, the Netherlands. **Invited lecture**		
- *Van hormonen tot chemotherapie: de behandeling van neuroendocriene tumoren in 2014* Ipsen onbijtsymposium Erasmus Endocrinologie Cursus, Noordwijkerhout, the Netherlands. **Invited lecture**	2014	2
- *2013 ENETS-Ipsen fellowship overview* 11th Annual ENETS Conference, Barcelona, Spain. **Invited lecture**	2014	2
- *Inducing, understanding and overcoming resistance to everolimus in pancreatic neuroendocrine tumors.* 11th Annual ENETS Conference, Barcelona, Spain. **Oral**	2014 2013	2 2
- *Biomarker discovery and pancreatic neuroendocrine tumor cell line characterization using whole exome sequencing.* VVGE Herfstsymposium, Brugge. **Invited lecture**	2013	2
- Today's treatment in neuroendocrine tumors. 1th "Perspectives in Gastro-oncology" symposium, Brussels, Belgium. **Invited lecture**	2013	2
- *Whole Exome Sequence Of BON-1 And QGP-1, Two Human Pancreatic Neuroendocrine Tumor Cell Lines, Reveals Homozygous Loss Of Function Mutations In TP53, HRNR and CYFIP2.* 10th Annual ENETS Conference, Barcelona, Spain		

2. Teaching activities

	Year	Workload (Hours/ ECTS)
Lecturing		
- "Interprofessioneel samenwerken in de gezondheidszorg 2" (IPSIG 2), Master na master specialistische geneeskunde/Master Verpleeg- en Vroedkunde/Master Huisartsgeneeskunde/Master Sociaal werk/Master Revalidatiewetenschappen en Kinesitherapie, Master in Ergotherapie, University of Antwerp, Antwerpen	2014 -2016	34
- Practical course "Hypercortisolism." 1th Bachelor of Medicine, Erasmus MC, Rotterdam	2013	2,5
Supervision of students		
- Masterthesis Anton Cuypers tot behalen van de title Master in Medicine, Faculteit Geneeskunde en Gezondheidswetenschappen, Universiteit Antwerpen, Antwerpen, België		5
- Masterthesis Matthias Beyens tot behalen van de titel Master in de Biomedische wetenschappen, Faculteit Biomedische Wetenschappen, Universiteit Antwerpen, Antwerpen, België		5
- Scriptie Emilia Van Hecke tot behalen van de titel Bachelor in de Medische Labortoriumtechnieken, Karel De Grote hogeschool, Antwerpen, België		5

Awards and prices

- Best Poster award, Science Days Internal Medicine Erasmus MC, Antwerp Belgium	2014
- BSMO Best poster presentation award. 16th Annual BSMO Meeting, Brussels, Belgium	2014
- European Cancer Congress 2013 Fellowship grant, awarded by the European Cancer Congress to attend the European Cancer Congress 2013, Amsterdam, the Netherlands	2013
- ENETS-Ipsen 2013 Translational Research Fellowship, awarded by the European Neuroendocrine Tumor Society (ENETS)	2013
- ENETS Abstract Prizes “Basic science related to cancer biology”, 3rd prize awarded by the European Neuroendocrine Tumor Society (ENETS)	2012
- FWO Travel grant for a long stay abroad at the Erasmus MC, Rotterdam, the Netherlands,	-2013
- Antwerp Doctoral School (ADOC) ‘Omkadering van jonge onderzoekers’ – OJO grant for a research visit abroad at the Erasmus MC, Rotterdam, the Netherlands	2012 2012
- PhD scholarship of CWO (Commissie Wetenschappelijk Onderzoek), the Faculty of Medicine and Health Sciences, the University of Antwerp, Antwerp, Belgium	2012

Awards and prices

-	VVGE aanmoedingsbeurs, awarded by the Flemisch Society for Gastroenterology (VVGE), Elewijt, Belgium	2012
-	MOCA research grant for translational research in oncology 2012, awarded by the Multidisciplinair Oncologisch Centrum Antwerpen, Antwerp University Hospital, Edegem, Belgium	2012
Total		**96**

Acknowledgements – Dankwoord

From the first letter to the last, this thesis has been 9 years in the making. Almost a decade since my first foray into the lab, these years have been filled with challenging but interesting experiments, many thought-provoking discussions and lots of ~~writing~~ re-writing. Luckily, many people have helped and supported me during this great endeavor. Without them, this thesis would never have come to fruition and I'm glad that I can finally offer a well-deserved "thank you"!

I would like to start by thanking prof. dr. W.N.M. Dinjens, prof. dr. J. Martens and prof. dr. G.D. Valk for studying this manuscript in detail as members of the small committee of the jury. In addition, I would like to thank all members of the jury for taking the time to discuss my research during my promotion. I look forward to your opposition, as only through discussion good ideas become great ideas!

This thesis started when an inexperienced student entered the office of prof. dr. Marc Peeters, asking whether he could do research on neuroendocrine tumours. Prof. Peeters, I cannot imagine how different things would've been if you hadn't taken a chance on me. Not only did you give me the opportunity to start doing research, you have also proven to be a mentor for many aspects of my career, even giving me the chance to start working within your department at the Antwerp University Hospital.

One of the first actions of prof. Peeters proved to be vital for this thesis: he introduced me to prof. dr. Leo J. Hofland at the Erasmus MC. Dear Leo, when a Belgian delegation entered your office in 2012, none of us could have foreseen what would follow. You've hosted this Belgian for a year in your lab in person, but more than that, have guided me through the mysteries of neuroendocrine tumour research. You are one of the sharpest minds I have ever encountered. I'm still trying to find a paper on NETs that you haven't read! Even more than an inspiring researcher, you are a kind person. It is truly a highlight when we can meet up (nowadays mainly virtually) to discuss research, because one way or another, we'll end up discussing life in general. You are a promotor in the truest sense of the word: you bestow your wisdom onto your students and make them better people.

Prof. dr. Pauwels, dear Patrick, as always in oncology, "tissue is the issue". Your essential support as promotor in finding, selecting and extracting the samples we needed for our research, are only a small part of your involvement in my thesis. In discussions, you've always proved to have the latest insights on pathology and genomics readily available and you have hence pushed my thesis to the next level.

Prof. dr. Op de Beeck, Ken, you were there from the very start, guiding an enthusiastic young student in his first steps in the lab. Undoubtedly, some of those "first steps" were quite shaky and you've spent considerable time explaining to this physician exactly how those genetic techniques worked and how to use a

pipette. Thank you for your patience! More than your patience, your insights really put this project and, thus, neuroendocrine research in Antwerp, on the rails. Hence, I'm very glad to be able to call you "promotor".

Next to the vital role of my promotors in my thesis, I have had the luck of meeting some people throughout my PhD that I consider "mentors", such as Prof. dr. de Herder. Dear Wouter, if it wasn't for a tennis match somewhere in the Middle East that both you and prof. Peeters watched, this thesis might have never existed. You have helped not only by facilitating my research, but also by allowing me to follow your consultations in the NET clinic, effectively kickstarting my career as a NET clinician. Other than that, I tremendously enjoyed our non-clinical, barely scientific, discussions as well. For instance, I fondly remember the day we spent driving around the Dutch countryside to visit patients at home and collect samples.

Prof. dr. Van Camp, dear Guy, what started as a much-needed introductory course in genetics and genetic techniques for this unknowing PhD student, soon became a masterclass as you adopted me into your lab at the Center of Medical Genetics. Your genetic insights and enthusiasm for the oncogenetic field - always looking for better ways to answer the research question - was essential for this project. I would like to thank you not only for hosting me but also pushing the research in this thesis forward!

To counter all these jury members, mentors and promotors, I

have found two amazing paranymphs willing to stand by me. Dear Marije, you were the first person to speak to me in Leo's lab, and provided me with an opening line that still follows me to this day: "I'm a little strange". You didn't stay a stranger for very long as we started talking and never stopped. What started as a joint interest in NET quickly transformed into a joint interest in life. I'm very glad to count you as one of my dearest friends. Dear Tobit, being the first in the family to obtain a PhD is quite historical. Despite starting a few years later than me, you reached the finish line first. Luckily, today I can follow in your footsteps and, in doing so, have a "real" doctor supporting me during my defense. Hopefully, you can feel some of the pride I felt when my big "little" brother defended. I truly admire the uncompromising truthfulness by which you navigate your life. I aspire every day to be as authentic in my decisions!

One of the highlights of my PhD journey was the amazing group of peers that I got to know and that supported me all the way through to the end.

I want to start by thanking Matthias Beyens. Dear Matthias, when you first set foot in our lab for your master thesis, you blew me away with your keen intellect, great insights and a wet lab mastery I will never possess. Hence, I was very lucky that you decided to pursue a PhD in NET. Only a couple of months into your PhD, you decided to become a bioinformatician. As people that know you can attest, when you put your mind to something, nothing can stop you. Your transformation into a bioinformatics whizz kid

was truly impressive. It allowed us to lift our research to the next level, resulting in many of the papers in this thesis. In addition to being an excellent researcher, you are a genuinely nice guy with a strong focus on every project you undertake, whether it is research, cycling or your friends. I'm very happy for all the times we got the chance to discuss both research and life over a couple of beers!

Towards the end of my time in the lab, Gitta Boons joined our research group. Dear Gitta, it is a true honor to have been able to do research together, as you challenged me to become a better scientist. I really enjoyed our discussions on all your exciting new findings, even though sometimes I needed to convince you exactly how exciting these findings were. Through your research, you helped me to keep the "goesting" for science, even when I was swamped with clinical work. I look forward to your PhD defense which will undoubtedly be excellent!

The first year of my PhD, I spent in the endocrinology lab at the Erasmus MC, surrounded by a group of "neuroendo gekkies" (for some reason the name "Hairy tumours", that we used as group name in a pub quiz, didn't really stick despite leading us close to victory). Thomas, Federico, Sabine, Roxanne, Sara, Stephanie, Gerard, Sanne, Vincent, Kimberly, and Mesut, it was great sharing offices and laughs over the years. Thomas and Federico, as fellow foreigners in the Dutch ecosystem, we relied on each other to understand some of the intricacies of the Erasmus MC. I'm glad that I could introduce you to some Belgian beers, but prefer that

you stay away from the Jameson, Federico! Thomas, you had the questionable honor of being the first person that I had to accompany to the police station to report a car theft. I'm really glad that I managed to see you both in your "natural" habitat and hope that we'll soon have the chance to meet up again! Sabine, a psychologist in an endocrinology lab, it was great getting to know you and I'm happy that you found your place in life. Roxanne, although our paths only crossed briefly, we managed to publish together and have a great time doing so. Kimberly, about as enthusiastic about research as about rowing, it was great discussing clinical NET studies with you. Stephanie, although not really sharing a research interest, we did share beers and laughs. Gerard, you are one of the nicest people that worked in the lab, it was great to be able to hang out. Sanne, you always fill the room with your warmth wherever you go. It was great getting to know you. Vincent, dear Vincent, so many discussions we've had, some even about science. You definitely broadened my world. Sara, your research skyrocketed, fueled by your personality. I wish you all the best. Mesut, despite never having shared an office, we did share a room during the Science days, which was enough to realize that you are a great guy! I wish you and the other people in the lab all the best!

Fadime and Peter, undoubtedly you are the beating heart of the neuro-endo lab. Your knowledge of cells and techniques is a safe haven for any beginning PhD student, especially when it is a physician who has never seen a lab from the inside. Thank

you for supporting me in my first steps in the lab and for your kindness in helping me salvage the experiments that had failed!

After my stay at the Erasmus MC, I returned to Antwerp, where I received a warm welcome in the Center for Medical Genetics. The "DOOF" group was not really a silent bunch. Nele, Lieselot and Marieke, you were unfortunate enough to have to share an office space with me. Probably your PhDs might have been even more impressive, if we hadn't been talking for so many valuable research hours about nothing and everything all at once. Nele and Marieke even were taken on an expedition through the Ghent nightlife by me, which included a long walk in the wrong direction. Hopefully you can forgive me by now? Manou and Hanne, you were "from the other side" but, despite your lack of interest in oncology, you have proven to be amazing colleagues and we shared many fun meals. Hanne, I promise you, I will never ever again ask you for a "small favor", which consisted of rewriting the entire PhD policy of the Antwerp University. I guess I still owe you an apology for that. Anne, as a lab technician, you provided the much-needed stability in our dynamic DOOF office. Thank you for all your help in all our PhD's. You have been a cornerstone for all of us.

Over the course of my PhD, I got involved in setting up NETwerk, a collaboration of nine hospitals around NET care. I would like to thank all people involved in making NETwerk the success it is today. Special thanks go to Willem Lybaert, who has been a driving force for NET care and a great personal inspiration. NETwerk would not have been possible without the initial help

of Greetje, who soon was joined by Lesley. Lesley, thank you for helping me navigate all the ongoing NETwerk projects, effectively serving as an "external memory". I had a great time during the many hours we discussed NETwerk and so many other things. I wish you all the best in your new job! Of note, I would also like to thank Marc Simoens for introducing me to the world of NET with my first publication, long before there was any mention of this thesis or NETwerk.

Some of the ideas we used to set up NETwerk were undoubtedly inspired by Wanda Geilvoet. Dear Wanda, you're the "original" NET nurse and an all-round nice person. I learned a great deal from you at the Erasmus MC and afterwards.

Outside of work, I would like to thank two people without whom not a single letter of this thesis would have been written: my parents. Thank you for supporting me through my very, very, very long school career. I can finally say: "I'm finished". The fact that you can hold this beautiful book, is thanks to my sister: Esther. Dear sis, thank you for finding the time in between a journey around the world, two jobs and a renovation project to put the layout cherry on top of my thesis. Your energy is an inspiration!

Dear Valérie, as long as you've known me, this thesis has been following me around. Thank you for your patience, not only with my thesis but with me in general. You are the most impressive person I have ever met and I'm still amazed every day that you choose me!

Dear Odile, I would like to dedicate this thesis to you. You are far too young to understand what is written, but I will gladly explain this to you in the future. In the meantime, you show me the world through your eyes and it is a beautiful one. You have changed my life in less than two years far more than any research could and for that I would like to thank you.